Insights into Transition Metal Catalysed Asymmetric Transformations

Ruchuta Ardkhean

Lady Margaret Hall

University of Oxford

A thesis presented in partial fulfilment of the requirements for the award of the degree of

Doctor of Philosophy

Michaelmas 2018

Author's Declaration

This thesis describes work carried out in the Chemistry Research Laboratory, Oxford, between October 2014 and August 2018 under the supervision of Dr Stephen Fletcher and Dr Robert Paton, and at Vertex Pharmaceuticals (Europe) Ltd, 86-88 Jubilee Avenue, Milton Park, OX14 4RW, UK between April 2017 to June 2017 under the supervision of Dr Michael Mortimore. The thesis is a result of my own work, except when stated otherwise, and has not been submitted for any other degree at this or any other university.

Ruchuta Ardkhean

November 2018

Acknowledgement

A wise woman once told me that to obtain a Ph.D., there will be a stage where you have face challenges that will teach you a philosophy of a lifetime. I did not think that it would be such a big deal as it is just another degree at the end of the day… until I realised that she was absolutely right.

There are many people who I owed my DPhil to. First and foremost, I would like to thank my main supervisor, Steve who has changed the way I handle research and has been a great supervisor. Rob for his help on the computational side of things. And Mike for his advice and help with the placement.

My family, especially my mom and my dad who always give me support when I need it most. Roger, Loraine and Plum for being like a family-far-from-home.

The 4 year DPhil would not be as joyful and interesting as it has been without the incredible team from both experimental and computational lab – Sarah, Mire, Nisha, Jacqueline, Kiran, Alex(2), Reece, Rob, Lucy, David, Chus, Iuliia, Thomas, Philipp, Zhenbo, Xing, Joseph, Wieland, Ignacio, Andrew, Qian, Fernanda, Chu, Manu, Masha, Elena, Sedef, Shiny, and many more than I can name here.

SBM CDT team who have given me so much more than just funding but a team and friendship that would last a lifetime. DPST who has given me an opportunity to come to the UK to study.

My housemates – Ping, Pui, Jin and Kukkik for making me feel at home around you guys. Lucas, Faye and Jing who added a positive twist towards the end of my DPhil journey.

And finally thanks to all my previous supervisors, teachers, friends and colleagues who I am lucky to have met you all.

Abstract

A longstanding challenge in asymmetric catalysis is the discovery and development of a suitable chiral catalyst. There are no fixed rules or paths to follow when it comes to designing new catalysts. Traditionally, chemists have started by screening existing ligands and then analysing the experimental results using logical induction based on chemical knowledge and experience. To shift away from the reliance on trial and error for catalyst design, we have pursued a systematic approach that integrates experimental screening with a regression model – a quantitative structure-selectivity relationship (QSSR). In theory this approach is versatile and can be applied to any transformation, and any ligand (**Scheme 1**).

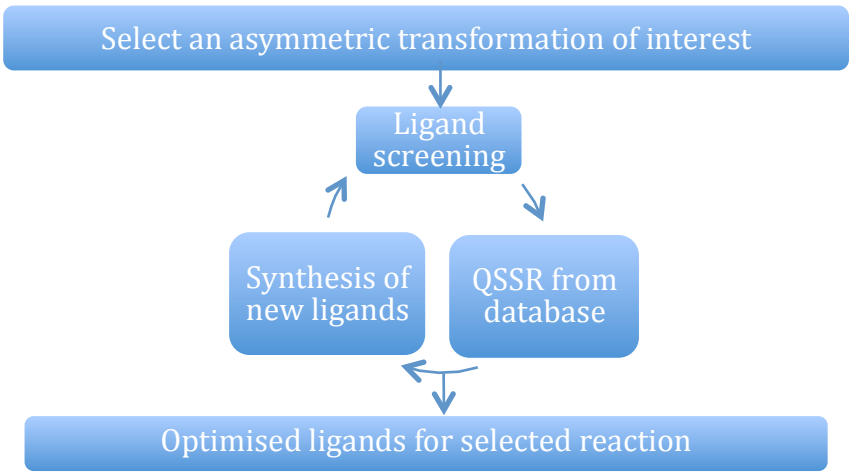

Scheme 1 Systematic approach to ligand design.

In this thesis, this systematic approach has been used in three different reactions. First, we demonstrated the use of this approach on an established system to shed light on the role of chiral phosphoramidite ligands on the enantioinduction of copper catalysed asymmetric conjugate addition to cyclohexenones. We analysed the experimental results using QSSR models and DFT calculations to aid our understanding of enantioinduction (**Scheme 2**).

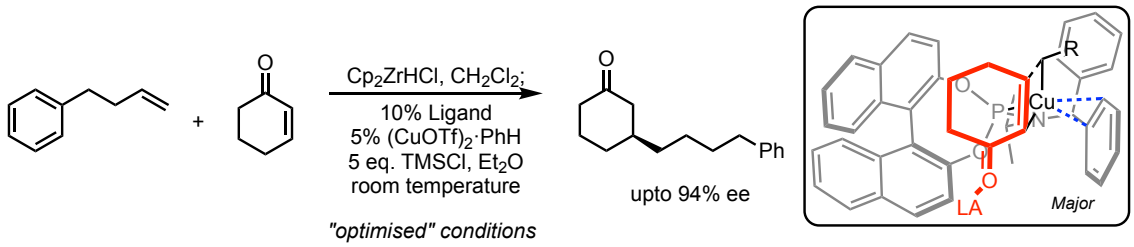

Scheme 2. **Chapter 2:** Copper catalysed conjugate addition of a cyclohexenone.

Then we illustrate the use of this systematic approach on developing suitable chiral ligands for a challenging substrate, a β-substituted cyclopentenone, in copper catalysed conjugate additions. The QSSR model has led us to discover novel ligands with improved selectivity. Enantioinduction of the system was also established using QSSR and DFT calculations. The synthetic value of this approach was demonstrated by a range of substrates which gave up to 97% isolated yield and 92% ee for 16 examples, some bearing functional groups that are generally not tolerated by other methods in the literature (**Scheme 3**).

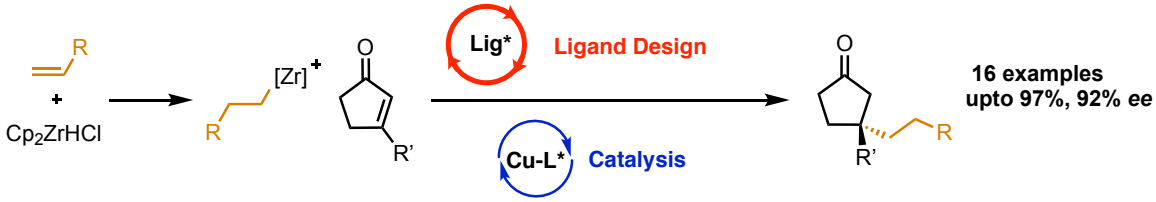

Scheme 3. **Chapter 3:** Copper catalysed conjugate addition of a β-substituted cyclopentenone.

Finally we have applied the approach to optimise an iridium-catalysed asymmetric hydrogenation of a dihydroisoquinoline, a precursor of Almorexant®. The initial ligand screening on 37 chiral ligands gave a yield and ee in the range of 4-100% yield and 2-80% ee. The project is subjected to on-going investigation (**Scheme 4**).

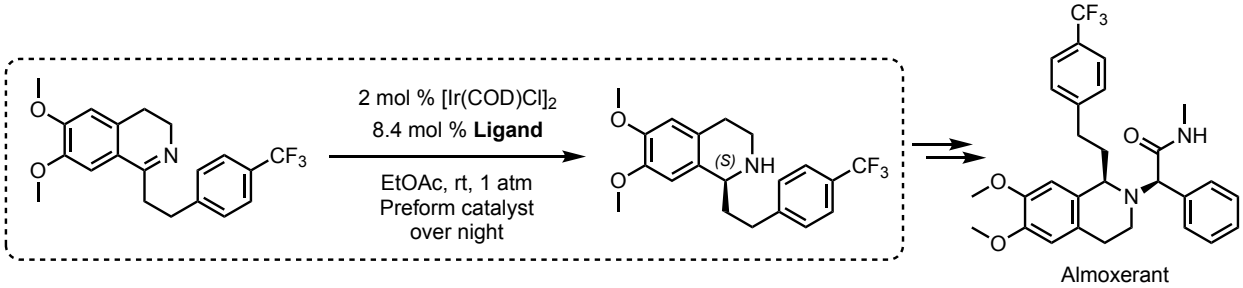

Scheme 4. **Chapter 4:** iridium catalysed hydrogenation of dihydroisoquinoline.

Abbreviation

Ac	Acetate/acetyl
ACA	Asymmetric Conjugate Addition
AD	Domain of applicability or applicability domain
Aq.	Aqueous
atm	Atmosphere
br	Broad
Bu	Butyl
c	cyclo-
ca.	Circa
cm	Centimetres
COD	1,5-cyclooctadiene
COSY	Homonuclear correlation spectroscopy
Cp*	Pentamethyl cyclopentadiene
CPK	Corey-Pauling-Koltun
Cv	Cross validation
Cy	Cyclohexane
d	doublet
DCM	Dichloromethane
DEPTQ	Distortionless Enhancement by Polarisation Transfer with retention of Quaternaries
DFT	Density functional theory
DPPP	1 ,3-Bis(diphenylphosphino)propane
ee	Enantiomeric excess
EIE	Equilibrium isotope effect
EPR	Electron Paramagnetic Resonance
Et	Ethyl
eq.	Equivalent(s)
EWG	Electron-withdrawing group
Ext	External
FF	Force field
Hex	Hexyl
Hept	Heptyl
HOMO	Highest Occupied Molecular Orbital
HPLC	High Performance Liquid Chromatography
HRMS	High resolution mass spectrometry
hr	Hour(s)
HSQC	Heteronuclear Single-Quantum Correlation
HTS	High Throughput Screening
IPA	Isopropylamine
iPr	Isopropyl
iBu	Isobutyl
IR	Infra-red
KIE	Kinetic isotope effect
kJ	Kilo Joules
l	Liquid
lig.	ligand

MLR	Multivariate linear regression
Me	Methyl
Mol	Moles
MM	Molecular mechanic
mmol	Millimoles
mCPBA	Meta-chloroperbenzoic acid
MLR	Multivariate linear regression
MP	Melting point
mm	Millimetres
MS	Mass spectrometry
Naph	Naphthyl
NBO	Nonbonding orbital
NMR	Nuclear magnetic resonance
^{n}Bu	Normal butyl
NCI	Non-colvalent interaction
Oct	Octyl
OLS	Ordinary least square regression
ONIOM	our own n-layered integrated molecular orbital and molecular mechanics
ovn	overnight
Ph	Phenyl
Pr	Propyl
QM	Quantum mechanic
QSSR	Quantitative Structure-Selectivity Relationship
R	Rectus (right-handed)
rt	Room temperature
quant.	Quantitative
rel	Relative
S	Sinister (left-handed)
s.	solid
s	singlet
sat.	Saturated
SCF GIAO	Self-consistent field gauge-including atomic orbital
SFC	Supercritical fluid chromatography
Smd	Solvation model based on density
^{t}Bu	Tert-butyl
TES	Triethyl Silyl
(x)Tf	Triflate (x = O)/Triflimide (x = N)
THF	Tetrahydrofuran
TIPS	Triisopropyl Silyl
TLC	Thin Layer Chromatography
TMS	Trimethyl Silyl
TS	Transition states
UV-vis	Ultraviolet - visible spectroscopy
vs	Versus
XPS	X-ray photoelectron spectroscopy

Table of Contents

1 Introduction

1.1 Chirality in life and medicine

The word 'chiral' is derived from χείρ (*cheir)*, a Greek word meaning hand. It was first used in science by Sir William Thompson in 1884.[1] Chirality, in the context of molecules, is the when the molecules possess a non-superimposable mirror image. The left and right "handed" forms of a molecule are called enantiomers (from ἐναντίος (enantios), meaning opposite). Enantiomeric excess (ee) is defined as the percentage difference between one enantiomer and the other. The sense of chirality can be assigned based on different rules, but in here we will use the Cahn-Ingold-Prelog system i.e., *R* or *S* which is universally used (**Equation 1-1**).[2]

Equation 1-1

$$\text{ee} = \frac{|R - S|}{R + S} \times 100 = |\%R - \%S|$$

Where *R* and *S* denote the amount of *R* and *S* enantiomer respectively

The physical and chemical properties of enantiomers are identical. Only when they are placed in a chiral environment will they behave differently.

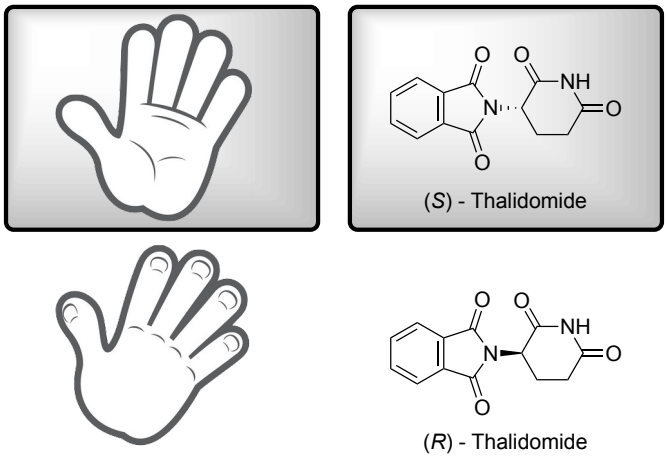

Figure 1-1 Right hand and (*R*)-Thalidomide and their mirror images.

Most chiral molecules found in living organisms and organic materials are enantiopure. Much work has been done to explain how and why, yet this remains an active and exciting research area.[3,4] The study of chirality not only serves the fundamental curiosity regarding the chemical origins of homochirality, but also plays an important role in our standard of living through innovations in medicines and agriculture. Failures to account for the different properties of enantiomers in medicine can have profound and lasting effects. For example, the use of Thalidomide during pregnancies led to a range of birth defects.[5] Although the biological mechanisms are still unclear, it was claimed that the (*R*)-enantiomer of Thalidomide has a sedative effect whereas, the (*S*)-enantiomer is teratogenic (**Figure 1-1**). In fact, (*S*)- and (*R*)-thalidomide enantiomers interconvert rapidly *in vivo* with both oral and intravenous dosing, meaning that both enantiomers could contribute to toxicity. Nevertheless, this tragedy led to stricter regulations of approval of medicines in many countries including the US and the UK. This emphasises the importance of the ability to control production of enantiopure molecules.

1.2 Access to enantioenriched materials

There are multiple approaches that allow chemists to gain access to enantioenriched materials; using natural enantiomerically pure starting materials (the *chiral pool*[6,7]), separating enantiomers by resolution[8] and by using a chiral auxiliary[9]. Some examples for each approach are shown in **Figure 1-2**).

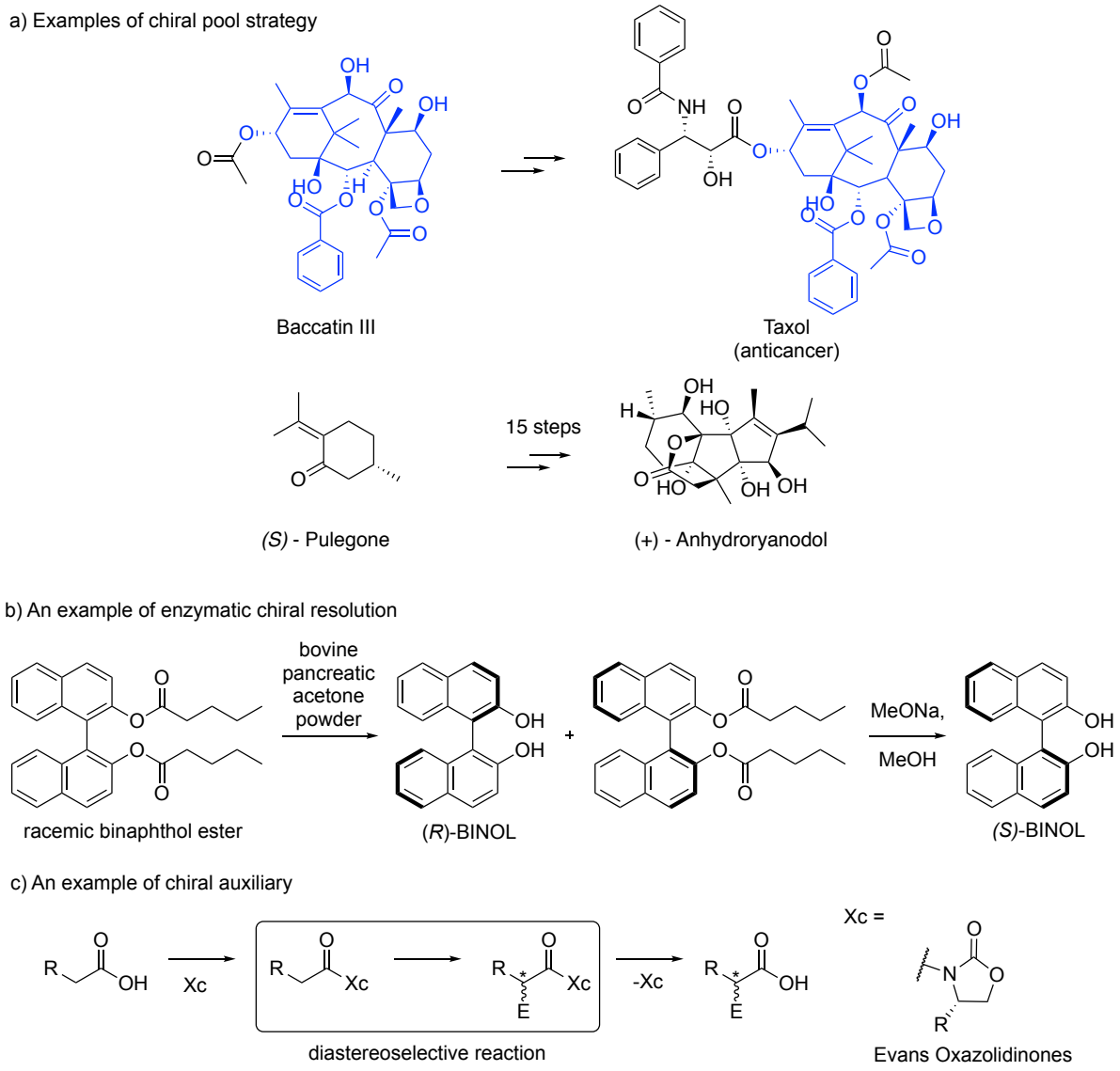

Figure 1-2 Some examples of chiral pool, chiral resolution, and chiral auxiliaries.

Alternatively, a more modern approach involves using *asymmetric catalysis*. This allows selective synthesis for enantioenriched materials using only a catalytic amount of a chiral species. Compared to the other approaches, asymmetric synthesis

is desirable because there is no need to rely on availability of the natural enantiomer (chiral pool) or wasting materials (50% of mass in kinetic resolutions is unwanted, and use of chiral auxiliaries require additional steps to introduce the auxiliary and liberate the desired molecule). In addition, the development of a catalytic system uses sub-stoichiometric chiral species to accelerate the reaction. These considerations add to the overall efficiency and atom economy of an asymmetric reaction.[10]

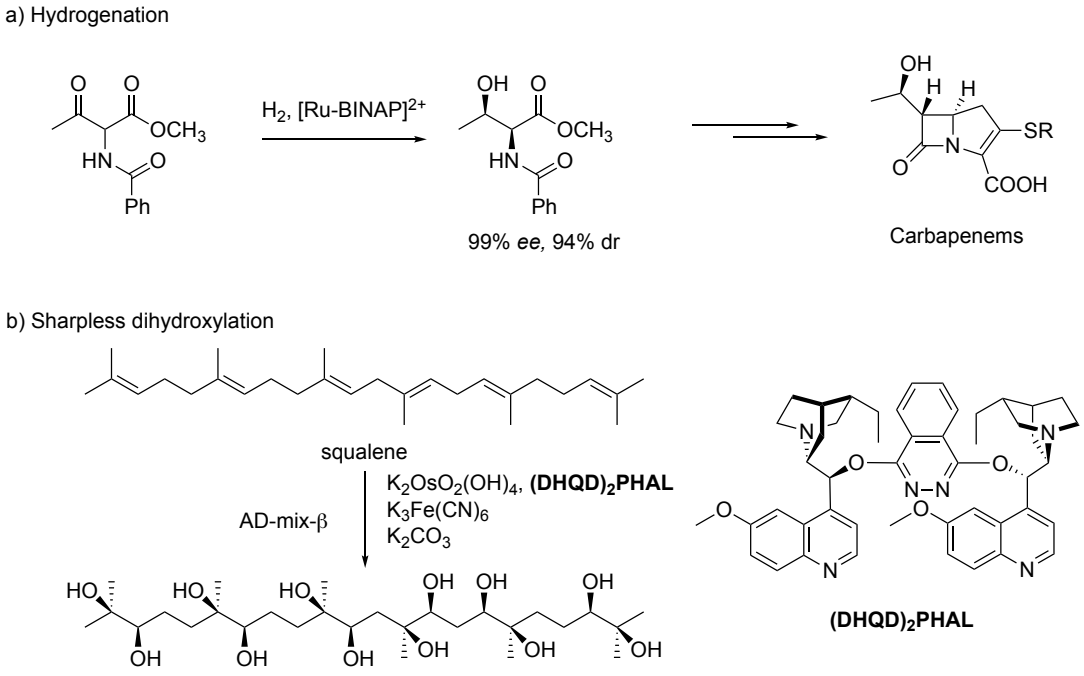

Figure 1-3 Examples of asymmetric catalytic reactions: a) asymmetric hydrogenation by Noyori and b) asymmetric dihydroxylation by Sharpless.

The impact of asymmetric catalysis in chemistry was recognised by the 2001 Nobel Prize, shared by three chemists: William S. Knowles, Ryoji Noyori, and Barry K. Sharpless for their work on catalytic asymmetric hydrogenation and oxidation (**Figure 1-3**). An example of Noyori's asymmetric hydrogenation of a carbonyl is shown in **Figure 1-3a**. This reaction used a chiral Ru complex which led to high yield, enantio- and diastereoselectivity of the product which is a precursor of the last resort antibiotic, Carbapenems.[11] **Figure 1-3b** shows an example of Sharpless

asymmetric dihydroxylation of squalene where 6 C=C bonds are functionalised in a single step.[12,13]

1.3 Privileged ligands; phosphoramidites

Metal-ligand complexes activate many transformations and in enantiopure, chiral form they can be used to effect asymmetric catalysis. A particular class of chiral ligand which functions across a wide variety of chemical transformations, is often referred to as a 'privileged' ligand.[14] These ligands are able to induce good to excellent levels of enantioselectivity in various reactions, even though the ligated metal and the associated reaction mechanisms may drastically differ. Examples of privileged ligands include BINOL (1,1′-Bi-2-naphthol)[8], BINAP ((2,2′-bis(diphenylphosphino)-1,1′-binaphthyl[15], used in Diels-Alder reactions, hydrogenation, Heck reactions, Aldol reactions, etc.), Brintzinger's ligand[16] (used in alkene and imine reduction, Ziegler-Natta polymerisation, etc.), TADDOL[17] (used in Diels-Alder reaction, aldehyde alkylation, iodolactonisation, etc.) and Bisoxazoline[18] (used in Diels-Alder reaction, Mukaiyama aldol, conjugate addition, cyclopropanation, etc.).[14] This array of ligands emphasises that the source of chirality may come from stereogenic centres or from axial chirality due to restricted rotation about a biaryl bond.

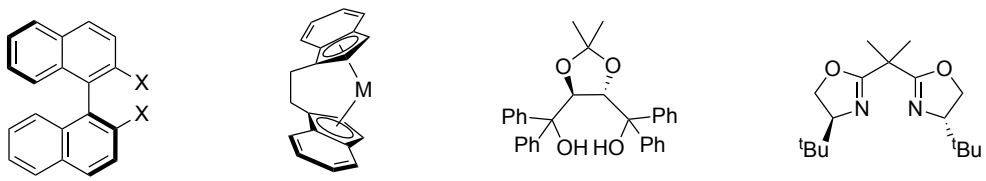

X = OR BINOL
X = PR_2 BINAP based ligands

Brintzinger's ligand

TADDOLate ligand

Bisoxazoline

Figure 1-4 Examples of privileged chiral ligands

Privileged structures such as BINOL also feature as a core structural element in more complex ligands. For example, a BINOL sub-unit is commonly found as a *chiral backbone* in phosphoramidite ligands used with a transition metal, where some of these ligands show versatility towards a wide range of transformations such as conjugate addition, 1,2-addition, allylic substitutions, cross-couplings, cycloaddtion and hydroborylation/hydrosilylations.[19,20] Many of these transformations show a large substrate scope with very good to excellent ee, for instance, an asymmetric hydrogenation where known substrate scope includes α-amino acids, β-amino acids, dicarboxylic acids, esters, cinnamic acids, amines and heterocycles.[19] Many of these types of ligands are commercially available eg. MonoPhos and Feringa's ligand (**Figure 1-5**).

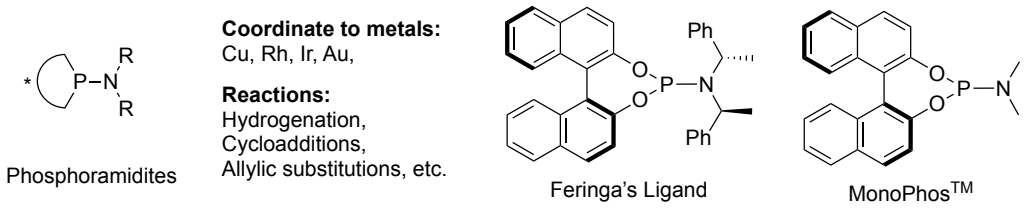

Figure 1-5 Phosphoramidite ligands

Some common structural features present in many privileged ligands are relatively rigid structures, C_2-symmetry, and bearing heteroatoms able to bind strongly with the transition metals.[14] However, such criteria are neither necessary nor sufficient to create an effective chiral catalyst. It is possible to synthesise chiral ligands with all of these features which do not perform well and *vice versa*. This means that the search for a chiral ligand that performs well for a given transformation of interest remains extremely challenging and still relies on trial and error. In this search for new ligands, phosphoramidite scaffolds are attractive due to their modular structure. This ensures that structures, and therefore reactivity and selectivity, are

tunable parameters. In addition, the BINOL backbone is commercially available in both *R* and *S* forms, so that the choice of enantiomers is not limited like in ligands derived from some chiral pool structures such as ligands derived from carbohydrates.[21]

1.4 Approaches for ligand design in asymmetric catalysis

It is highly likely that there is no general catalyst: it is not plausible to make a general catalyst or chiral ligand capable of catalysing *all* chemical transformations in high selectivity. As new target molecules constantly emerge, the need to discover new methods and to develop new chiral ligands naturally follows. However, the selection or design of the most appropriate chiral ligand and catalyst remains a challenge without a straightforward solution.

When a new system is being developed, in the most widely practised approach is to take a group of selected ligands and catalysts and test them for desirable catalytic properties for the reaction. This ligand development is rightfully guided by the accumulated expertise of trained chemists. This approach has inherent sense of trial and error and often more so than a sense of design. Trial and error thus been beneficial in catalyst discovery but generally, any developer/designer of a system would prefer to minimise reliance on randomness to save time and effort.

In this chapter, we will discuss three approaches for ligand design 1) Serendipitous discovery and high throughput screening 2) Mechanistically driven ligand discovery, and 3) Quantitative model-lead ligand discovery.

1.4.1 Serendipitous discovery and high throughput screening (HTS)

Serendipity has played an important role in chemical discovery as exemplified by discoveries such as the classic Friedel-Crafts and Wittig olefination reactions.[22] Enabled by modern technology, such as automated robotic systems, it is possible to accelerate the process of trial-and-error experimentation to generate results rapidly. For example, Macmillan has used high throughput screening and GC-MS as a means to analyse product formation, leading to a discovery of a novel photoredox catalysed α-amino C-H arylation reaction, terming the procedure 'accelerated serendipity' (**Figure 1-6**).[23]

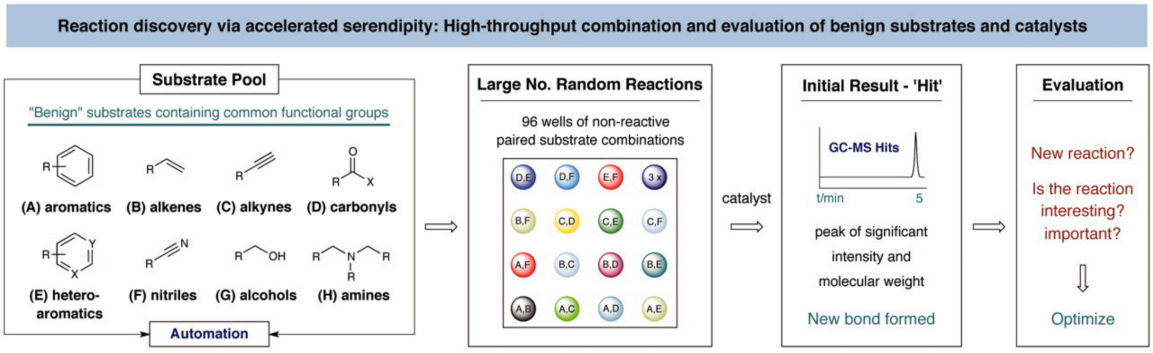

Figure 1-6 Macmillan's approach to accelerated serendipity. Reprinted with permission.[23]

Examples of rapid screening platforms for asymmetric catalysis have been illustrated by de Vries and Lefort, in asymmetric hydrogenation. Here, the *in situ* synthesis of 32 BINOL-derived phosphoramidite ligands and 64 hydrogenation reactions were carried out by Premex 96-multireactor within two days (**Figure 1-7a**).[24] Feringa, de Vries and Minnaard also applied this approach to rhodium catalysed asymmetric addition of arylboronic acids by synthesising 20 chiral phosphoramidite ligands *in situ* and used them in the subsequent reaction giving up to 87% ee of the desired product (**Figure 1-7b**).[25]

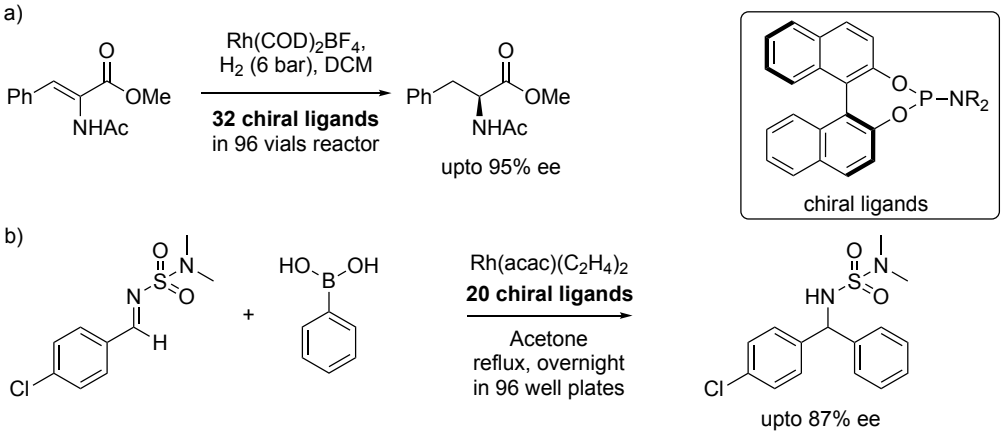

Figure 1-7 Asymmetric reactions with parallel chiral ligands screening.

The ability to screen multiple reactions at a time is a promising approach, however, the reliable analysis of reaction progress, product formation and selectivity is equally as important. The traditional approach of analysing enantioselectivity using chiral HPLC becomes a bottleneck in this regard. Therefore, recent advances in ee determination procedures make HTS more attractive. With supercritical fluid chromatography, Regalado and Welsh (at Merck) have shown that the ee of 50 racemic compounds can be analysed in less than a minute each on customised short chiral columns (1-2 cm).[26] Others have developed, to a certain extent, more specialised (in a sense, less widely used) systems; Anslyn and co-workers have developed a circular dichroism based host-guest system to determine ee of vicinal diols, α-hydroxyacids, vicinal diamines, cyclohexanones, amines, α-chiral aldehydes, carboxylates, amino acids, and secondary alcohols within ± 7% or lower average error (**Figure 1-8a**).[27] For chiral amines and amino acids, a few other methods have been developed to analyse their ee's[28] such as NMR/ fluorescence detection of chiral boronate and amine assembly by Anzenbacher (**Figure 1-8b**)[29,30], ^{19}F NMR probing chiral palladium pincer complex with chiral amines developed by Zhao and

Swager[31] (**Figure 1-8c**), and Heemstra used a DNA biosensor to detect the chiral amino acid tyrosinamide (**Figure 1-8d**).[32]

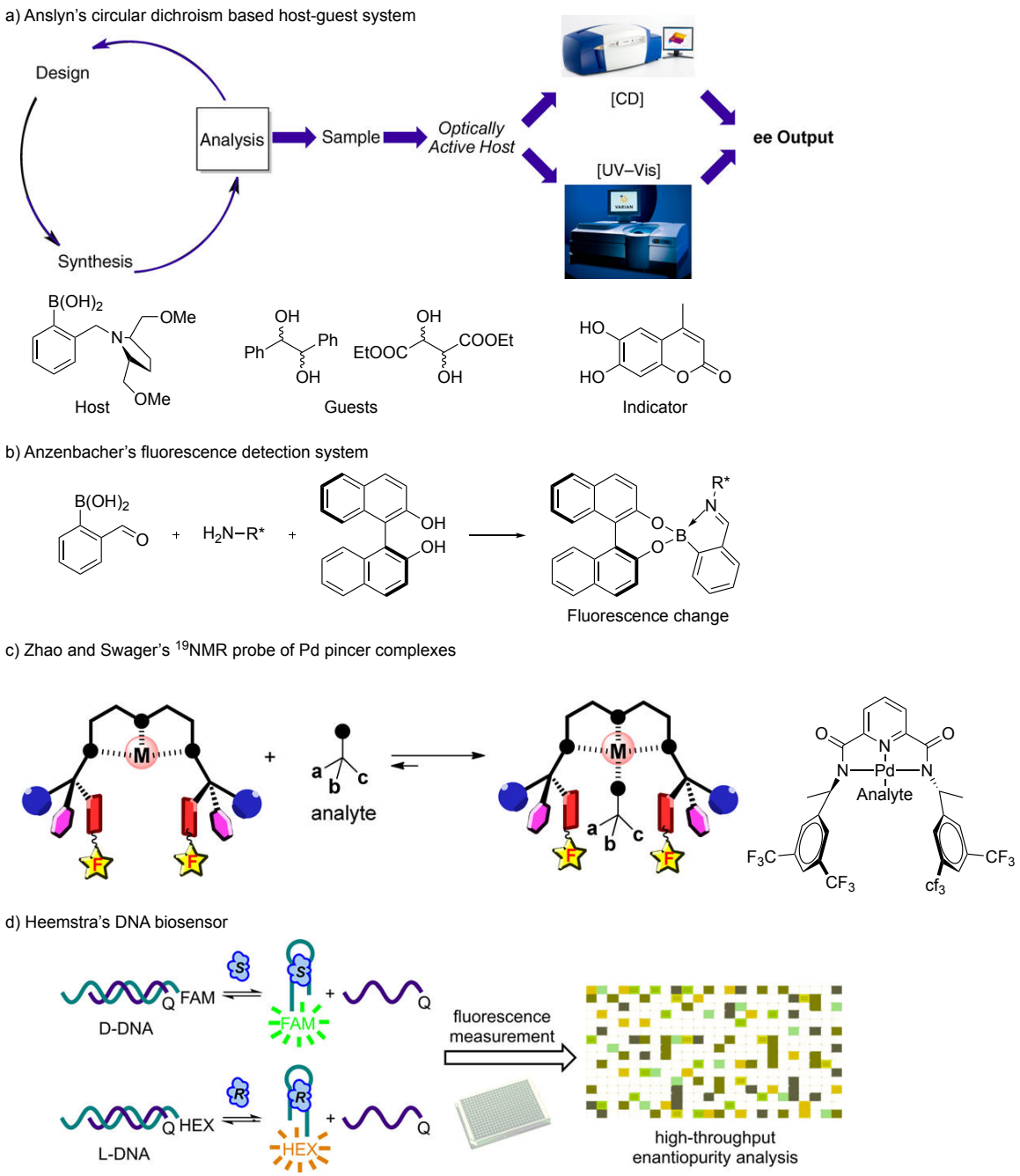

Figure 1-8 Examples of ee detection techniques: a) Anslyn's circular dichroism based host-guest system, b) Anzenbacher's fluorescence detection system, c) Zhao and Swager's ^{19}NMR probe of Pd pincer complexes and d) Heemstra's DNA biosensor. Reprinted with permissions.[27,31,32]

Despite the promising accomplishments this approach has achieved so far, some drawbacks remain. Firstly, specialised tools or chemical systems are often required

for screening and analysis. Secondly, there is no guarantee that screening will yield any promising results neither does it offer a systematic way to improve upon in the context of reaction development. Lastly, this approach generates a lot of waste data (which can be useful when used in conjunction with other approaches, see section 1.4.3).

1.4.2 Mechanistically driven ligand discovery

The most rational strategy to ligand design is to tackle the problem bottom-up. This approach is based on drawing logical assumptions from established reaction mechanisms and knowledge about how the enantioselectivity in the product is induced. However, the elucidation of the reaction mechanism and identification of the factors governing the enantioinduction pose a challenge in itself. The computational cost of modelling has been made more efficient since the 1960s and continues to do so. The emergence of quantum computing may result in the availability of even more versatile calculations in the near future, but the prediction of small-molecule catalysts using the computational infrastructure of today is now firmly embedded in the first line of attack in catalyst design.[33] Computational modelling of a chemical system on its own still faces key challenges such as narrowing the plausible reaction pathways from multiple possibilities, modelling solvation, evaluating dispersion energy in large complexes, sampling the conformations of large and flexible species and the breakdown of statistical rate-theories.[34] To this end, collaborative and combinatorial approaches have shown to be most promising, particularly with the use of a computational modelling in combination with experimental results. A plethora of successful mechanistic studies prior to 2014 have been highlighted by Wu, showing examples where experimental

findings were explained by modelling, models substantiated or eliminated by experimental results, and cases which led to the development of more powerful solutions to reactivity or selectivity problems.[35] Combined computational and experimental mechanistic studies continue to flourish. Some recent examples are; Stępień's mechanistic study on palladium mediated double C-H activation using NMR spectroscopy and density functional theory (DFT) calculations[36] and Wang's mechanistic study on copper catalysed oxidative cross coupling of arenes and boronic acids using XPS, EPR, NMR, HRMS, and UV–vis and computational calculations (**Figure 1-9**)[37].

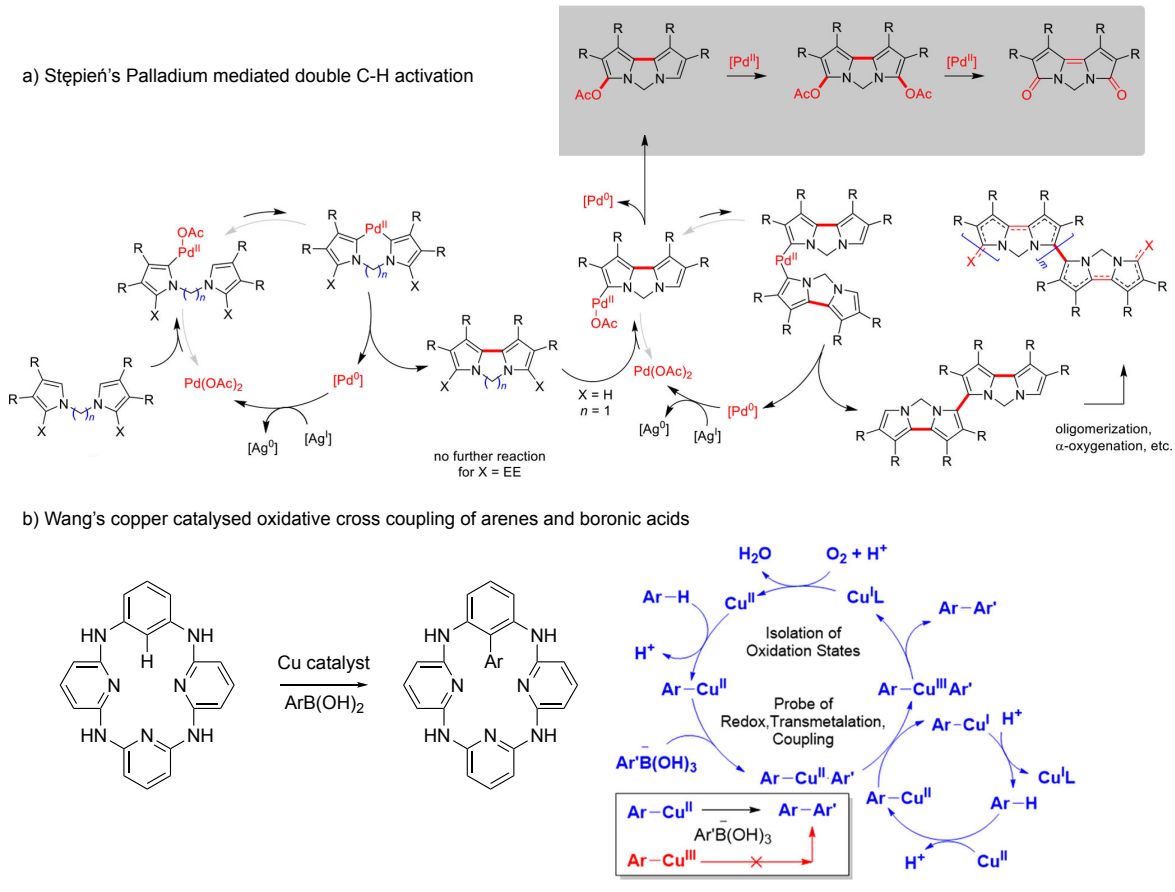

Figure 1-9 Examples of combinatorial mechanistic studies: a) Stępień's palladium mediated double C-H activation and b) Wang's copper catalysed oxidative cross coupling of arenes and boronic acids. Reprinted with permissions.[36,37]

1.4.2.1 QM based methods

Qualitative models often provide satisfying rationalizations of experimental results but lack the ability to make quantitative predictions. Real reactions may have idiosyncrasies not accounted for by qualitative general rules. Modelling (and hopefully predicting) enantioselectivity requires quantitative numerical calculations. The difference between the free energies of activation for the formation of opposite enantiomers determines their ratio. Because of the logarithmic dependence, less accuracy is needed to predict high enantioselectivities correctly than to predict low values. For example, a prediction that $\Delta\Delta G^{\ddagger} = 0 \pm 0.25$ kcal/mol means that the reaction will proceed with 0 ± 20 % ee, while a prediction $\Delta\Delta G^{\ddagger} = 2.5 \pm 0.25$ kcal/mol means that a reaction will proceed with 97 ± 1 % ee (**Figure 1-10**). Nonetheless, the relatively small Gibbs energy differences, means that enantioselectivies can be difficult to predict.[38]

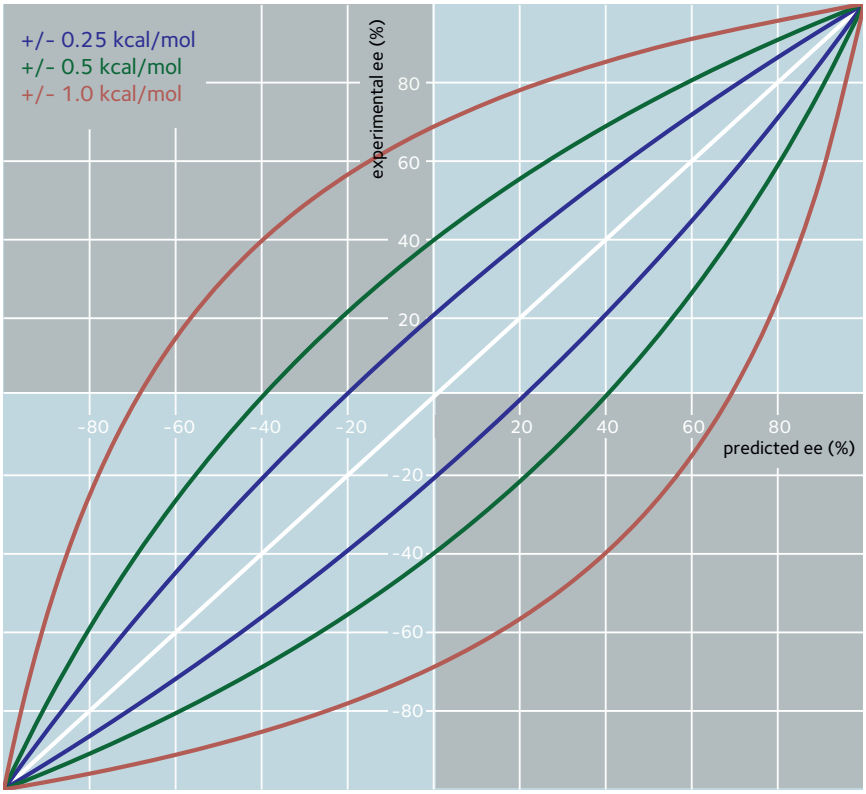

Figure 1-10 Enantiomeric excess error plot in predicted ee (kcal/mol) at different levels of enantioselectivity.

Enantiomeric enrichment arises from the difference in the rate of irreversible stereodetermining steps of competing pathways involving diastereomeric transition state structures ($\Delta\Delta G^{\ddagger}$ in **Figure 1-11**). The subtle energy difference between competing diastereomeric transition states means that an error of 3 kcal/mol in calculations translates to predicting a racemic product or a perfect selectivity of 99% ee at rt. In conformationally flexible catalysts, the energy changes due to the change in conformation alone could overwhelm the actual energy difference underlying the stereoselectivity.[38] This emphasises the necessity in thorough and comprehensive conformational sampling of the transition structures.

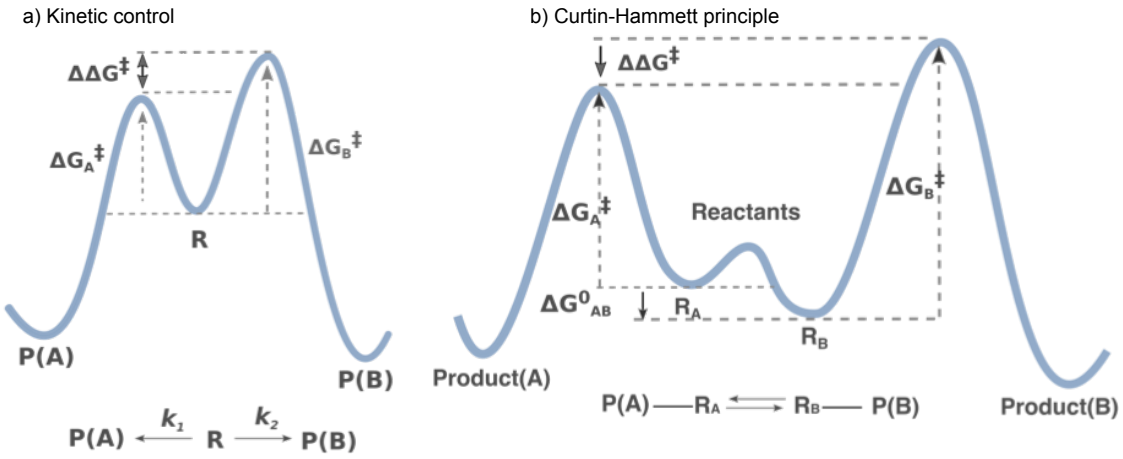

Figure 1-11 Schematic energy profile under a) Kinetic control and b) Curtin-Hammett regime where A and B are diastereomeric complexes between a chiral ligand and each enantiomer of reactants and products.

The benefit of modelling diastereomeric species using DFT is that (hopefully) calculations will benefit from systematic error cancellation. Recent mechanistic studies in asymmetric catalysis which led to better ligands was achieved by many, for examples, Anderson and Paton achieved enantio- and diastereoselective cycloisomerisation in a combined experimental and computational pursuit.[39] This reaction was successfully catalysed by rhodium and Feringa's ligand (96%, 98% ee) and was further improved to 99.9% ee. The improvement of the ligand selectivity owed to the recognition of Rh-arene interaction at the transition states in an unexpected pathway discovered by DFT calculations. (**Figure 1-12a**).

In 2014, Houk and Schafmeister designed a theozyme based on a spiroligozyme (spirol bicyclic macromolecule derived from bis-aminoacids) for aromatic Claisen rearrangement of substituted coumarins (**Figure 1-12b**).[40] With the knowledge of the key two-point hydrogen bonding interaction mimicking ketosteriod isomerase's active site, the most active catalyst was predicted to have the highest rate compared to the uncatalysed reaction, which was synthetically proven. The theozyme even contains carboxylic acids and phenols which were considered unusual functional

features of organocatalysis for Claisen rearrangements at that time. This is a nice example of the deviation from the usual synthetic ideas in catalysts led by theoretical calculations.

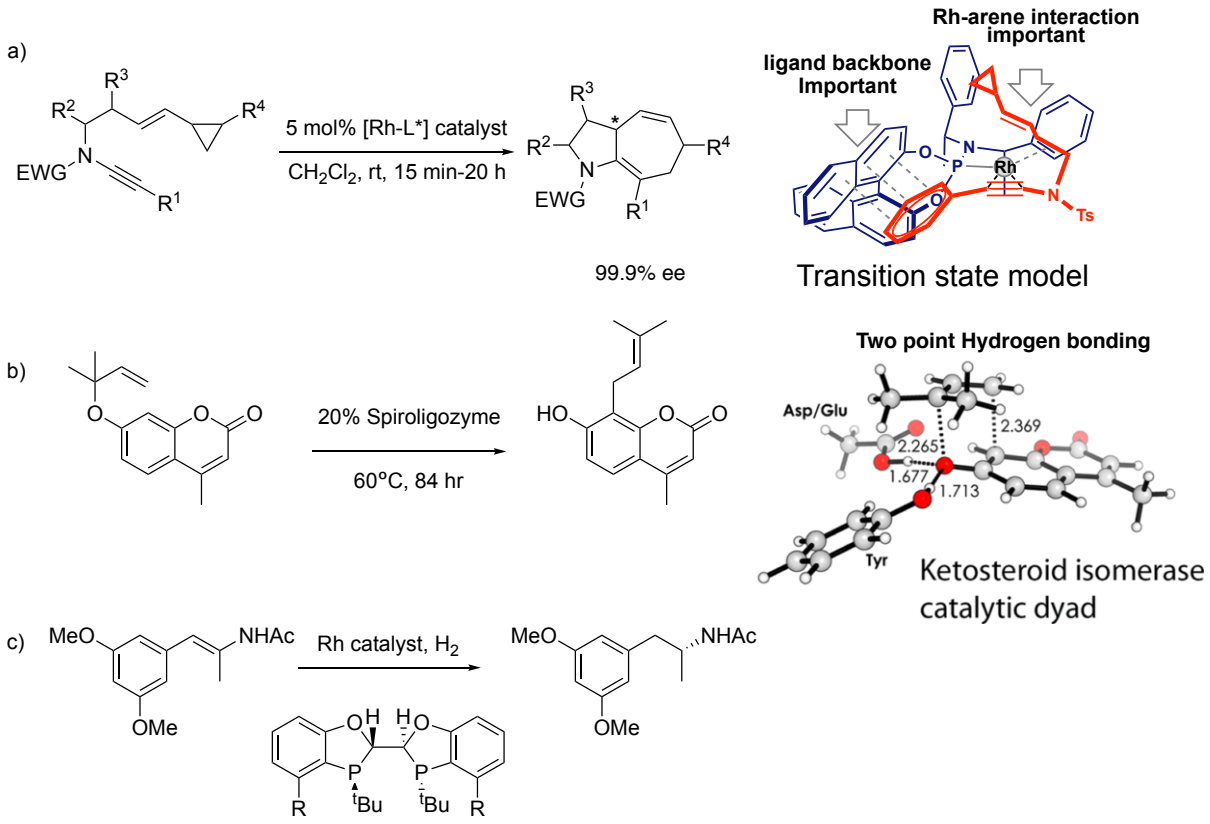

Figure 1-12 a) Asymmetric cycloisomerisation of ynamide b) Aromatic Claisen rearrangement of allyl coumarins and c) Rh catalysed hydrogenation optimised with AARON. Reprinted with permissions.[39,40]

In 2017, Wheeler reported an automated reaction optimiser for new catalysts (AARON) based on DFT screening which was applied to enantioselective rhodium catalysed asymmetric hydrogenation of enamines (**Figure 1-12c**).[41] This tool was invented for calculating ee of asymmetric reactions where the mechanism is established and many possible transition structures at the stereodetermining step exist. However, the errors of the predicted ee range from 0-23% ee, or 0-3.7 kcal/mol which are not insignificant. This needs to be improved before this method becomes broadly applicable.

In a large and flexible system, QM based methods are much too expensive for this purpose. One can make the assumption that only key functional groups and a certain portion of the chemical structure is relevant to enantioinduction and therefore simply truncate the real chemical systems to a smaller model system. This assumes that the model system behaves like the real system which requires further validation. Alternatively, a lower level of theory such as cheaper DFT funtionals or molecular mechanics (MM) can be used on parts of molecules deemed chemically less relevant, whereas the important portion is treated with QM. This hybrid treatment is called ONIOM or QM/MM methods. More details of these methods and their application can be found elsewhere.[42,43]

1.4.2.2 Force field approach

Norrby and Wiest have developed a transition state specific force field (TSFF) method for enantioselectivity prediction using molecular mechanics. The parameterisation of the force field (FF) is fitted based on QM data, thus the term quantum guided molecular mechanics (Q2MM).[44] The method has been successfully applied to various transition metal catalysed transformations such as rhodium catalysed hydrogenations to predict the enantioselectivity of new chiral ligands and reactants (**Figure 1-13**).[44,45]

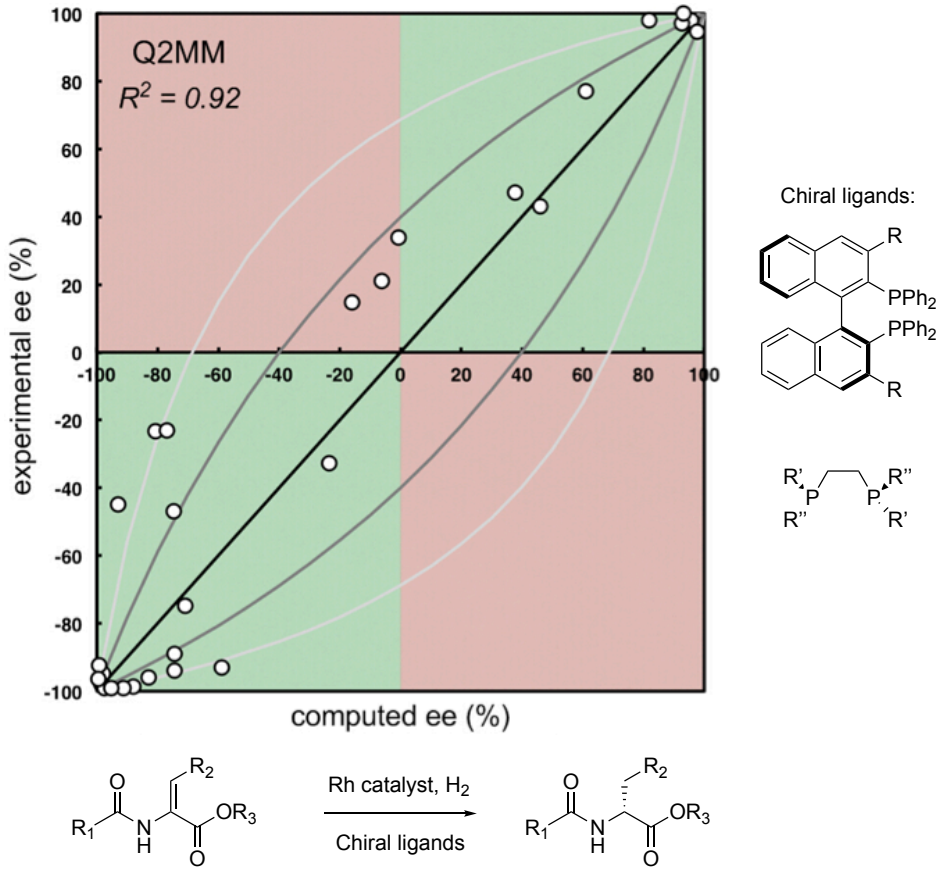

Figure 1-13 Q2MM calculation of ee in rhodium catalysed hydrogenation.[35]

The computational cost of sampling using Monte Carlo method (random sampling) of the transition structures are much reduced compared to QM level of theory. Q2MM allows for a fast prediction of enantioselectivity of new catalyst/substrate. However, much effort needs to be invested in development of the FF itself. Once the FF is developed, it is reaction specific, so new FF needs to be developed every time for a new reaction.

1.4.3 Quantitative-structure-selectivity relationship (QSSR)

Quantitative structure-activity relationship (QSAR) have been used by biologists and medicinal chemists for more than six decades.[46] Unlike a traditional ligand screening approach where only a small portion of data offers insightful information, this tool exploits all data collected (both positive and negative results) with the aim

to predict behaviour of compounds of interest. Linear free energy relationships have been used by organic chemists since 1930s following the pioneering work from Hammett.[47,48] QSAR operates on the same fundamental assumption that a relationship between features and properties of chemical compounds or reaction conditions and biological activities exists. In the context of asymmetric catalysis, we relate more to enantioselectivity, thus the quantitative structure-selectivity relationship (QSSR). This also bears a fundamental assumption that relationships between ligands/catalyst/substrates/chiral additive structures, hence their properties, and the resultant enantio/diastereoselectivity of the reaction exists. Model creation only requires a set of input data without any requirement of the mechanistic understanding. We can essentially treat a system as a black box problem where knowledge about the relationship is not required before hand. We intend to make use of QSSR as a tool to faciliate our research.

1.4.3.1 QSAR best practices

Comprehensive guidelines to construct QSAR models starting from data collection to model interpretation can be found in these dedicated publications; Tropsha summarised a rigorous protocol for QSAR practices.[46] Dearden, Cronin and Kaiser published a critical review on QSAR model construction with a checklist of errors to be aware of, supported by case studies.[49], Sigman has recently published a review on multivariate linear regression (MLR) for reaction development[50], and finally, detailed terminologies, definitions and practices regarding QSAR models and case studies can be found in Organisation for Economic Co-operation and Development (OECD) guidelines.[51]

Distilled from the literature, we summarise the most widely accepted QSAR practises in a flowchart displayed below (**Figure 1-14**).

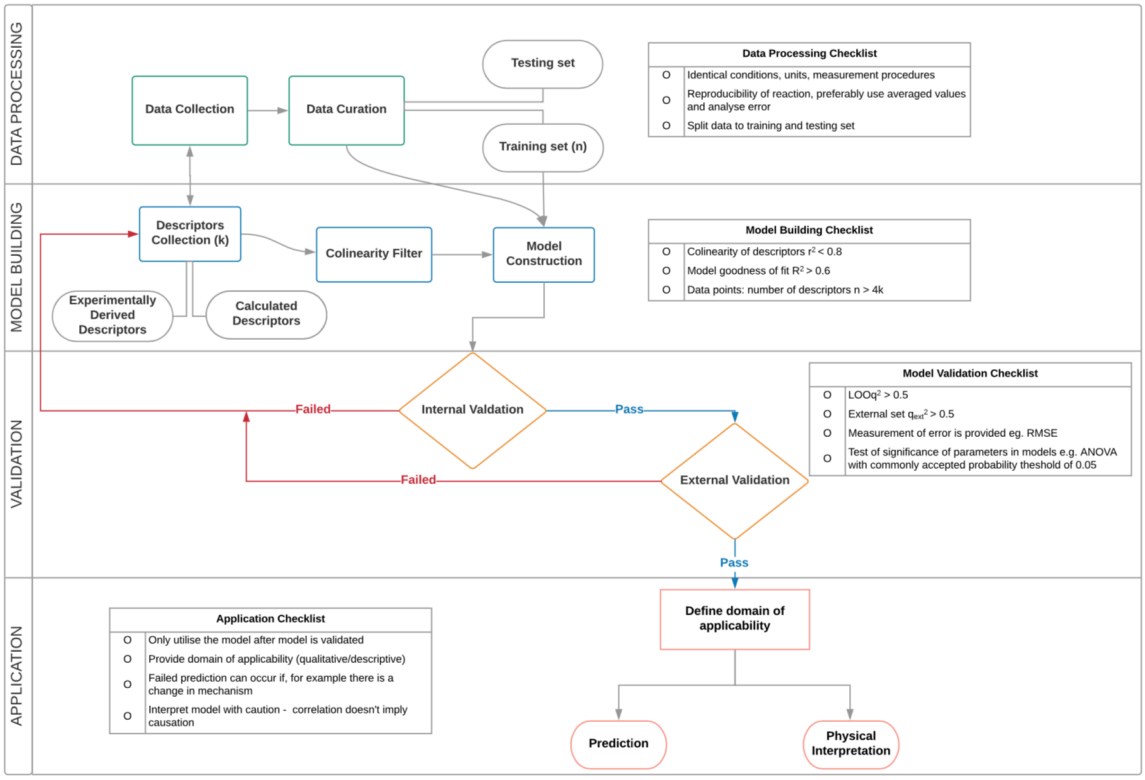

Figure 1-14 Flowchart and checklist for QSSR model construction and application.

The process can be divided into 4 stages starting with data collection and processing, model building, model validation (which is intertwined with model building in a feedback loop), and application. In each step on the flowchart above, requirements and generally accepted criteria are summarised in a form of checklist boxes. For examples, in the first step of data processing, it is crucial that all the data are homogenous, i.e. have identical units and collected in identical manner to avoid any random artefacts incurred during data collection. In addition, repeats are important to show that the data is reproducible and to minimise random error. Moving forward to model construction, data (dependent parameter, Y_i) is split into training (used in model construction) and testing (to validate the model) sets.

Chemical descriptors for the training data are collected and most relevant are selected during model construction. The models are then validated prior to application. If they fail validation, new descriptors needs to be collected and/or new forms of models needs to be generated. Only models that pass external validation can be used to predict or have any physical meaning drawn from them. Details for each step are discussed below.

1.4.3.1.1 Collecting descriptors

A crucial part of QSSR model building is collecting or generating the physiochemical descriptors (independent parameters, X_i which describes the chiral ligands/catalyst/substrates/additive structures). These parameters can be obtained empirically or by calculations. Data curation is required for treatment of empirical data in similar manner to the dependent parameters (Y_i). Numerous sources of physiochemical descriptors are available in the literature such as empirical and computed steric parameters; (A parameters,[52] B parameters,[53] Charton parameters,[54,55] Taft parameters[56]) Veerloop's Sterimol parameters,[57] Bo's three dimensional descriptors,[58] Electronic parameters; Hammett parameters, Charges, orbital energies, and other parameters such as spectroscopic parameters (IR frequencies, NMR shielding tensors, etc.) and descriptors developed especially for P donors ligands such as Tolman's angles.[59–61] Further treatment of these data by standardisation is sometimes practised (**Equation 1-2**). This transforms the raw data to dimensionless data with mean = 0 and standard deviation (SD) = 1.

Equation 1-2:

$$x = \frac{x_i - \bar{x}}{s}$$

Where $\bar{x} = \frac{1}{n}\sum_{i=1}^{n} x_i$ (sample mean), n = number of data points,

$$s = \sqrt{\frac{1}{n-1}\sum_{i=1}^{n}(x_i - \bar{x})^2}$$ (sample standard deviation of x).

It is recommended that any co-linearity among parameters should be avoided or used with caution in multivariate linear regression (MLR). There are no hard criteria on correlation limits but $r^2 > 0.8$ is highly discouraged.[49]

1.4.3.1.2 Model construction

Two main questions in model construction are; which type of the regression to be used and which descriptors to include in the final model. Some studies suggested that choices of chemical descriptors affect the prediction performance of QSAR models to greater extent than choices of model optimisation techniques.[46] Both of the questions will be discussed in detail below.

Types of regression

Regression is a study of relationships. There are many types of regression used in QSAR studies. In here we focus on types of regressions which have been applied to asymmetric catalysis. A list of merits and drawbacks of each method are presented.

1. Ordinary least squares regression (OLS)

This type of regression has been most commonly used in asymmetric catalysis. For models with only one independent parameter, it is called univariate linear (or non-linear) regression. A model that contains multiple independent parameters is called multiple least square regression. This can take linear or non-linear form. The linear form is termed multivariate linear regression (MLR).

✓ most transparent

✓ easily reproducible

✗ not suitable for confounded parameters (highly correlated parameters)

2. Partial least squares regression (PLS)

PLS is similar to OLS but the independent parameters are treated with principle component analysis (PCA). PCA reduces the number of descriptors by applying linear combination to sets of parameters. This reduces dimensions of the model.

✓deal with larger data with many variables.

✗ can be hard to interpret model and identify outliers

When large data set is available, machine learning algorithms such as K-nearest neighbour can be used to generate QSSR models but so far, there has generally not been enough experimental data generated in asymmetric catalysis experiments to meet the requirement to train the algorithm, unlike in QSAR studies.

Selecting parameters

Most commonly used in QSSR is MLR. PCA and PLS are used more in QSAR.[58] In MLR, automated parameters selection algorithms can be found in various sources including an open access platform in *R*.[62] Forward selection starts with an empty model or an initial model. Then parameters are included one parameter at time to improve the model based on a set criteria to determine quality of the model, such as adjusted coefficient of determination (R^2_{adj}), or Akaike information criterion (AIC), or significance (P-value) until the model cannot be further improved. On the other

hand, backward elimination starts with a full model with all parameters included and eliminates one parameter at a time.

1.4.3.1.3 Evaluation of fit, robustness for MLR

MLR has been most often used in asymmetric catalysis. The following guidelines and criteria are collected from the literature regarding MLR.[49,51,63,64] Notably, criteria are somewhat varied among different experts and no consensus has been entirely agreed. Nevertheless, it is useful for any researchers that are interested in QSSR to be aware of these standard practices and criteria.

Evaluation of fit and over-fit

Most common statistical treatment to measure goodness of fit of MLR is correlation coefficient, R^2 (**Equation 1-3**). If $R^2 > 0.5$, this means the explained variance is greater than unexplained variance. The acceptable value is up to user's judgement. Recommended values by Tropsha is $R^2 > 0.6$.[63]

Equation 1-3

$$R^2 = 1.0 - \frac{\sum_{i=1}^{n}(Y_i - \hat{Y}_i)^2}{\sum_{i=1}^{n}(Y_i - \bar{Y})^2}$$

Where $Y_i, \hat{Y}_i, \bar{Y}$= measured, predicted and averaged dependent variable, n = number of data points

Over-fitting is a phenomenon where too many parameters (k) are used, this leads to models with better fit but reduced predictive ability because models also account for random errors specific to the training set.[65] Adjusted correlation coefficient R^2_{adj} (**Equation 1-4**) penalises the use of additional parameters so over-fitted model can be better captured.[51]

Equation 1-4

$$R^2_{adj} = 1.0 - \frac{\sum_{i=1}^{n}(Y_i - \hat{Y}_i)^2/(n-k-1)}{\sum_{i=1}^{n}(Y_i - \bar{Y})^2/(n-1)}$$

Where $Y_i, \hat{Y}_i, \bar{Y}$= measured, predicted and averaged dependent variable, n = number of data points, k = number of independent variables in the model.

Another 'rule of thumb' is that the amount of data points (n) must be 4 times larger than the number of parameters (k) : n > 4k[63] or n > 3k[66] etc.

1.4.3.1.4 Model validation

Evaluation of significance is needed in any statistic model in order to estimate how certain one can be between the true correlation and random occurrences. In *R*, when *lm* function is used, it also runs a significant test which gives probability (p-value) as an output for each independent parameter included in the model. P-value lower than a specified level of significance justifies the rejection of the null hypothesis that the linear correlation occurred by chance. A commonly accepted significance threshold (α) is 0.05.

Analysis of variance (ANOVA), particularly the T-test and the F-test are also commonly used. The null hypothesis is that the coefficients of each of the parameters within the model are equal to zero. So if the statistic is *larger* than the set criteria i.e. for a T-Test at threshold of 0.05 at specified degree of freedom, we can reject the null hypothesis and therefore say that the parameters or the model show statistically significant correlation with the confidence level of 95%.[67]

Once models are generated and filtered to only a small number that have a good fit, not over-fit, and are statistically significant, the next step is to validate the models. This can be divided into internal and external validation. These internal validations

are now considered necessary but not sufficient.[64] It is considered necessary that external validation be carried out prior to application of the model.

Internal validation

Variety of internal validation methods are available.[63] Leave-one-out (LOOCV) or leave-many-out cross-validation (LMOCV) are among the most used in asymmetric catalysis QSSR. In LMOCV or LOOCV, a number (M) or one (O) data point are left out as a test set and the rest of the data is used as a training set. The measure of fit of the resultant models called a predictive squared correlation coefficient, q^2 is calculated (**Equation 1-5**). Because there are many possible ways to split the data when M>1, fixed iterations of LMOCV are commonly used within affordable computational time required. As a consequence, not all the possible combinations of data splitting is evaluated. This means the q^2 from non-exhaustive LMOCV may not be the same for different observers depending on how the data is split. This is not a problem for LOOCV. The recommended value for LOOCV q^2 is 0.6.[63] There are many other methods for QSSR validation such as Bootstrapping[68] and Y randomisation[69].

Equation 1-5

$$q^2 = 1.0 - \frac{\sum_{i=1}^{n}(Y_i - \hat{Y}_i)^2}{\sum_{i=1}^{n}(Y_i - \bar{Y}_{tr})^2}$$

Where Y_i, $\hat{Y}_i$, $\bar{Y}_{tr}$= measured, predicted and averaged dependent variable, n = number of data points in the training set.

External validation

A set of data that has not been used to train the model is called the external testing set. It is highly recommended that the external testing set must be a fair representative of the whole range of both dependent and independent parameters.

The predictive power of a QSSR model can be quantified with predictive squared correlation coefficient, q^2_{ext} (**Equation 1-5**) with respect to $\bar{Y}$ from the testing data or, alternatively, the training set. However, the latter has been shown to give too optimistic values in some case studies.[70,71] The recommended criteria is $q^2_{ext} > 0.5$.[63]

Outliers

Outliers reflect error in measurements or actually indicate something interesting like competing side reactions or a change in mechanism. This is why it is crucial to make sure data is reproducible. Ways to quantify boundaries to identify outliers by statisticians are discussed elsewhere.[72] In QSSR, Sigman has calculated the degree of deviation to quantify the error of the extrapolation data and showed that it was within 10 - 20% error and thus argued that they are not outliers.[73] Lipnick recommended that outliers lie three or four standard deviations away from the mean of residual.[74]

1.4.3.1.5 Applicability domain (AD)

Like all models, regressions capture parts of reality. Therefore, all models are inherently *incorrect* but are likely to be useful within a certain limit. Models are highly dependent upon the inputs. They will breakdown if we try to predict unseen data that differ drastically from the input data. This is a common problem around extrapolation (prediction that falls outside the domain covered by the training data).

'Domain of applicability' or 'applicability domain' (AD) is a non-rigid limit between extrapolation and interpolation (prediction that falls within the domain covered by the training data). In practice, the line between performance of chemicals within AD

and outside is not a sharp one. The change in predictability of a model is a gradual rather than a sudden drop across AD. AD therefore acts as a guide which needs to be substantiated by expert judgement. AD helps define a quantitation limit (where predictions are not quantitative anymore), or define the domain of linearity of the model (outside this, it is not necessarily linear anymore). Defining an AD with QSSR should help the end-user of the model balance the validity of a predicted value. Some argue that defining an AD is in fact inappropriate because the utilisation of the model outside the AD isn't outright invalid, only less reliable. Furthermore, predictions of compounds within a model AD should still be treated with caution in certain cases.[75] AD therefore helps the end-user to be aware of the approximate limits of a model, between extrapolation and interpolation, and to make choices accordingly.

Simplest AD: Qualitative description of AD

One definition of AD is *"The applicability domain of a (Q)SAR model is the response and chemical structure space in which the model makes predictions with a given reliability."*[51] This means we can just outline the AD descriptively based on the training data set and the observed properties (dependent variables). For more rigorous evaluation of AD, i.e. quantitative AD can be found elsewhere.[51]

When a model disappoints…

Even when compounds appear to be within the AD, there is no guarantee that the prediction of such compounds will be reliable.[51] In QSAR, an activity landscape might contains 'cliffs' where a sudden change in activity is observed with subtle structural changes. In the presence of these activity cliffs, even interpolation can fail.

Arguably, activity landscape is much more complicated than energy landscape for asymmetric transformations with one or a few saddle points in an otherwise relatively flat landscape. An equivalence of the notorious activity cliffs seen in QSAR in QSSR is perhaps the change in mechanistic pathways which can be informative and potentially provide insight to alternative reaction pathways.

1.4.3.1.6 Model Utilisation

Utilisation of regression is categorised into two types: prediction and physical interpretation.[76] Often in QSAR, one trades a meaningful model for a highly predictive one. However, in QSSR for asymmetric catalysis, in some cases, applications of regression can lie in the sweet spot where the models have been illustrated to be both predictive and not too complicated which allows for meaningful interpretations.[77]

Chemists have used QSSR to aid the improvement of enantioselectivity only since the turn of the 21st century.[67,78–80] Since then, much work has been published from a few groups.[81–85] We select the most recent examples on the frontier of QS(A/S)R applied to asymmetric catalysis to discuss here.

1.4.3.2 Predicting enantioselectivity

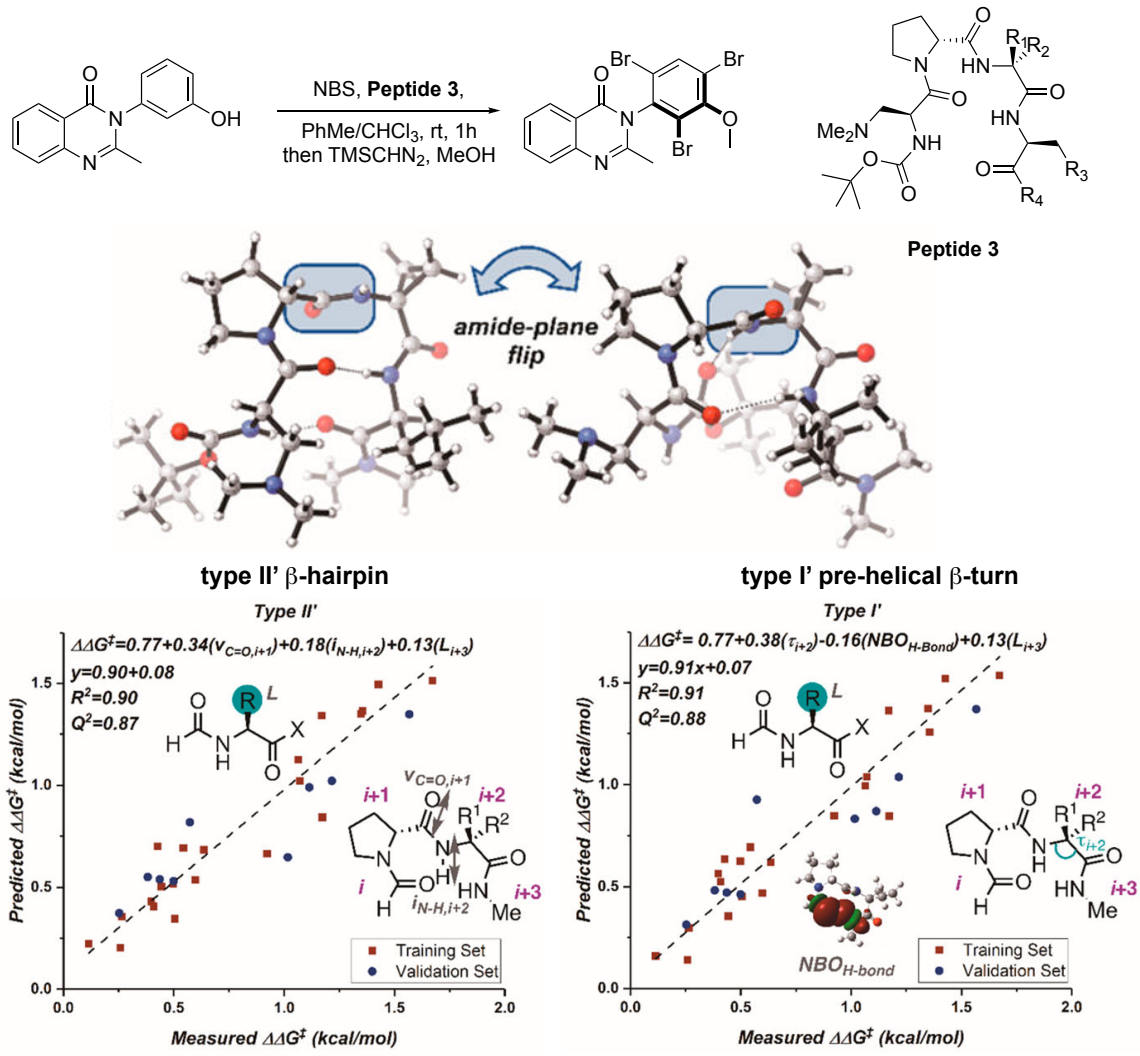

Figure 1-15 QSSR model for atroposelective bromination of arylquinazolinones using tetrapeptide catalyst. Reprinted with permission.[86]

Sigman is a pioneer in the reviving the use of QSSR in asymmetric organic transformations. He has published numerous examples of the use of regression assisted reaction optimisation and mechanistic elucidation.[79,87–89] In one of his most recent papers, an atroposelective bromination of arylquinazolinones using tetrapeptide catalyst, they discovered that the enantiomeric excess of the atrotopic products can be expressed in terms of calculated parameters: NBO charges, IR stretches, a multidimensional steric parameter called Sterimol L parameter (see **Figure 2-1** for the definitions of Sterimol parameters) and a crystallographically

derived parameter; main chain angles (**Figure 1-15**).[86] The QSSR models derived from different conformations of peptides suggest that the multiple conformers of the peptide β-turn contribute to the stereodetermining transition structures.

1.4.3.3 Predicting Yield

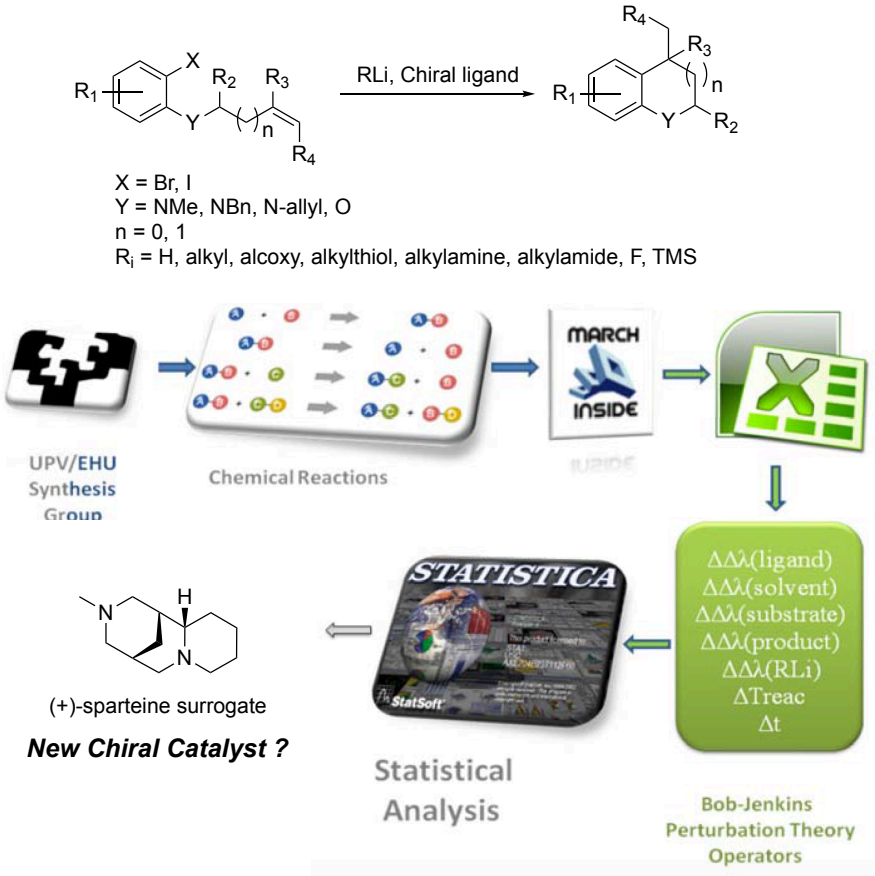

Figure 1-16 QSPR-perturbation theory of enantioselective intramolecular carbolithiations. Reprinted with permission [90]

Cordeiro and Gonzalez-Diaz have produced a QSPR-perturbation theory model to partially quantify the yield or enantioselectivity of intramolecular carbolithiations (**Figure 1-16**).[90] Their model was expressed in a complex function of multiple variables such as variation of chiral ligands, organolithiums and additives, solvents, and temperatures and time. Rather than giving prediction outcome that converts directly to % yield or % ee, the mode calculated perturbation of reaction outcome from the referenced state; $\lambda_{new} = \lambda_{reference}$ + perturbation functions. Where λ_i are

binary functions that takes value of 1 or -1 according to a preset cutoff value. For example, λ gives a value of 1 for a reaction yield greater than 95% and enantiomeric excess greater than 90%, otherwise λ takes value of -1. The authors show that the model works for a testing set. Some limitations in this model are that its prediction is binary and does not offer exact value of ee, and also a physical interpretation of such complex model is inhibited.

1.4.3.4 Predicting product distribution

Toste and Sigman have recently published a mechanistic investigation into Pd catalysed enantioselective diarylation of benzyl acrylates with chiral anion phase transfer catalyst (CAPT) (**Figure 1-17**).[88] The products of this reaction contain a stereogenic centre at the β-carbon. This competes with a by-product, which is a result of an unwanted Heck reaction. The QSSR was used to separately model enantioselectivity and product distribution. They found that product:Heck by-product ratio (P:H) correlates to steric properties of chiral phosphate catalyst. The P:H ratio was found to be positively correlated with Sterimol B_5 of substituent at C-6 position ($B5_6$) and a more subtle negatively correlated with Sterimol L parameter at C-4 position (L_4) of the catalyst. Further experiments showed that the phosphate catalyst can act as a base to aid formation of by-product. Therefore, the QSSR supports the finding that more sterically hindered phosphate slows down the formation of the by-product, hence decreasing the kinetically competing Heck by-product formation compared to the desirable arylation product.

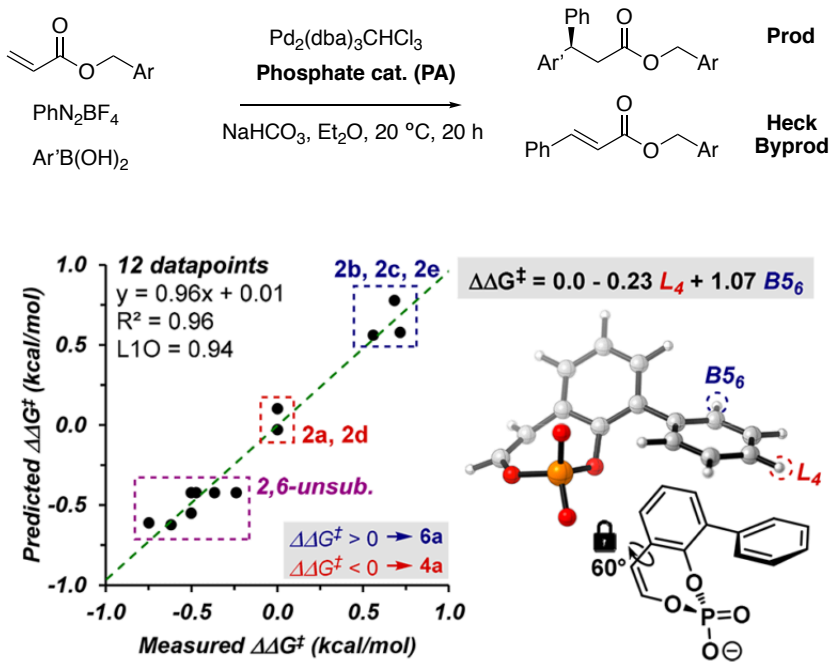

Figure 1-17 QSSR for Pd catalysed enantioselective diarylation of benzyl acrylates. Reprinted with permission.[88]

1.5 Project aims

To compliment the traditional strategy for ligand design, we aimed to execute a systematic combinatorial approach for chiral ligand discovery and optimisation. This approach started with experimental ligand screening, followed by QSSR model construction where we focused on producing the simplest predictive model based on computed physiochemical descriptors using a transparent model optimisation technique like a least square regression. The validated model could then be used for virtual screening prior to the experimental screening. The interpretation of the QSSR models was aided by DFT calculations to make sense of the correlation and search for factors responsible for enantioinduction. In principle, there is no restriction on the type of reaction this approach is applicable to. This approach could be applied to any asymmetric transformation of interest. In this thesis we presented three chemical systems. Each of them followed this strategy.

2 Experimental and computational exploration of asymmetric induction for copper catalysed conjugate addition with chiral phosphoramidite ligands

Materials present in this chapter have been published in 2017.*[91]*

2.1 Introduction

Conjugate additions to prochiral Michael acceptors are well studied in synthetic organic chemistry and are among the most common synthetic tools for the construction of C-C bonds.[92] The first asymmetric conjugate addition was developed in 1975 by Wynberg, and later on (in 1988) the first enantioselective copper catalysed conjugate addition by Lippard[93] with Grignard reagents. Since then, many other groups have developed efficient asymmetric conjugate addition (ACA) methods, especially with dialkylzinc species. Accordingly, a plethora of specific ACA reaction conditions have been developed. These often require highly customised conditions specific to the type of electrophile used,[94] for example, copper catalysed conjugate addition with diethylzinc and Grignard reagents (**Scheme 2-1**). The scheme illustrates that different electrophiles require different chiral ligand scaffolds (eg. with cyclohexenone, cycloheptenone, a linear enone and a macrocylic enone).

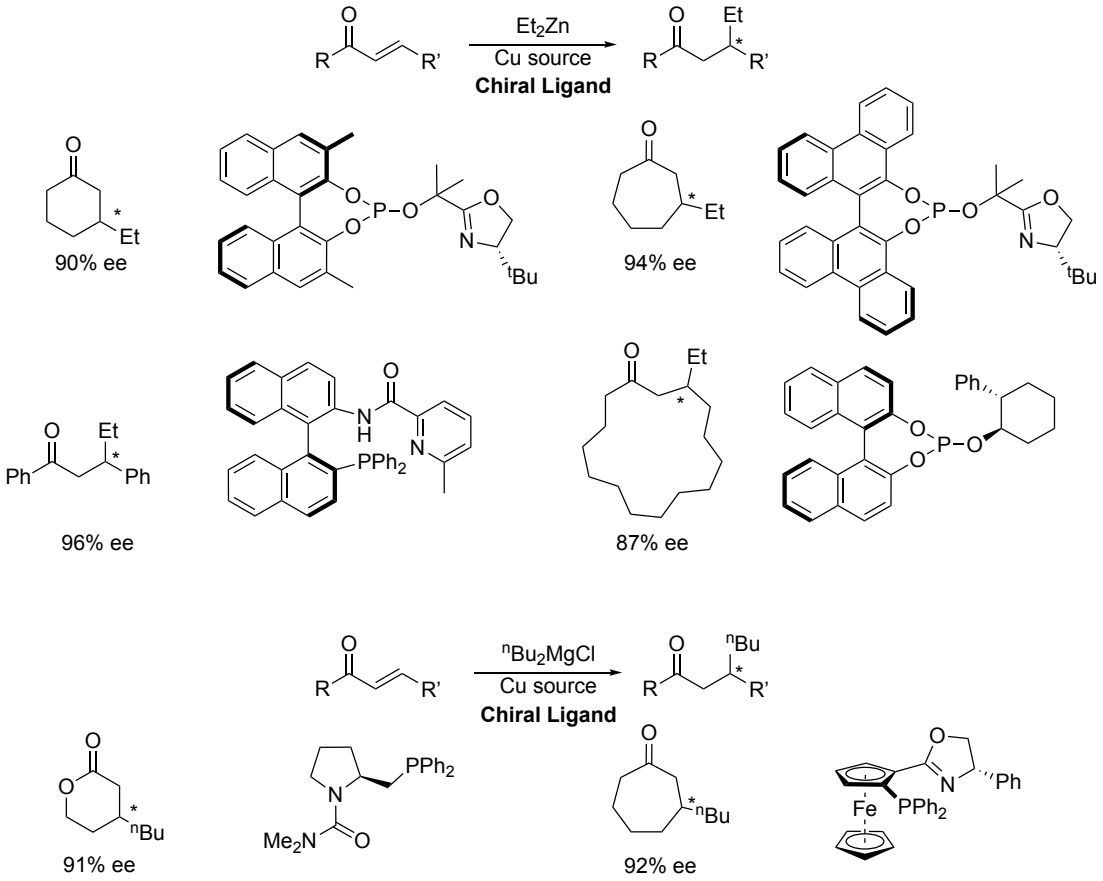

Scheme 2-1 Examples of Cu-catalysed ACA with different organometallic reagents, electrophiles and chiral ligands.[94]

Among the chiral ligands used, phosphoramidites were first used by Feringa[95,96] and Alexakis[97] in copper catalysed ACA, and have been shown to be very efficient at inducing high enantioselectivity for many substrates (**Scheme 2-2**).[98–100]

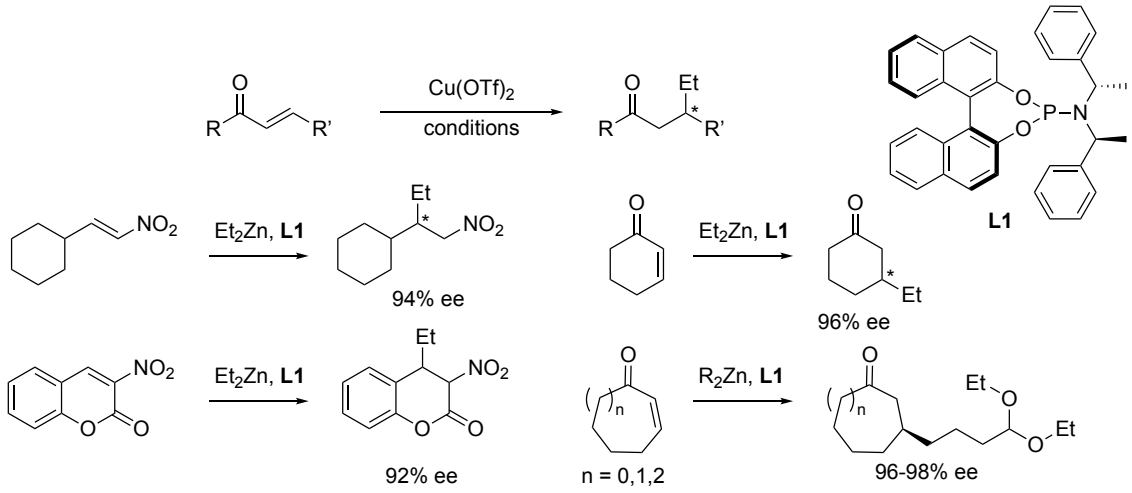

Scheme 2-2 Examples of Cu catalysed ACA with **L1**. [94]

We reported a copper catalysed asymmetric conjugate addition of alkylzirconium species to Michael acceptors such as acyclic and cyclic enones **Scheme 2-1**. [101–107] As shown in **Scheme 2-1** and **Scheme 2-3**, slightly different chiral ligands and/or catalysts are needed when the electrophile structure is altered.

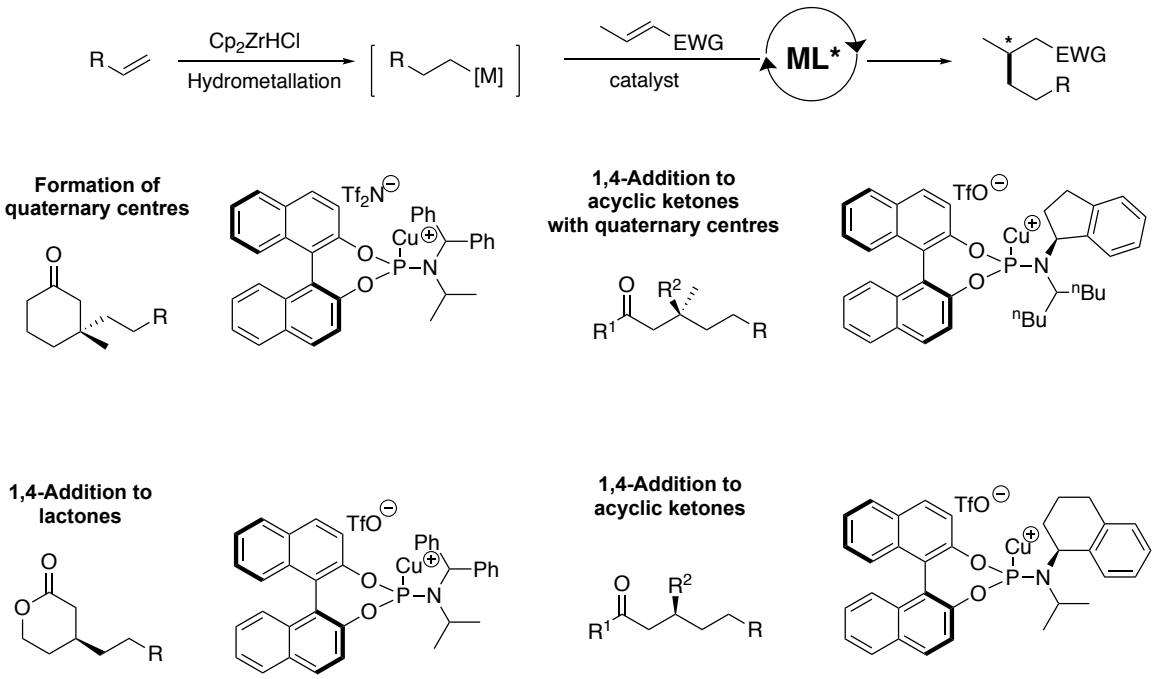

Scheme 2-3 Examples of Cu-catalysed conjugate addition with organozirconocene by the Fletcher group. [105–108]

The chiral phosphoramidite ligands are our ligands of choice. The ligands' modular structures enable quick synthetic variation of their structures, which in turn allows us to study the effect of the ligand structure on the enantioselectivity of the reaction.

For most cases, new catalytic systems need to be developed when the desired product is not in the scope of existing synthetic methods. The discovery of the appropriate chiral ligands is still a formidable task in asymmetric ACA. This is especially true for reactions where mechanistic data, particularly concerning the stereodetermining step, is unknown. The knowledge of the underlying factors that give rise to asymmetric induction is key to the rational design and improvement of

chiral catalysts. Relating to our system, the mechanism of copper catalysed ACA with Grignard reagents has been studied[109] but the mechanism of our reaction with alkylzirconocenes is still unclear.

Traditional approaches to the discovery and development of enantioselective catalytic reactions involve serendipity, chemical intuition, and systematic screening. To increase the information gained from the experimental ligand screening, we intend to use multiple tools to aid our development of new chiral ligands. We were inspired by the work done by Sigman on the analysis of an asymmetric reaction using a multidimensional parameter called Sterimol.[79] Sterimol was originally developed by Verloop for quantitative structure–activity relationships (QSAR) in medicinal chemistry.[57] These parameters provide a more detailed description of steric bulk of a substituent by capturing the spatial anisotropy of the substituent (**Figure 2-1**). There are up to 6 parameters in total for the two generations of the Sterimol parameters. The first generation of Sterimol parameters consists of L, B_1, B_2, B_3 and B_4 parameters. L is defined as the length of the substituent along the direction of its attachment to the rest of the molecule. B parameters are all perpendicular to L. The magnitudes of these vectors are in the following order: $B_1 \geq B_2 \geq B_3 \geq B_4$ where B_1 and B_2 are at 90° to B_3 and B_4. Because B_2, B_3, and B_4 are defined based on the vector B_1, this definition, even though was useful in many cases, can be ambiguous where multiple vectors satisfy the condition mentioned above for B_1 i.e. any vector along an arc of a circle, which means B_2-B_4 can be different depending on which vector is selected as B_1. Consequently, the second generation of Sterimol parameter was developed. It consists of 3 parameters: L, B_1

and B_5. L and B_1 are defined as above. B_5 is defined as the longest parameter perpendicular to L.

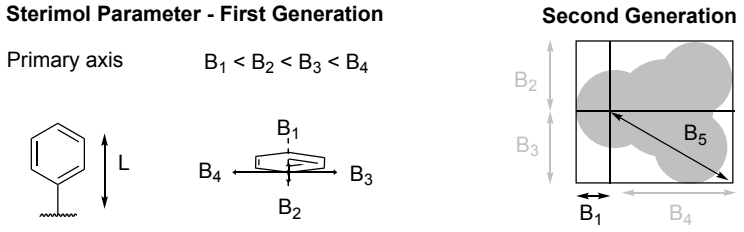

Figure 2-1 Sterimol parameters: the first (L, B_1-B_4) and the second generation (L, B_1 and B_5).

The use of Sterimol parameters in understanding asymmetric synthesis has been shown to provide mechanistic insight into key elements of asymmetric induction.[57] Only in the past decade, Sigman[79,110] and others[81,82,111] have applied Sterimol parameters as steric descriptors for quantitative structure-selectivity relationships (QSSR) and applied the approach to the study of enantioselectivity in catalytic asymmetric reactions (see section 1.4.3.2).

2.1.1 Project aim

Despite the value of phosphoramidites as privileged ligands, to our knowledge, no one has identified the enantiocontrolling factors for phosphoramidite ligands in copper catalysed ACA.[109,112,113]

Our aim was to elucidate the important interactions that govern the enantioselectivity of ACA products induced by chiral phosphoramidite ligands. To achieve this, we used a combination of quantitative analysis of the effects of ligand-structural variation on the resulting enantioselectivity, spectroscopic study of the metal-ligand complexes, and DFT calculations.

2.2 Results and discussion

2.2.1 Experimental Ligand screening

All the experiments regarding ligand screening and reaction optimisation were carried out by Philippe Roth and Rebecca Maksymowicz.

2.2.1.1 Screening reaction conditions

For the purpose of chiral ligand screening, a model reaction was selected from an established method published earlier by us; a conjugate addition to a cyclohexenone.[102] The reaction starts with *in situ* generation of an alkylzirconocene nucleophile, from a reaction of a terminal alkene and Schwartz reagent (Cp_2ZrHCl).[114,115] In a separate flask, a catalytic copper source and a chiral ligand were stirred at rt to form a Cu-ligand complex. The Cu-ligand complex suspension was then transferred using a syringe filter into the preformed nucleophile solution, followed by an addition of the enone. We found that two reaction conditions gave approximately the same results; using $(CuOTf)_2$·PhH complex or CuOTf (produced *in situ* from CuCl and AgOTf) as a copper source (**Scheme 2-4**). Both of these conditions were reproducible, giving repeats within ±2% ee and were exclusively used for all of the ligand screening experiments.

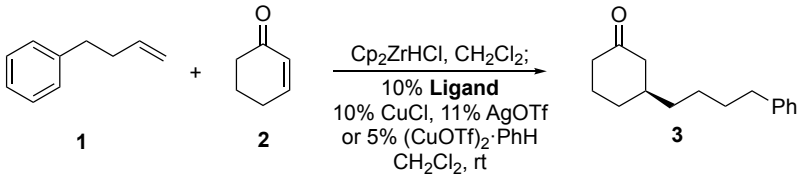

Scheme 2-4 Ligand screening conditions.

2.2.1.2 Ligand screening results

Variation of backbone

We started by exploring different chiral backbones while maintaining the bis-1-(phenylethyl)amine moiety (**Figure 2-2**). Under these conditions, commercially available Feringa's ligand (**L1**) already gave 80% ee. The stereochemistry of the amine did not strongly affect the level of enatioselectivity (74% ee in *(S,R,R)*-**L1** vs 80% ee in *(S,S,S)*-**L1**). The catechol and biphenyl backbone performed poorly (17-25% ee, **L2** and **L3**). The spirobiindanediol backbone, a partially reduced BINOL, and 7,7'-dibromo BINOL gave moderate ee (64-68% ee, **L4**-**L6**). A derivative of the binaphthyl backbone gave relatively lower ee than BINOL (74% ee, **L7**). All three of the 3,3'-disubstituted BINOLs did not give higher ee (28-65% ee, **L8**-**L10**).

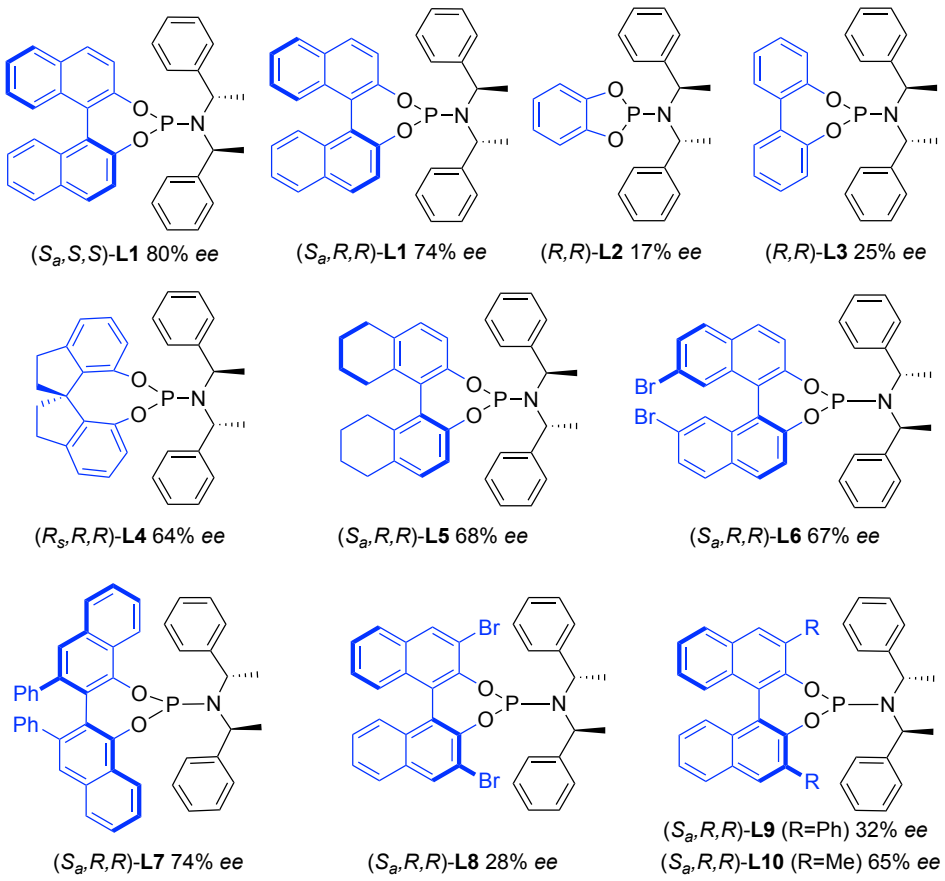

Figure 2-2 Enantiomeric excess (%) of product **3** as a result of varying ligand's backbone. Reported ee was determined by HPLC using a chiral non-racemic stationary phase of the crude reaction mixture.

Variation of amido substituents

Next we examined the effects of the amido substituent on the level of observed enantioselectivity (**Table 2-1**). We ranked the substituents on the amido part based on their steric bulk. The larger substituent on N atom was split into two parts; R_1 and R_2 at the α-carbon where R_1 is larger than R_2, and R_3 denotes the other smaller substituent on the N-atom. In every case examined with BINOL based backbones, the absolute stereochemistry of the product was solely determined by the stereochemistry on the BINOL backbone rather than the stereochemistry of the amido substituents. For ligands containing *(S)*-BINOL, ee's are reported as positive values and with *(R)*-BINOL, they are reported as negative values.

For ligands with simple alkyl substituents on the amine, ee increased with the size of substituents to a maximum point and then decreased (17-56% ee, **L11**-**L15**). **L16**-**L18** are derivatives of **L1**, and did not perform as well (43-76% ee). Bicyclic and tricyclic amido substituents gave a maximum ee of 76% (**L19**-**L23**). We then retained one amido substituent as a chiral moiety where R_1 = 2-naphthyl and R_2 = methyl and only varied R_3 (**L24**-**L32**). Again we observed a general trend that an increase in the size of the substituent R_3 increases the ee up to an optimal point before ee starts to decrease with the increase in the steric bulk of R_3 (15-73% for **L24**-**L27** and 70% down to 5% for **L28** to **L30**). When R_3 was benzyl or a phenyl, the observed ee's were low (38% and 17%, **L31** and **L32**). When we changed the substituent pattern of R_1 from 2-naphthyl to 1-naphthyl while keeping the rest of the ligand unmodified (compare **L24** to **L33** and **L26** to **L34**), we either observed no change or a reduction in ee (15% ee for both **L24** and **L33**, or 49% ee for **L34** vs 68% ee for **L26**). This suggests that the effects of the substituents are not

independent from each other, which in other words, meant that they are not additive.

Table 2-1 Enantiomeric excess (%) of product **3** as a result of varying the ligand's amido substituents. Reported ee was determined by HPLC using a chiral non-racemic stationary phase of the crude reaction mixture.

Variation of amido substituents

Alkyl substituents

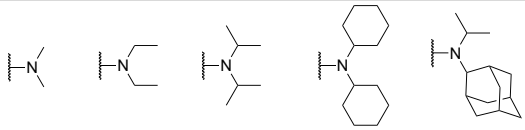

L11 -17% *ee* **L12** 7% *ee* **L13** -59% *ee* **L14** -56% *ee* **L15** -17% *ee*

Ligands similar to L1

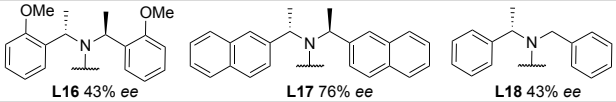

L16 43% *ee* **L17** 76% *ee* **L18** 43% *ee*

Bicyclic and tricyclic substituents

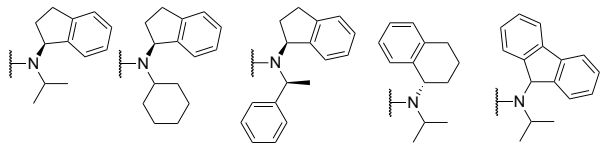

L19 75% *ee* **L20** 72% *ee* **L21** 76% *ee* **L22** 67% *ee* **L23** -53% *ee*

Achiral substituents

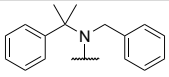

L44 -55% *ee*

Ligand	Ligand substituents R1	R2	R3	ee (%)
L45	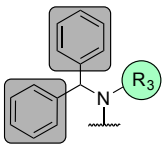		Isopropyl	78
L46			Cyclopentyl	78
L47			Cyclohexyl	86
L48	R_1, R_2 = Phenyl		Cyclooctyl	77

Ligand	Ligand substituents R1	R2	R3	ee (%)
Variation of single N substituent (R_3)				
L24[b]	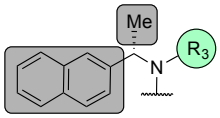		Methyl	15
L25[b]			Ethyl	26
L26[b]			Isopropyl	68
L27[b]			Cyclohexyl	73
L28[b]			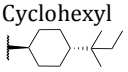	70
L29[b]			Cycloheptyl	48
L30[b]	R_1 = 2-Naphthyl, R_2 = Methyl		Adamantyl	5
L31[b]			Benzyl	38
L32[b]			Phenyl	17
L33[b]	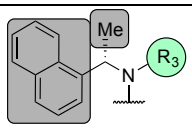		Methyl	15
L34[b]	R_1 =1-Naphthyl, R_2 = Methyl		Isopropyl	49
Variation of aromatic substituent (R_1)				
L35[b]	Phenyl			51
L36[b]	4-Me-C_6H_4			64
L37[b]	4-FC_6H_4			60
L38[b]	4-Cl-C_6H_4			67
L39[b]	3-Cl-C_6H_4	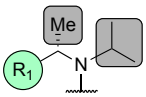		65
L40[a,c]	3-Br-C_6H_4	R_2 = Methyl, R_3 = Isopropyl		-67
L41[b]	4-MeO-C_6H_4			72
L42[b]	3-MeO-C_6H_4			69
L43[b]	2-MeO-C_6H_4			66

[a]Ligands bearing (*R*)-BINOL, otherwise (*S*)-BINOL, [b](*S*)-Amine, [c](*R*)-Amine.

On the other hand, when the aryl moiety R_1 was varied while R_2 and R_3 were fixed as a methyl and isopropyl group respectively, their influence on ee was subtle (51-72% ee, **L35-L43**). Among a variety of substituted aryls, the phenyl ring gave the worst ee of 51% (**L35**). *Para*-methyl, halides and methoxy substituents all increased the ee by 10% to 20%. From these results, it is hard to draw any conclusions about the electronic effects on the ee for these sets of ligands. With chloro and methoxy

substituents, the change in substituent pattern also caused slight but measurable changes in the ee, where *para*-, *meta*- and *ortho*- substituents induced slightly lower ee in that order (Cl: 67, 65% ee, **L38**, **L39** and OMe: 72, 69, 66 % ee, **L41**-**L43**).

Pleasingly, when achiral amines are used, we are able to achieve good enantioselectivity of up to 86% ee, **L24**-**L28**). However, only one ligand was more selective than **L1** (86% ee, **L47**). Notably, **L45** gave a comparable ee to its structural isomer, **L1** (78% ee, **L45** vs 80% ee, **L1**). This opens up an opportunity for a new class of ligands with an achiral amido moiety. Using ligands with achiral amido part reduces complications that may arise from asymmetric synthesis of amines and the separation of diastereomers during the final step of ligand synthesis.

2.2.1.3 Achiral amido ligand testing set

Following up from the lead achiral amido moiety, a set of ligands where R_1 = R_2 = aryl rings were synthesised and tested (**Figure 2-3**). Compared to phenyl, the substituted phenyl rings all gave worse ee (up to 70% ee, **L49**-**L54**, compared to 78% ee, **L45**). Ligands bearing electron-withdrawing groups performed particularly poorly (55% ee and 20% ee, **L53** and **L54**). For ligands with R_3 = isopropyl, the ligand bearing 2-naphthyl rings gave comparable ee to the ligand bearing phenyl rings (76% ee, **L55** vs 78% ee, **L45**). A ligand with 1-naphthyl rings gave the best ee out of this set of ligands (85% ee, **L56**). When we kept the aryl moiety as 1-naphthyl but changed R_3 to another secondary alkyl, a cyclohexyl, this slightly reduced the ee (80% ee, **L57**). This data was used as an external testing set for model I represented as blue data points (**Figure 2-4**).

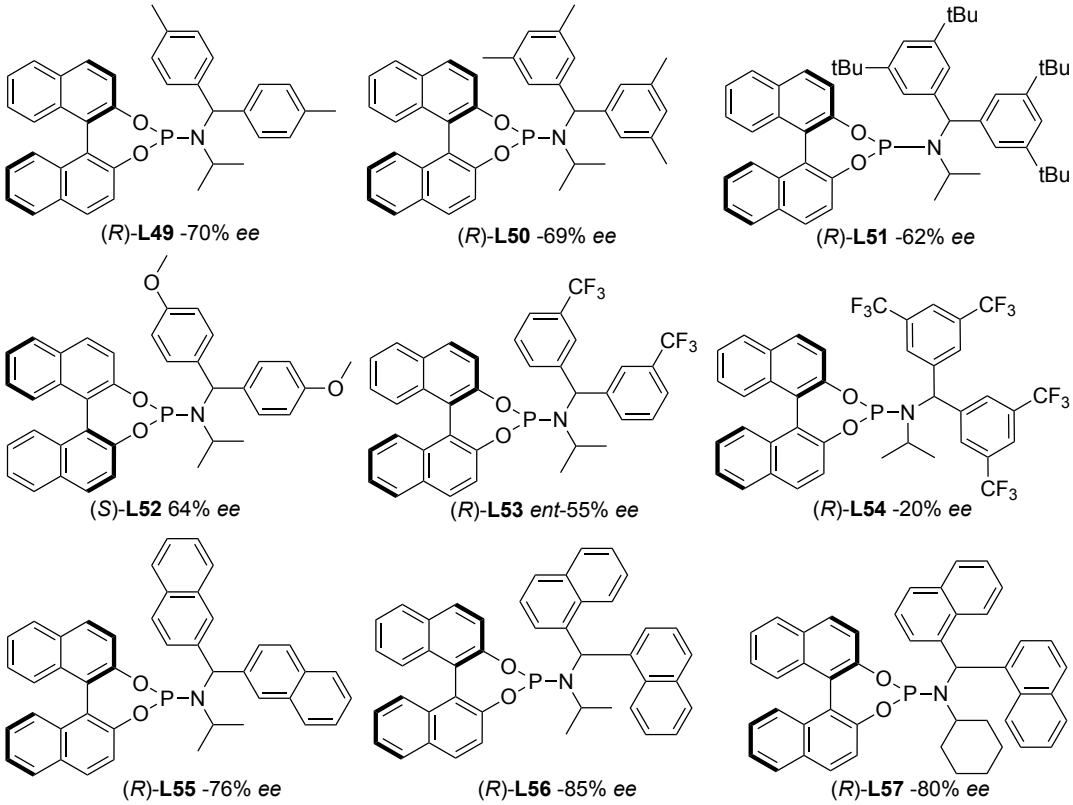

Figure 2-3 Enantiomeric excess (%) of product **3** as a result of varying ligand's amido moiety. Reported ee was determined by HPLC using a chiral non-racemic stationary phase of the crude reaction mixture

2.2.2 Combinatorial studies for enantioinduction: QSSR models and DFT studies

2.2.2.1 QSSR model I – first preliminary steric model

With the current information from ligand screening, we aimed to gain extra information by generating statistical models relating experimental selectivity with ligand structures. We started with a linear model where we only considered ligands with an isopropyl group as one of the substituents at the N-atom (R_3 = ^{i}Pr).

The models were created using an open access R-statistics package.[62] The parameters considered are the second generation Sterimol parameters (L, B_1 and B_5), and the distance from the closest carbon atom to the Cu-center in the structure of the optimized Cu:phosphoramidite complex to quantify the metal-arene

interaction (See **Table 2-3**). We envisaged that this Cu—C distance would be suitable for the model, since it would capture any interaction with the metal centre. However, this did not give a good correlation with the observed enantioselectivity.

After manual selection of the parameters for the model based on the correlation coefficient (R^2), we found that only two steric parameters; Sterimol L parameter for R_1 and R_2 substituents gave a degree of correlation (for the definition of Sterimol parameters, see **Figure 2-1**). A two-dimensional scatter plot showing the experimental ee on the y-axis and the calculated ee on the x-axis is shown in **Figure 2-4**: $\Delta\Delta G^{\ddagger}$pred (kJ/mol) = 4.36 + 0.25 L_{R1} + 0.91 L_{R2}. The model has a poor fit, R^2 = 0.48 (black data points. n = 13) with a root-mean-squared error (RMSE) of 0.46 kJ/mol. Statistical significance of the parameters and the models are tested based on F-statistics. The L_{R1} parameter is not statistically significant at 5% level of confidence whereas L_{R2} is. Other steric parameters such as Sterimol B_1 and B_5 parameters gave models with a much worse fit.

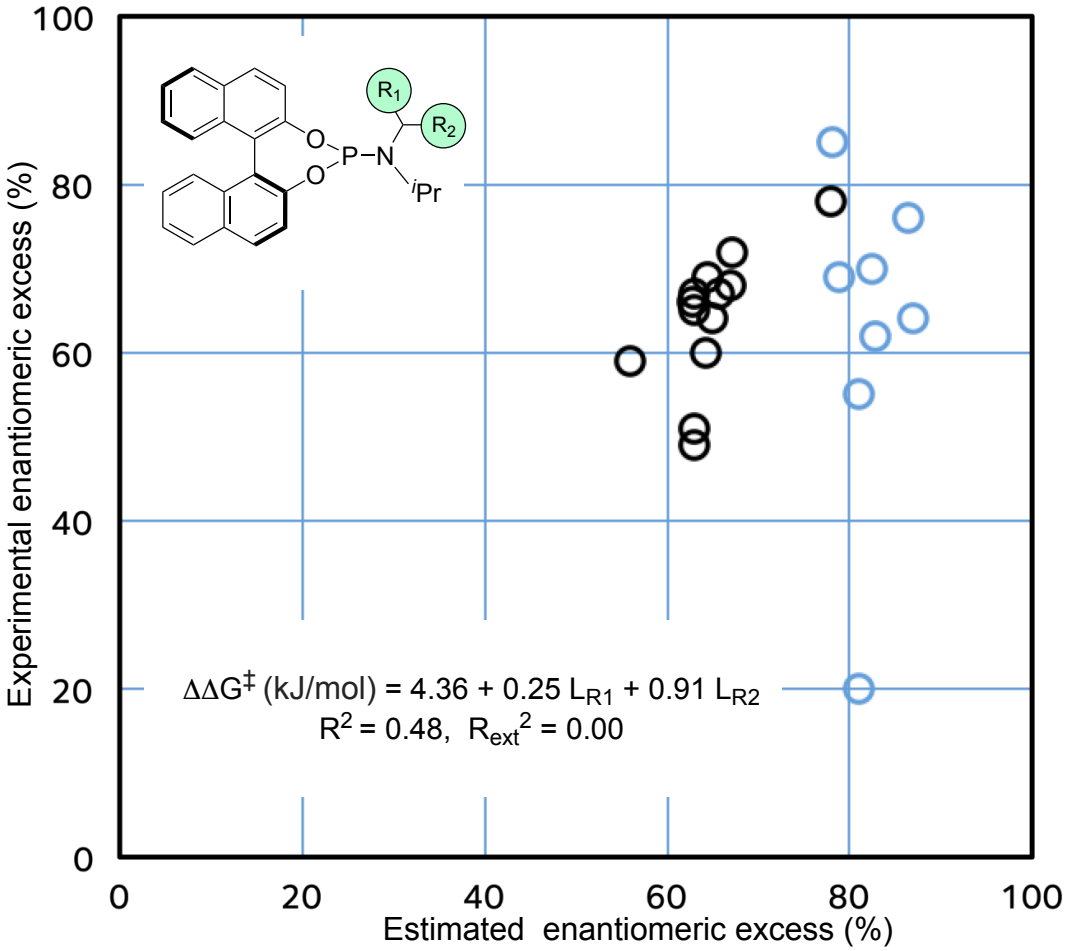

Figure 2-4 Model I: correlation between experimental ee and calculated ee (%) for chiral ligands with R_3= ^{i}Pr. Black = training ligands, Blue = testing ligands.

The model was applied to unseen data (**Figure 2-3**) shown in blue. The testing set R^2 is zero, meaning that the model failed the validation. This is not surprising since the model does not have a good fit and one of the parameters is not statistically significant. However, this provided a basis for further optimisation of QSSR models. In addition, the electron-withdrawing groups clearly reduced the ee and the model was missing electronic descriptors. This result demonstrated that the initial training set lacked sufficient electronic variation.

2.2.2.2 QSSR model II – second preliminary model

To improve upon the first steric model and gain more insight into the enantioinduction, we went back to construct a new QSSR model for the ligands. Like before, we only considered ligands with R_3 = ^{i}Pr. We anticipate that the correlation of any electronic or steric factors with the experimentally observed ee can provide information on the factors that are important in the enantioinduction. This correlation is shown in **Figure 2-5**.

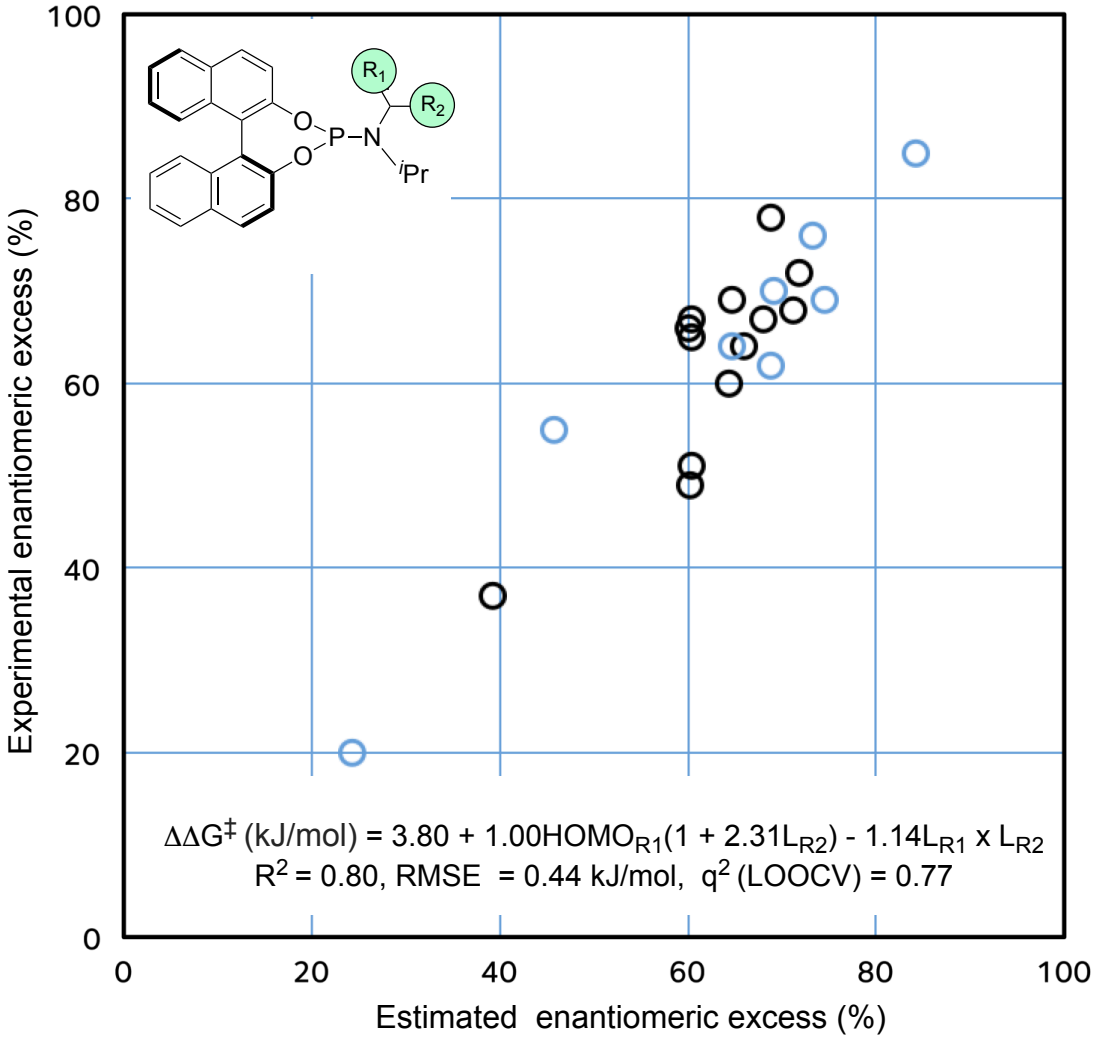

Figure 2-5 Model II: correlation between experimental ee and calculated ee (%) for chiral ligands with R_3= ^{i}Pr. Black = training ligands, Blue = previous testing ligands now also included as training ligands.

The enantiomeric excess is calculated from the two steric parameters; L_{R1} and L_{R2} previously seen in Model I (**Figure 2-4**), and an electronic term; a HOMO energy of the truncated R_1 substituent, capped with a methyl group (**Figure 2-6**). The HOMO energy was computed at the B3LYP/6-31G(d) level of theory.[116]

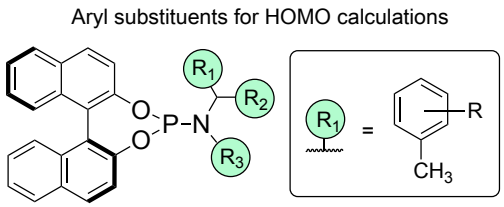

Figure 2-6 Schematic representation of methyl capped R_1 substituent.

The exact expression is in a non-linear format: $\Delta\Delta G_{expt}^{\ddagger} = 3.80 + 1.00HOMO_{R1}(1 + 2.31L_{R2}) - 1.14L_{R1} \times L_{R2}$. The root-mean-square error (RMSE) of model II is 0.44 kJ/mol. This model showed a good fit (R^2 = 0.80). It also passed commonly accepted internal validation criteria of leave-one-out cross-validation with q^2 = 0.77.

This model, however, only accounts for ligands where R_3 = ^{i}Pr. We then expanded the ligand scope to all ligands that can be distinctively defined as R_1, R_2 and R_3, (**Figure 2-7**) and excluded ligands where R_1 and R_2 cannot be defined (e.g. **L14**-**L23** where R_1 and R_2 represent a single cyclic substituent).

2.2.2.3 QSSR model III – a generalised model

In this final model (model III, n = 38), we are able to account for almost twice as many ligands compared to model II (n = 21) by the introduction of a Gaussian term which describes the steric bulk of R_3. Once again *R*-statistics package[62] was used to obtain the Gaussian term ($\exp(-m(x-n)^2)$). This term consists of constants *m* and *n* which were evaluated from a linear fitting of logarithmic equation: $\ln(\mathbf{\Delta\Delta G^{\ddagger}}) = -m(x)^2 + 2m \cdot n(x) - m \cdot n^2$ where *x* is steric parameter describing R_3. We explored

Sterimol B_1, Charton[54,55] and Taft[56] parameters for *x*. However, as Charton and Taft parameters were taken from the literature, these parameters were not available for all the ligands used. In comparison to B_1, we discovered that Charton parameters also gave an equally good fit (R^2 = 0.79, **Figure 2-7**). Nonetheless, due to their limited availability, we used Sterimol B_1 parameters, which can be computed "on demand" for any future predictions prior to ligand synthesis.

The calculated ee's are derived from this expression: $\Delta\Delta G_{expt}^{\ddagger} = -0.35 + 0.92HOMO_{R1}(1 + 1.99L_{R2}) - 1.04L_{R1} \times L_{R2} + 5.86\exp(-0.28(B1_{R3} - 1.18)^2)$ (**Figure 2-7**). The model showed good correlation (R^2 = 0.79) with RMSE of 0.76 kJ/mol. Leave-one-out cross-validation of the final model resulted in a good cross-validated correlation coefficient of q^2 = 0.73. The correlation between parameters is low ($r^2 < 0.10$) for all parameters.

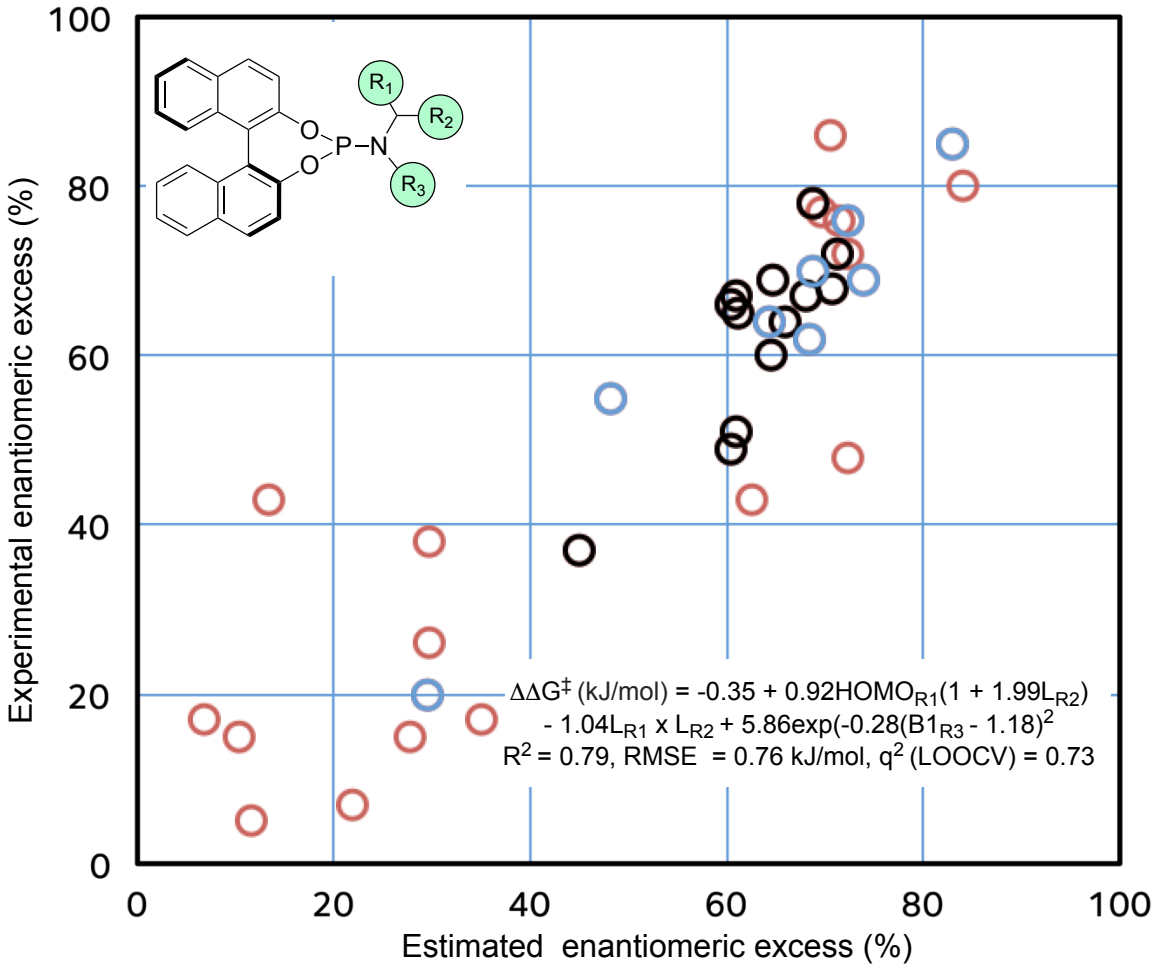

Figure 2-7 Model III: correlation between experimental ee and calculated ee (%) for chiral ligands with well defined R_1, R_2 and R_3. Black = training ligands, Blue = previous testing ligands now also included as training ligands, Red = ligands which $R_3 \neq {}^{i}Pr$.

The newly introduced Gaussian term maximised around 1.18 which is equvalent to B_{1R3} of 2.39 Å, an estimated 'ideal' width for R_3. The shallow curve near the maximum means that small deviation of B_1 from this ideal value will not drastically lower the enatioselectivity. This means that in addition to an isopropyl group, a range of groups with 'suitable size' to R_3 can also achieve the desirable effect e.g. α-methylnaphthyl, and cyclohexyl substituents. We rationalised that the substituent this size can fit under the BINOL ring such that the other substituents (R_1 and R_2) can adopt conformations that do not disrupt any favourable interaction between the

copper and R_1. This spatial arrangement was supported by the NOE and NOESY experiments of the Ligand:CuOTf complexes.[91]

Both of the new models suggested the positive influence of the electron richness of the ligand. The positive $HOMO_{R1}$ term showed a correlation that the more electron rich the R_1 group is, the better the enantiomeric excess. The model also illustrates the importance of the length of both R_1 and R_2 to the ee. Correlation does not necessary imply causation so we sought to explain the relations by further experimental and DFT studies.

2.2.2.4 Test for non-linear effects

To probe the nature of the active catalyst at the stereodetermining TS, we performed a test for non-linear effects.[117] We used 4 scalemic mixtures of **L1**, a racemic and an enantiopure **L1**. The result is plotted in **Figure 2-8**. We observed a linear relationship between the ligand enantiomeric excess and the enantiomeric excess of the product, which is consistent with 1:1 metal:ligand stoichiometry in the chiral catalyst .

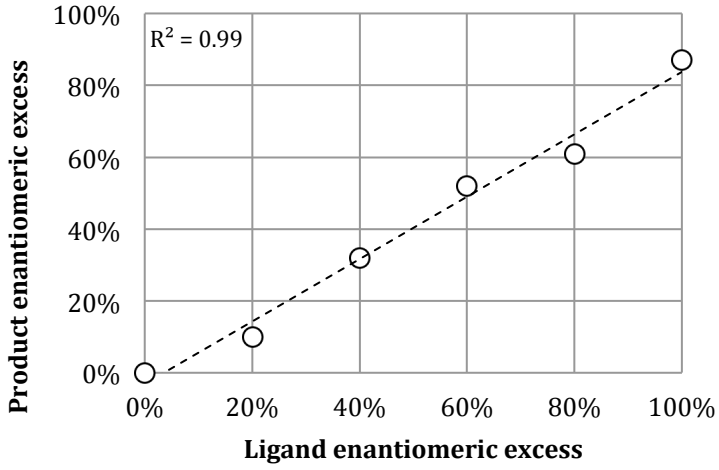

Figure 2-8 Relationship between the *ee* of the ligand and the *ee* of the conjugate addition product under the optimised reaction condition.

2.2.2.5 DFT studies of the competing TS at the stereodetermining step

All the DFT calculations were done by Qian Peng

We examined several conformations of the Cu complex transition states at the stereodetermining carbocupration step. Only the two lowest energy conformations of the complex with **L45** are presented here (**Figure 2-9**). To increase the computational tractability, we truncated the alkyl nucleophile derived from 4-phenyl-1-butene to an ethylene. The predicted stereochemistry of the resulting products with either $ZrCp_2Cl$ or TMS as a Lewis acid agreed with the experimentally observed stereochemistry (screening vs. optimised reaction conditions, see 2.2.3).

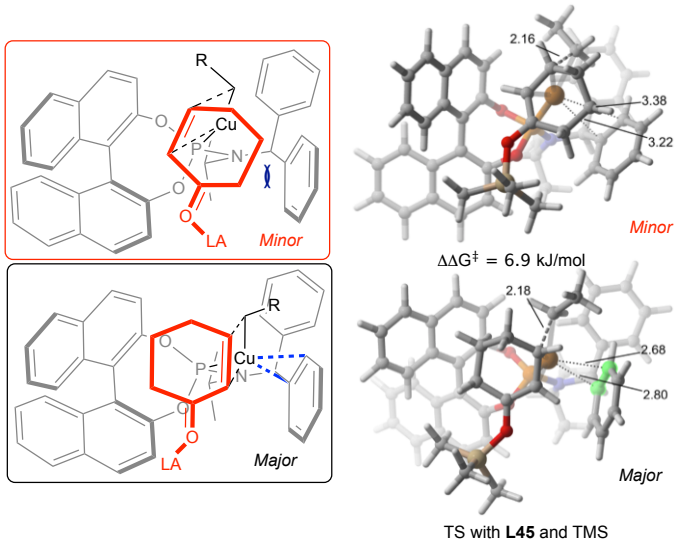

Figure 2-9 Stereodetermining TSs with ligand **L45** and TMS as a Lewis acid. SMD(DCM)-B97D/def2TZVPP//B97D/6-31G(d)&LANL2DZ $\Delta\Delta G^{\ddagger}$ (298 K); selected distances in Å

In addition to the TS of **L45**-TMS, the competing pair of TS's with ligands **L45** (with $ZrCp_2Cl$), **L54** and **L56** with TMS as the Lewis acid were optimised at SMD(DCM)-B97D/def2TZVPP//B97D/6-31G(d)&LANL2DZ level of theory. The distances between Cu and the closest carbon atom in the aromatic ring of the ligand were plotted against the experimentally observed enantioselectivity expressed as $\Delta\Delta G^{\ddagger}$ in kJ/mol (**Figure 2-10**). In all of the cases considered, clear difference in the distances

between copper and the aromatic rings in the competing pair of TS's illustrates that there is a favourable copper-arene interaction that is more emphasised in the more stable diastereomer of the TS which leads to the major enantiomer of the product. This spatial organisation was also seen in the ground states complexes.[91]

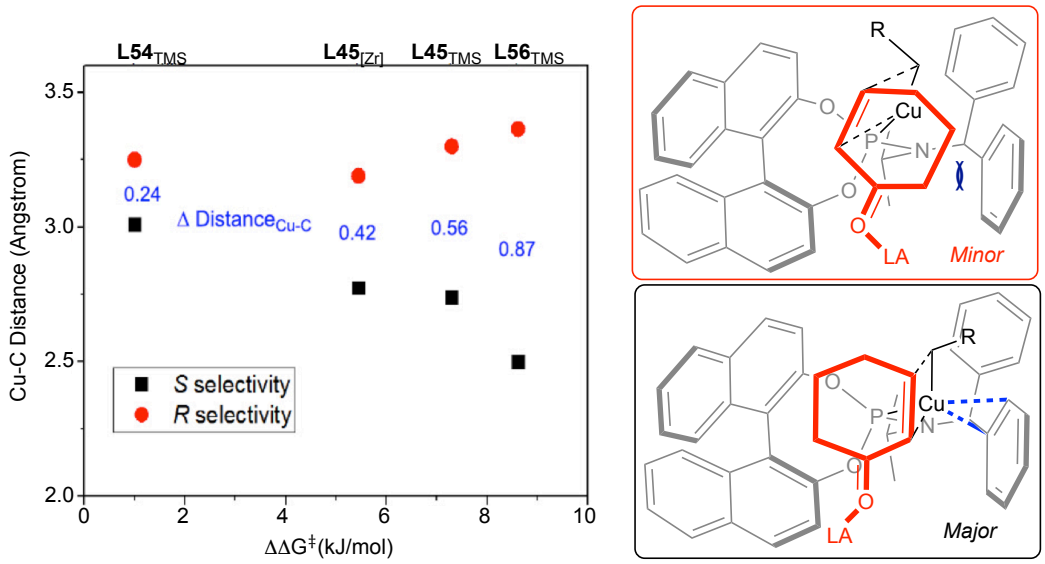

Figure 2-10 Experimental ΔΔG‡ against Cu-arene distances (Å) for ligands **L45**, **L54** and **L56** with different Lewis acids. In black, data extracted from the lowest energy transition structures which lead to the major enantiomer of the product. In red, TSs that lead to the minor enantiomer of the product. (LA = Lewis acid)

These DFT models also aided in the interpretation of the QSSR models. In the QSSR model, HOMO energy of the aryl ring contributed favourably to the calculated enantioselectivity. A higher energy HOMO of substituents indicates that they are better electron donors. Thus they can form stronger interactions with copper, increasing the energy difference between the competing TS and therefore enhance the level of enantioselectivity.

2.2.3 Optimising reaction conditions

All the experiments regarding ligand screening and reaction optimisation were carried out by Philippe Roth and Rebecca Maksymowicz.

By subjecting the best three ligands (*(S,S,S)*-**L1**, **L47**, **L56**) to an optimised reaction condition previously reported[102], the ee was further improved for **L1** and **L56** to 90% and 94% respectively but the ee remained constant for **L47** at 86% ee (**Scheme 2-5**).

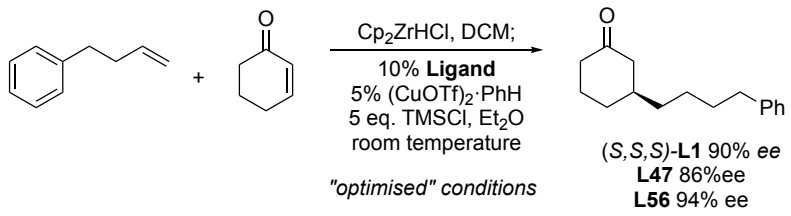

Scheme 2-5 Conjugate addition with **L1**, **L47** and **L56** under the optimised condition.

Under these optimised conditions, 5 eq. of TMSCl was added and the solvent for the reaction was switched to Et_2O. The exact role of TMSCl is under investigation by our group. There are multiple roles that TMSCl can play in facilitating the conjugate addition such as activating the enone as a Lewis acid, as well as stabilising the enolate. In terms of the increases in enantioselectivity, the TMS-coordinated substrate could provide better fit in the Cu-ligand chiral environment, which is less pronounced in the other diastereomer of the TS that leads to the minor enantiomer of the product. Alternatively it could promote the asymmetric pathway compared to the racemic background reaction that arises from the organocopper species without chiral ligand.

2.3 Summary

The role of the chiral phosphoramidite ligands in asymmetric conjugate addition of alkylzirconocenes to cyclic enones was studied using experimental and computational experiments. The BINOL backbone of the phosphoramidites were shown to be responsible for the absolute stereochemistry of the product. The

modular amido part of the ligands influenced the level of enantioselectivity of reaction, not the absolute stereochemistry.

Statistical regression models were created for enantioselectivity prediction based on mathematical expressions of electronics and steric parameters of the ligand substituents. HOMO energy of the R_1 substituents was found to positively correlate with the observed enantioselectivity. DFT calculations of the competing TS helped interpret this HOMO term as an important interaction between the metal centre and one of these aromatic groups. This copper-arene interaction is responsible for an enhanced affinity, and is conserved in the favoured transition state structure leading to the major enantiomer of the product. The QSSR model gave an 'optimal' size of the amido substituent R_3 where the deviation from that value reduced the ee. We reason that this is the most suitable size of the substituent such that it allows for ligands to adopt the conformation that R_1 can be in close proximity to the copper atom. In the end, a model that could fit all 38 cases was trained on ligands where R_i is alkyl or aryl substituents. The best ligands were subjected to optimised reaction conditions and showed enhanced enantioselectivity of up to 94% ee.

2.4 Experimental Section

2.4.1 Reproducibility

As a standard protocol in our lab to verify the quality of new batches of reagents, a test reaction using Feringa's ligand (**L1**) is carried out under the screening conditions (**Scheme 2-4**). If the reagents are of good quality, the test reaction gives 80±2% ee. These reactions were performed multiple times. Reproducibility of the enantioselectivity of the reaction with 7 representative ligands is tabulated below.

Table 2-2 Reproducibility of measured enantioselectivity in copper catalysed conjugate addition.

Ligand	Repeats	Measured *ee* (%)	ΔΔG‡ (kJ/mol)
L1	2	80%	5.44
	8	79%	5.31
	2	81%	5.59
	1	82%	5.73
	avg.	**80%**	**5.44**
L13	1	37%*	1.93*
	1	59%	3.56
	1	59%	3.56
	avg.*	**59%**	**3.56**
L24	2	15%	0.75
	avg.	**15%**	**0.75**
L27	1	72%	4.50
	1	74%	4.71
	avg.	**73%**	**4.61**
L43	1	66%	3.93
	1	69%	4.20
	1	64%	3.76
	avg.	**66%**	**3.96**
L45	2	78%	5.18
	1	77%	5.06
	avg.	**78%**	**5.14**
L56	3	85%	6.22
	avg.	**85%**	**6.22**

*This result is likely due to a low quality batch of ligand so it was excluded from the averaged value and from the QSSR model.

2.4.2 Test for non-linear effects

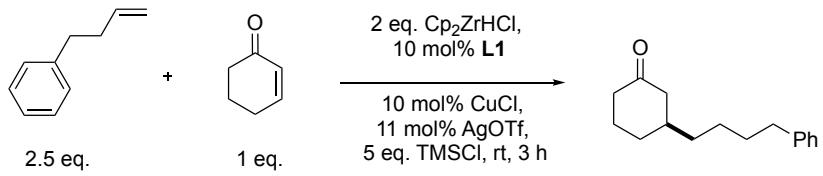

Scheme 2-6 Conditions used to test for non-linear effects.

Taking the optimised reaction conditions (Et_2O, TMSCl, 0.40 mmol scale), a series of conjugate reactions were carried out with varied ratio of the enantiomers of **L1** (**Scheme 2-6**). Six different ratios of *(S)* and *(R)*-**L1** were tested and the corresponding enantiomeric excess of the product was illustrated. The results revealed a linear relationship between the enantiomeric excess (ee) of the ligand and the ee of the resultant product with high coefficient of determination (R^2 = 0.99).

Enantiomeric excess was determined by HPLC [Chiralpak® IC; flow: 1.0 mL/min; hexane/^{i}PrOH: 95:5; λ = 210 nm; (+)-(*R*)-3-(4-phenylbutyl)cyclohexanone, t_R = 13.8 min; (–)-(*S*)-3-(4-phenylbutyl)cyclohexanone, t_R = 14.8 min].

2.5 Computational experimental section

2.5.1 Calculation of steric and electronic parameters for amido R_1/R_2 substituents

Sterimol L, B_1 and B_5 parameters of R_1 and R_2 groups were computed from the geometries of B97D[116]/6-31G(d) optimised structures (using Gaussian09)[118] of the R_i group truncated by a methyl group using *Molecular Pro Plus 7.0* program.[119] The original CPK definition of atomic van der Waals radii implemented by Verloop was used throughout. We have compared the quantitative parameters against those obtained from the original Fortran77 program, finding strong linear correlation.[57] Parameters were converted to dimensionless quantities x' expressing them in terms of the standard deviation from the mean value from all ligands examined (see **Equation 1-2**), as has been performed in previous studies (**Table 2-3** and **Table 2-4**). This has no effect on the correlation of the models generated, although does in principle allow for an unbiased comparison between the terms present in the model.

Table 2-3 Training set of ligands used for model building (R_3 = ^{i}Pr).

Lig.	R_1	L	B_1	B_5	HOMO	R_2	L	B_1	B_5	ee[a] (%)	$\Delta\Delta G^{\ddagger a}$ (kJ/mol)
L13	Me	-2.52	-0.44	-1.68	-3.25	Me	-0.66	-0.18	-0.53	59	3.56
L26	2-Naph	0.99	-0.19	0.22	0.55	Me	-0.66	-0.18	-0.53	68	4.11
L34	1-Naph	-0.37	-0.19	1.37	0.56	Me	-0.66	-0.18	-0.53	49	2.66
L35	Ph	-0.39	-0.19	-0.83	0.01	Me	-0.66	-0.18	-0.53	51	2.79
L36	4-MeC_6H_4	0.28	0.51	-0.82	0.21	Me	-0.66	-0.18	-0.53	64	3.76
L37	4-FC_6H_4	0.07	-0.19	-0.83	0.06	Me	-0.66	-0.18	-0.53	60	3.43
L38	4-ClC_6H_4	0.53	-0.19	-0.83	-0.02	Me	-0.66	-0.18	-0.53	67	4.02
L39	3-ClC_6H_4	-0.39	-0.19	0.62	-0.12	Me	-0.66	-0.18	-0.53	65	3.84
L40	3-BrC_6H_4	-0.39	-0.19	0.62	-0.04	Me	-0.66	-0.18	-0.53	67	4.02

L41	4-MeOC$_6$H$_4$	1.08	0.29	-0.82	0.45	Me	-0.66	-0.18	-0.53	72	4.50
L42	3-MeOC$_6$H$_4$	0.13	0.21	0.60	0.35	Me	-0.66	-0.18	-0.53	69	4.20
L43	2-MeOC$_6$H$_4$	-0.40	-0.04	1.37	0.39	Me	-0.66	-0.18	-0.53	66	3.93
L45	Ph	-0.39	-0.19	-0.83	0.01	Ph	1.01	0.06	0.26	78	5.18

[a]Experimentally obtained values.

Table 2-4 Test set of ligands used for model validation (achiral amido part, R_3 = ^{i}Pr).

Lig.	R_1	L	B_1	B_5	HOMO	R_2	L	B_1	B_5	ee[a] (%)	ΔΔG‡ (kJ/mol)
L49	4-MeC$_6$H$_4$	0.28	0.51	-0.82	0.21	4-MeC$_6$H$_4$	1.53	0.70	0.27	70	4.30
L50	3,5-diMeC$_6$H$_3$	-0.28	-0.19	0.42	0.20	3,5-diMeC$_6$H$_4$	1.10	0.06	1.42	69	4.20
L51	3,5-di^{t}BuC$_6$H$_3$	0.34	5.36	1.46	0.22	3,5-di^{t}BuC$_6$H$_4$	1.58	5.18	2.39	62	3.59
L52	4-MeOC$_6$H$_4$	1.08	0.29	-0.82	0.45	4-MeOC$_6$H$_4$	2.15	0.49	0.27	64	3.76
L53	3-CF$_3$C$_6$H$_4$	0.04	0.10	0.82	-0.30	3-CF$_3$C$_6$H$_4$	1.34	0.33	1.79	55	3.06
L54	3,5-diCF$_3$C$_6$H$_3$	0.03	0.76	0.82	-0.60	3,5-diCF$_3$C$_6$H$_3$	1.34	0.93	1.80	20	1.00
L55	2-Naph	0.99	-0.19	0.22	0.55	2-Naph	2.09	0.06	1.24	76	4.94
L56	1-Naph	-0.37	-0.19	1.37	0.56	1-Naph	1.02	0.06	2.31	85	6.22

[a]Experimentally obtained values.

2.5.2 Calculation of steric and electronic parameters for amido substituents ($R_3 \neq {}^i$Pr)

Steric parameters describing R groups including Charton parameters, Sterimol L and B_1 parameters were converted to dimensionless quantities and tabulated in **Table 2-5**. As before, the Sterimol parameters were computed from the geometries of B97D/6-31G(d) optimized structures of the R_i group truncated by a methyl group using *Molecular Pro Plus 7.0* program.[119] Charton parameters are not available for all the substituents and were collected from the literature.[54,55,79]

Table 2-5 Set of ligands with $R_3 \neq {}^i$Pr.

Lig.	R_1	L	HOMO	R_2	L	R_3	B1	Charton	ee[b] (%)	ΔΔG‡[b] (kJ/mol)
-	n/a	-	-	n/a	-	^{i}Pr	0.09	-0.02	-	-
L11	H	-3.06	-3.17	H	-1.08	Me	-1.26	-1.61	17	0.85
L12	Me	-2.52	-3.25	H	-1.08	Et	-1.19	-1.34	7	0.35
L16	2-MeOC$_6$H$_4$	-0.40	0.39	Me	-0.66	α-Me-2-OMePh	0.16	1.50[a]	43	2.28
L17	2-Naph	0.99	0.55	Me	-0.66	α-Me-Naph	0.12	1.50[a]	76	4.94
L18	Ph	-0.39	0.01	Me	-0.66	Bn	-1.19	-0.42	43	2.28
L24	2-Naph	0.99	0.55	Me	-0.66	Me	-1.26	-1.61	15	0.75
L25	2-Naph	0.99	0.55	Me	-0.66	Et	-1.19	-1.34	26	1.32

L27	2-Naph	0.99	0.55	Me	-0.66	Hex	0.16	0.71	73	4.61
L29	2-Naph	0.99	0.55	Me	-0.66	Hep	0.16	1.57	48	2.59
L30	2-Naph	0.99	0.55	Me	-0.66	adamantyl	4.50	3.75	5	0.25
L31	2-Naph	0.99	0.55	Me	-0.66	Bn	-1.19	-0.42	38	1.98
L32	2-Naph	0.99	0.55	Me	-0.66	Ph	-1.01	-1.28	17	0.85
L33	1-Naph	-0.37	0.56	Me	-0.66	Me	-1.26	-1.61	15	0.75
L46	Ph	-0.39	0.01	Ph	1.01	Pent	0.09	-0.35	78	5.18
L47	Ph	-0.39	0.01	Ph	1.01	Hex	0.16	0.71	86	6.41
L48	Ph	-0.39	0.01	Ph	1.01	Oct	2.24	-	77	5.06
L57	1-Naph	-0.37	0.56	1-Naph	1.02	Hex	0.16	0.71	80	5.44

[a]Assumed to be the same as α-Me-Ph. [b]Experimentally obtained values.

2.5.3 R outputs

Regression fitting outputs from *R* for each QSSR models are shown below:

Model I:

A linear least squared regression was generated using *lm* function. The dependent variable is the experimentally observed ee (expressed in kJ/mol), denoted as ddG. The dependent variables are Sterimol L parameters. Sterimol L parameter of R_i is denoted as Li. The script below is the outcome from *R* using standardised data points tabulated above.

```
Call: lm(formula = ddG ~ L1 + L2)

Residuals:
     Min       1Q   Median       3Q      Max
-1.01031 -0.07297  0.12261  0.35291  0.46734

Coefficients:
            Estimate Std. Error t value Pr(>|t|)
(Intercept)   4.3580     0.2280  19.113 3.34e-09 ***
L1            0.2501     0.1698   1.473   0.1715
L2            0.9072     0.3275   2.770   0.0198 *
---
Signif. codes:  0 ‘***’ 0.001 ‘**’ 0.01 ‘*’ 0.05 ‘.’ 0.1 ‘ ’ 1

Residual standard error: 0.5228 on 10 degrees of freedom
Multiple R-squared:  0.4798,    Adjusted R-squared:  0.3757
F-statistic: 4.611 on 2 and 10 DF,  p-value: 0.03811
```

Model II:

We first defined non-linear terms (cross terms) involving HOMO energy and Sterimol parameters as Ti terms. The HOMO energy of the R_1 substituent is denoted as E1. Sterimol L parameter of R_i is denoted as R1L.

```
T1 <- E1*R2L
T2 <- R1L*R2L
```

A linear least squared regression was again generated using *lm* function. The dependent variable is the experimentally observed ee (expressed in kJ/mol), denoted as ddG. The dependent variables are HOMO energy of R_1 substituent (E1) and the two cross terms defined as above. The script below is the outcome from *R* using standardised data points tabulated previously.

Fitting the regression:

```
Call:
lm(formula = ddG ~ E1 + T1 + T2)

Residuals:
     Min       1Q   Median       3Q      Max
-0.71981 -0.31737 -0.02226  0.27926  0.90486

Coefficients:
            Estimate Std. Error t value Pr(>|t|)
(Intercept)   3.8025     0.1141  33.337  < 2e-16 ***
E1            0.9969     0.1638   6.087 1.21e-05 ***
T1            2.3040     0.2909   7.921 4.18e-07 ***
T2           -1.1413     0.2032  -5.618 3.07e-05 ***
---
Signif. codes:  0 ‘***’ 0.001 ‘**’ 0.01 ‘*’ 0.05 ‘.’ 0.1 ‘ ’ 1

Residual standard error: 0.4943 on 17 degrees of freedom
Multiple R-squared:  0.8041,    Adjusted R-squared:  0.7695
F-statistic: 23.26 on 3 and 17 DF,  p-value: 2.996e-06
```

Leave one out cross validation:

To carry out leave-one out cross validation, we call an existing library in *R* called ‘*cvq2*’. The result below is the output obtained from using *cvq2* function on **Modell II**.

```
---- CALL ----
cvq2(modelData = m2, formula = ddG ~ E1 + T1 + T2)

---- RESULTS ----

-- MODEL CALIBRATION (linear regression)
#Elements:        21

mean (observed):  3.8605
mean (predicted):        3.8605
rmse (nu = 0):           0.4448
r^2:                     0.8041

-- PREDICTION PERFORMANCE (cross validation)
#Runs:                           1
#Groups:                 21
#Elements Training Set:  20
#Elements Test Set:              1

mean (observed):  3.8605
mean (predicted):        3.8755
rmse (nu = 1):           0.5238
q^2:                     0.7652
```

Model III:

Model III was created using two regressions. Firstly, to obtain coefficients in the Gaussian term, we expressed the experimentally observed enantioselectivities (ddG in kJ/mol) in a logarithmic scale (lnddG). We then used *lm* function in *R* to obtain a linear regression between lnddG (a dependent variable) and Sterimol B_1 parameter of R_3 (B_1^{R3}) substituent (an independent variable) and a squared term of B_1^{R3} denoted as B12.

Fitting Gaussian term based on Sterimol parameter B1:

```
lnddG <- log(ddG)
B12 <- R3B1^2
```

Fitting the regression:

```
Call:
lm(formula = lnddG ~ B12 + R3B1)
Residuals:
     Min       1Q   Median       3Q      Max
-0.49727 -0.30611  0.08405  0.16538  0.57084

Coefficients:
            Estimate Std. Error t value Pr(>|t|)
```

```
(Intercept)  1.27555    0.18559   6.873 0.000468 ***
B12         -0.27606    0.04728  -5.839 0.001112 **
R3B1         0.65260    0.17306   3.771 0.009278 **
---
Signif. codes:  0 ‘***’ 0.001 ‘**’ 0.01 ‘*’ 0.05 ‘.’ 0.1 ‘ ’ 1

Residual standard error: 0.4006 on 6 degrees of freedom
Multiple R-squared:  0.8796,    Adjusted R-squared:  0.8395
F-statistic: 21.93 on 2 and 6 DF, p-value: 0.001743
```

Full regression:

Once the coefficients for the Gaussian term were obtained, we expressed these terms as an exponential function of B_1^{R3} as shown below named gR3B1. Then we include the previous cross terms T1 and T2 as described previously and used these terms as dependent parameters to generate a regression with *lm* function.

```
gR3B1 <- exp(-0.2761*(R3B1-1.182)^2)
```

Fitting the regression:

```
Call:
lm(formula = ddG ~ E1 + T1 + T2 + gR3B1)

Residuals:
     Min       1Q   Median       3Q      Max
-1.95844 -0.54902  0.08892  0.45371  1.95291

Coefficients:
            Estimate Std. Error t value Pr(>|t|)
(Intercept)  -0.3529     0.3891  -0.907 0.371069
E1            0.9243     0.2485   3.720 0.000740 ***
T1            1.8420     0.3674   5.013 1.77e-05 ***
T2           -1.0437     0.2685  -3.888 0.000462 ***
gR3B1         5.8562     0.5987   9.782 2.80e-11 ***
---
Signif. codes:  0 ‘***’ 0.001 ‘**’ 0.01 ‘*’ 0.05 ‘.’ 0.1 ‘ ’ 1

Residual standard error: 0.8185 on 33 degrees of freedom
Multiple R-squared:  0.788,     Adjusted R-squared:  0.7623
F-statistic: 30.67 on 4 and 33 DF,  p-value: 1.071e-10
```

Leave one out cross validation:

To carry out leave-one out cross validation, we call an existing library in *R* called ‘*cvq2*’. The result below is the output obtained from using *cvq2* function on **Model III**.

```
---- CALL ----
cvq2(modelData = m3, formula = ddG ~ E1 + T1 + T2 + gR3B1)

---- RESULTS ----

-- MODEL CALIBRATION (linear regression)
#Elements:        38

mean (observed):  3.3411
mean (predicted):        3.3411
rmse (nu = 0):           0.7627
r^2:                     0.7880

-- PREDICTION PERFORMANCE (cross validation)
#Runs:                          1
#Groups:                 38
#Elements Training Set:  37
#Elements Test Set:              1

mean (observed):  3.3411
mean (predicted):        3.3482
rmse (nu = 1):           0.8983
q^2:                     0.7286
```

Fit Gaussian term based on Charton parameter B_1:

An analogous model to **Model III** but with Charton parameter rather than Sterimol B_1 parameter (describing R_3 substituent) was created. The methods are essentially identical to the method for generating **Model III** and are shown below.

```
charton2 <- charton^2
```

Fitting the regression:

```
Call:
lm(formula = lnddG ~ charton2 + charton)

Residuals:
       1        2        3        4        5        6        7        8
 0.20445 -0.36344  0.09376  0.11764  0.27795 -0.01938 -0.05519 -0.25577

Coefficients:
            Estimate Std. Error t value Pr(>|t|)
(Intercept)  1.33145    0.12503   10.65 0.000126 ***
charton2    -0.33401    0.03258  -10.25 0.000152 ***
charton      0.54199    0.08338    6.50 0.001287 **
---
Signif. codes:  0 ‘***’ 0.001 ‘**’ 0.01 ‘*’ 0.05 ‘.’ 0.1 ‘ ’ 1

Residual standard error: 0.2618 on 5 degrees of freedom
Multiple R-squared:  0.956,     Adjusted R-squared:  0.9384
F-statistic: 54.28 on 2 and 5 DF,  p-value: 0.0004067

RMSE = 0.7627204
```

Full regression:

```
gchar <- exp(-0.33401*(charton-0.81134)^2)
```

Fitting the regression:

```
Call:
lm(formula = ddG ~ E1 + T1 + T2 + gchar)

Residuals:
    Min      1Q  Median      3Q     Max
-1.6975 -0.4233  0.0169  0.5154  1.9298

Coefficients:
            Estimate Std. Error t value Pr(>|t|)
(Intercept)  -0.3700     0.3891  -0.951  0.34871
E1            0.8638     0.2477   3.487  0.00144 **
T1            1.7169     0.3648   4.706 4.66e-05 ***
T2           -0.8807     0.2683  -3.283  0.00249 **
gchar         5.1164     0.5264   9.719 4.53e-11 ***
---
Signif. codes:  0 ‘***’ 0.001 ‘**’ 0.01 ‘*’ 0.05 ‘.’ 0.1 ‘ ’ 1

Residual standard error: 0.8139 on 32 degrees of freedom
Multiple R-squared:  0.7907,    Adjusted R-squared:  0.7645
F-statistic: 30.21 on 4 and 32 DF,  p-value: 1.857e-10

RMSE = 0.7568928
```

Leave one out cross validation:

The result from using *cvq2* function on **Modell III** with Charton parameter is shown below.

```
---- CALL ----
cvq2(modelData = m3charton, formula = ddG ~ E1 + T1 + T2 + gChar)

---- RESULTS ----

-- MODEL CALIBRATION (linear regression)
#Elements:       37

mean (observed):  3.2946
mean (predicted):        3.2946
rmse (nu = 0):           0.7569
r^2:                     0.7907

-- PREDICTION PERFORMANCE (cross validation)
#Runs:                           1
#Groups:                 37
#Elements Training Set:  36
#Elements Test Set:              1

mean (observed):  3.2946
mean (predicted):        3.3028
rmse (nu = 1):           0.9012
q^2:                     0.7266
```

2.5.4 Model validation, full analysis of variance (ANOVA) and F-statistics.

Each model has been validated by leave-one-out cross-validation (using the *cvq2* package in the *R*).[62] One data point was left out at a time and the rest of the data were used to generate a new model, which was then used to predict the excluded data point. The cross-validated correlation coefficient (q^2) is given for each model (see spreadsheet, or manuscript **Figure 2** and **3**). The q^2 values of models with electronic and steric factors are higher than the generally recommended value of 0.5. For each correlation, the corresponding F-statistics and ANOVA analysis were carried out using *R*-statistics package and tabulated below. Critical values of the F-statistic necessary for rejecting the null hypothesis (correlation due to random occurrences rather than being statistically significant), at the 0.05 significance level are tabulated in **Table 2-6**. This requirement is met for each parameter except for L_{R1} of the preliminary steric only model.

Table 2-6 F-statistics, P-values and the corresponding critical value for F-statistics for models and ANOVA tests for their corresponding parameters.

Model/Parameters	F-statistics	P-values	$F_{0.05}$(DF1,DF2)
$\Delta\Delta G^{\ddagger} = 4.36 + 0.25\ L_{R1} + 0.91\ L_{R2}$	4.61	0.038	$F_{0.05}(2,10) = 4.103$
L_{R1}	1.55	0.242	$F_{0.05}(1,10) = 4.965$
L_{R2}	7.67	0.020	
$\Delta\Delta G^{\ddagger} = 3.73 + 1.33HOMO_{R1}(1 + 1.57L_{R2}) - 1.09L_{R1} \times L_{R2}$	23.26	3.00×10^{-6}	$F_{0.05}(3,17) = 3.197$
$HOMO_{R1}$	7.017	0.017	$F_{0.05}(1,17) = 4.451$
$HOMO_{R1}\times L_{R1}$	31.19	3.29×10^{-5}	
$L_{R1} \times L_{R2}$	31.56	3.07×10^{-5}	
$\Delta\Delta G^{\ddagger} = -0.29 + 1.15HOMO_{R1}(1 + 1.65L_{R2}) - 1.00L_{R1} \times L_{R2} + 5.63\exp(-0.28(B1_{R3} - 1.18)^2)$	30.67	1.07×10^{-10}	$F_{0.05}(4,33) = 2.659$
$HOMO_{R1}$	11.28	1.99×10^{-3}	$F_{0.05}(1,33) = 4.139$
$HOMO_{R1}\times L_{R2}$	6.32	0.017	
$L_{R1} \times L_{R2}$	9.40	0.00430	
$\exp(-0.276(B1_{R3} - 1.18)^2$	95.68	2.81×10^{-11}	

3 Copper Catalysed Asymmetric Conjugate addition to β-substituted cyclopentenones forming quaternary centres with the aid of quantitative structure-selectivity relationship (QSSR)

Materials present in this chapter have been published in 2018.*[120]*

3.1 Introduction

All-carbon quaternary centres are found in many natural products and bioactive molecules (**Figure 3-1**).[121–126] Compounds containing this motif play an important role in chemistry and pharmaceuticals.[127] The value and the interests in this area can be illustrated by a number of reviews highlighting the progress in enantioselective construction of these quaternary centres, but introducing these centres enantioselectively remains a challenge. [128–132] Substantial progress has been made in certain areas such as enantioselective conjugate addition to cyclohexenones. However, this is not the case for other ring rizes.[98,128]

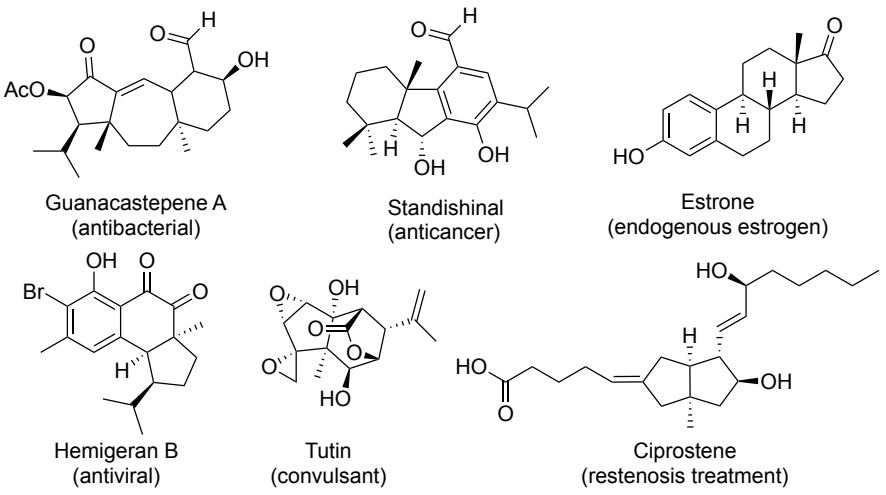

Figure 3-1 Examples of biologically active compounds containing five membered ring with quaternary centres.

Five-membered enones are often referred to as particularly challenging substrates for asymmetric conjugate addition (ACA).[20,94,98,128,133] One of the reasons is that they are relatively flat therefore they exhibit weaker intrinsic conformational preference unlike the cyclohexenones.[98]

Synthetic methods for ACAs that are suitable for six-membered rings are not necessarily suitable or are more limited in scope when applied to 5-membered rings.[129,134–144] For example, Alexakis has established many Cu-catalysed ACA that worked well on substrates containing a 6-membered ring containing substrates but those conditions did not work as well for 5-membered rings (**Scheme 3-1**).

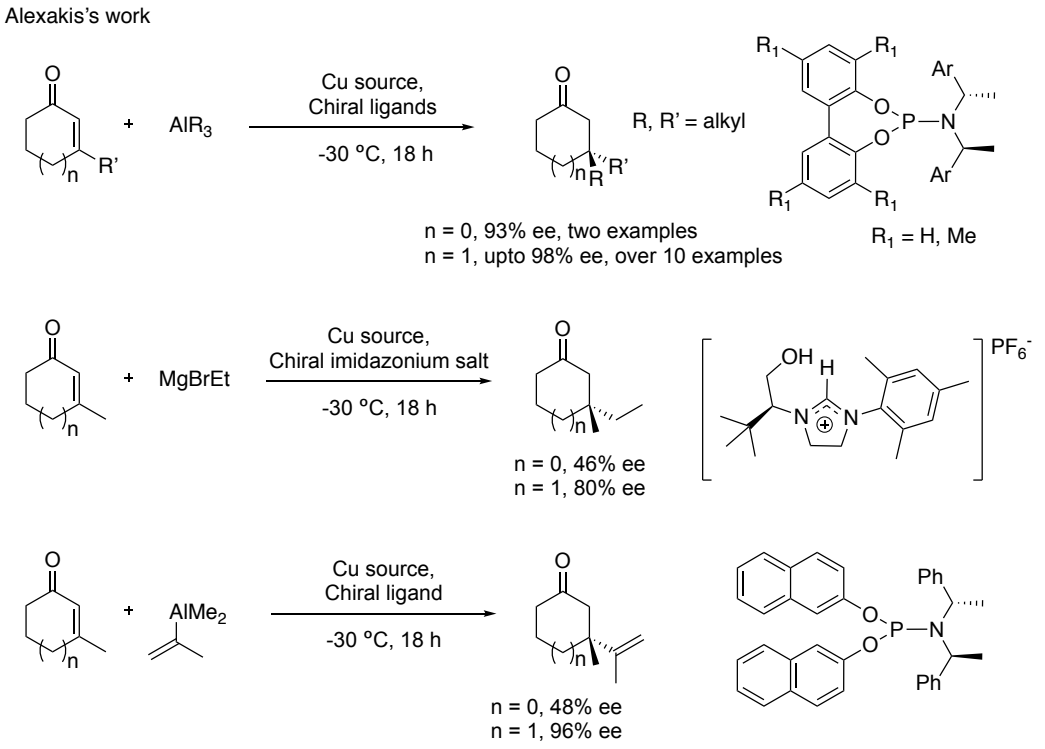

Scheme 3-1 Alexakis's contribution on copper catalysed ACA with 6 and 5 membered ring enones forming quaternary Csp^3-Csp^3 centres.

Combining the two separate challenges of 5-membered ring substrates and constructing quaternary centres makes the development of an enantioselective ACA of β-substituted cyclopentenones difficult. Relatively few methods exist for this.[145–148] Among these, even fewer address the formation of quaternary centres that are bound to all four sp^3-hybridised carbons. For example, in 2007, Alexakis reported the first example of ACA to β-substituted cyclopentenones using organoaluminium nucleophiles (AlR_3, R = Me and Et).[144,149] In the following year, Hoveyda disclosed, to our knowledge, the only other suitable ACA method for unactivated β-substituted cyclopentenones. This method showed good substrate scope but was limited to simple alkyl nucleophiles (10 examples using AlR_3 where R = Me, Et, ^{i}Bu).[145] (**Scheme 3-2**)

Hoveyda's work

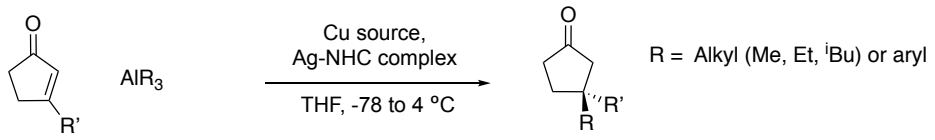

10 examples upto 97% yield, 97% ee (R = alkyl)
9 examples upto 85% yield, 98% ee (R = aryl)

Scheme 3-2 Hoveyda's work on conjugate addition to β-substituted cyclopentenones.

Some unstabilised nucleophiles used in the copper catalysed ACA include Grignard reagents, organozinc[99], organoaluminium[134] and organozirconocenes[150]. These organometallic species are very reactive, while some are pyrophoric. The commercially available reagents are often limited to aryls and simple alkylmetal species except organozinc reagents where some esters and nitriles are tolerated. The unstabilised organometallic reagents such as Grignard and organozinc can be generated from more stable precusors but this activation process often requires cryogenic conditions due to their reactivity and functional group tolerance is relatively poor.

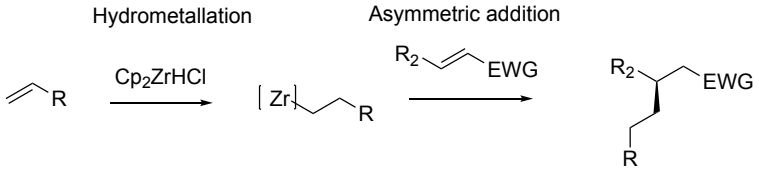

Scheme 3-3 Hydrozirconation of a terminal alkene to form an organozirconium *in situ* followed by trapping with an electrophile in ACA.

On the other hand, alkenes are easy to handle and variety of alkenes are commercially available compared to the organometallic reagents. They can be used to generate organozirconiums (also unstabilised nucleophiles where pKa~50) *in situ* with Schwartz reagents at rt to be used in conjugate addition (**Scheme 3-3**).[150] These reagents were shown to be compatible to more functional groups compared to Grignard, organozinc, or organoaluminium species.[101]

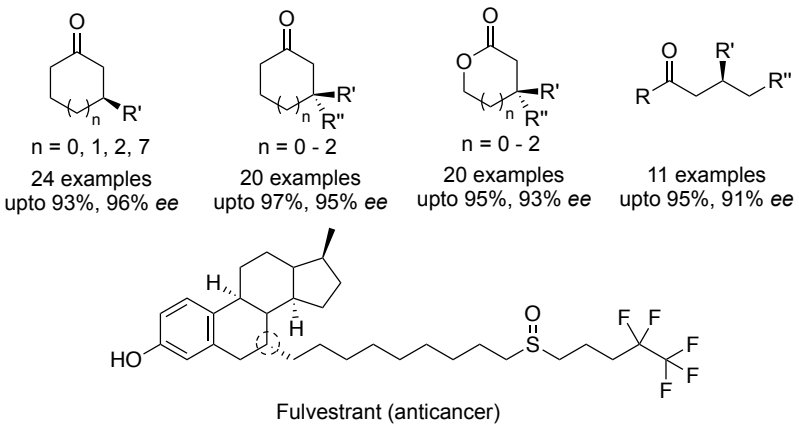

Figure 3-2 Selected examples for the copper-catalysed ACA using *in situ* generated organozirconium species in our lab.

In our lab, we developed copper catalysed ACAs for cyclic[151,152] and acyclic[107] enones, lactones[106], dieneones[153], thioesters[154] and functionalised enones[155,156] using alkylzirconium nucleophiles (**Figure 3-2**).[101] To form quaternary centres, we developed protocols involving β-substituted cyclic[103] and linear substrates[105]. However, we were unable to develop effective asymmetric additions to the 5-membered ring substrates for quaternary centres formation (**Scheme 3-4**).[108]

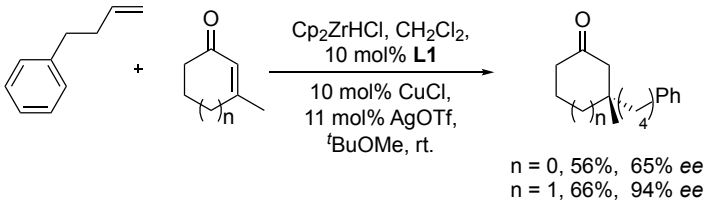

Scheme 3-4 Copper-catalysed ACA optimised conditions for cycloenones forming quaternary centres developed by our lab.

3.2 Aim

Our aim was to develop a highly enantioselective protocol for the conjugate addition to β-substituted cyclopentenones to form a quaternary centre. We planned to use the same approach as the previous chapter for developing new chiral ligands (see chapter 2). This started with the experimental ligand screening and we used these data to construct a QSSR model which would hopefully be predictive and provide us

some clues about important factors governing the enantioinduction. DFT calculations were then used to help interpreting the QSSR models and shed some light to the enantiocontrolling factors operating at the transition structures. These tools would then be used in combination towards designing the better chiral ligands.

3.3 Results and discussion

3.3.1 Reaction condition screening

We started with changing the reaction conditions that were optimised for cyclohexenones to observe the effects of each reagents and additives to the product yield or enantioselectivity (**Table 3-1**). Most of the reaction yields in this chapter are quoted based on the ^{1}H NMR spectrum of the crude reaction mixture with $MeNO_2$ as an internal standard. Comparison between NMR yields and the isolated yields showed a good correlation and the calibration plot is shown in the experimental section (**Figure 3-13**).

Table 3-1 Screening of reaction conditions

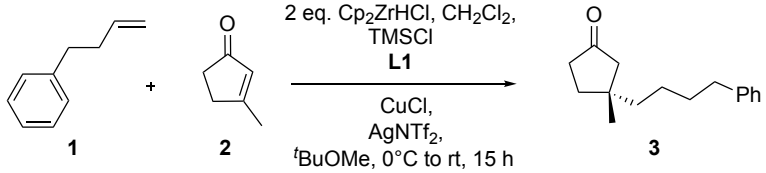

Entry	CuCl (mol%)	Ligand (mol%)	Alkene	TMSCl	Scale (mmol)	Yield[a]	*ee*
1	10	-	5 eq.	5 eq.	0.2	22%[g]	
2	10	-	2.5 eq.	5 eq.	0.2	85%	-
3	-	10	2.5 eq.	5 eq.	0.2	0%	-
4	10	10	5 eq.	-	0.2	11%[g]	1%
5	10	10	2.5 eq.	1 eq.	0.2	31%	65%
6[b]	10	10	1.5 eq.	5 eq.	0.2	32%	65%[c]
7	10	10	2.5 eq.	5 eq.	0.2	69%	62%
8[d]	10	10	2.5 eq.	5 eq.	0.2	21%	65%
9	20	20	2.5 eq.	5 eq.	0.2	60%	64%[c]
10	10	20	2.5 eq.	5 eq.	0.2	67%	59%
11[e]	10	10	2.5 eq.	5 eq.	0.2	56%[e]	49%
12[f]	10	10	2.5 eq.	5 eq.	0.2	78%	61%
13	10	10	2.5 eq.	5 eq.	1.0	70%	69%

[a]Yield based on NMR of the crude reaction mixture, [b]1.1 eq. Cp_2ZrHCl, [c] *ee* from crude mixture, [d]rt, [e] $AgNTf_2$ from commercial source, [f] New $AgNTf_2$ synthesised in-house, [g]isolated yield.

From these condition screenings, we found that a racemic background reaction can occur which can erode the observed ee (entries 1,2). As a consequence, for future ligand screening, 11 mol% of ligand is used with 10 mol% CuCl. Adding too much alkene reduces the yield (entries 1 and 4). A copper salt is crucial for reactivity (entry 3).

TMSCl (distilled, stored with $CaH_{2(s)}$) is essential for yield and selectivity. Without TMSCl, enone starting material was fully consumed but the yield of product is low and there was no selectivity (entry 4 vs 5 vs 6). It is interesting to note that the cyclohexenone analogue gave good yield and ee without TMSCl but TMSCl also improves the ee (see chapter 2). Adding 5 eq. of TMSCl with 2.0 eq of the Schwartz reagent and 2.5 eq. of the alkene with 10% Cu-ligand loading at 0 °C gave the best result (entry 7). These conditions were taken forward for further screening. Doing the reaction at room temperature slightly increases the ee but yield is reduced (entry 8). Adding twice as much catalyst or double the chiral ligand do not dramatically change the result (entries 9 and 10). The quality of $AgNTf_2$ is crucial for good yield and ee (entries 11 and 12). Carrying out the reaction at larger scale (1 mmol) increased the ee (entry 13).

Screening of other Lewis acids namely $B(O^iPr)_3$, TESCl, did not lead to better results (**Table 3-2**). When TIPSCl or isopropoxy pinacol borate was used, the enone starting material was consumed but no indication of product formation was observed with less than 50% of enone starting material remaining unreacted.

Table 3-2 Screening Lewis acids

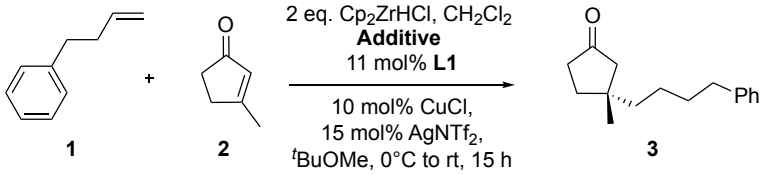

Entry	Additive	Yield		*ee*
		^{1}H	isolated	
1	1 eq. B(O*i*Pr)$_3$	<4%	nd	61%[c]
2	5. eq.TESCl	nd	33%	15%
3	5 eq. TIPSCl	0%	0%	-
4	5 eq. 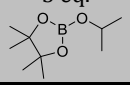	0%	0%	-

Nd = not determined, [c] *ee* from crude mixture.

Keeping all other condition fixed and only change the identity of the solvent, we found that ethereal solvents (^{t}BuOMe, Et_2O) gave the best yields and ees (**Table 3-3**).

Table 3-3 Screening solvents

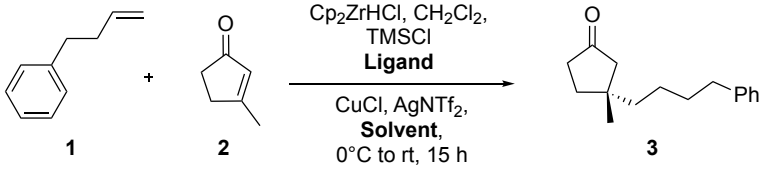

Entry	Solvent	Scales (mmol)	Yield		*ee*	Remarks
			^{1}H	isolated		
1	^{t}BuOMe	0.2	69%	nd	62%	
2	THF	0.2	68%	nd	56%	
3	DCM	0.2	62%	nd	45%	
4	Toluene	0.2	55%	nd	1%	
5	^{t}BuOMe	1.0	70%	73%	69%	1 mmol scale
6	Et_2O	1.0	90%	85%	69%	1 mmol scale

THF and DCM gave lower ee's. Toluene gave essentially racemic product. The scale of reaction improves ee (entries 5-6). Both ether solvents examined gave the same ee with Et_2O giving slightly higher yield on a 1 mmol scale.

3.3.2 Ligand screening

We used the condition shown in entry 7, **Table 3-1** for the rest of the ligand screening. First we varied the backbone of the ligand (**Scheme 3-5**) while keeping

the bis-1-(phenylethyl)amine part. The commercially available Feringa's ligands bearing a BINOL backbone **L1** gave 35% ee. The mismatched isomer (S_a,*R*,*R*)-**L2** gave slightly lower ee (20%). The ligands with 1,1'-disubstituted BINOL backbones gave essentially the same or lower ee (4-36% ee, **L3**-**L5**). The ligand with a partially reduced BINOL backbone gave poor ee (7% ee, **L6**). Achiral biaryl backbones gave less than 10 % ee in all three cases tested (**L7**-**L9**). The ligand with chiral spirobiindanediol backbone gave poor ee (15% ee, **L10**). The ligand with TADDOL backbone gave essentially racemic product (2% ee, **L11**). These poor selectivities observed with a range of different ligands emphasised the challenge often observed with this 5-membered ring enone.

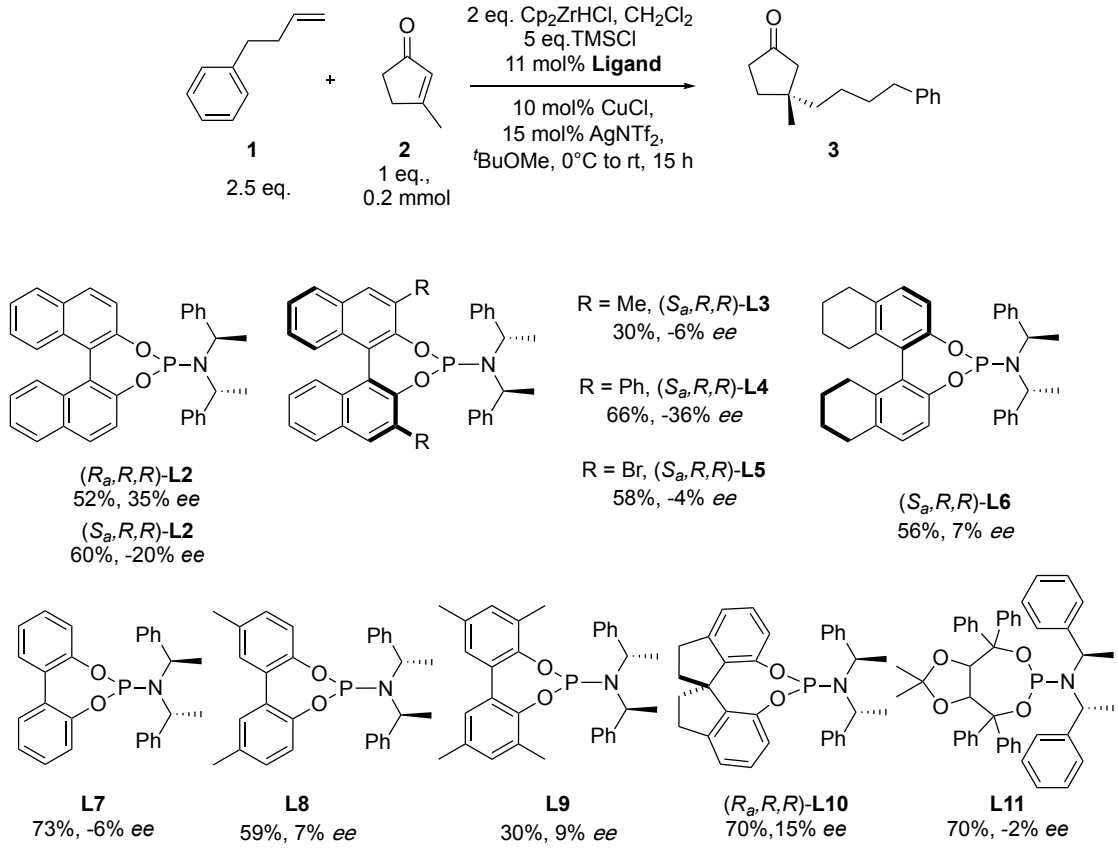

Scheme 3-5 The ligand screening conditions and the ligand screening results with different backbones. Yield based on ^{1}H NMR spectroscopy with $MeNO_2$ as internal standard of the crude reaction mixture. Ee's were determined by HPLC using a non-racemic stationary phase.

Then we varied the substituents on amido moiety while keeping the BINOL backbone. In all cases, the absolute stereochemistry of the product was determined by the axial chirality of the BINOL. The notation from this point onwards is that *(R)*-BINOL yields majorly *(R)*-**3** and the corresponding ee values are reported as positive number where as *(S)*- BINOL yields majorly *(S)*-**3** and those ee's are given as negative numbers.

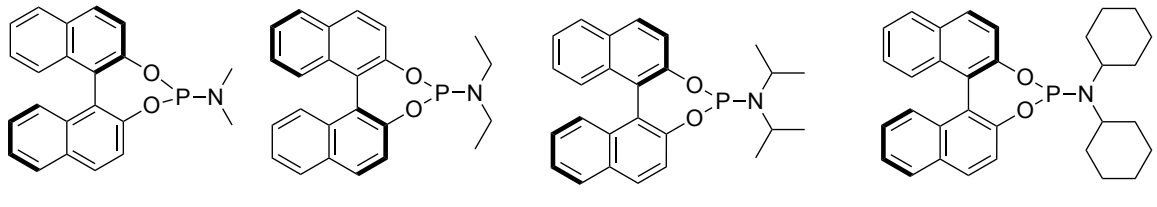

Figure 3-3 The ligand screening results with different symmetrical amines. Yield based on ^{1}H NMR spectroscopy with $MeNO_2$ as internal standard of the crude reaction mixture. Ee's were determined by HPLC using a non-racemic stationary phase.

Starting with the simplest alkyl substituents on the amido group, we observed a weak trend that increases in the substituent size slightly increases the ee (4-24% ee, **L12-L15**, **Figure 3-3**).

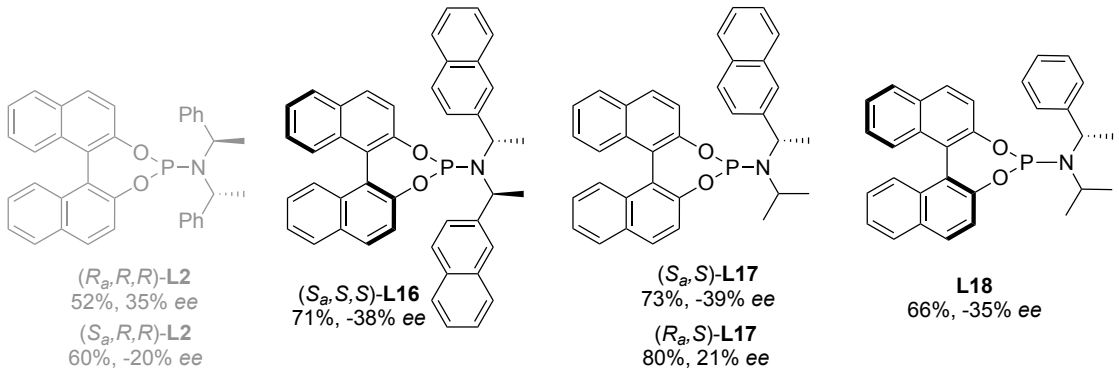

Figure 3-4 The ligand screening results with different chiral amido substituents. Yield based on ^{1}H NMR spectroscopy with $MeNO_2$ as internal standard of the crude reaction mixture. Ee's were determined by HPLC using a non-racemic stationary phase.

Compared to the commercial ligand **L2** which was shown to be good at catalysing many reactions,[19] the larger binaphthyl derivative of this ligand did not give

significantly better ee values (38% ee, **L16**). Swapping one of the chiral substituents on the amido group to a simple isopropyl group did not dramatically change the yield (**L18** vs **L2** and **L17** vs **L16**). The absolute configuration of the BINOL backbone and the N-substituent can be matched or mismatched in their sense of enantioinduction: we observed that mismatched ligands (i.e. R_a,*S*) gave slightly reduced ee than the matching ligands (i.e. R_a,*R*) in comparable yields, with the product absolute configuration being dictated by the BINOL configuration.

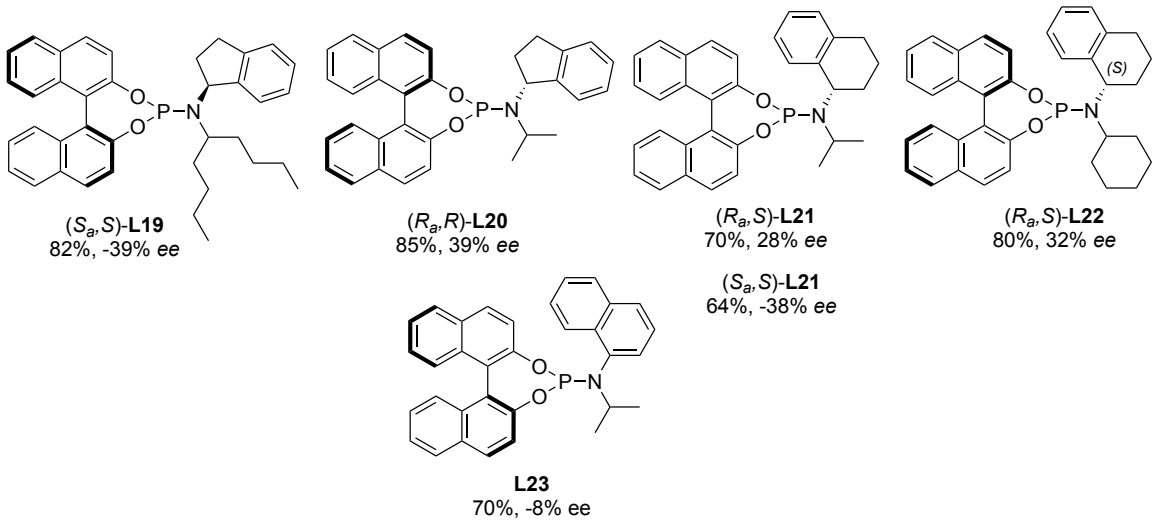

Figure 3-5 The ligand screening results with different bicyclic amido substituents. Yield based on ^{1}H NMR spectroscopy with $MeNO_2$ as internal standard of the crude reaction mixture. Ee's were determined by HPLC using a non-racemic stationary phase.

We explored **L19** which is our commercialised ligand that was shown to be efficient at catalysing linear substrates in ACA.[105,153] It gave comparable ee to **L2** (-39% ee). Truncating the *n*-butyl chain to a methyl group did not affect the ee (**L20** vs **L19**). Switching an indane moiety to a tetrahydronaphthalene also did not affect the ee (**L21** vs **L20**). Once again, we saw the matching ligand is preferred compared to mismatch ligands (28% ee *(R_a,S)*-**L21** vs -38% ee *(S_a,S)*-**L21**). Replacing the ^{i}Pr group to a cyclohexyl group reduces the ee a little (32% ee, **L22**). These modification of structures did not lead to significant changes in the ee therefore, we did not

investigate further modification. A ligand featuring a naphthyl ring gave poor ee (8% ee, **L23**).

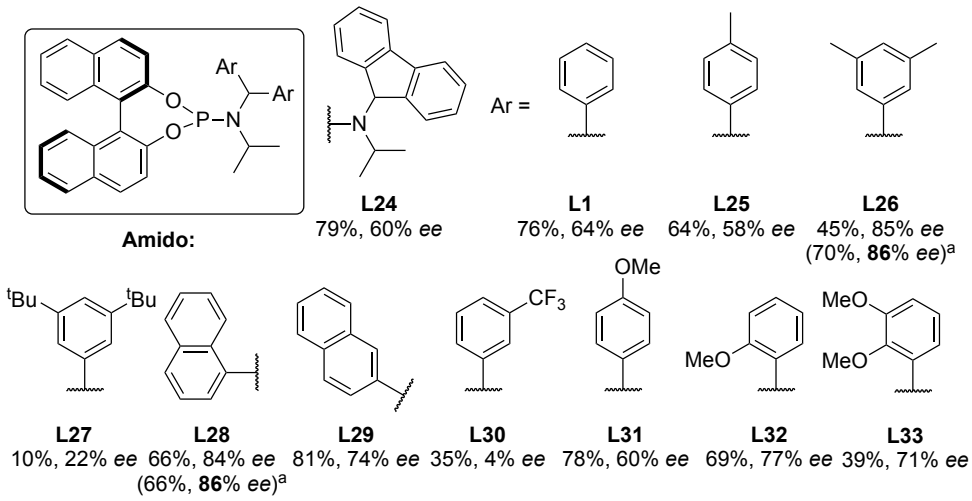

Figure 3-6 The ligand screening results with different diaryl amines. Yield based on ^{1}H NMR spectroscopy with $MeNO_2$ as internal standard of the crude reaction mixture. Ee's were determined by HPLC using a non-racemic stationary phase. [a]Results from the reaction which give the highest ee out of all repeats.

When we went back to studying derivatives of **L1** and now changed only the aromatic substituents, things became more interesting (**Figure 3-6**). The observed *ee* values drastically changed with the structure of the aryl from nearly racemic (4% *ee* with **L30**) to 86% *ee* observed with **L26** and **L28**. Fluorenyl ring (**L24**) and *para*-substituted phenyl ring (**L25**) gave slightly lower ee's compared to the phenyl ring (**L1**). A 3,5-dimethyl substituted ring gave one of the best ee's (**L26**). Replacing the methyl group with a larger ^{t}Bu group dramatically decreases the ee and yield (10%, 22% ee, **L27**). The ligand with 1-naphthyl ring also gave one of the best ee's (**L28**). We saw slight drops in ee when the substituent pattern was changed to 2-naphthyl (**L29**). A dramatic drop in ee was seen when electron-withdrawing group was used (4% ee, **L30**). Having a strong electron donating group like a methoxy group at *para* position of the aryl ring did not change the ee compared to the unsubstituted ring (60% ee, **L31**) while an *ortho*-substituted ligands gave better ee (77% ee, **L32**). The

ligand with two methoxy groups actually decreased the ee compared to a mono *o*-methoxy substituted ligand (71% ee, **L33**).

In summary, these aryl groups are clearly important in modulating the level of selectivity. An electron-withdrawing group is detrimental to the ee. However, to improve the ee, it was less obvious how to identify which properties of aryls/ligands should be tuned to obtain a better ee. This non-intuitive trends in ligand structure/product ee relationships are often observed in asymmetric catalysis, especially a transition-metal catalysed reactions.[157] To gain more information from these screening results, we subsequently used these results in a more quantitative way.

3.3.3 QSSR models for training set: Model I

As seen in **Figure 3-6**, the aryl moiety was shown to be the most influential part of the ligand to the value of ee. The average values of the ee were used except for some exceptions where repeats could not be carried out (see section 3.5.1). Next, we constructed a QSSR model to help guide us to design better ligands. To do this, we explored a linear regression between observed and calculated enantioselectivity (in kJ/mol).

To create a set of parameters describing the ligand's structure and properties, we computed 28 parameters for either ligands as a whole or just the aromatic substituents (see section 3.6.1). Only computed parameters for ligands were collected here rather than experimentally derived parameters because this way we could use the model prior to the synthesis of the new ligands. We have done our best to divide the nature of these parameters in to "steric" and "electronic" groupings,

however, in practice, these effects may not be fully decoupled and often go hand-in-hand.

To select parameters to be included in the model, we used an automated algorithm - a stepwise forward selection (see experimental section 3.6.2). These parameters were checked that the correlation between them is within recommended value (r^2 < 0.7, recommended < 0.8). Too high a correlation between parameters leads to problems of linear dependency during model building.

Our model contains the DFT-computed HOMO energy of the aryl rings as the electronic parameter. The HOMO is of π-character, and we considered that this captures the ability of these rings to interact/coordinate with substituents in a way which partial atomic charges, which are influenced by σ-contributions, cannot. The "steric" component of the model was described by the first generation Sterimol parameters: L, B_1 and B_3, quantifying different dimensions of the aryl rings (**Figure 3-7**).

The L parameter describes the length of the ring along the bond that connects the substituent to the rest of the ligand. In cases of flat aryl rings, B_1 represents the thickness of the ring (minimum width) and B_3 represents the width of the ring (width perpendicular to B_1). The calculated ee was a function of ligand descriptors as follows: $\Delta\Delta G^{\ddagger}$ (kJ/mol) = $1.27E_{HOMO} - 1.61B_1 + 1.13B_3 - 0.57L + 3.46$

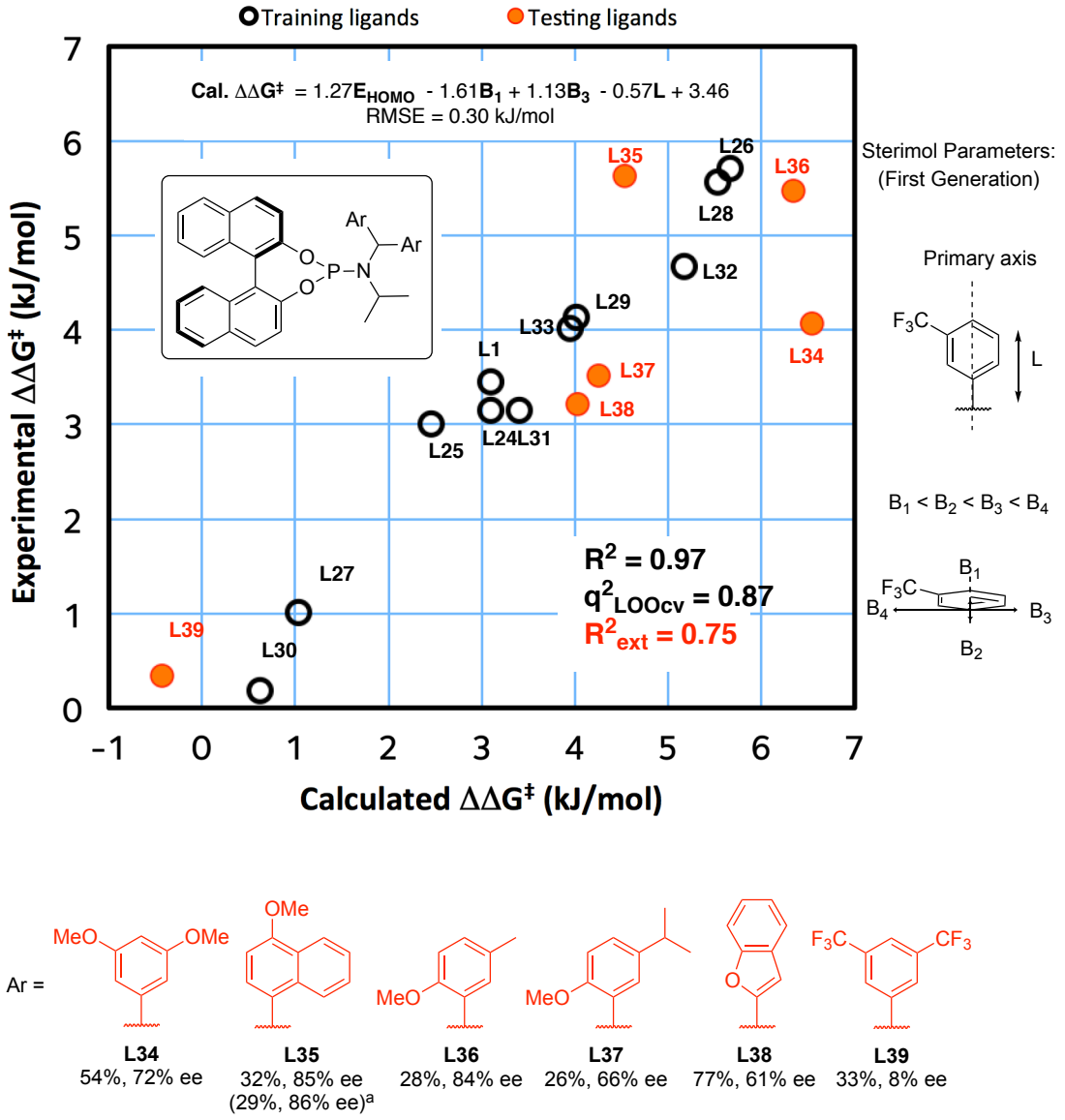

Figure 3-7 Model I: Correlation of experimentally observed enantioselectivity and calculated enantioselectivity (reported in kJ/mol) and results from the testing ligands. Yield based on ^{1}H NMR spectroscopy with $MeNO_2$ as internal standard of the crude reaction mixture. Enantiomeric excesses were determined by HPLC using a non-racemic stationary phase. [a]Results from the reaction which give the highest *ee* out of all repeats.

This model has a good fit of data as measured by the correlation coefficient (R^2) of 0.97 with root mean squared deviation (RMSD) of 0.30 kJ/mol. To validate the model, leave-one-out cross-validation (LOOCV) was carried out, giving a predictive squared correlation coefficient (q^2) of 0.87. To further validate the model's predictive power, a set of six new ligands was synthesised and tested (shown in red,

Figure 3-7). The model also performed acceptably for these testing ligands, with an $R^2_{ext} = 0.75$.

The testing set ligand spanned a range of ee's from 8-86% ee. The best ligand, **L35** gave ee's just as good as the training set. Analysis of variance (ANOVA) showed that the model and each parameter is statistically significant at 5% level of confidence (see experimental section 3.6.3). Having validated the model, we can be more confident in using it for guiding the synthesis of a better ligand, or drawing chemical interpretation behind the correlation.

3.3.4 Planned synthesis of better ligands

A virtual screen of novel chiral ligands that could give higher ee was performed (**Figure 3-8**). Only ligands whose starting materials were accessible in a few steps were considered. The model suggested that a flat (negative B_1) and wide ring (positive B_3) with high HOMO (positive E_{HOMO}) should be beneficial to the ee of the product (it should be remembered that although raw HOMO energies are themselves negative, the normalization process of converting the quantities into dimensionless quantities means that higher HOMO energies are in fact positive in the statistical model). Unfortunately, our attempts to synthesise these ligands were not successful.

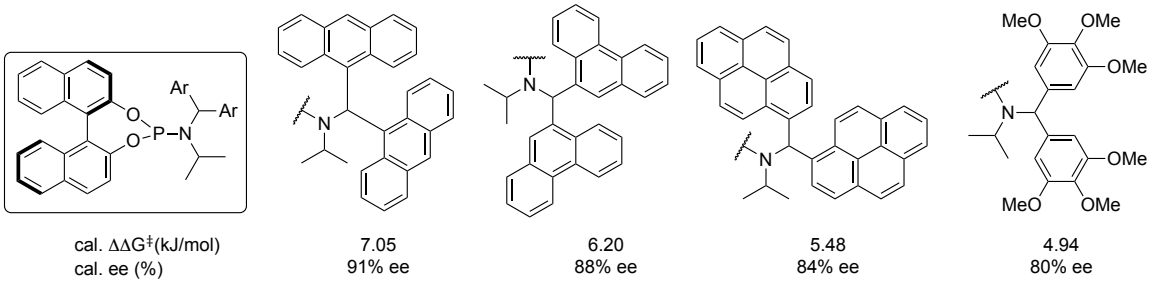

Figure 3-8 Predicted ee (reported in kJ/mol as well as % ee) for ligands in virtual screening.

3.3.5 DFT studies

We performed DFT calculations of competing transition structures (TSs) of the stereodetermining carbocupration step at the SMD(DCM)-B97D/def2-TZVPP//B97D/6-31G(d)&LANL2DZ level of theory (see experimental section 3.7 for details). Only the three lowest energy TSs are shown in **Figure 3-9**. **TS1** and **TS3** are the lowest energy TS and the third lowest energy TS which lead to the major enantiomer of the product. **TS2** is the second lowest energy TS which leads to the minor enantiomer of the product.

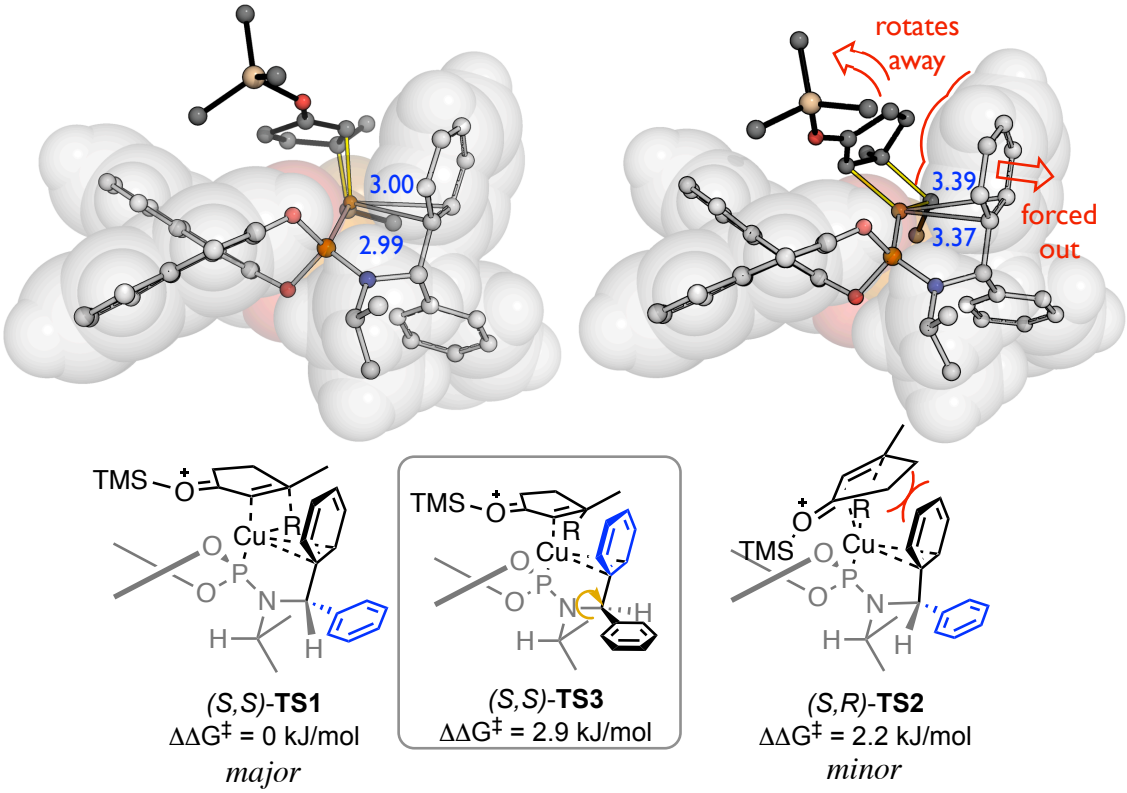

Figure 3-9 Competing transition structures, SMD(DCM)-B97D/def2-TZVPP//B97D/6-31G(d)&LANL2DZ level of theory. Distances between Cu and C_{Ar} (in blue, Å).

Diagrams of the 3D structures of the favoured TS (**TS1**) and the disfavoured TS (**TS2**) are also shown with Cu-C distances (Å) highlighted. Like in the 6-membered

ring, the favoured TS showed shorter Cu-C distances to one of the aryl ring (see section 2.2.2.5). Our calculations suggest a favourable non-covalent interaction between Cu and one of the aryl rings – as suggested by the interatomic separations (sum of van der Waals radii of Cu and C bond is 3.10 Å)[158]and computational e.g. NCI (see experimental section 3.7) and NBO analyses.[91] This Cu-arene interaction is more favourable in **TS1** leading to the major enantiomer. In the minor pathway *via* **TS2**, we reasoned that the bulk of the enone ring forced the aromatic substituent away from the Cu centre thus disrupting this interaction.

To interpret the electronic term (E_{HOMO}) in the QSSR model, we suggested that the favourable Cu-arene interaction is enhanced by aromatic electron-donating ability, and favours the major enantiomer: a positive correlation between enantioselectivity and E_{HOMO} is therefore expected.

The steric terms in the QSSR models are harder to interpret. This is partly because all the enantioselectivity data was obtained from ligands with two identical aryl rings. The current data offered no information about whether these steric terms (B_1, B_3, L) were in fact related to the blue or the black aryl ring which are diastereotopic to each other. Fortunately, there is also a probability that **TS1** and **TS3** which are related by a C-N bond rotation (indicated by a yellow arrow, **Figure 3-9**) can both play a role in inducing ee when the aryls are not identical and we might be able to synthesise ligands where only one aryl ring has a donor ability to interact with the Cu and the other aryl group has suitable steric bulk or may not even play a role at all. For these reasons, we saw the need to synthesise more ligands with non-identical aryl rings.

3.3.6 QSSR the second generation: Modell II

To further understand the meaning underlying the steric terms in QSSR and to obtain better ligands, we synthesised 19 new ligands with unsymmetrical diaryl moieties. These ligands we designed with two goals in mind; (1) to obtain ligands that are predicted to yield better *ee* as suggested by **Model I** (**Figure 3-7**), and (2) to have a set of ligands that spans suitable chemical space where they are varied in both steric bulk and electronic properties (**Figure 3-10**).

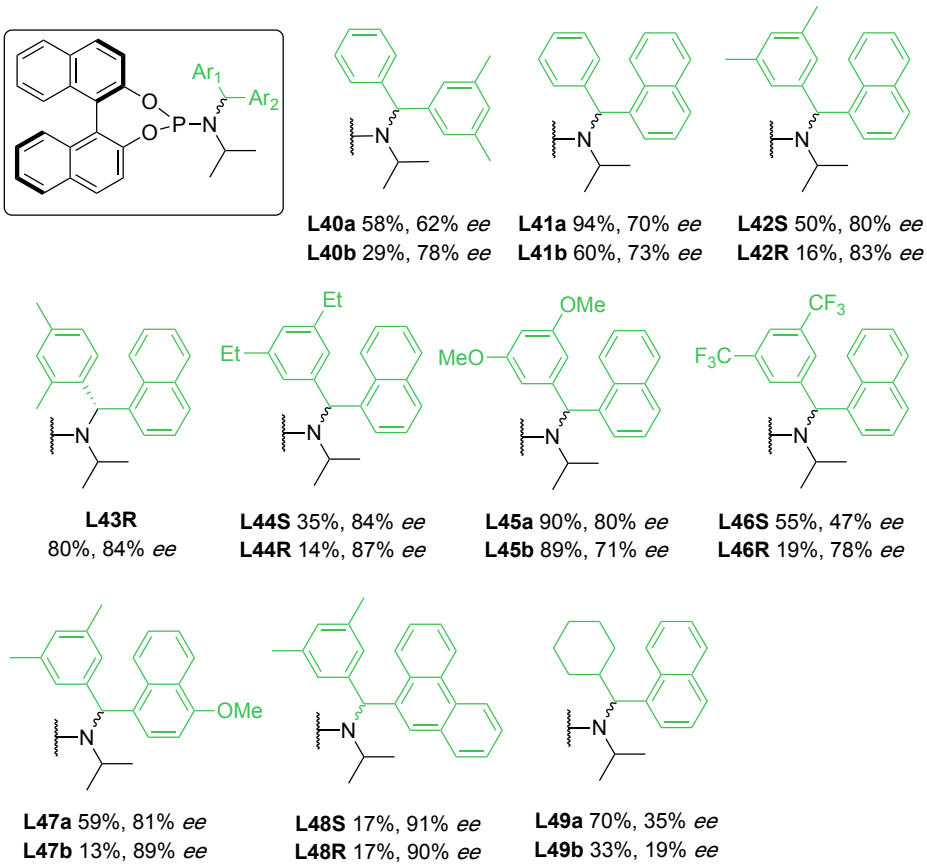

Figure 3-10 The ligand screening results with different chiral diaryl amido substituents. Yield based on ^{1}H NMR spectroscopy with $MeNO_2$ as internal standard of the crude reaction mixture. Ee's were determined by HPLC using a non-racemic stationary phase.

These new ligands contain a stereogenic centre at the benzylic carbon. We synthesised racemic amine precursors of the ligands. The amines were separated by HPLC using a non-racemic stationary phase by the team at Vertex pharmaceutical, Abingdon, UK and then subjected to condensation with PCl_3 and the enantiopure

(R)-BINOL backbone. For these new ligands, we did not know the absolute stereochemistry of the amines except for those identified by X-ray crystallography (**L42R**, **L43R** and **L48S**). For the rest of the ligands where the stereochemistry of the amines was unknown, we assumed that the diastereomer of the ligand that yielded higher ee corresponded to the stereochemistry that would place the aryl with higher HOMO energy next to the copper on **TS1** (**Figure 3-11**).

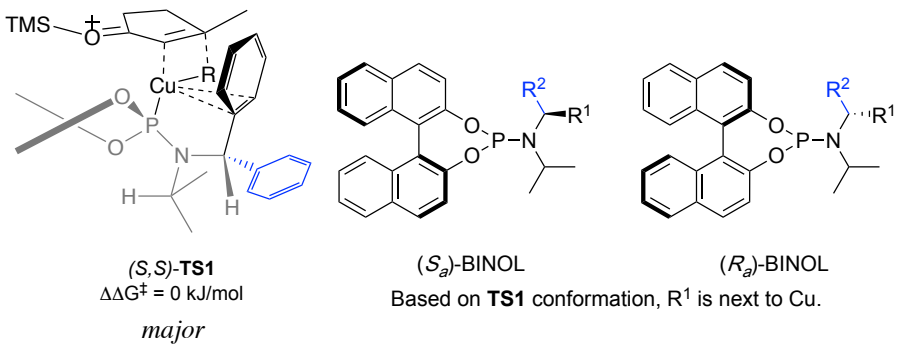

Figure 3-11 The lowest energy TS: **TS1** with ligand **L1** and the represention of R^1 (in black) with (R_a)- and (S_a)-BINOL

With these newly acquired data, we combined it with the previous training data set and derived a new QSSR model for all 30 ligands. Once again, these parameters were checked that there was no strong correlation between them (r^2 < 0.20). The new QSSR model took a form of the equation below, **Model II** (**Figure 3-12**)**:**

$$\Delta\Delta G^{\ddagger}\,(\text{kJ/mol}) = 0.74E_{HOMO}{}^{R1} + 0.59E_{HOMO}{}^{R2} - 1.10B_1{}^{R1} + 0.65B_3{}^{R1} + 0.51B_3{}^{R2} + 4.17$$

The previous set of ligands (**L24** – **L33**) is shown as black circles and the new ligands (**L40** – **L49**) are shown in green. Four of the new ligands give higher ee values (87-91% ee, **Figure 3-10**) than the previous set (86% ee in for **L26**, **L28** (**Figure 3-6**) and **L35**, (**Figure 3-7**)).

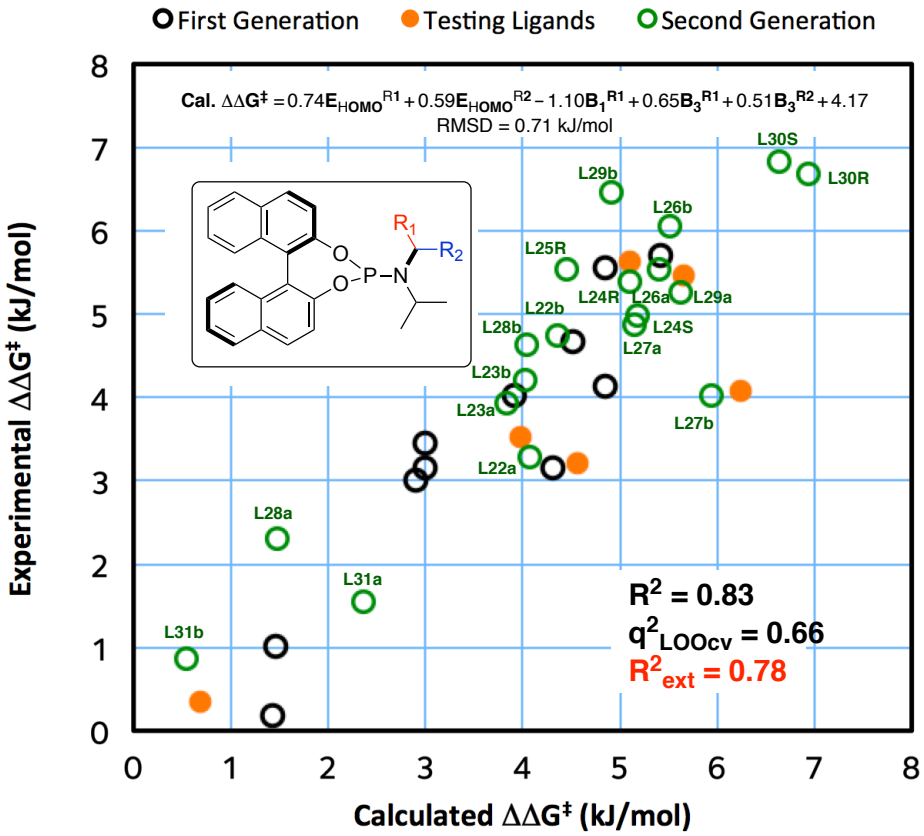

Figure 3-12 Model II: Correlation of experimentally observed enantioselectivity and calculated enantioselectivity (reported in kJ/mol) for the first (black) and second (green) generation training ligands and the testing ligands (red). Yield based on ^{1}H NMR spectroscopy with $MeNO_2$ as internal standard of the crude reaction mixture. Enantiomeric excesses were determined by HPLC using a non-racemic stationary phase. [a]Results from the reaction which give the highest *ee* out of all repeats.

The model has good fit (R^2 = 0.83) with RMSD = 0.71 kJ/mol. Internal validation with LOOCV gave q^2 = 0.65. The testing set ligands data gave good correlation (R^2_{ext} = 0.78). ANOVA showed that the model and each parameter are statistically significant at a 5% level of confidence except for the term B_3^{R2} which lies at the borderline (see section 3.6.3).

Similar models where the other steric terms are included or excluded gave slightly better or poorer fit. This model was balanced between a good fit and using few parameters. Inclusion of an L^{R2} term resulted in a new model with a slightly better fit but with fewer degrees of freedom, while exclusion of B_3^{R2} gave a worse fit (see experimental section 3.6.2.5).

Comparing the previous and this model, they both showed positive correlations of enantioselectivity with the aromatic HOMO energy and with the B_3 parameter, and a negative correlation with B_1 parameter. The duplicate of E_{HOMO} and B_3 terms for both aromatic substituents (R_1 and R_2) indicated that both rings may coordinate to copper, and that transition structures corresponding to both conformations are populated and contributed to the observed enantioselectivity.

3.3.7 Substrate scope

The QSSR models have led us to synthesise ligands with better ee's. In these screening reactions, the reactions are carried out in identical conditions. We often observed that the reactions with ligands that gave better ee are inherently slower than with the ligands that gave moderate ee's. We decided to compromise between product yield and ee and chose **L28** as a ligand to further explore the substrate scope of this reaction under optimised conditions (see experimental section 3.5.2 for further screening of conditions). Under the optimised conditions, we used Et_2O as a solvent rather than ^{t}BuOMe and carried out the reaction at 0.40 mmol scale (**Scheme 3-6**). The optimised conditions were applied to other simple aliphatic alkenes (**4**-**8**) giving up to 97% yield and 92% ee. The method has shown to be compatible with functionalised nucleophiles such as silyl, bromide, benzyl-protected alcohol and internal alkynyl groups (**9**-**13**; 57-82%, 85-90% ee). β-Substituted cyclopentenones bearing simple alkyl and a CH_2CH_2Ph substituent were also tested giving moderate yield and good ee's (**14**-**16**; 54-66%, 82-87% ee).

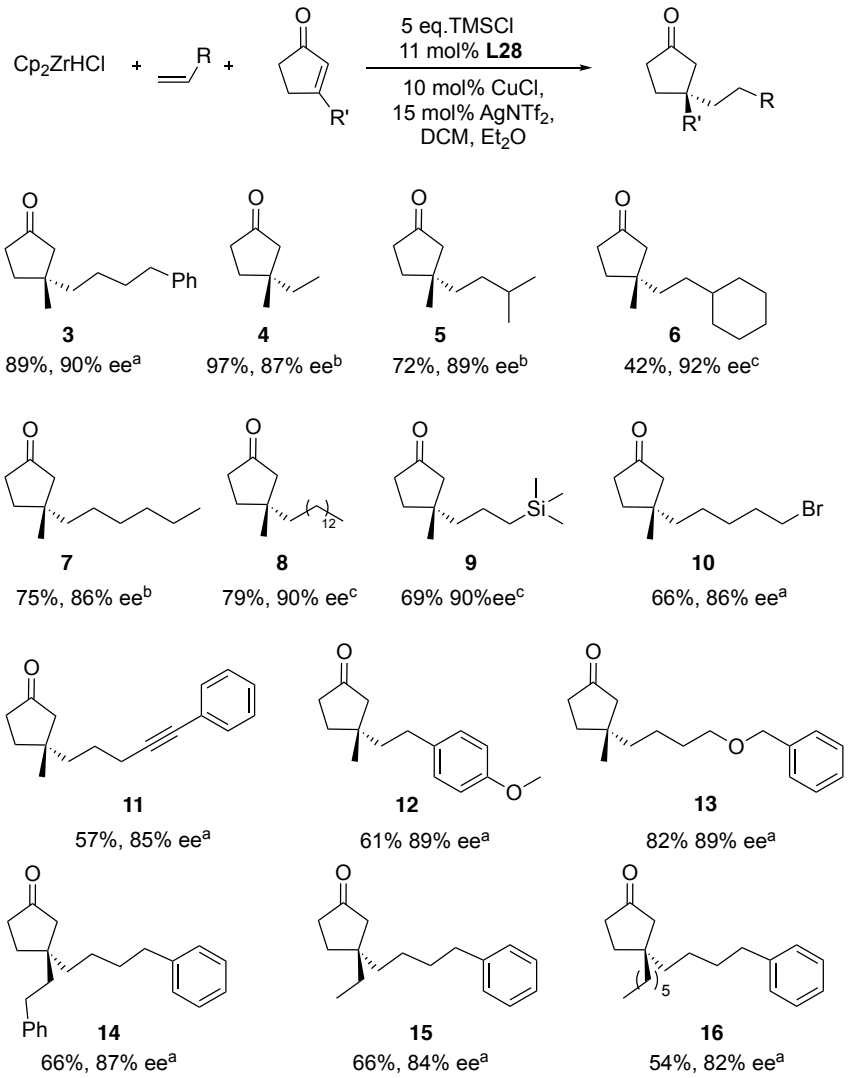

Scheme 3-6 Optimised condition and substrate scope for both reaction partners. Ee determined by [a]HPLC using a non-racemic stationary phase or SFC, [b]Chiral GC, [c]Derivatisation followed by HPLC.

3.4 Summary

We have developed a method for asymmetric conjugate addition to β-substituted cyclopentenones giving up to 97% yield and 92% ee with simple and functionalised nucleophiles. The approach for designing more enantioselective chiral ligands started with ligand screening and followed by construction of QSSR models to aid ligand design. A non-covalent interaction that plays an important role in the enantioinduction of product was identified as the interaction between the copper and aryl moieties which was established in QSSR models and was structurally

substantiated by DFT calculations. This has led to the development of new phosphoramidite ligands that give higher enantioselectivities.

3.5 Experimental Section

The isolated yields and the corresponding calculated yields of **3** based on the ^{1}H NMR of the crude reaction mixture with $MeNO_2$ as an internal standard is shown in **Figure 3-13**.

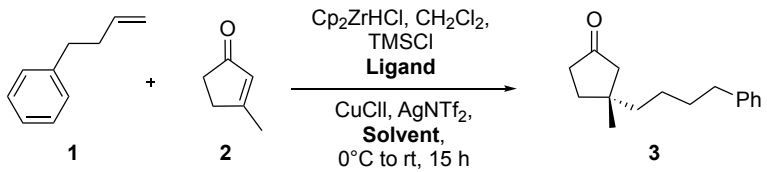

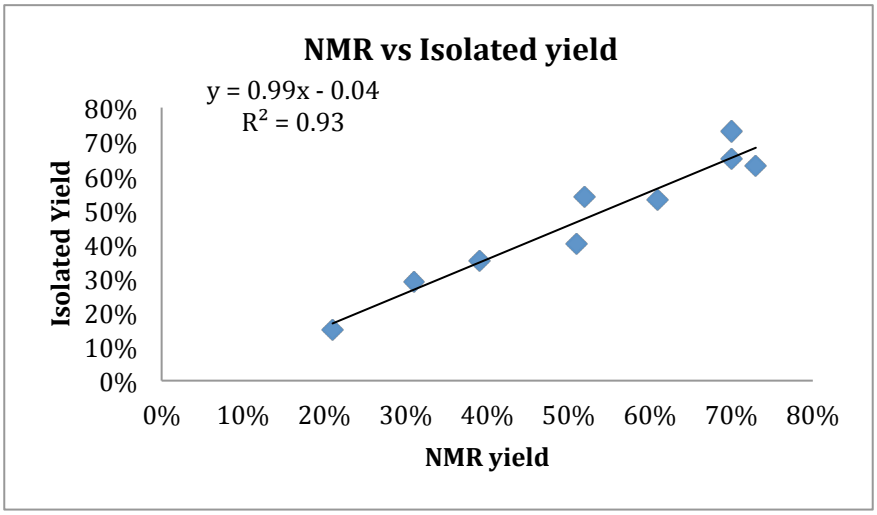

Figure 3-13 The isolated and calculated yields based on 1H NMR of the crude reaction mixture using $MeNO_2$ as an internal standard.

3.5.1 Reproducibility

Multiple repeats (2-6) are carried out using the screening reaction condition (**Scheme 3-5**) with different ligands. Average yield and ee of these repeats are tabulated in **Table 3-4**. The yield and ee are dependent on the quality of Schwartz reagent (Cp_2ZrHCl), the quality of silver salt ($AgNTf_2$). The inert atmosphere and TMSCl are required for reactivity. The Schwartz reagent is synthesised in a large

batch. The use of slightly older Schwartz reagent at the end of the batch resulted in slightly decreased in ee and noticeable reduction in yield. To test the quality of reagents, test reactions with ligand **L26** are carried out to give ee of 85% (±3%).

Table 3-4 The average yields and ee's over multiple repeats for ACA with different chiral ligands.

Ligand	Ligand Structure	Number of Repeats	Averaged Yield	Averaged ee (%)	Averaged ΔΔG‡ (kJ/mol)	RMSE ΔΔG‡ (kJ/mol)
L1	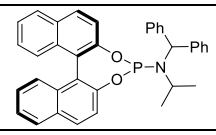	2	76%	64%	3.45	0.21
L27	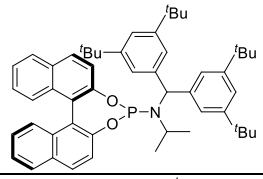	2	10%	22%	1.02	0.14
L26	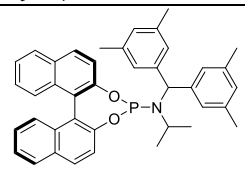	6	45%	85%	5.71	0.09
L28	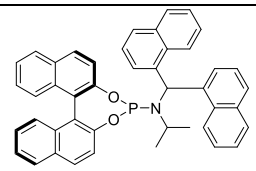	2	66%	84%	5.56	0.44
L29	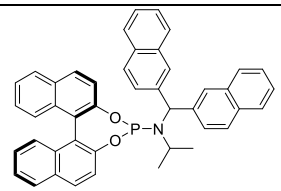	2	78%	72%	4.13	0.27
L32	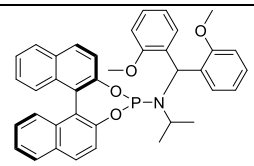	2	69%	77%	4.67	0.64
L33	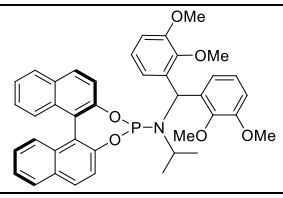	3	39%	71%	4.02	0.46
L34	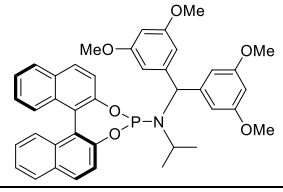	2	54%	72%	4.07	0.07

L35	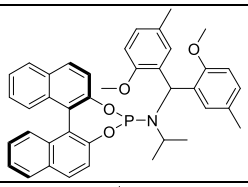	2	28%	84%	5.47	0.11
L35	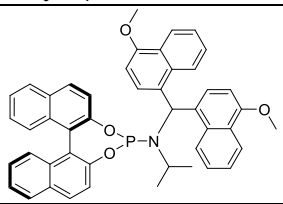	2	32%	85%	5.63	0.34
L45a	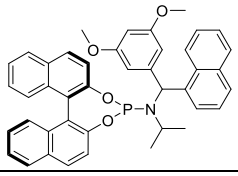	2	90%	80%	4.93	0.09
L45b	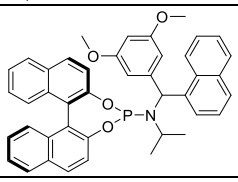	2	89%	71%	3.98	0.06
L46S	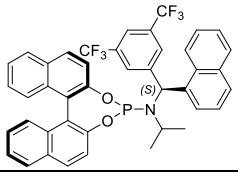	3	55%	47%	2.30	0.30
L46R	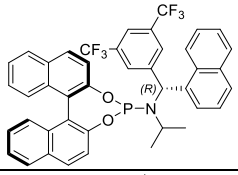	2	19%	78%	4.75	0.16
L47a	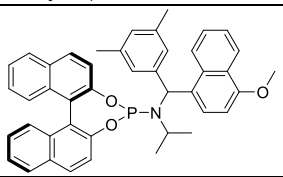	2	59%	81%	5.06	0.27
L47b	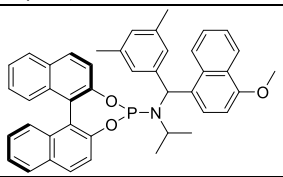	2	13%	89%	6.35	0.15
L48S	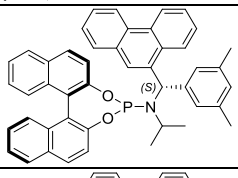	2	17%	91%	6.83	0.54
L48R	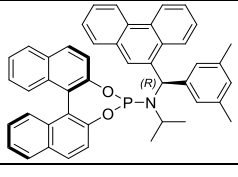	2	17%	90%	6.68	0.00

L49a	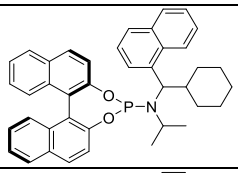	2	70%	35%	1.66	0.15
L49b	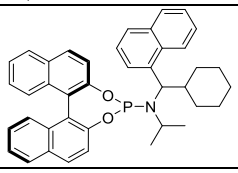	2	33%	19%	0.85	0.03

Reported yields are based on the ^{1}H NMR of the crude reaction mixture with $MeNO_2$ as internal standard, ee's were determined by HPLC using a non-racemic stationary phase.

3.5.2 Optimisation of condition

We selected a few ligands and screened the Cu and Ag sources, the solvents and temperatures to establish a new optimised reaction condition (**Table 3-5**, **Figure 3-14** and **Table 3-6**).

Table 3-5 Screening of copper and silver salts.

Entry	Ligand	Ag Salt[a]	Yield[b]	ee	Remarks
1	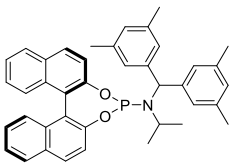 **L26**	$AgNTf_2$	31%	89%	~11% enone left
2		$AgNTf_2$	30%	40%	Anhydrous CuCl beads (white)
3		AgOTf	0%		„
4		$AgSbF_6$	0%		„
5		$AgClO_4$	17%	19%	<40% enone left
6		CuBr	trace	nd	
7		CuBr	trace	nd	~13% enone left
8		CuI + $AgNTf_2$	16%	88%	

[a]CuCl was used unless specified, [b]Yield based on ^{1}H NMR spectroscopy with $MeNO_2$ as internal standard of the crude reaction mixture..

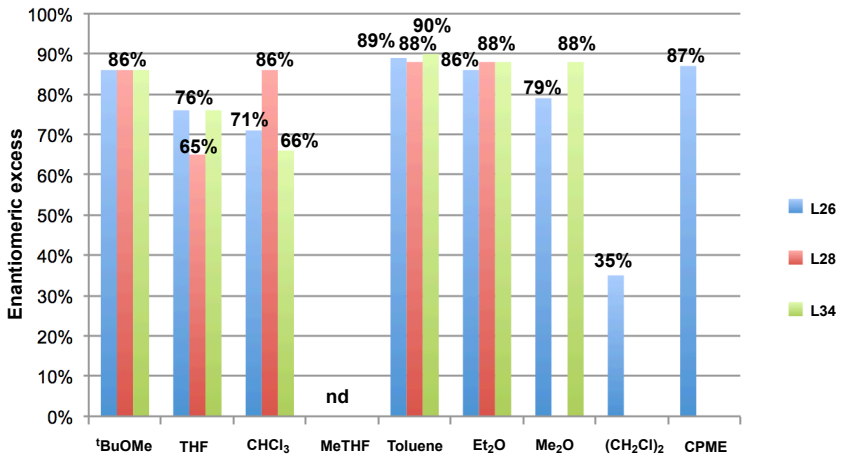

Figure 3-14 Solvent dependencies of enantiomeric excess (%) for **L26**, **L28** and **L34**.

The solvent for hydrozirconation step was always DCM and was omitted from the solvent screening plot and table (**Figure 3-14** and **Table 3-6**). Only the major solvent used in the reaction was shown.

Table 3-6 Temperatures and solvents screening

Entry	Ligand	solvent	Temp, time	Yield		*ee*	Remarks
				^{1}H	isolated		
1	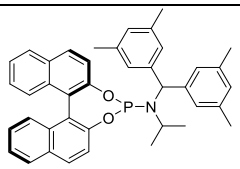 **L26**	^{t}BuOMe	0 °C	36%	-	86%	
2		^{t}BuOMe	rt	0%			
3		toluene	rt, 2.5h	20%	-	82%	<39% enone left
4		toluene	0 °C	31%	-	89%	~11% enone left
5		Et_2O	-10 °C	80%	-	52%	14% enone
6		toluene, Et_2O	0 °C	64%	-	89%	15% enone
7		toluene, Et_2O	0 °C, 1h	36% [c]	-	87%	
8		toluene, Et_2O	0 °C, 5h	71% [c]	-	89%	
9		toluene, Et_2O	0 °C, 9h	78% [c]	-	88%	
10		toluene, Et_2O	0 °C, 24h	87% [c]	-	88%	Trace of enone
11		toluene, Et_2O	0 °C	80%	-	60%	9% enone
12		toluene, Et_2O	-10 °C, 21h	46%	-	89%	26% enone
13		toluene	-10 °C	32%	-	89%	3 eqv. [Zr] <54% enone left
14		toluene	-10 °C	31%	-	89%	20mol% [Cu] <49% enone left
15		toluene	-10 °C	26%	-	91%	<47% enone left
16		toluene	-30 °C	0%	-	-	<70% enone left
17	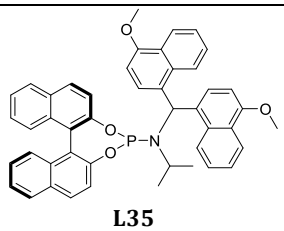 **L35**	toluene	rt, 2.5h	15%	-	75%	<43% enone left
18		toluene	0 °C	27%	7%	90%	~27% enone left
19		toluene	-10 °C	32%	10%	91%	20mol% [Cu], 46% enone
20		toluene, Et_2O	-10 °C, 38 h	43%		83%	0.40mmol

3.5.3 General experimental information

All reactions were performed under an $Ar_{(g)}$ atmosphere. Anhydrous Et_2O, DCM and THF were obtained from mBraun SPS-800 solvent purification system equipped with anhydrous alumina columns. Anhydrous ^{t}BuOMe was dried in 4 Å molecular

sieves. Anhydrous MeOH and other solvents were used as purchased. Preformed ligand-copper complexes were filtered under $Ar_{(g)}$ atmosphere through polytetrafluorethane syringe filter (13 mm, 0.2 μm). Freshly distilled PCl_3 and distilled TMSCl in $CaH_{2(s)}$ were used. Thin layer chromatography (TLC) plates were examined under UV light (λ_{max} = 254 nm) and stained using ceric ammonium molybdate (CAM) or potassiumpermanganate ($KMnO_4$) solutions.

^{1}H, ^{13}C and ^{31}P NMR spectra were measured by Bruker AVIII400, AVII400, and Ascend™ 400 MHz machines in $CDCl_3$ solvent. Chemical shifts were reported in part per million, referenced to solvent residue peaks. Scalar coupling patterns were described as singlet (s), doublet (d), triplet (t), quartet (q) or multiplet (m). Broad peaks are indicated as (br). Coupling constants (*J*) were quoted to one decimal place. Chemical shifts were quoted to two decimal places in ^{1}H NMR and one decimal place in ^{13}C NMR and ^{31}P NMR. HSQC, COSY, DEPTQ and HMBC based experiments were performed to aid the assignment of spectra.

Chiral HPLC separations were achieved using an Agilent 1260 Infinity series normal phase HPLC unit and HP Chemstation software. Preparative chiral SFC separations were carried out by the analytical group at Vertex Pharmaceuticals, Milton Park, Abingdon using a Waters SFC 100 or a Berger Minigram. Chiral columns (250x20 mm (SFC 100) or 250x10 mm (Minigram)) were used as specified in the text. Chiral GC measurements were conducted on a HP6890 (H2 as vector gas) or HP6850 (H_2 as vector gas) with the stated column in the characterization. Temperature programs are described as follows: initial temperature (°C) - initial time (min) - temperature gradient (°C/min) –[certain temperature – holding time - temperature gradient (°C/min)]- final temperature (°C) – holding time. Retention times (t_R) are given in

min. Chiralpak® columns (250×4.6 mm), fitted with matching Chiralpak® Guard Cartridges (10×4 mm), were used as specified in the text. Chiral SFC (supercritical fluid chromatography) separations were conducted on a Waters Acquity UPC^2 system using Waters Empower software. Chiralpak® columns (150 × 3 mm, particle size 3 μm) were used. Solvents used were of HPLC grade (Fisher Scientific, Sigma Aldrich or Rathburn). Solvents used were of HPLC grade (Fisher Scientific, Sigma Aldrich or Rathburn); all eluent systems were isocratic.

Infra-red spectra were recorded on a Bruker Tensor 27 FTIR spectrometer equipped with a PIKE Miracle Attenuated Total Reflectance sampling accessory using a solid sample or thin film for liquid compounds. IR data was reported in wavenumbers (cm^{-1}).

High Resolution Mass spectra were carried out by the internal service at the university of Oxford. (1) Electron spray ionisation (ESI+) were recorded on a Fisons Platform II. (2) Electron ionisation (EI)/Chemical ionisation (CI): Analyses were performed on an Agilent 7200 quadrupole time of flight (Q-ToF) instrument equipped with a direct insertion probe supplied by Scientific instrument Manufacturer (SIM) GmbH. Instrument control and data processing were performed using Agilent MassHunter software. The system was calibrated on the day of the analysis and its mass accuracy with external calibration (as used for these experiments) is better than 5ppm for 24 hours following calibration. Source conditions for both EI and CI were adjusted to maximise sensitivity, the reagent gas used in CI was either methane or ammonia (and should be apparent in the metadata associated with the data). (3) Atmospheric pressure chemical ionisation (APCI+): Analyses were performed using a Thermo Exactive mass spectrometer equipped

with Waters Acquity liquid chromatography system. Instrument control and data processing were performed using Thermo Xcalibur Software. The system was calibrated on the day of the analysis and its mass accuracy with external calibration (as used for these experiments) is better than 5ppm for 24 hours following calibration. The mass spec was operated using the APCI probe and resolution was set to 50,000. APCI source conditions were adjusted to maximise sensitivity. A mixture of 10% water, 89.9% methanol and 0.1% formic acid was used to transport samples to the mass spectrometer at a flow rate of 0.2 mL/min.

Chemical names were generated from CambridgeSoft ChemBioDraw Ultra 17.1 programme. Optical rotations ($[\alpha]_D^T$) were recorded from a Perkin Elmer 241 Polarimeter and are reported in degree·ml(·g·dm)$^{-1}$. Samples were prepared at concentration (c) measured in mg·ml^{-1}.

3.5.4 General procedures

Schwartz reagent (Cp_2ZrHCl) was prepared according to procedure developed by Wipf[159]. $AgNTf_2$ was prepared according to procedure developed by Huber and Rolling[160].

General procedure A – conjugate addition

In an aluminium foil wrapped, flame dried round bottom flask equipped with a stirrer bar, $CuCl_{(s)}$ (0.10 eq.), $ligand_{(s)}$ (0.11 eq.), and solvent (1.0 ml) were added and stirred at rt for 1 h. $AgNTf_{2(s)}$ (0.15 eq.) was added and the mixture was stirred for further 30 mins. In the meantime, in a separate, dried, foil wrapped round bottom flask, dried DCM (0.20 ml) $alkene_{(l)}$ and Schwartz $reagent_{(s)}$ (Cp_2ZrHCl, 0.20 eq.) was stirred at rt in the dark. Once a clear yellow/orange solution of

organozirconium was obtained, the ligand mixture was filtered throughto the organozirconium flask and the combined solution was stirred at 0 ˚C for 25 mins. Enone (1 eq.) and $TMSCl_{(l)}$ (5 eq.) was added and the reaction mixture was stirred while left to slowly warm up to rt over 15 h. Et_2O (ca.3 ml) and 1 M $NH_4Cl_{(aq)}$ (ca.2 ml) were added to the reaction and stirred for 30 mins before the mixture was partitioned into aqueous and organic phases. The aqueous layer was then extracted with Et_2O three times. The combined organic layer was washed with sat.$NaHCO_{3(aq)}$ and dried with anhydrous $Na_2SO_{4(s)}$. The solvent was evaporated under reduced pressure. The crude mixture was purified by flash column chromatography.

The stereochemistry of the conjugate addition products were assigned compared to literature known compounds or based on chirality of the BINOL backbone of the ligand used.

Ligand screening:

Screening of ligands was carried out according to **procedure A** with 4-phenyl-1-butene (2.5 eq.).

Yields were calculated based on ^1H NMR of the crude mixture with $MeNO_2$ as an internal standard. The crude mixture was filtered through silica gel (petrol/EtOAc = 95:5) and solvent was removed *in vacuo* prior to ee analysis by chiral HPLC.

General Procedure B – Amine synthesis[161]

Ketone (1.0 eq.) was dissolved in DCM and cooled in an ice bath. After 10 mins, $TiCl_4$ solution in DCM (1.0 M, 1.1 eq.) was added dropwise to the solution of the ketone at 0 ˚C. The ice bath was removed and the stirring solution was slowly warmed up to rt.

After 10 mins, a solution of amine (2.2-3.0 eq.) was diluted in THF and was added dropwise to the stirring solution of the ketone. The mixture was stirred at rt for 3 h. A solution of $NaB(CN)H_3$ dried under high vacuum before used, 1.2-5.0 eq.) in THF was slowly added to the stirring reaction mixture followed by the addition of anhydrous MeOH and the suspension was stirred at rt for a specified length of time. $NaOH_{(aq)}$ (2 M) was then added while stirring. The mixture was filtered through Celite/EtOAc. $NaHCO_{3(sat.)}$ was added and the mixture was partitioned between organic and aqueous phase. The aqueous layer was extracted by Et_2O three times. The combined organic layer was concentrated *in vacuo* and acidified with concentrated HCl. The acidic mixture was partitioned and the ethereal layer was extracted with 1 M HCl three times. The combined acidic aqueous layer was basified with 25% NaOH until pH≈14. The basic layer was extracted with DCM three times. The combined DCM fraction was dried with $MgSO_{4(s)}$. The mixture was filtered before the solvent was remove *in vacuo* and dried or freeze-dried under high vacuum.

Alternative purification techniques:

$NaHCO_{3(sat)}$ was then added while stirring. The mixture was filtered through Celite/EtOAc. The biphasic solution was concentrated *in vacuo* and the aqueous layer was extracted by EtOAc three times. The combined organic layer was dried with $MgSO_{4(s)}$ and was concentrated *in vacuo* and filtered through a strong cation exchange column ISOLUTE® SCX-2 (propylsulfonic acid) with MeOH to wash off non-basic component followed by ammonia solution in MeOH (2 M). The ammonium solution was concentrated and dry under high vacuum.

General procedure C - Ligand Synthesis[162]

Freshly distilled $PCl_{3(l)}$ (1.1 eq.) was diluted in DCM and cooled in an ice bath. Et_3N (5.0 eq.) was added dropwise to the cooled, stirring solution of PCl_3. The ice bath was removed and the solution was left to slowly warm up to rt over 10 mins. The amine (1.0 eq.) in DCM was added dropwise to the stirred solution of Et_3N. The reaction mixture was stirred at rt for 5 h before enaniopure BINOL (1.3 eq.) was added and the mixture was stirred overnight at rt. The mixture was filtered through Celite/DCM and solvent was evaporated under reduced pressure. The crude mixture was purified by flash column chromatography.

Procedures for ligands that were not synthesised by the author but were used in this work can be found in previously reported procedures.[91]

General procedure D – Derivatisation of ketone[163]

To a flamed dried round bottom flask with a stirrer bar, ketone (1.0 eq.), DCM (0.5 M) and mCPBA (2.6 eq.) were added and stirred under $Ar_{(g)}$. The flask was placed in an ice bath and wrapped in an aluminium foil before trifluoroacetic $acid_{(l)}$ (1.0 eq.) was added dropwise over 10 mins. The reaction mixture was stirred overnight and slowly warm up to rt. The conversion of the ketone starting material was monitored by TLC with $KMnO_4$ stain. Once the starting material is consumed, the reaction mixture was washed with $Na_2SO_{3\,(aq)}$ (5% solution, ca. 2 ml), $NaHCO_{3(sat)}$ and $H_2O_{(l)}$. The organic layer was dried with $MgSO_{4(s)}$. The crude reaction mixture was used in the subsequent step without further purification.

To a flamed dried round bottom flask with a stirrer bar, the crude reaction mixture (1.0 eq.), DCM (0.1 M) and $AlMe_3$ (1.6 eq.) were added and stirred under $Ar_{(g)}$. The flask was placed in ice bath before $benzylamine_{(l)}$ (2.0 eq.) was added dropwise. The

reaction mixture was stirred overnight and slowly warm up to rt. The conversion of the ketone starting material was monitored by TLC with $KMnO_4$ stain. Once the starting material is consumed, $HCl_{(aq)}$ (1 M, ca. 3 ml) was added and the aqueous layer was extracted by DCM (ca. 5 ml) three times. The combined organic layer was dried with $MgSO_{4(s)}$ and dried *in vacuo*. The crude reaction mixture was filtered through silica gel with EtOAc:Et_3N eluent and the solvent was removed *in vacuo*.

3.5.5 Experimental details

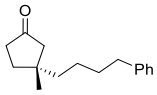

(+)-*(R)*-3-methyl-3-(4-phenylbutyl)cyclopentan-1-one **3**

General procedure A: $CuCl_{(s)}$ (4.0 mg, 0.04 mmol, 0.10 eq.), (R_a)-*N*-(di(naphthalen-1-yl)methyl)-*N*-isopropyldinaphtho[2,1-*d*:1',2'-*f*][1,3,2]dioxaphosphepin-4-amine (28.2 mg, 0.22 mmol, 0.11 eq.), Et_2O (2.0 ml), $AgNTf_{2(s)}$ (23.8 mg, 0.06 mmol, 0.15 eq.), DCM (0.4 ml) 4-phenyl-1-butene$_{(l)}$ (150 µl, 1.0 mmol, 2.5 eq.), Cp_2ZrHCl (206.2 mg, 0.80 mmol, 2.0 eq.), 3-methyl-2-cyclopentenone (40 µl, 0.40 mmol, 1 eq.) and $TMSCl_{(l)}$ (0.25 ml, 1.0 mmol, 5.0 eq.)

The crude mixture was treated as described above and was purified by flash column chromatography [SiO_2, pentane/EtOAc = 95:5] to afford colourless oil of (+)-*(R)*-3-methyl-3-(4-phenylbutyl)cyclopentan-1-one (82.3 mg, 89%).

^{1}H NMR (400 MHz, $CDCl_3$) δ_H: 7.38 – 7.26 (m, 2H, $2C_{Ar}H$), 7.25 – 7.17 (m, 3H, $3C_{Ar}H$), 2.70 – 2.61 (m, 2H, $CH_2CH_2CH_2Ph$), 2.39 – 2.21 (m, 2H, CH_2CH_2CO), 2.18 – 1.98 (m, 2H, $MeCCH_2CO$), 1.89 – 1.71 (m, 2H, CH_2CH_2CO), 1.73 – 1.54 (m, 2H, CH_2CH_2Ph), 1.52 – 1.21 (m, 4H, CH_2Ph and $MeCCH_2$), 1.06 (s, 3H, CH_3).

^{13}C NMR (101 MHz, $CDCl_3$) δ_C: 220.2, 142.6, 128.5 (2C), 128.4 (2C), 125.8, 52.4, 41.7, 39.7, 36.9, 36.0, 35.4, 32.2, 25.2, 24.5.

IR υ_{max} (l): 2930, 1738, 1496, 1153, 698.

HRMS (ESI^+) $[C_{16}H_{22}ONa]^+$ predicted 253.1568, found 253.1563 (Δ –0.1 ppm).

HPLC analysis indicated an enantiomeric excess of 90% [Chiralpak® AY-H; flow: 1 mL/min; hexane/^{i}PrOH = 95:5; λ = 210 nm; minor enantiomer (–)-(*S*)-3-methyl-3-(4-phenylhexyl)cyclopentanone, t_R = 7.77 min; major enantiomer (+)-(*R*)-3-methyl-3-(4-phenylhexyl)cyclopentanone, t_R = 8.30 min].

$[\alpha]_{589}^{25}$ = +27.4 (*c* 1.00, $CHCl_3$).

Data was consistent with previously reported values.[108]

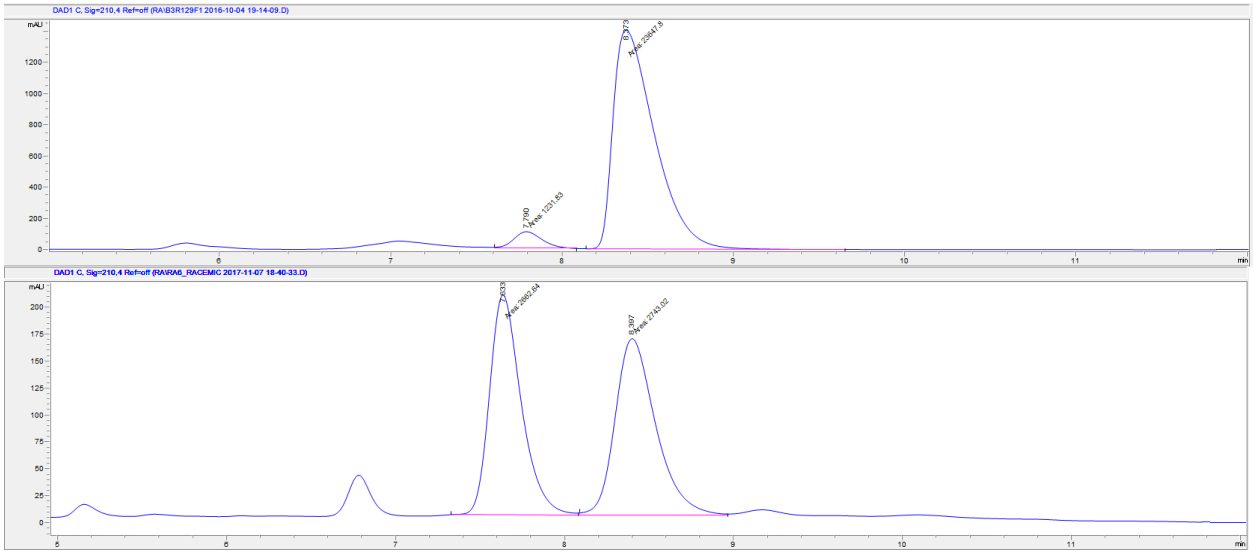

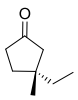

(*R*)-3-ethyl-3-methylcyclopentan-1-one **4**

General procedure A: $CuCl_{(s)}$ (4.0 mg, 0.4 mmol, 0.10 eq.), ligand *(Ra)-N*-(di(naphthalen-1-yl)methyl)-*N*-isopropyldinaphtho[2,1-*d*:1',2'-

f][1,3,2]dioxaphosphepin-4-amine$_{(s)}$ (28.2 mg, 0.04 mmol, 0.11 eq.), Et_2O (2.0 ml), $AgNTf_{2(s)}$ (23.8 mg, 0.06 mmol, 0.15 eq.), DCM (0.40 ml), Cp_2ZrHCl (206.0 mg, 0.80 mmol, 2.0 eq.) in ethene$_{(g)}$ atmosphere (balloon), 3-methyl-2-cyclopentenone (40 µl, 0.40 mmol, 1.0 eq.) and $TMSCl_{(l)}$ (0.25 ml, 2.0 mmol, 5.0 eq.)

The crude mixture was treated as described above as described above and was purified by flash column chromatography [SiO_2, pentane/EtOAc = 96:4] to afford pale yellow oil of (*R*)-3-ethyl-3-methylcyclopentan-1-one (49.1 mg, 97%).

GC analysis indicated an enantiomeric excess of 87% [Macherey & Nagel, Lipodex® E; 60-30 λ = 210 nm; major enantiomer, t_R = 16.8 min; minor enantiomer, t_R = 19.5 min].

^{1}H NMR (400 MHz, $CDCl_3$) δ_H: 2.38 – 2.22 (m, 2H, COC*H*$_2$), 2.12 – 1.95 (m, 2H, COC*H*$_2$), 1.88 – 1.66 (m, 2H, C*H*$_2$), 1.44 (q, *J* = 7.6 Hz, 2H, C*H*$_2$CH$_3$), 1.03 (s, 3H, C*H*$_3$), 0.90 (t, *J* = 7.5 Hz, 3H, CH$_2$*CH*$_3$).

^{13}C NMR (101 MHz, $CDCl_3$) δ_C: 220.4, 52.0, 39.9, 37.0, 34.9, 34.1, 24.7, 9.2.

IR υ_{max} (film): 3051, 2980, 1737, 777.

$[\alpha]_{589}^{25}$ = +28.7 (*c* 1.00, $CHCl_3$).

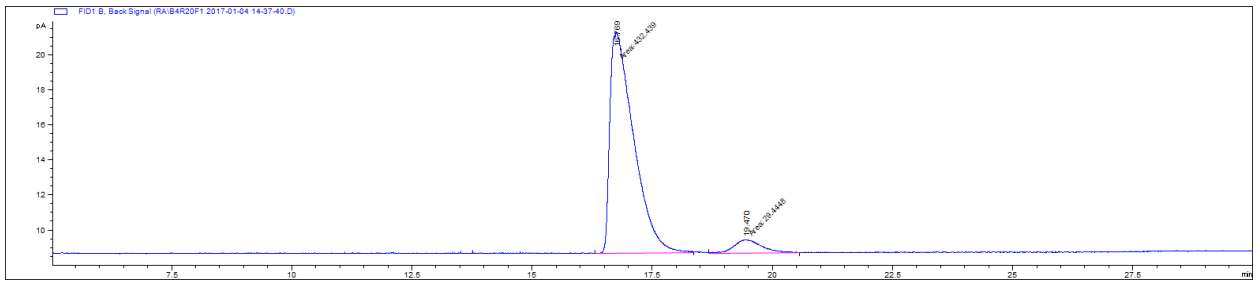

Data was consistent with previously reported values.[144]

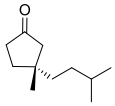

(*R*)-3-isopentyl-3-methylcyclopentan-1-one **5**

General procedure A: $CuCl_{(s)}$ (4.0 mg, 0.4 mmol, 0.10 eq.), ligand *(R_a)-N*-(di(naphthalen-1-yl)methyl)-*N*-isopropyldinaphtho[2,1-*d*:1',2'-*f*][1,3,2]dioxaphosphepin-4-amine$_{(s)}$ (28.2 mg, 0.04 mmol, 0.11 eq.), Et_2O (2.0 ml), $AgNTf_{2(s)}$ (23.8 mg, 0.06 mmol, 0.15 eq.), DCM (0.40 ml) 3-methylbut-1-ene$_{(l)}$ (70 mg, 1.00 mmol, 2.5 eq.), Cp_2ZrHCl (206.0 mg, 0.80 mmol, 2.0 eq.), 3-methyl-2-cyclopentenone (40 µl, 0.40 mmol, 1.0 eq.) and $TMSCl_{(l)}$ (0.25 ml, 2.0 mmol, 5.0 eq.)

The crude mixture was treated as described above and was purified by flash column chromatography [SiO_2, pentane/EtOAc = 97:3] to afford colourless oil of 3-isopentyl-3-methylcyclopentan-1-one (48.5 mg, 72%).

GC analysis indicated an enantiomeric excess of 89% [Macherey & Nagel, Lipodex® E; 60-30-0.1-70-10, λ = 210 nm; major enantiomer, t_R = 61.3 min; minor enantiomer, t_R = 65.0 min].

^{1}H NMR (400 MHz, $CDCl_3$) δ_H: 2.36 – 2.17 (m, 2H, COC*H*$_2$), 2.10 – 1.93 (m, 2H, COC*H*$_2$), 1.85 – 1.67 (m, 2H, C*H*$_2$), 1.52 – 1.32 (m, 3H, C*H*$_2$, C*H*), 1.25 – 1.06 (m, 2H, C*H*$_2$), 1.02 (s, 3H, C*H*$_3$), 0.87 (d, *J* = 6.6 Hz, 6H, CH(C*H*$_3$)$_2$).

^{13}C NMR (101 MHz, $CDCl_3$) δ_C: 220.3, 66.0, 52.4, 39.6, 39.5, 36.9, 35.3, 33.9, 28.7, 25.2, 25.1, 22.8, 22.7, 15.4 (2C).

HRMS (ESI^+) $[C_{11}H_{21}O]^+$ predicted 169.15869, found 169.15880 (Δ 0.63 ppm).

IR υ_{max} (film): 1954, 2962, 2870, 1739, 1137.

$[\boldsymbol{\alpha}]_{589}^{25}$ = +28.7 (*c* 1.00, $CHCl_3$).

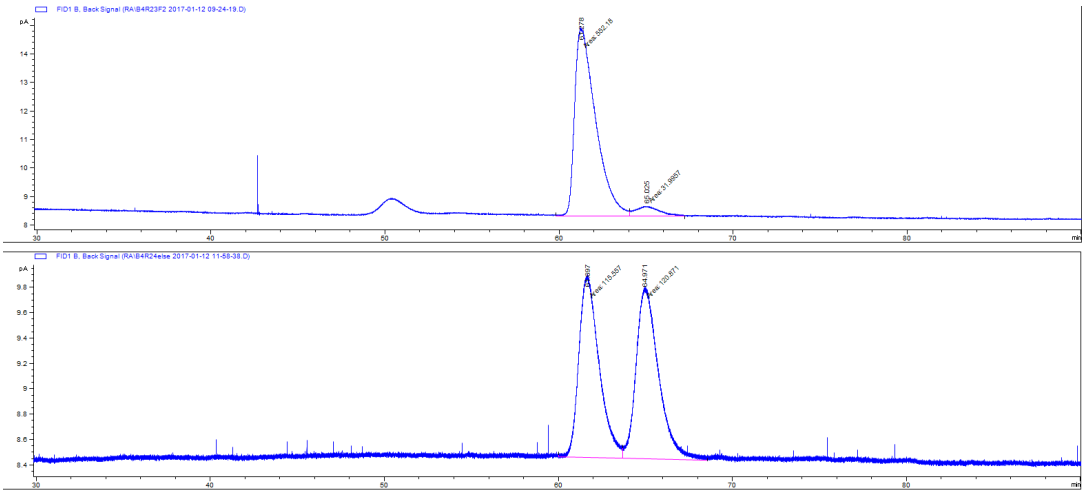

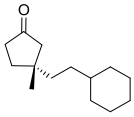

(*R*)-3-(2-cyclohexylethyl)-3-methylcyclopentan-1-one **6**

General procedure A: $CuCl_{(s)}$ (4.0 mg, 0.4 mmol, 0.10 eq.), ligand *(R_a)-N*-(di(naphthalen-1-yl)methyl)-*N*-isopropyldinaphtho[2,1-*d*:1',2'-*f*][1,3,2]dioxaphosphepin-4-amine$_{(s)}$ (28.2 mg, 0.04 mmol, 0.11 eq.), Et_2O (2.0 ml), $AgNTf_{2(s)}$ (23.8 mg, 0.06 mmol, 0.15 eq.), DCM (0.40 ml) vinylcyclohexane$_{(l)}$ (140 µl, 1.00 mmol, 2.5 eq.), Cp_2ZrHCl (206.0 mg, 0.80 mmol, 2.0 eq.), 3-methyl-2-cyclopentenone (40 µl, 0.40 mmol, 1.0 eq.) and $TMSCl_{(l)}$ (0.25 ml, 2.0 mmol, 5.0 eq.)

The crude mixture was treated as described above and was purified by flash column chromatography [SiO_2, pentane/EtOAc = 98:2] to afford colourless oil of 3-(2-cyclohexylethyl)-3-methylcyclopentan-1-one (70.5 mg, 42%).

The enantiomeric excess of the product was determined by chiral SFC after two steps derivatisation (**General procedure D**).

SFC analysis indicated an enantiomeric excess of 92% [Chiralpak® IA-3; 1500 psi, 30 °C, flow: 1.5 mL/min; 1% to 30% MeOH in 8 min; λ = 210 nm; major enantiomer, t_R = 4.39 min; minor enantiomer, t_R = 4.57 min].

^{1}H NMR (400 MHz, $CDCl_3$) δ_H: 2.37 – 2.22 (m, 2H, COC*H*$_2$), 2.13 – 1.95 (m, 2H, COC*H*$_2$), 1.85 – 1.58 (m, 9H, 4(C*H*$_2$), C*H*$_a$H$_b$), 1.43 – 1.33 (m, 2H, C*H*$_2$), 1.28 – 1.06 (m, 4H, C*H*, C*H*$_2$, CH$_a$*H*$_b$), 1.02 (s, 3H, C*H*$_3$), 0.93 – 0.80 (m, 2H, C*H*$_2$).

^{13}C NMR (101 MHz, $CDCl_3$) δ_C: 220.5, 52.4, 39.6, 39.1, 38.4, 37.0, 35.3, 33.6, 33.5, 32.5, 26.8, 26.5 (2C), 25.2.

HRMS (ESI$^+$) $[C_{14}H_{25}O]^+$ predicted 209.19026, found 209.18999 (Δ 1.29 ppm).

IR υ_{max} (film): 2989, 2920, 2851, 1740, 1449, 1380, 1163, 957.

$[\boldsymbol{\alpha}]_{589}^{25}$ = +29.6 (*c* 1.00, $CHCl_3$).

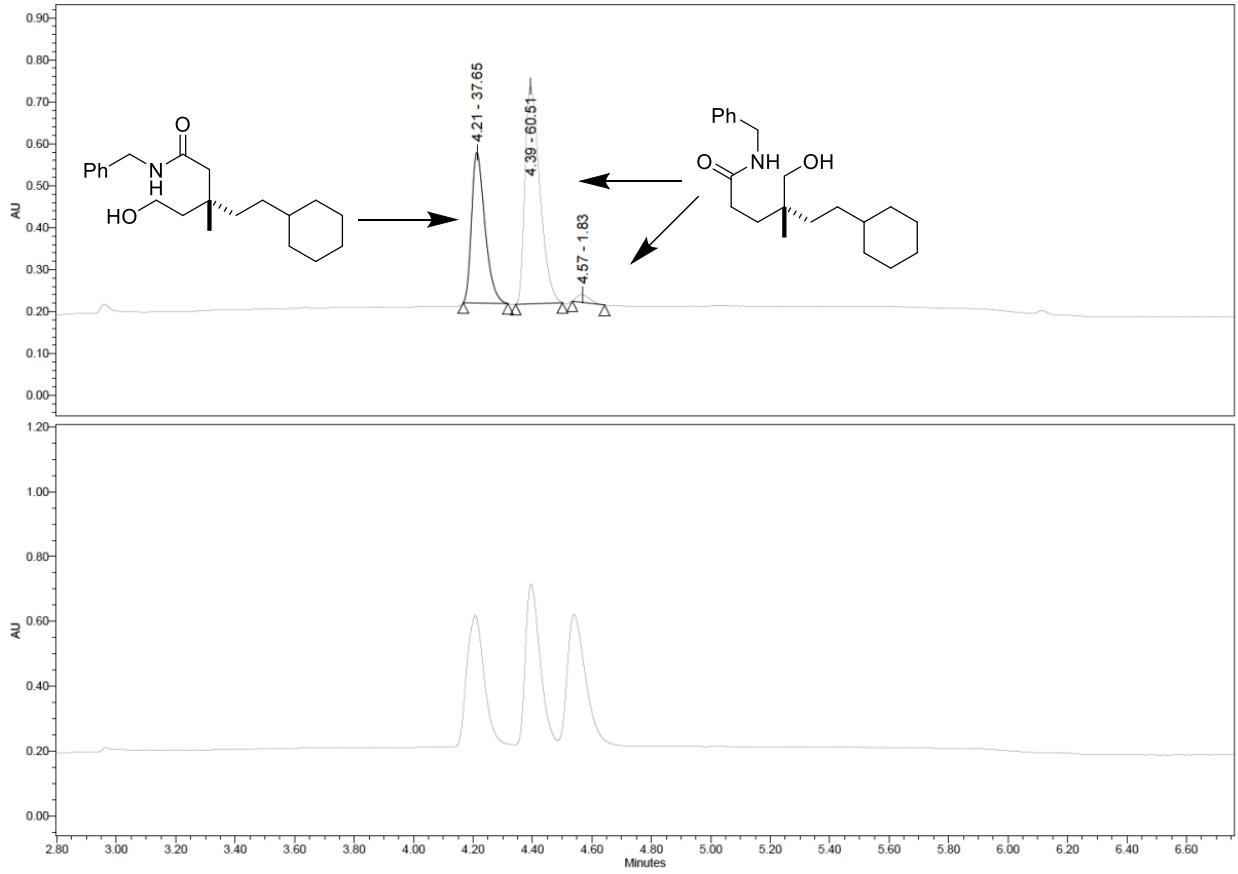

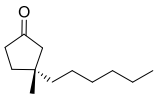

(*R*)-3-hexyl-3-methylcyclopentan-1-one **7**

General procedure A: $CuCl_{(s)}$ (4.0 mg, 0.4 mmol, 0.10 eq.), ligand *(R_a)-N*-(di(naphthalen-1-yl)methyl)-*N*-isopropyldinaphtho[2,1-*d*:1',2'-*f*][1,3,2]dioxaphosphepin-4-amine$_{(s)}$ (28.2 mg, 0.04 mmol, 0.11 eq.), Et_2O (2.0 ml), $AgNTf_{2(s)}$ (23.8 mg, 0.06 mmol, 0.15 eq.), DCM (0.40 ml) 1-hexene$_{(l)}$ (124 µl, 1.00 mmol, 2.5 eq.), Cp_2ZrHCl (206.0 mg, 0.80 mmol, 2.0 eq.), 3-methyl-2-cyclopentenone (40 µl, 0.40 mmol, 1.0 eq.) and $TMSCl_{(l)}$ (0.25 ml, 2.0 mmol, 5.0 eq.)

The crude mixture was treated as described above and was purified by flash column chromatography [SiO_2, pentane/EtOAc = 92:8] to afford pale yellow oil of 3-hexyl-3-methylcyclopentan-1-one (55.0 mg, 75%).

GC analysis indicated an enantiomeric excess of 86% [Macherey & Nagel, Lipodex® E; 70-30-0.2-85-10, λ = 210 nm; major enantiomer, t_R = 79.3 min; minor enantiomer, t_R = 82.4 min].

^{1}H NMR (400 MHz, $CDCl_3$) δ_H: 2.36 – 2.21 (m, 2H, COC*H*$_2$), 2.11 – 1.94 (m, 2H, COC*H*$_2$), 1.85 – 1.67 (m, 2H, C*H*$_2$), 1.39 – 1.20 (m, 10H, 5C*H*$_2$), 1.03 (s, 3H, CC*H*$_3$), 0.91 – 0.83 (m, 3H, CH_2C*H*$_3$).

^{13}C NMR (101 MHz, $CDCl_3$) δ_C: 220.4, 52.4, 41.9, 39.6, 36.9, 35.4, 31.9, 30.1, 25.2, 24.8, 22.8, 14.2.

HRMS (ESI^+) $[C_{12}H_{22}O^{23}Na]^+$ predicted 205.15633, found 205.15629 (Δ 0.19 ppm).

IR υ_{max} (film): 2955, 2927, 1740, 1464, 1405, 1379, 1166, 1134.

$[\alpha]_{589}^{25}$ = +32.8 (*c* 1.00, $CHCl_3$).

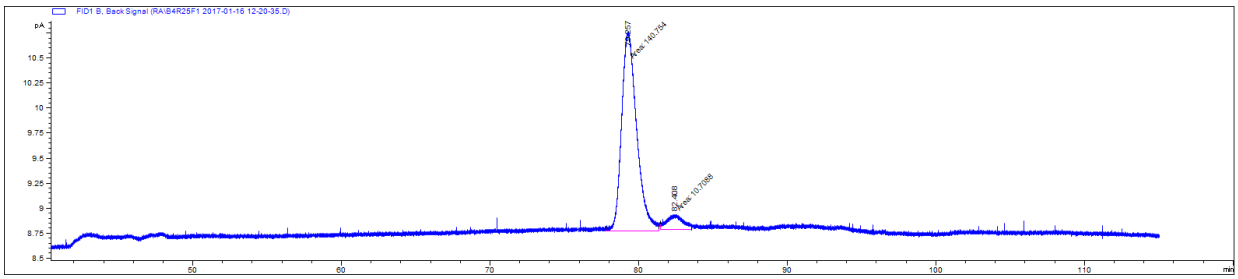

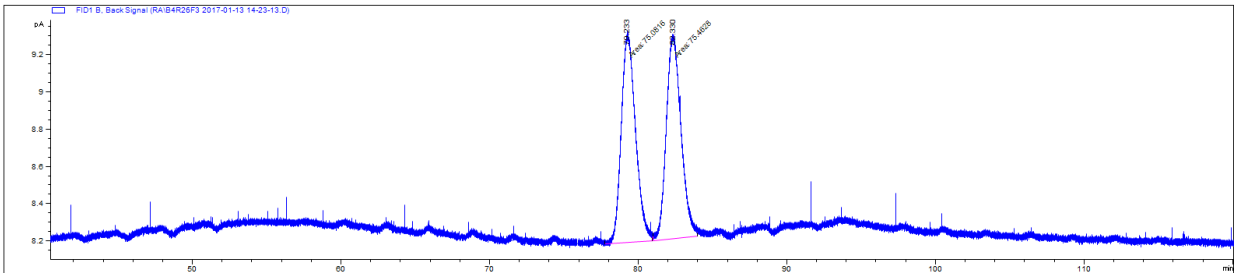

^{1}H and IR spectra are consistent with previously reported values.[164]

 (*R*)-3-methyl-3-tetradecylcyclopentan-1-one **8**

General procedure A: $CuCl_{(s)}$ (4.0 mg, 0.4 mmol, 0.10 eq.), ligand **L***(R_a)-N*-(di(naphthalen-1-yl)methyl)-*N*-isopropyldinaphtho[2,1-*d*:1',2'-*f*][1,3,2]dioxaphosphepin-4-amine$_{(s)}$ (28.2 mg, 0.04 mmol, 0.11 eq.), Et_2O (2.0 ml), $AgNTf_{2(s)}$ (23.8 mg, 0.06 mmol, 0.15 eq.), DCM (0.40 ml) 1-tetradecene$_{(l)}$ (253 µl, 1.00 mmol, 2.5 eq.), Cp_2ZrHCl (206.0 mg, 0.80 mmol, 2.0 eq.), 3-methyl-3-tetradecylcyclopentan-1-one (40 µl, 0.40 mmol, 1.0 eq.) and $TMSCl_{(l)}$ (0.25 ml, 2.0 mmol, 5.0 eq.)

The crude mixture was treated as described above and was purified by flash column chromatography [SiO_2, pentane/Et_2O = 97:3] to afford colourless oil of 3-methyl-3-tetradecylcyclopentan-1-one (92.5 mg, 79%).

The enantiomeric excess of the product was determined by chiral HPLC after two steps derivatisation (**General procedure D**).

SFC analysis indicated an enantiomeric excess of 90% [Chiralpak® IG-3; 1500 psi, 30 °C, flow: 1.5 mL/min; 1% to 30% MeOH in 10 min; λ = 211.9 nm; minor enantiomer, t_R = 9.58 min; major enantiomer, t_R = 94.78 min].

^{1}H NMR (400 MHz, $CDCl_3$) δ_H: 2.31 – 2.21 (m, 2H, COCH_2), 2.07 (d, *J* = 17.9 Hz, 1H, COCH_AH$_B$), 1.99 (d, *J* = 17.9 Hz, 1H, COCH$_A$$H_B$), 1.85 – 1.67 (m, 2H, C$H_2$), 1.43 – 1.18 (s, 26H, 13CH_2), 1.03 (s, 3H, CCH_3), 0.87 (t, *J* = 6.8 Hz, 3H, CH_2CH_3).

^{13}C NMR (101 MHz, $CDCl_3$) δ_C: 220.3, 52.4, 42.0, 39.6, 36.9, 35.4, 32.1, 30.5, 29.8, 29.8 (5C), 29.8, 29.5, 25.2, 24.9, 22.8, 14.3.

HRMS (CI$^+$) $[C_{20}H_{38}O]^+$ predicted 295.2987, found 295.2987 (Δ 3.32 ppm).

IR υ_{max} (l): 2980, 2957, 2922, 2853, 1742, 1464, 1152, 721.

$[\boldsymbol{\alpha}]_{589}^{25}$ = +25.5 (*c* 1.09, $CHCl_3$).

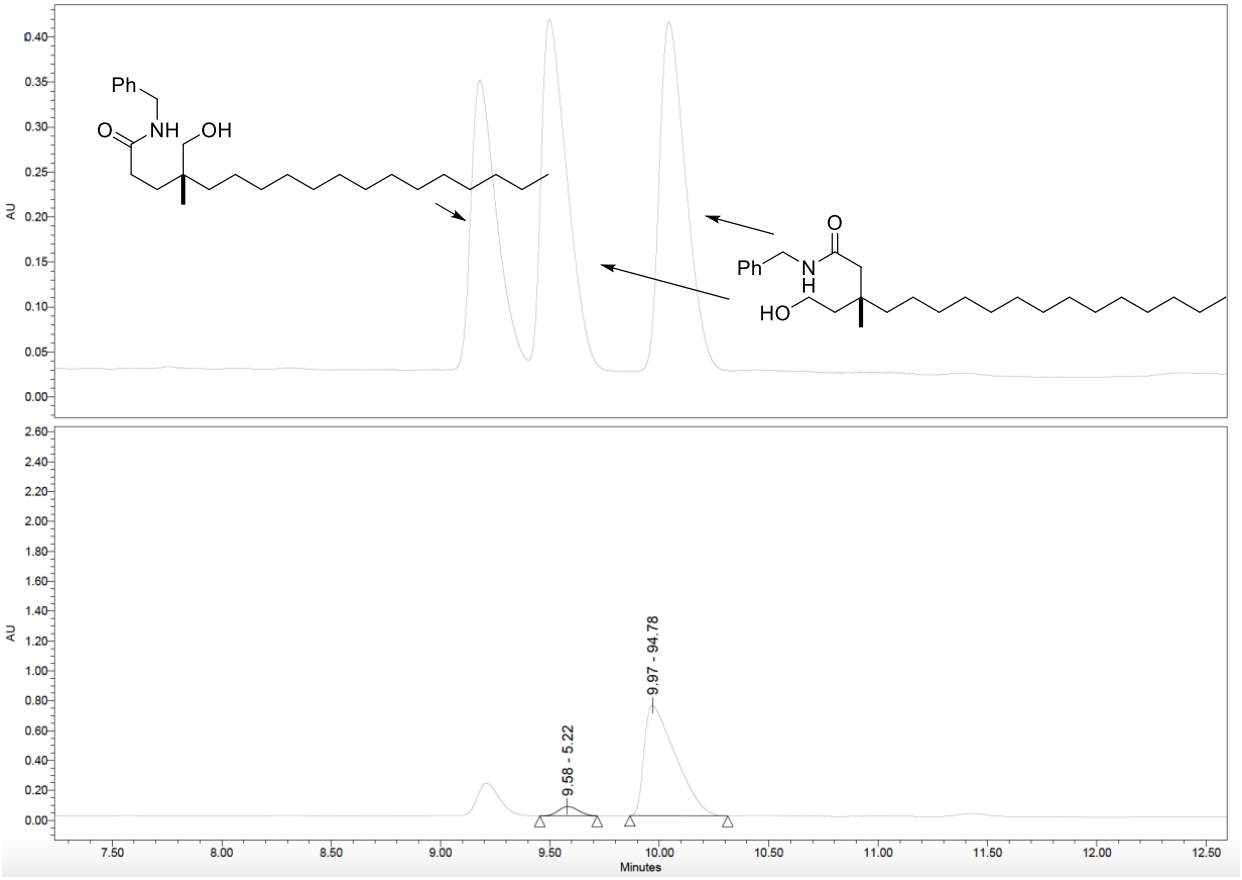

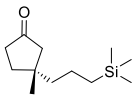

(S)-3-methyl-3-(3-(trimethylsilyl)propyl)cyclopentan-1-one **9**

General procedure A: $CuCl_{(s)}$ (4.0 mg, 0.4 mmol, 0.10 eq.), ligand *(R_a)-N*-(di(naphthalen-1-yl)methyl)-*N*-isopropyldinaphtho[2,1-*d*:1',2'-*f*][1,3,2]dioxaphosphepin-4-amine$_{(s)}$ (28.2 mg, 0.04 mmol, 0.11 eq.), Et_2O (2.0 ml), $AgNTf_{2(s)}$ (23.8 mg, 0.06 mmol, 0.15 eq.), DCM (0.40 ml) allyltrimethylsilane$_{(l)}$

(159 µl, 1.00 mmol, 2.5 eq.), Cp_2ZrHCl (206.0 mg, 0.80 mmol, 2.0 eq.), 3-methyl-2-cyclopentenone (40 µl, 0.40 mmol, 1.0 eq.) and $TMSCl_{(l)}$ (0.25 ml, 2.0 mmol, 5.0 eq.)

The crude mixture was treated as described above and was purified by flash column chromatography [SiO_2, pentane/EtOAc = 92:8] to afford pale yellow oil of 3-methyl-3-(3-(trimethylsilyl)propyl)cyclopentan-1-one (58.5 mg, 69%).

The enantiomeric excess of the product was determined by chiral HPLC after two steps derivatisation (**General procedure D**).

HPLC analysis indicated an enantiomeric excess of 90% [Chiralpak® ID; flow: 1 mL/min; hexane/^{i}PrOH = 92:8; λ = 210 nm; major enantiomer, t_R = 18.5 min; minor enantiomer, t_R = 20.7 min].

^{1}H NMR (400 MHz, $CDCl_3$) δ_H: 2.33 – 2.20 (m, 2H, COCH_2), 2.10 – 1.93 (m, 2H, COCH_2), 1.84 – 1.66 (m, 2H, CH_2), 1.47 – 1.13 (m, 4H, 2CH_2), 1.02 (s, 3H, CCH_3), 0.50 – 0.41 (m, 2H, CH_2Si), -0.04 (s, 9H, Si(CH_3)$_3$).

^{13}C NMR (101 MHz, $CDCl_3$) δ_C: 220.2, 52.3, 46.1, 39.7, 36.8, 35.4, 25.1, 19.1, 17.5, -1.5 (3C).

HRMS (EI^+) $[C_{12}H_{24}OSi]^+$ predicted 212.1596, found 213.1664 (Δ 2.3 ppm).

IR υ_{max} (film): 2953, 2923, 1743, 1247, 861, 837.

$[\boldsymbol{\alpha}]_{589}^{25}$ = +29.2 (*c* 1.00, $CHCl_3$).

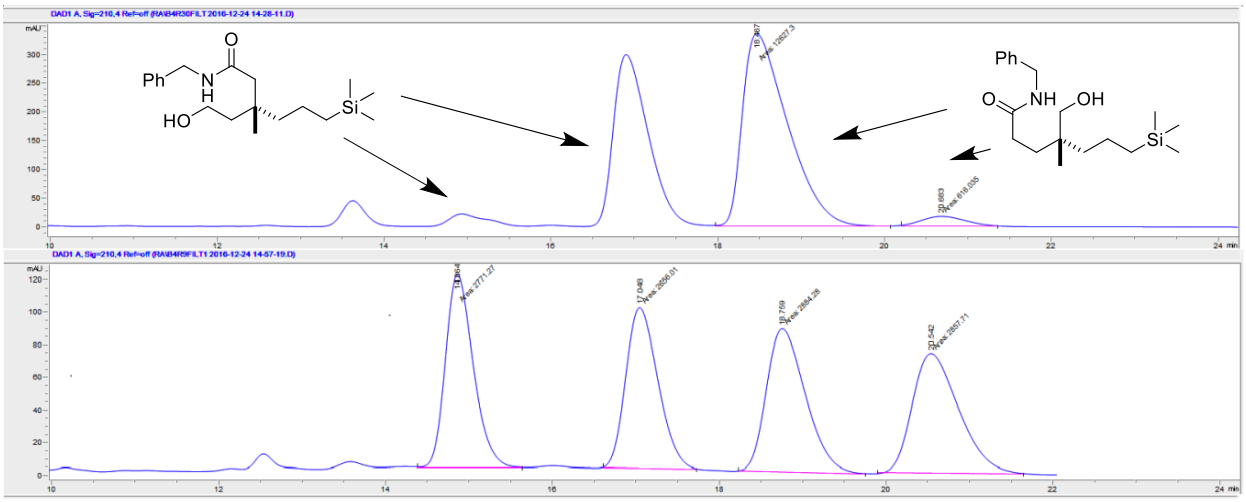

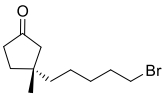

(R)-3-(5-bromopentyl)-3-methylcyclopentan-1-one **10**

General procedure A: $CuCl_{(s)}$ (4.0 mg, 0.4 mmol, 0.10 eq.), ligand *(R_a)-N*-(di(naphthalen-1-yl)methyl)-*N*-isopropyldinaphtho[2,1-*d*:1',2'-*f*][1,3,2]dioxaphosphepin-4-amine$_{(s)}$ (28.2 mg, 0.04 mmol, 0.11 eq.), Et_2O (2.0 ml), $AgNTf_{2(s)}$ (23.8 mg, 0.06 mmol, 0.15 eq.), DCM (0.40 ml) 5-bromopentene$_{(l)}$ (118 µl, 1.00 mmol, 2.5 eq.), Cp_2ZrHCl (206.0 mg, 0.80 mmol, 2.0 eq.), 3-methyl-2-cyclopentenone (40 µl, 0.40 mmol, 1.0 eq.) and $TMSCl_{(l)}$ (0.25 ml, 2.0 mmol, 5.0 eq.)

The crude mixture was treated as described above and was purified by flash column chromatography [SiO_2, pentane/EtOAc = 95:5] to afford colourless oil of 3-(5-bromopentyl)-3-methylcyclopentan-1-one (65.3 mg, 66%).

HPLC analysis indicated an enantiomeric excess of 86% [Chiralpak® AY-H; flow: 1 mL/min; hexane/^{i}PrOH = 95:5; λ = 210 nm; major enantiomer (+)-(*R*)- 3-(5-bromopentyl)-3-methylcyclopentan-1-one, t_R = 12.1 min; minor enantiomer (–)-(*S*)-3-(5-bromopentyl)-3-methylcyclopentan-1-one, t_R = 13.7 min].

^{1}H NMR (400 MHz, $CDCl_3$) δ_H: 3.38 (t, *J* = 6.8 Hz, 2H, C*H*$_2$Br), 2.30 – 2.17 (m, 2H, COC*H*$_2$), 2.09 – 1.98 (m, 2H, COC*H*$_2$), 1.91 – 1.79 (m, 2H, C*H*$_2$), 1.79 – 1.69 (m, 2H, C*H*$_2$), 1.48 – 1.37 (m, 2H, C*H*$_2$), 1.42 – 1.34 (m, 2H, C*H*$_2$), 1.38 – 1.18 (m, 2H, C*H*$_2$), 1.02 (s, 3H, C*H*$_3$).

^{13}C NMR (101 MHz, $CDCl_3$) δ_C: 219.9, 52.3, 41.7, 39.5, 36.8, 35.3, 33.9, 32.8, 28.9, 25.1, 24.1.

HRMS (ESI$^+$) $[C_{11}H_{20}O^{79}Br]^+$ predicted 247.0694, found 247.0692 (Δ 0.66 ppm).

IR υ_{max} (l): 2931, 1738, 1462, 1404, 1255, 1151.

$[\boldsymbol{\alpha}]_{589}^{25}$ = +5.4 (*c* 0.25, $CHCl_3$).

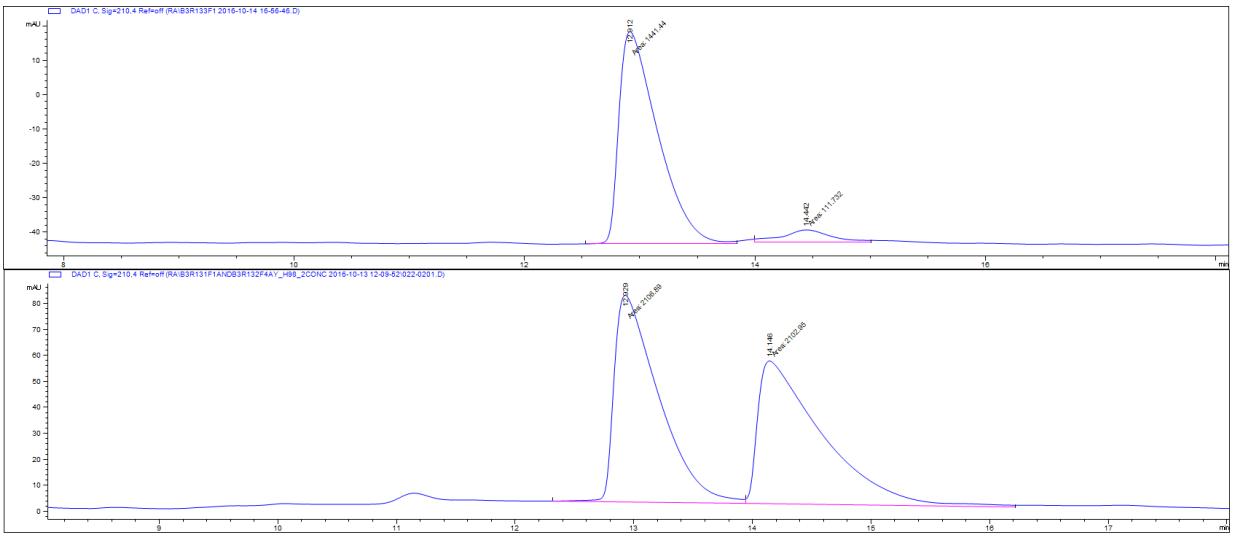

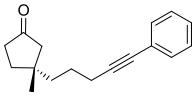

(*R*)-3-methyl-3-(5-phenylpent-4-yn-1-yl)cyclopentan-1-one **11**

General procedure A: $CuCl_{(s)}$ (4.0 mg, 0.4 mmol, 0.10 eq.), ligand *(R$_a$)-N*-(di(naphthalen-1-yl)methyl)-*N*-isopropyldinaphtho[2,1-*d*:1',2'-

f][1,3,2]dioxaphosphepin-4-amine$_{(s)}$ (28.2 mg, 0.04 mmol, 0.11 eq.), Et_2O (2.0 ml), $AgNTf_{2(s)}$ (23.8 mg, 0.06 mmol, 0.15 eq.), DCM (0.40 ml) 1-phenyl-4-penten-1-yne$_{(l)}$ (152 µl, 1.00 mmol, 2.5 eq.), Cp_2ZrHCl (206.0 mg, 0.80 mmol, 2.0 eq.), 3-methyl-2-cyclopentenone (40 µl, 0.40 mmol, 1.0 eq.) and $TMSCl_{(l)}$ (0.25 ml, 2.0 mmol, 5.0 eq.)

The crude mixture was treated as described above and was purified by flash column chromatography [SiO_2, pentane/EtOAc = 95:5] to afford colourless oil of 3-methyl-3-(5-phenylpent-4-yn-1-yl)cyclopentan-1-one (62.7 mg, 65%).

HPLC analysis indicated an enantiomeric excess of 88% [Chiralpak® IB; flow: 1 mL/min; hexane/^{i}PrOH = 95:5; λ = 238 nm; minor enantiomer (–)-(*R*)-3-methyl-3-(5-phenylpent-4-yn-1-yl)cyclopentan-1-one, t_R = 15.1 min; major enantiomer (+)-(*S*)-3-methyl-3-(5-phenylpent-4-yn-1-yl)cyclopentan-1-one, t_R = 19.3 min].

^{1}H NMR (400 MHz, $CDCl_3$) δ_H: 7.36 – 7.26 (m, 2H, 2C$_{Ar}$*H*), 7.20 (dd, *J* = 5.0, 2.0 Hz, 3H, 3C$_{Ar}$*H*), 2.41 – 2.29 (m, 2H, C*H*$_2$CCPh), 2.26 – 2.15 (m, 2H, C*H*$_2$CO), 2.09 – 1.91 (m, 2H, C*H*$_2$CO), 1.84 – 1.66 (m, 2H, C*H*$_2$), 1.63 – 1.43 (m, 4H, C*H*$_2$), 1.00 (s, 3H, C*H*$_3$).

^{13}C NMR (101 MHz, $CDCl_3$) δ_C: 219.7, 131.5, 128.2, 127.6, 123.8, 89.8, 81.0, 52.3, 41.1, 39.4, 36.8, 35.2, 25.0, 24.3, 20.0.

HRMS (ESI$^+$) $[C_{17}H_{21}O]^+$ predicted 241.1589, found 241.1587 (Δ 0.88 ppm).

IR υ_{max} (l): 2953, 1737, 1490, 1156, 756, 692.

$[\boldsymbol{\alpha}]_{589}^{25}$ = +22.8 (*c* 1.00, $CHCl_3$).

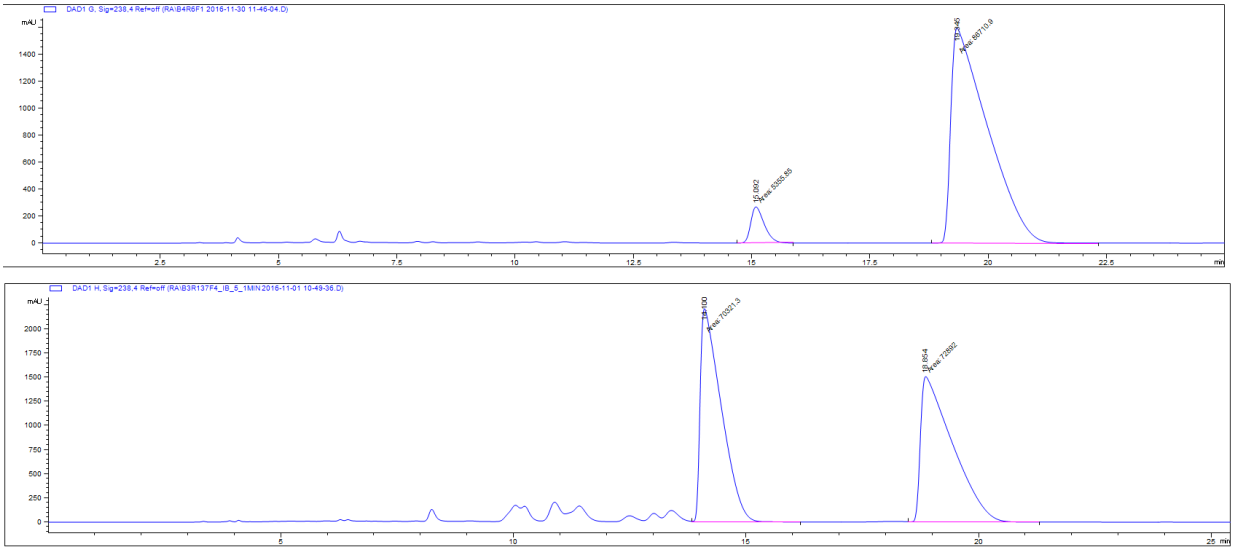

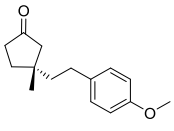

(*R*)-3-(4-methoxyphenethyl)-3-methylcyclopentan-1-one **12**

General procedure A: $CuCl_{(s)}$ (4.0 mg, 0.4 mmol, 0.10 eq.), ligand *(R_a)-N*-(di(naphthalen-1-yl)methyl)-*N*-isopropyldinaphtho[2,1-*d*:1',2'-*f*][1,3,2]dioxaphosphepin-4-amine$_{(s)}$ (28.2 mg, 0.04 mmol, 0.11 eq.), Et_2O (2.0 ml), $AgNTf_{2(s)}$ (23.8 mg, 0.06 mmol, 0.15 eq.), DCM (0.40 ml) 1-methoxy-4-vinylbenzene $_{(l)}$ (134 µl, 1.00 mmol, 2.5 eq.), Cp_2ZrHCl (206.0 mg, 0.80 mmol, 2.0 eq.), 3-methyl-2-cyclopentenone (40 µl, 0.40 mmol, 1.0 eq.) and $TMSCl_{(l)}$ (0.25 ml, 2.0 mmol, 5.0 eq.)

The crude mixture was treated as described above and was purified by flash column chromatography [SiO_2, pentane/EtOAc = 95:5] to afford colourless oil of 3-(4-methoxyphenethyl)-3-methylcyclopentan-1-one (56.6 mg, 61%).

HPLC analysis indicated an enantiomeric excess of 89% [Chiralpak® IB; flow: 1 mL/min; hexane/^{i}PrOH = 98:2; λ = 210 nm; major enantiomer, t_R = 11.8 min; minor enantiomer, t_R = 13.1 min].

^{1}H NMR (400 MHz, $CDCl_3$) δ_H: 7.16 – 7.08 (m, 2H, 2C$_{Ar}H$), 6.90 – 6.82 (m, 2H, 2C$_{Ar}H$), 3.81 (s, 3H, OCH_3), 2.70 – 2.49 (m, 2H, CH_2), 2.39 – 2.24 (m, 2H, CH_2), 2.21 – 2.04 (m, 2H, COCH_2), 1.95 – 1.80 (m, 2H, CH_2), 1.77 – 1.68 (m, 2H, CH_2), 1.16 (s, 3H, CCH_3).

^{13}C NMR (101 MHz, $CDCl_3$) δ_C: 219.9, 157.9, 134.5, 129.2 (2C), 114.0 (2C), 55.4, 52.3, 44.3, 39.7, 36.8, 35.4, 30.5, 25.0.

HRMS (EI$^+$) $[C_{15}H_{20}O_2]^+$ predicted 232.1463, found 232.1463 (Δ −2.6 ppm).

IR υ_{max} (l): 2954, 1736, 1490, 1511, 1243, 1035, 821.

$[\boldsymbol{\alpha}]_{589}^{25}$ = +21.1 (*c* 1.00, $CHCl_3$).

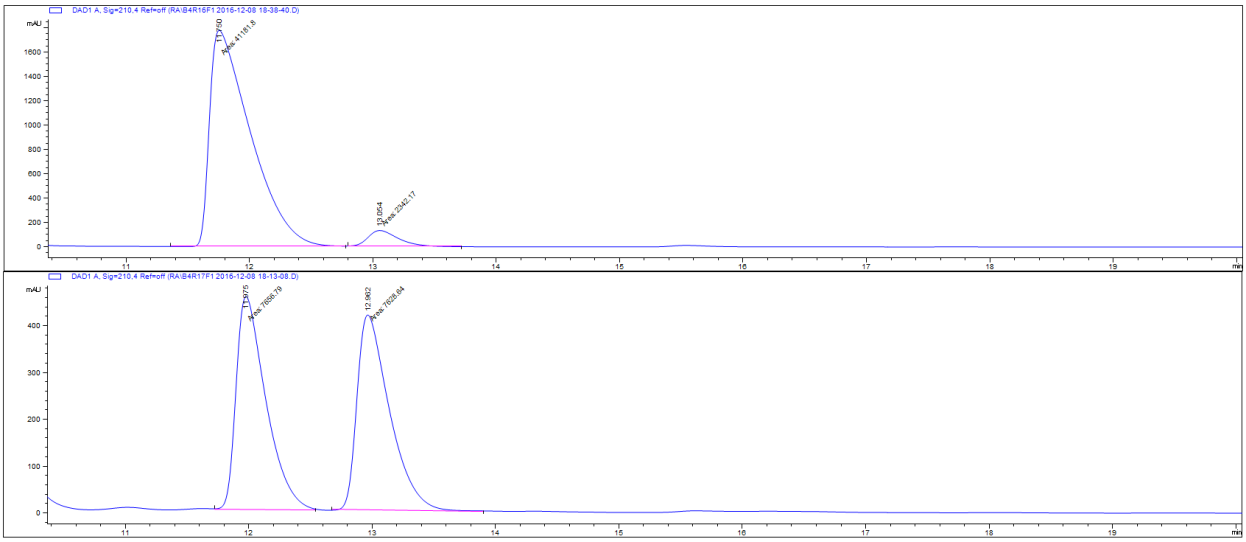

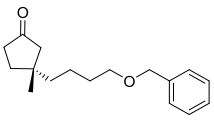

(*R*)-3-(4-(benzyloxy)butyl)-3-methylcyclopentan-1-one **13**

General procedure A: $CuCl_{(s)}$ (4.0 mg, 0.4 mmol, 0.10 eq.), ligand *(R$_a$)-N*-(di(naphthalen-1-yl)methyl)-*N*-isopropyldinaphtho[2,1-*d*:1',2'-*f*][1,3,2]dioxaphosphepin-4-amine$_{(s)}$ (28.2 mg, 0.04 mmol, 0.11 eq.), Et_2O (2.0 ml),

$AgNTf_{2(s)}$ (23.8 mg, 0.06 mmol, 0.15 eq.), DCM (0.40 ml) ((but-3-en-1-yloxy)methyl)benzene$_{(l)}$ (162 mg, 1.00 mmol, 2.5 eq.), Cp_2ZrHCl (206.0 mg, 0.80 mmol, 2.0 eq.), 3-methyl-2-cyclopentenone (40 µl, 0.40 mmol, 1.0 eq.) and $TMSCl_{(l)}$ (0.25 ml, 2.0 mmol, 5.0 eq.)

The crude mixture was treated as described above and was purified by flash column chromatography [SiO_2, pentane/EtOAc = 95:5] to afford colourless oil of 3-(4-(benzyloxy)butyl)-3-methylcyclopentan-1-one (85.3 mg, 82%).

HPLC analysis indicated an enantiomeric excess of 89% [Chiralpak® IB; flow: 1 mL/min; hexane/^{i}PrOH = 95:5; λ = 210 nm; minor enantiomer, t_R = 11.6 min; major enantiomer, t_R = 14.0 min].

^{1}H NMR (400 MHz, $CDCl_3$) δ_H: 7.31 – 7.14 (m, 5H, $5C_{Ar}H$), 4.42 (s, 2H, ArCH_2), 3.40 (t, *J* = 6.4 Hz, 2H, OCH_2), 2.29 – 2.11 (m, 2H, COCH_2), 2.03 – 1.87 (m, 2H, COCH_2), 1.76 – 1.62 (m, 2H, CH_2), 1.59 – 1.45 (m, 2H, CH_2), 1.39 – 1.19 (m, 4H, 2CH_2), 0.96 (s, 3H, CH_3).

^{13}C NMR (101 MHz, $CDCl_3$) δ_C: 220.1, 138.6, 128.4 (2C), 127.7 (2C), 127.6, 73.0, 70.2, 52.3, 41.7, 39.6, 36.8, 35.2, 30.4, 25.0, 21.5.

HRMS (EI$^+$) $[C_{15}H_{20}O_2]^+$ predicted 232.1463, found 232.1463 (Δ −2.6 ppm).

IR υ_{max} (l): 2934, 2863, 1737, 1163, 735, 697.

$[\boldsymbol{\alpha}]_{589}^{25}$ = +25.3 (*c* 1.00, $CHCl_3$).

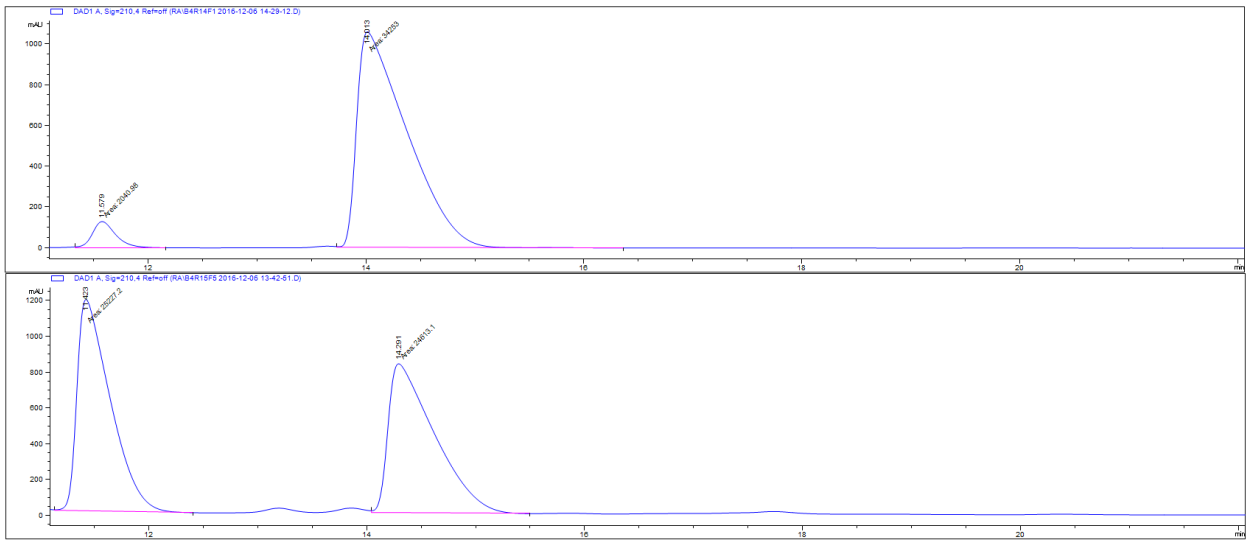

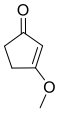

3-Methoxycyclopent-2-en-1-one

3-Methoxycyclopent-2-en-1-one was synthesized based on the procedure reported by Zubaidha.[165]

To a dried round bottom flask with a magnetic stirrer bar, cyclopentane-1,3-dione (25 g, 255 mmol, 1.0 eq.) and MeOH (600 ml, 0.4 M) was added followed by $I_{2(s)}$ (1.94 g, 7.6 mmol, 0.03 eq.). The reaction mixture was stirred and heated to 30 °C overnight. After that, the reaction was left to cool to room temperature before $Na_2SO_{4(s)}$ was added and the reaction was stirred for 5 mins. Then the reaction mixture was filtered though a small amount of silica gel and was washed with EtOAc. The solvent was removed *in vacuo*. The purification by flash column chromatography [SiO_2, EtOAc] and recrystallisation in Et_2O resulted in 3-methoxycyclopent-2-en-1-one as white solid (7.57 g, 26%).

^{1}H NMR (400 MHz, $CDCl_3$) δ_H: 5.30 – 5.21 (m, 1H, C=C*H*), 3.78 (s, 3H, CH_3), 2.60 – 2.52 (m, 2H, CH_2), 2.45 – 2.36 (m, 2H, CH_2).

^{13}C NMR (101 MHz, $CDCl_3$) δ_C: 206.0, 191.3, 104.5, 58.8, 34.2, 28.3.

Data was consistent with previously reported values.[165]

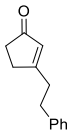

3-Phenethylcyclopent-2-en-1-one

3-Phenethylcyclopent-2-en-1-one was synthesized based on the procedure reported by Buchwald.[166]

To a dried multi-neck round bottom flask with a condenser attached, $Mg_{(s)}$ (865 mg, 36 mmol, 2.0 eq.), $I_{2(s)}$ (1 crystal) and THF (8 ml) was stirred at 40 ˚C for 30 mins. Then 1-bromo-2-phenylethane (4.9 ml, 35.6 mmol, 2.0 eq.) in THF (10 ml) was added and the stirring mixture was heated to reflux (70 ˚C) for 5 h.

To a separate dried round bottom flask containing 3-methoxycyclopent-2-en-1-one (2.0 g, 17.8 mmol, 1.0 eq.) in THF (18 ml), the reaction of premade Grignard reagent at rt was added dropwise. The suspension was stirred at rt for 16 h. Then distilled H_2O (10 ml), $HCl_{(aq.)}$ (2 M, ca. 10 ml) and Et_2O were added to the suspension until no effervescence was observed. The mixture was partitioned between the aqueous and organic layer. The aqueous layer was extracted by Et_2O three times. The combined organic layer was dried with anhydrous $MgSO_{4(s)}$ and the solvent was removed *in vacuo*. The crude mixture was purified by column chromatography [SiO_2, hexane/EtOAc = 10:1 to 5:1] to afford 3-phenethylcyclopent-2-en-1-one as a yellow viscous oil which turned to soft solid upon standing (2.88 g, 87%).

^{1}H NMR (400 MHz, $CDCl_3$) δ_H: 7.23 – 7.14 (m, 2H, 2$C_{Ar}H$), 7.14 – 7.05 (m, 3H, 3$C_{Ar}H$), 5.91 – 5.76 (m, 1H, C=C*H*), 2.88 – 2.74 (m, 2H, CH_2), 2.71 – 2.56 (m, 2H, CH_2), 2.55 – 2.42 (m, 2H, CH_2), 2.35 – 2.20 (m, 2H, CH_2).

^{13}C NMR (101 MHz, $CDCl_3$) δ_C: 209.7, 181.7, 140.4, 129.6, 128.4 (2C), 128.0 (2C), 126.2, 35.1, 34.8, 33.1, 31.5.

Data was consistent with previously reported values.[166]

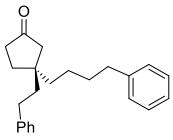

(*S*)-3-phenethyl-3-(4-phenylbutyl)cyclopentan-1-one **14**

General procedure A: $CuCl_{(s)}$ (4.0 mg, 0.4 mmol, 0.10 eq.), ligand *(R_a)-N*-(di(naphthalen-1-yl)methyl)-*N*-isopropyldinaphtho[2,1-*d*:1',2'-*f*][1,3,2]dioxaphosphepin-4-amine$_{(s)}$ (28.2 mg, 0.04 mmol, 0.11 eq.), Et_2O (2.0 ml), $AgNTf_{2(s)}$ (23.8 mg, 0.06 mmol, 0.15 eq.), DCM (0.40 ml) 4-phenyl-1-butene$_{(l)}$ (150 mg, 1.00 mmol, 2.5 eq.), Cp_2ZrHCl (206.0 mg, 0.80 mmol, 2.0 eq.), 3-phenethylcyclopent-2-en-1-one (73 µl, 0.40 mmol, 1.0 eq.) and $TMSCl_{(l)}$ (0.25 ml, 2.0 mmol, 5.0 eq.)

The crude mixture was treated as described above and was purified by flash column chromatography [SiO_2, pentane/Et_2O = 95:5] to afford a colourless oil of 3-phenethyl-3-(4-phenylbutyl)cyclopentan-1-one (85.1 mg, 66%).

SFC analysis indicated an enantiomeric excess of 87% [Chiralpak® IA-3; 1500 psi, 30 °C, flow: 1.5 mL/min; 1% to 30% MeOH in 8 min; λ = 210 nm; minor enantiomer, t_R = 3.82 min; major enantiomer, t_R = 4.58 min].

^{1}H NMR (400 MHz, $CDCl_3$) δ_H: 7.25 – 7.17 (m, 4H, $4C_{Ar}H$), 7.16 – 7.08 (m, 4H, $4C_{Ar}H$), 7.06 – 7.00 (m, 2H, $2C_{Ar}H$), 2.58 (dd, J = 8.5, 6.8 Hz, 2H, CH_2), 2.55 – 2.34 (m, 2H, CH_2), 2.21 (t, J = 8.0 Hz, 2H, $COCH_2CH_2$), 2.05 (s, 2H, $COCH_2C$), 1.78 (t, J = 8.0 Hz, 2H, $COCH_2CH_2$), 1.66 – 1.53 (m, 4H, $2CH_2$), 1.48 – 1.16 (m, 4H, $2CH_2$).

^{13}C NMR (101 MHz, $CDCl_3$) δ_C: 219.8, 142.4, 142.4, 128.6 (2C), 128.5 (2C), 128.5 (2C), 128.3 (2C), 126.0, 125.9, 51.2, 42.6, 40.1, 37.4, 36.6, 35.9, 33.4, 32.1, 31.0, 23.9.

HRMS (APCI$^+$) $[C_{23}H_{29}O]^+$ predicted 321.22129, found 321.22137 (Δ 0.26 ppm).

IR υ_{max} (l): 2930, 2858, 2360, 1739, 1454, 1157, 699.

$[\boldsymbol{\alpha}]_{589}^{25}$ = +2.8 (c 1.00, $CHCl_3$).

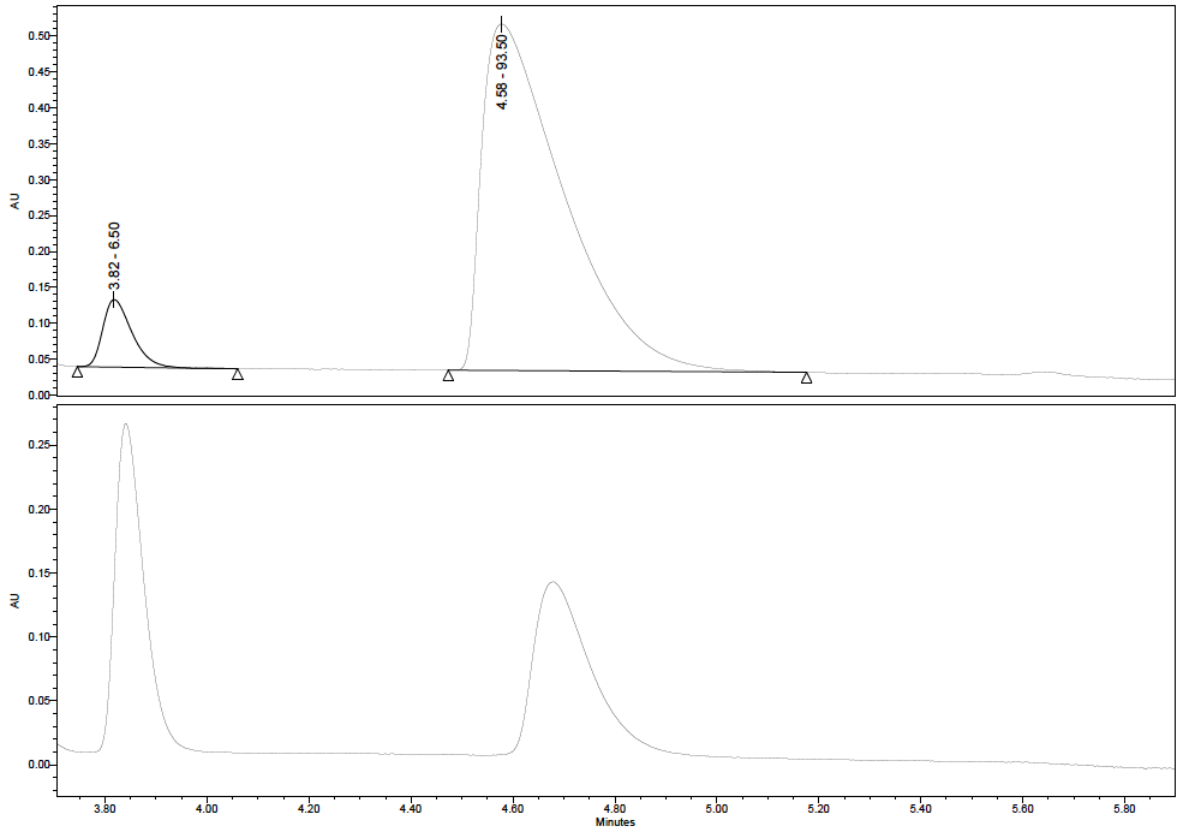

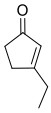

3-Ethylcyclopent-2-en-1-one

3-Ethylcyclopent-2-en-1-one was synthesised based on the procedure reported by Buchwald.[166]

To a dried round bottom flask containing 3-methoxycyclopent-2-en-1-one (1.5 g, 13.4 mmol, 1.0 eq.) in ^{t}BuOMe (26 ml), the solution of ethylmagnesium bromide (8.9 ml, 26.8 mmol, 2.0 eq., 3 M in Et_2O) was added dropwise at 0 °C. The suspension was stirred at rt for 2 h. Then distilled H_2O (10 ml), $HCl_{(aq.)}$ (2 M, ca. 10 ml) and Et_2O were added to the suspension until no effervescence was observed. The mixture was partitioned between the aqueous and organic layer. The aqueous layer was extracted by Et_2O three times. The combined organic layer was dried with anhydrous $MgSO_{4(s)}$ and the solvent was removed *in vacuo*. The crude mixture was purified by column chromatography [SiO_2, pentane/EtOAc = 100:15 to 1:1] to afford 3-ethylcyclopent-2-en-1-one as a viscous oil (252 mg, 17%).

^{1}H NMR (400 MHz, $CDCl_3$) δ_H: 5.94 – 5.87 (m, 1H, C=C*H*), 2.59 – 2.51 (m, 2H, CH_2), 2.43 – 2.33 (m, 4H, CH_2), 1.14 (t, *J* = 7.4 Hz, 3H, CH_3).

^{13}C NMR (101 MHz, $CDCl_3$) δ_C: 210.2, 184.6, 128.7, 35.4, 31.5, 26.8, 11.5.

Data was consistent with previously reported values.[166]

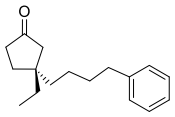

(*R*)-3-ethyl-3-(4-phenylbutyl)cyclopentan-1-one **15**

General procedure A: $CuCl_{(s)}$ (4.0 mg, 0.4 mmol, 0.10 eq.), ligand *(R_a)-N*-(di(naphthalen-1-yl)methyl)-*N*-isopropyldinaphtho[2,1-*d*:1',2'-*f*][1,3,2]dioxaphosphepin-4-amine$_{(s)}$ (28.2 mg, 0.04 mmol, 0.11 eq.), Et_2O (2.0 ml),

$AgNTf_{2(s)}$ (23.8 mg, 0.06 mmol, 0.15 eq.), DCM (0.40 ml) 4-phenyl-1-$butene_{(l)}$ (150 mg, 1.00 mmol, 2.5 eq.), Cp_2ZrHCl (206.0 mg, 0.80 mmol, 2.0 eq.), 3-ethylcyclopent-2-en-1-one (43 µl, 0.40 mmol, 1.0 eq.) and $TMSCl_{(l)}$ (0.25 ml, 2.0 mmol, 5.0 eq.)

The crude mixture was treated as described above and was purified by flash column chromatography [SiO_2, pentane/Et_2O = 5:1] to afford colourless oil of 3-ethyl-3-(4-phenylbutyl)cyclopentan-1-one (64.7 mg, 66%).

SFC analysis indicated an enantiomeric excess of 84% [Chiralpak® IA-3; 1500 psi, 30 °C, flow: 1.5 mL/min; 1% to 30% MeOH in 5 min; λ = 210 nm; minor enantiomer, t_R = 2.63 min; major enantiomer, t_R = 2.85 min].

^{1}H NMR (400 MHz, $CDCl_3$) δ_H: 7.24 – 7.15 (m, 2H, $2C_{Ar}H$), 7.14 – 7.06 (m, 3H, $3C_{Ar}H$), 2.59 – 2.48 (m, 2H, ArCH_2), 2.17 (t, *J* = 8.0 Hz, 2H, COCH_2CH_2), 1.97 (s, 2H, COCH_2C), 1.77 – 1.62 (m, 2H, $COCH_2CH_2$), 1.58 – 1.49 (m, 2H, CH_2), 1.42 – 1.12 (m, 6H, $3CH_2$), 0.76 (t, *J* = 7.5 Hz, 3H, CH_3).

^{13}C NMR (101 MHz, $CDCl_3$) δ_C: 220.3, 142.5, 128.4 (2C), 128.4 (2C), 125.8, 50.8, 42.7, 37.1, 36.6, 35.9, 32.8, 32.2, 30.0, 24.0, 8.7.

HRMS (ESI^+) $[C_{17}H_{25}O_2]^+$ predicted 245.18999, found 245.19007 (Δ 0.33 ppm).

IR υ_{max} (l): 3026, 2962, 2931, 2859, 2630, 1740, 1456, 699.

$[\alpha]_{589}^{25}$ = –4.1 (*c* 1.04, $CHCl_3$).

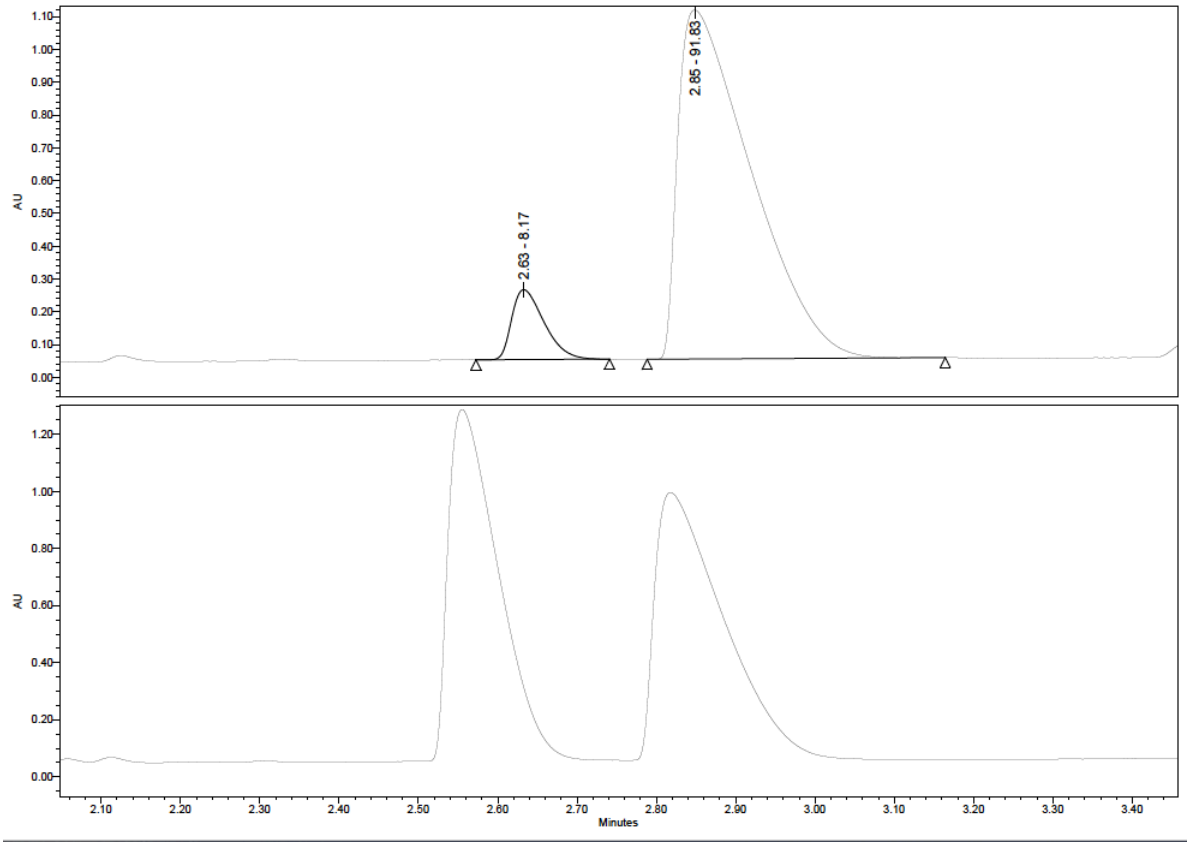

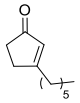

3-Hexylcyclopent-2-en-1-one

3-Hexylcyclopent-2-en-1-one was synthesised based on the procedure reported by Buchwald.[166]

To a dried round bottom flask containing 3-methoxycyclopent-2-en-1-one (2.0 g, 17.8 mmol, 1.0 eq.) in THF (10 ml), the solution of hexylmagnesium bromide (44.5 ml, 35.6 mmol, 2.0 eq., 0.8 M in THF) was added dropwise at 0 °C. The suspension was stirred at rt for 2 h. Then distilled H_2O (10 ml), $HCl_{(aq.)}$ (2 M, ca. 10 ml) and Et_2O were added to the suspension until no effervescence was observed. The mixture was partitioned between the aqueous and organic layer. The aqueous layer was extracted by Et_2O three times. The combined organic layer was dried with anhydrous $MgSO_{4(s)}$ and the solvent was removed *in vacuo*. The crude mixture was

purified by column chromatography [SiO_2, petrol/EtOAc = 1:0 to 10:1] to afford 3-hexylcyclopent-2-en-1-one as a viscous brown oil (1.74 g, 71%).

^{1}H NMR (500 MHz, $CDCl_3$) δ_H: 5.96 – 5.91 (m, 1H, C=C*H*), 2.60 – 2.54 (m, 2H, CH_2), 2.44 – 2.36 (m, 4H, 2CH_2), 1.63 – 1.51 (m, 2H, CH_2), 1.39 – 1.13 (m, 6H, 3CH_2), 0.94 – 0.84 (m, 3H, CH_3).

^{13}C NMR (126 MHz, $CDCl_3$) δ_C: 210.3, 183.3, 35.5, 33.7, 31.7, 31.7, 29.2, 27.2, 22.7, 14.2.

^{1}H spectroscopy was consistent with previously reported values.[167]

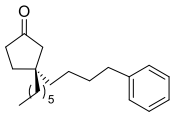

(*R*)-3-hexyl-3-(4-phenylbutyl)cyclopentan-1-one **16**

General procedure A: $CuCl_{(s)}$ (4.0 mg, 0.4 mmol, 0.10 eq.), ligand *(R_a)-N*-(di(naphthalen-1-yl)methyl)-*N*-isopropyldinaphtho[2,1-*d*:1',2'-*f*][1,3,2]dioxaphosphepin-4-amine $_{(s)}$ (28.2 mg, 0.04 mmol, 0.11 eq.), Et_2O (2.0 ml), $AgNTf_{2(s)}$ (23.8 mg, 0.06 mmol, 0.15 eq.), DCM (0.40 ml) 4-phenyl-1-butene$_{(l)}$ (150 mg, 1.00 mmol, 2.5 eq.), Cp_2ZrHCl (206.0 mg, 0.80 mmol, 2.0 eq.), 3-hexylcyclopent-2-en-1-one (70 µl, 0.40 mmol, 1.0 eq.) and $TMSCl_{(l)}$ (0.25 ml, 2.0 mmol, 5.0 eq.)

The crude mixture was treated as described above and was purified by flash column chromatography [SiO_2, pentane/Et_2O = 100:15] to afford colourless oil of hexyl-3-(4-phenylbutyl)cyclopentan-1-one (65.5 mg, 54%).

SFC analysis indicated an enantiomeric excess of 82% [Chiralpak® ID-3; 1500 psi, 30 °C, flow: 1.5 mL/min; 1% to 30% MeOH in 5 min; λ = 210 nm; minor enantiomer, t_R = 2.61 min; major enantiomer, t_R = 3.17 min].

^{1}H NMR (400 MHz, $CDCl_3$) δ_H: 7.25 – 7.16 (m, 2H, 2$C_{Ar}H$), 7.13 – 7.06 (m, 3H, 3$C_{Ar}H$), 2.59 – 2.50 (m, 2H, $C_{Ar}CH_2$), 2.17 (t, *J* = 8.0 Hz, 2H, $COCH_2CH_2$), 1.98 (s, 2H $COCH_2C$), 1.75 – 1.65 (m, 2H, $COCH_2CH_2$), 1.60 – 1.48 (m, 2H, CH_2), 1.41 – 0.97 (m, 14H, 7CH_2), 0.88 – 0.76 (m, 3H, CH_3).

^{13}C NMR (101 MHz, $CDCl_3$) δ_C: 220.5, 142.6, 128.5 (2C), 128.4 (2C), 125.8, 51.3, 42.5, 37.8, 37.7, 36.6, 35.9, 33.4, 32.2, 31.9, 30.1, 24.3, 24.0, 22.8, 14.2.

HRMS (APCI$^+$) $[C_{21}H_{33}O]^+$ predicted 301.25259, found 301.25259 (Δ 1.53 ppm).

IR υ_{max} (l): 2927, 2857, 2360, 1740, 1455, 699.

$[\boldsymbol{\alpha}]_{589}^{25}$ = –3.1 (*c* 1.08, $CHCl_3$).

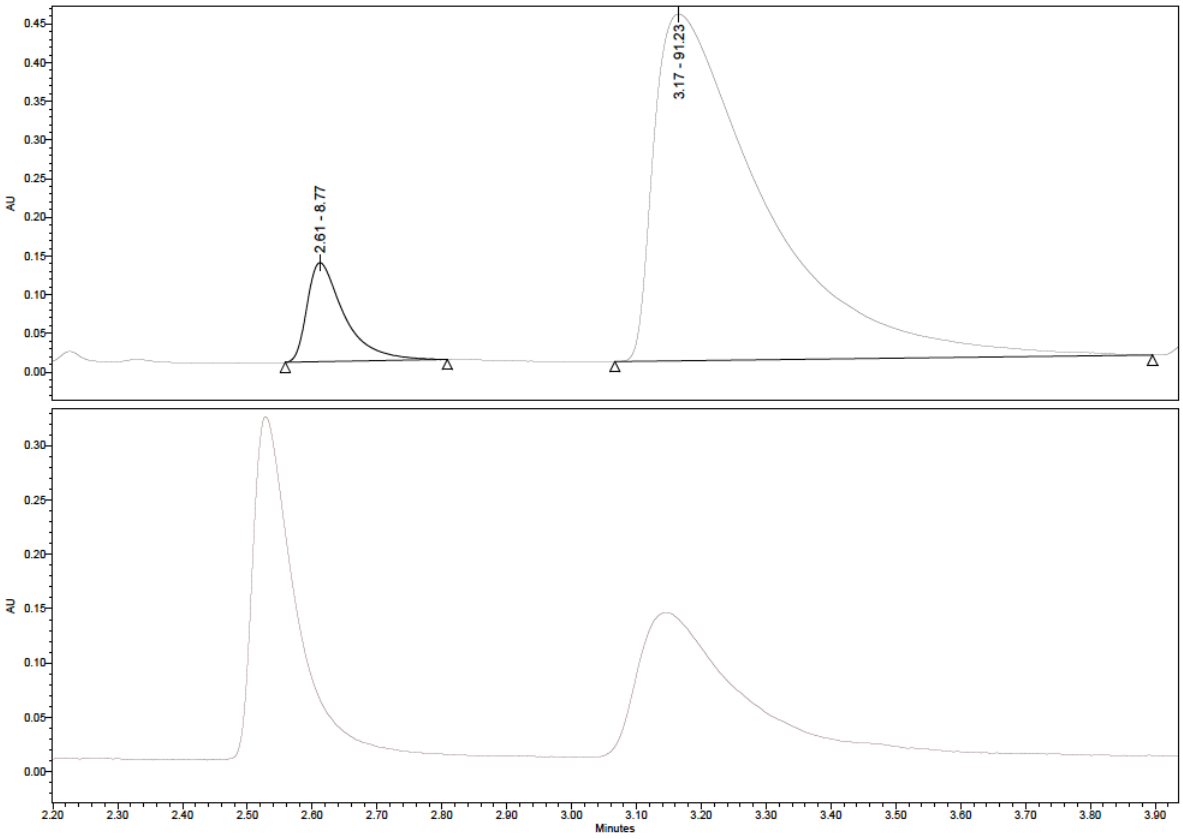

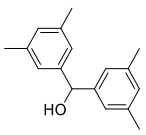

Bis(3,5-dimethylphenyl)methanol

To a dried multi-neck round bottom flask with a condenser attached, $Mg_{(s)}$ (948 mg, 39 mmol, 1.8 eq.), $I_{2(s)}$ (1 crystal) and THF (5 ml) was stirred at 40 ˚C for 30 mins. Then 1-bromo-3,5-dimethylbenzene (4.28 ml, 31.5 mmol, 1.49 eq.) in THF (10 ml) was added and the stirring mixture was heated to reflux (70 ˚C) for 5 h. The mixture was cooled to rt and 3,5-dimethylbenzaldehyde (2.84 g, 21.1 mmol, 1.0 eq.) in THF (15 ml) was added and the condenser was removed. The suspension was stirred at rt for 16 h. Then distilled H_2O (10 ml), $HCl_{(aq.)}$ (2 M, *ca.* 5 ml) and Et_2O were added to the suspension until no effervescence was observed. The mixture was partitioned between the aqueous and organic layer. The aqueous layer was extracted by Et_2O

three times. The combined organic layer was dried with anhydrous $MgSO_4$(s) and the solvent was removed *in vacuo* to afford bis(3,5-dimethylphenyl)methanol as a white solid (5.02 g, 99%).

^{1}H NMR (400 MHz, $CDCl_3$) δ_H: 7.03 (br s, 4H, 4*o*-$C_{Ar}H$), 6.90 (br s, 2H, 2*p*-$C_{Ar}H$), 5.70 (s, 1H, $CHAr_2$), 2.30 (s, 12H, 4CH_3).

^{13}C NMR (101 MHz, $CDCl_3$) δ_C: 144.0 (2C), 138.1 (4C), 129.3 (2C), 124.4 (4C), 76.5 , 21.5 (4C).

Data was consistent with previously reported values.[168]

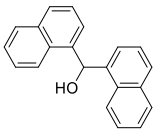

Di(naphthalen-1-yl)methanol

To a dried multi-neck round bottom flask with a condenser attached, $Mg_{(s)}$ (948 mg, 39 mmol, 1.3 eq.), $I_{2(s)}$ (1 crystal) and THF (5 ml) was stirred at 40 ˚C for 30 mins. Then 1-bromonaphthalene (4.40 ml, 31.5 mmol, 1.05 eq.) in THF (10 ml) was added and the stirring mixture was heated to reflux (70 ˚C) for 5 h. The mixture was cooled to rt and 1-naphthaldehyde (4.69 g, 29.9 mmol, 1.0 eq.) in THF (15 ml) was added and the condenser was removed. The suspension was stirred at rt for 16 h. Then distilled H_2O (10 ml), $HCl_{(aq.)}$ (2 M, ca. 5 ml) and Et_2O were added to the suspension until no effervescence was observed. The mixture was partitioned between the aqueous and organic layer. The aqueous layer was extracted by Et_2O three times. The combined organic layer was dried with anhydrous $MgSO_{4(s)}$ and the solvent was removed *in vacuo* to afford di(naphthalen-1-yl)methanol as a white solid with minor impurity (9.19 g, quantitative yield).

^{1}H NMR (400 MHz, $CDCl_3$) δ_H: 8.10 – 8.03 (m, 2H, $2C_{Ar}H$), 7.92 (dd, *J* = 7.7, 1.7 Hz, 2H, $2C_{Ar}H$), 7.84 (d, *J* = 8.0 Hz, 2H, $2C_{Ar}H$), 7.55 – 7.37 (m, 8H, $8C_{Ar}H$), 7.33 (br s, 1H, O*H*), 2.40 (br s, 1H, O*H*).

^{13}C NMR (101 MHz, $CDCl_3$) δ_C: 138.5 (2C), 134.0 (2C), 131.2 (2C), 129.0 (2C), 128.7 (2C), 126.6 (2C), 125.9 (2C), 125.6 (2C), 125.1 (2C), 123.8 (2C), 69.8.

Data was consistent with previously reported values.[169]

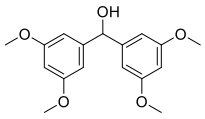

Bis(3,5-dimethoxyphenyl)methanol

To a dried multi-neck round bottom flask with a condenser attached, $Mg_{(s)}$ (583 mg, 24.3 mmol, 1.8 eq.), $I_{2(s)}$ (1 crystal) and THF (4 ml) was stirred at reflux for 30 mins until the suspension decolourised. Heating was halted before 1-bromo-3,5-dimethoxybenzene (4.34 ml, 20.0 mmol, 1.50 eq.) was added dropwise and the stirring mixture was heated to reflux (70 ˚C) for 3.5 h. The mixture was cooled to rt. To a stirring solution of 3,5-dimethoxybenzaldehyde (2.21 g, 13.3 mmol, 1.0 eq.) in THF (13 ml), the organomagnesium solution was added by syringe at 0 ˚C. The suspension was stirred at rt for 16 h. Then distilled H_2O (10 ml), $HCl_{(aq.)}$ (2 M, *ca.* 5 ml) and Et_2O were added to the suspension until no effervescence was observed. The mixture was partitioned between the aqueous and organic layer. The aqueous layer was extracted by Et_2O three times. The combined organic layer was dried with anhydrous $MgSO_{4(s)}$ and the solvent was removed *in vacuo* to afford bis(3,5-dimethoxyphenyl)methanol as a white solid (3.28 g, 54%).

^{1}H NMR (400 MHz, $CDCl_3$) δ_H: 6.55 (d, *J* = 2.2 Hz, 4H, 4C_{Ar}*H*), 6.36 (t, *J* = 2.3 Hz, 2H, 2C_{Ar}*H*), 5.68 (s, 1H, C*H*), 3.77 (s, 12H, 4C*H*$_3$), 2.18 (s, br, 1H, O*H*).

^{13}C NMR (101 MHz, $CDCl_3$) δ_C: 161.0 (4C), 146.1 (2C), 104.6 (4C), 99.6 (2C), 76.4, 55.5 (4C).

Data was consistent with previously reported values.[170]

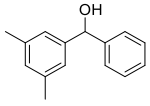

(3,5-Dimethylphenyl)(phenyl)methanol

To a dried multi-neck round bottom flask with a condenser attached, $Mg_{(s)}$ (94.8 mg, 3.9 mmol, 1.8 eq.), $I_{2(s)}$ (1 crystal) and THF (1 ml) was stirred at reflux for 30 mins until the suspension decolourised. Heating was halted before 1-bromo-3,5-dimethybenzene (0.57 ml, 4.3 mmol, 1.4 eq.) was added dropwise and the stirring mixture was heated to reflux (70 ˚C) for 3.5 h. The mixture was cooled to rt. To a stirring solution of benzaldehyde (305 µl, 3.0 mmol, 1.0 eq.) in THF (8 ml), the organomagnesium solution was added by syringe at 0 ˚C. The suspension was stirred at rt for 16 h. Then distilled H_2O (10 ml), $HCl_{(aq.)}$ (2 M, ca. 5 ml) and Et_2O were added to the suspension until no effervescence was observed. The mixture was partitioned between the aqueous and organic layer. The aqueous layer was extracted by Et_2O three times. The combined organic layer was dried with anhydrous $MgSO_{4(s)}$ and the solvent was removed *in vacuo*. The crude mixture was purified by column chromatography [SiO_2, pentane/EtOAc = 1:0 to 1:1] to afford (3,5-dimethylphenyl)(phenyl)methanol as a yellow viscous oil (512 mg, 80%).

^{1}H NMR (500 MHz, $CDCl_3$) δ_H: 7.44 – 7.40 (m, 2H, $2C_{Ar}H$), 7.39 – 7.34 (m, 2H, $2C_{Ar}H$), 7.31 – 7.27 (m, 1H, $C_{Ar}H$), 7.04 – 7.00 (m, 2H, $2C_{Ar}H$), 6.96 – 6.91 (m, 1H, $C_{Ar}H$), 5.80 (s, 1H, C*H*), 2.32 (s, 3H, CH_3), 2.32 (s, 3H, CH_3), 2.20 (s, br, 1H, O*H*).

^{13}C NMR (126 MHz, $CDCl_3$) δ_C: 144.1, 143.9, 138.2 (2C), 129.4, 128.6 (2C), 127.6, 126.6 (2C), 124.5 (2C), 76.5, 21.5 (2C).

HRMS (APCI$^+$) $[C_{15}H_{15}O]^+$ predicted 211.11174, found 211.11176 (Δ 0.06 ppm).

IR υ_{max} (film): 3347 (br), 2918, 1602, 701.

^{1}H NMR was consistent with previously reported values.[171]

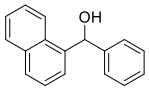

Naphthalen-1-yl(phenyl)methanol

To a dried multi-neck round bottom flask with a condenser attached, $Mg_{(s)}$ (1.30 g, 54.0 mmol, 1.8 eq.), $I_{2(s)}$ (1 crystal) and THF (30 ml) was stirred at reflux for 30 mins until the suspension decolourised. Heating was halted before 1-bromonaphthalene (6.30 ml, 45.0 mmol, 1.5 eq.) was added dropwise and the stirring mixture was heated to reflux (70 ˚C) for 3.5 h. The mixture was cooled to rt. To a stirring solution of benzaldehyde (3.05 ml, 30.0 mmol, 1.0 eq.) in THF (90 ml), the organomagnesium solution was added by syringe at 0 ˚C. The suspension was stirred at rt for 16 h. Then $HCl_{(aq.)}$ (2 M, ca. 40 ml) and Et_2O were added to the suspension until no effervescence was observed. The mixture was partitioned between the aqueous and organic layer. The aqueous layer was extracted by Et_2O three times. The combined organic layer was dried with anhydrous $MgSO_{4(s)}$ and the solvent was removed *in vacuo*. The crude mixture was purified by column chromatography [SiO_2,

petrol/EtOAc = 1:0 to 85:15] to afford naphthalen-1-yl(phenyl)methanol as a colourless viscous oil (6.53 g, 92%).

^{1}H NMR (500 MHz, $CDCl_3$) δ_H: 8.10 – 8.04 (m, 1H, $C_{Ar}H$), 7.93 – 7.82 (m, 2H, $2C_{Ar}H$), 7.67 (dt, *J* = 7.2, 1.0 Hz, 1H, $C_{Ar}H$), 7.55 – 7.43 (m, 5H, $5C_{Ar}H$), 7.39 – 7.33 (m, 2H, $2C_{Ar}H$), 7.32 – 7.27 (m, 1H, $C_{Ar}H$), 6.58 (s, 1H, C*H*), 2.33 (s, br, 1H, O*H*).

^{13}C NMR (126 MHz, $CDCl_3$) δ_C: 143.3, 139.0, 134.1, 130.9, 128.9, 128.7 (2C), 128.7, 127.8 (2C), 127.2, 126.3, 125.8, 125.5, 124.8, 124.1, 73.9.

Data was consistent with previously reported values.[172]

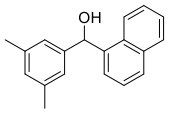

(3,5-Dimethylphenyl)(naphthalen-1-yl)methanol

To a dried multi-neck round bottom flask with a condenser attached, $Mg_{(s)}$ (94.8 mg, 3.9 mmol, 1.8 eq.), $I_{2(s)}$ (1 crystal) and THF (1 ml) was stirred at reflux for 30 mins until the suspension decolourised. Heating was halted before 1-bromo-3,5-dimethybenzene (0.57 ml, 4.3 mmol, 1.4 eq.) was added dropwise and the stirring mixture was heated to reflux (70 ˚C) for 3.5 h. The mixture was cooled to rt. To a stirring solution of naphthaldehyde (469 mg, 3.0 mmol, 1.0 eq.) in THF (8 ml), the organomagnesium solution was added by syringe at 0 ˚C. The suspension was stirred at rt for 16 h. Then distilled H_2O (10 ml), $HCl_{(aq.)}$ (2 M, ca. 5 ml) and Et_2O were added to the suspension until no effervescence was observed. The mixture was partitioned between the aqueous and organic layer. The aqueous layer was extracted by Et_2O three times. The combined organic layer was dried with anhydrous $MgSO_{4(s)}$ and the solvent was removed *in vacuo*. The crude mixture was

purified by column chromatography [SiO_2, pentane/EtOAc = 1:0 to 1:1] to afford (3,5-dimethylphenyl)(naphthalen-1-yl)methanol as a colourless solid (615 mg, 78%).

^{1}H NMR (500 MHz, $CDCl_3$) δ_H: 8.12 – 8.04 (m, 1H, $C_{Ar}H$), 7.91 – 7.88 (m, 1H, $C_{Ar}H$), 7.84 (d, *J* = 8.2 Hz, 1H, $C_{Ar}H$), 7.69 (dt, *J* = 7.0, 1.0 Hz, 1H, $C_{Ar}H$), 7.56 – 7.42 (m, 3H, $3C_{Ar}H$), 7.05 (s, 2H, $2C_{Ar}H$), 6.94 (s, 1H, $C_{Ar}H$), 6.53 – 6.49 (m, 1H, C*H*), 2.30 (s, 6H, CH_3), 2.26 (d, *J* = 3.7 Hz, 1H, O*H*).

^{13}C NMR (126 MHz, $CDCl_3$) δ_C: 143.2, 139.1, 138.3 (2C), 134.1, 130.9, 129.6, 128.9, 128.5, 126.3, 125.7, 125.5, 125.0 (2C), 124.6, 124.1, 73.8, 21.5 (2C).

HRMS (APCI$^+$) $[C_{19}H_{17}O]^+$ predicted 261.12739, found 261.12735 (Δ –0.16 ppm).

IR υ_{max} (s): 2981, 2360, 2342, 773.

M.P. = 95.0 - 96.6 ˚C.

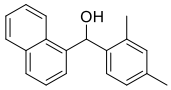

(2,4-Dimethylphenyl)(naphthalen-1-yl)methanol

To a dried multi-neck round bottom flask with a condenser attached, $Mg_{(s)}$ (1.30 g, 54.0 mmol, 1.8 eq.), $I_{2(s)}$ (1 crystal) and THF (30 ml) was stirred at reflux for 30 mins until the suspension decolourised. Heating was halted before 1-bromonaphthalene (6.30 ml, 45.0 mmol, 1.5 eq.) was added dropwise and the stirring mixture was heated to reflux (70 ˚C) for 3.5 h. The mixture was cooled to rt. To a stirring solution of 2,4-dimethylbenzaldehyde (4.18 ml, 30.0 mmol, 1.0 eq.) in THF (90 ml), the organomagnesium solution was added by syringe at 0 ˚C. The suspension was

stirred at rt for 16 h. Then $HCl_{(aq.)}$ (2 M, ca. 40 ml) and Et_2O were added to the suspension until no effervescence was observed. The mixture was partitioned between the aqueous and organic layer. The aqueous layer was extracted by Et_2O three times. The combined organic layer was dried with anhydrous $MgSO_{4(s)}$ and the solvent was removed *in vacuo*. The crude mixture was purified by column chromatography [SiO_2, petrol/EtOAc = 1:0 to 85:15] to afford (2,4-dimethylphenyl)(naphthalen-1-yl)methanol as a colourless residue (4.79 g, 61%).

^{1}H NMR (500 MHz, $CDCl_3$) δ_H: 8.07 – 8.00 (m, 1H, $C_{Ar}H$), 7.93 – 7.88 (m, 1H, $C_{Ar}H$), 7.86 – 7.80 (m, 1H, $C_{Ar}H$), 7.55 – 7.44 (m, 4H, $4C_{Ar}H$), 7.21 (d, *J* = 7.8 Hz, 1H, $C_{Ar}H$), 7.07 (s, 1H, $C_{Ar}H$), 7.00 (d, *J* = 8.0 Hz, 1H, $C_{Ar}H$), 6.74 (s, 1H, C*H*), 2.35 (d, *J* = 1.8 Hz, 6H, $2CH_3$), 2.12 (s, 1H, O*H*).

^{13}C NMR (126 MHz, $CDCl_3$) δ_C: 138.6, 138.2, 137.5, 135.8, 134.0, 131.6, 131.2, 128.9, 128.5, 127.0 (2C), 126.4, 125.8, 125.5, 124.6, 123.8, 70.1, 21.2, 19.3.

HRMS (ESI^+) $[C_{19}H_{17}O]^+$ predicted 261.12739, found 261.12741 (Δ 0.07 ppm).

IR υ_{max} (s): 2918, 2360, 1655, 1303, 781.

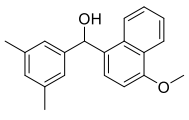

(3,5-Dimethylphenyl)(4-methoxynaphthalen-1-yl)methanol

To a dried multi-neck round bottom flask with a condenser attached, $Mg_{(s)}$ (707 mg, 29.1 mmol, 1.8 eq.), $I_{2(s)}$ (1 crystal) and THF (16 ml) was stirred at reflux for 30 mins until the suspension decolourised. Heating was halted before 1-bromo-3,5-dimethybenzene (5.0 g, 21.1 mmol, 1.3 eq.) was added dropwise and the stirring mixture was heated to reflux (70 ˚C) for 3.5 h. The mixture was cooled to rt. To a stirring solution of 4-methoxy-1-naphthaldehyde (2.18 ml, 16.2 mmol, 1.0 eq.) in

THF (40 ml), the organomagnesium solution was added by syringe at 0 ˚C. The suspension was stirred at rt for 16 h. Then distilled H_2O (10 ml), $HCl_{(aq.)}$ (2 M, ca. 5 ml) and Et_2O were added to the suspension until no effervescence was observed. The mixture was partitioned between the aqueous and organic layer. The aqueous layer was extracted by Et_2O three times. The combined organic layer was dried with anhydrous $MgSO_{4(s)}$ and the solvent was removed *in vacuo*. The crude mixture was purified by column chromatography [SiO_2, pentane/EtOAc = 1:0 to 8:2] to afford (3,5-dimethylphenyl)(4-methoxynaphthalen-1-yl)methanol as a colourless oil (985 mg, 21%).

^{1}H NMR (500 MHz, $CDCl_3$) δ_H: 8.58 – 8.51 (m, 1H, $C_{Ar}H$), 8.30 – 8.22 (m, 1H, $C_{Ar}H$), 7.75 – 7.65 (m, 3H, $3C_{Ar}H$), 7.28 – 7.24 (m, 2H, $2C_{Ar}H$), 7.14 (s, 1H, $C_{Ar}H$), 7.03 (d, *J* = 8.0 Hz, 1H, $C_{Ar}H$), 6.63 (d, *J* = 3.5 Hz, 1H, C*H*), 4.24 (s, 3H, OCH_3), 2.51 (s, 6H, $2CH_3$), 2.47 – 2.43 (m, 1H, O*H*).

^{13}C NMR (126 MHz, $CDCl_3$) δ_C: 155.5, 143.5, 138.1 (2C), 131.9, 131.2, 129.3, 126.8, 126.1, 125.2, 125.1, 124.9 (2C), 123.9, 122.7, 103.1, 73.7, 55.6, 21.5 (2C).

HRMS (ESI$^+$) $[C_{20}H_{20}O_2{}^{23}Na]^+$ predicted 315.13555, found 315.13565 (Δ 0.32 ppm).

IR υ_{max} (s): 3287, 2999, 2916, 1585, 767.

M.P. = 103 - 108 ˚C.

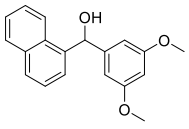

(3,5-Dimethoxyphenyl)(naphthalen-1-yl)methanol

To a dried multi-neck round bottom flask with a condenser attached, $Mg_{(s)}$ (1.30 g, 54.0 mmol, 1.8 eq.), $I_{2(s)}$ (1 crystal) and THF (30 ml) was stirred at reflux for 30 mins until the suspension decolourised. Heating was halted before 1-bromonaphthalene (6.30 ml, 45.0 mmol, 1.5 eq.) was added dropwise and the stirring mixture was heated to reflux (70 ˚C) for 3.5 h. The mixture was cooled to rt. To a stirring solution of 3,5-dimethoxybenzaldehyde (4.78 g, 30.0 mmol, 1.0 eq.) in THF (90 ml), the organomagnesium solution was added by syringe at 0 ˚C. The suspension was stirred at rt for 16 h. Then $HCl_{(aq.)}$ (2 M, ca. 40 ml) and Et_2O were added to the suspension until no effervescence was observed. The mixture was partitioned between the aqueous and organic layer. The aqueous layer was extracted by Et_2O three times. The combined organic layer was dried with anhydrous $MgSO_{4(s)}$ and the solvent was removed *in vacuo*. The crude mixture was purified by column chromatography [SiO_2, petrol/EtOAc = 1:0 to 85:15] to afford (3,5-dimethoxyphenyl)(naphthalen-1-yl)methanol as a colourless viscous oil (5.05 g, 61%).

^{1}H NMR (500 MHz, $CDCl_3$) δ_H: 8.09 (d, *J* = 2.5 Hz, 1H, $C_{Ar}H$), 7.90 – 7.85 (m, 1H, $C_{Ar}H$), 7.83 – 7.79 (m, 1H, $C_{Ar}H$), 7.60 (dt, *J* = 7.1, 1.0 Hz, 1H, $C_{Ar}H$), 7.51 – 7.43 (m, 3H, $3C_{Ar}H$), 6.59 (d, *J* = 2.4 Hz, 2H, $2C_{Ar}H$), 6.47 (d, *J* = 4.0 Hz, 1H, C*H*), 6.38 (t, *J* = 2.4 Hz, 1H, $C_{Ar}H$), 3.74 (s, 6H, $2OCH_3$), 2.31 (d, *J* = 4.0 Hz, 1H, O*H*).

^{13}C NMR (126 MHz, $CDCl_3$) δ_C: 161.1 (2C), 145.8, 138.7, 134.1, 131.0, 128.9, 128.7, 126.4, 125.8, 125.5, 124.9, 124.1, 105.3 (2C), 99.6, 73.8, 55.5 (2C).

HRMS (ESI^+) $[C_{19}H_{18}O_3{}^{23}Na]^+$ predicted 317.11482, found 317.11499 (Δ 0.55 ppm).

IR υ_{max} (film): 3421 (br), 2938, 2837, 2360, 1595, 1152, 780.

^{1}H NMR was consistent with previously reported values.[173]

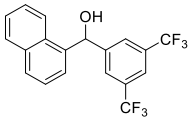

(3,5-Bis(trifluoromethyl)phenyl)(naphthalen-1-yl)methanol

To a stirring solution of 3,5-bis(trifluoromethyl)benzaldehyde (3.40 ml, 20.7 mmol, 1.0 eq.) in THF (21 ml), the premade naphthalen-1-ylmagnesium bromide solution (41 ml, 0.75 M, 31.0 mmol, 1.5 eq.) was added by syringe at 0 ˚C. The suspension was stirred at rt for 16 h. Then $HCl_{(aq.)}$ (2 M, ca. 40 ml) and Et_2O were added to the suspension until no effervescence was observed. The mixture was partitioned between the aqueous and organic layer. The aqueous layer was extracted by Et_2O three times. The combined organic layer was dried with anhydrous $MgSO_{4(s)}$ and the solvent was removed *in vacuo*. The crude mixture was purified by column chromatography [SiO_2, petrol/EtOAc = 1:0 to 85:15] to afford (3,5-bis(trifluoromethyl)phenyl)(naphthalen-1-yl)methanol as a white solid (2.71 g, 35%).

^{1}H NMR (500 MHz, $CDCl_3$) δ_H: 8.11 – 8.03 (m, 1H, $C_{Ar}H$), 7.95 – 7.85 (m, 4H, $4C_{Ar}H$), 7.81 (s, 1H, $C_{Ar}H$), 7.56 – 7.47 (m, 3H, $3C_{Ar}H$), 7.44 (dd, *J* = 7.2, 1.3 Hz, 1H, $C_{Ar}H$), 6.60 (s, 1H, C*H*), 2.55 (s, 1H, O*H*).

^{13}C NMR (126 MHz, $CDCl_3$) δ_C: 145.8, 137.6, 134.4, 131.8 (q, *J* = 33.3 Hz, 2C), 130.7, 129.8, 129.3, 127.0, 127.0 (2C), 126.3, 125.8, 125.5, 123.6, 123.5 (q, *J* = 272.7 Hz, 2C), 121.6 (p, *J* = 3.8 Hz), 73.1.

^{19}F NMR (471 MHz, $CDCl_3$) δ_F: −62.8 (s).

HRMS (ESI$^+$) $[C_{19}H_{11}OF_6]^+$ predicted 369.07086, found 369.07135 (Δ 1.33 ppm).

IR υ_{max} (s): 2981, 2360, 2342, 1276, 1125, 773.

M.P. = 89.5 - 94.7 ˚C.

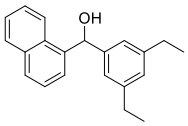

(3,5-Diethylphenyl)(naphthalen-1-yl)methanol

To a stirring solution of 3,5-diethylbenzaldehyde (1.00 g, 6.16 mmol, 1.0 eq.) in THF (6 ml), the premade naphthalen-1-ylmagnesium bromide solution (12.3 ml, 0.75 M, 9.24 mmol, 1.5 eq.) was added by syringe at 0 ˚C. The suspension was stirred at rt for 16 h. Then $HCl_{(aq.)}$ (2 M, ca. 40 ml) and Et_2O were added to the suspension until no effervescence was observed. The mixture was partitioned between the aqueous and organic layer. The aqueous layer was extracted by Et_2O three times. The combined organic layer was dried with anhydrous $MgSO_{4(s)}$ and the solvent was removed *in vacuo*. The crude mixture was purified by column chromatography [SiO_2, petrol/EtOAc = 1:0 to 85:15] to afford (3,5-diethylphenyl)(naphthalen-1-yl)methanol as a white solid (1.82 g, quantitative yield).

^{1}H NMR (500 MHz, $CDCl_3$) δ_H: 8.13 – 8.06 (m, 1H, $C_{Ar}H$), 7.91 – 7.83 (m, 1H, $C_{Ar}H$), 7.82 (dt, *J* = 8.2, 1.1 Hz, 1H, $C_{Ar}H$), 7.64 (dt, *J* = 7.2, 1.0 Hz, 1H, $C_{Ar}H$), 7.53 – 7.42 (m, 3H, $3C_{Ar}H$), 7.08 (d, *J* = 1.5 Hz, 2H, $2C_{Ar}H$), 6.97 (d, *J* = 1.8 Hz, 1H, $C_{Ar}H$), 6.52 (d, *J* = 3.9 Hz, 1H, C*H*), 2.60 (q, *J* = 7.6 Hz, 4H, $2CH_2$), 2.28 (d, *J* = 3.9 Hz, 1H, O*H*), 1.20 (t, *J* = 7.6 Hz, 6H, $2CH_3$).

^{13}C NMR (126 MHz, $CDCl_3$) δ_C: 144.7 (2C), 143.3, 139.2, 134.1, 131.0, 128.9, 128.5, 127.0, 126.2, 125.7, 125.5, 124.7, 124.1 (2C), 124.1, 73.9, 29.0 (2C), 15.7 (2C).

HRMS (ESI^+) $[C_{21}H_{22}O^{23}Na]^+$ predicted 313.15629, found 313.15631 (Δ 0.08 ppm).

IR υ_{max} (s): 3234 (br), 2964, 2361, 1598, 1456, 782.

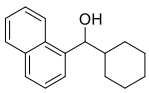

cyclohexyl(naphthalen-1-yl)methanol

To a stirring solution of cyclohexaldehyde (3.50 ml, 30.0 mmol, 1.0 eq.) in THF (52 ml), the premade naphthalen-1-ylmagnesium bromide solution (60 ml, 0.75 M, 45 mmol, 1.5 eq.) was added by syringe at 0 ˚C. The suspension was stirred at rt for 7 d. Then $HCl_{(aq.)}$ (2 M, ca. 40 ml) and Et_2O were added to the suspension until no effervescence was observed. The mixture was partitioned between the aqueous and organic layer. The aqueous layer was extracted by Et_2O three times. The combined organic layer was dried with anhydrous $MgSO_{4(s)}$ and the solvent was removed *in vacuo*. The crude mixture was purified by column chromatography [SiO_2, petrol/EtOAc = 1:0 to 8:2] to afford cyclohexyl(naphthalen-1-yl)methanol as a white solid (3.72 g, 52%).

^{1}H NMR (500 MHz, $CDCl_3$) δ_H: 8.16 (d, *J* = 8.1 Hz, 1H, $C_{Ar}H$), 7.90 – 7.85 (m, 1H, $C_{Ar}H$), 7.78 (d, *J* = 8.1, 1.0 Hz, 1H, $C_{Ar}H$), 7.59 (d, *J* = 7.1 Hz, 1H, $C_{Ar}H$), 7.55 – 7.43 (m, 3H, $3C_{Ar}H$), 5.20 (dd, *J* = 6.6, 3.1 Hz, 1H, C*H*OH), 2.02 – 1.95 (m, 1H, CH_aH_b), 1.95 – 1.87 (m, 2H, O*H*, C*H*CH_2), 1.81 – 1.73 (m, 1H, CH_aH_b), 1.70 – 1.60 (m, 2H, CH_aH_b, CH_aH_b), 1.46 – 1.38 (m, 1H, CH_aH_b), 1.24 – 1.12 (m, 5H, $5CH_aH_b$).

^{13}C NMR (126 MHz, $CDCl_3$) δ_C: 139.7, 134.0, 131.0, 129.0, 128.0, 125.9, 125.6, 125.4, 124.3, 123.8, 76.3, 44.5, 30.5, 28.4, 26.6, 26.5, 26.2.

Data was consistent with previously reported values.[174]

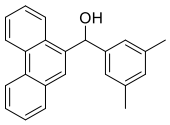

(3,5-Dimethylphenyl)(phenanthren-9-yl)methanol

To a stirring solution of phenanthren-9-al (1.32 mg, 6.40 mmol, 1.0 eq.) in THF (29 ml), the premade 3,5-dimethylphenylmagnesium bromide solution (16.6 ml, 0.50 M, 8.32 mmol, 1.3 eq.) was added by syringe at 0 °C. The suspension was stirred at rt for 2 d. Then $HCl_{(aq.)}$ (2 M, ca. 40 ml) and Et_2O were added to the suspension until no effervescence was observed. The mixture was partitioned between the aqueous and organic layer. The aqueous layer was extracted by Et_2O three times. The combined organic layer was dried with anhydrous $MgSO_{4(s)}$ and the solvent was removed *in vacuo*. The crude mixture was purified by column chromatography [SiO_2, petrol/EtOAc = 1:0 to 8:2] to afford (3,5-dimethylphenyl)(phenanthren-9-yl)methanol as a white solid (1.73 g, 87%).

^{1}H NMR (500 MHz, $CDCl_3$) δ_H: 8.79 – 8.68 (m, 2H, 2$C_{Ar}H$), 8.08 – 8.02 (m, 1H, $C_{Ar}H$), 8.03 (s, 1H, $C_{Ar}H$), 7.99 – 7.93 (m, 1H, $C_{Ar}H$), 7.75 – 7.59 (m, 3H, 3$C_{Ar}H$), 7.60 – 7.51 (m, 1H, $C_{Ar}H$), 7.09 (d, *J* = 1.5 Hz, 2H, 2$C_{Ar}H$), 6.95 (s, 1H, $C_{Ar}H$), 6.49 (s, 1H, C*H*), 2.36 (s, 1H, O*H*), 2.30 (s, 6H, 2CH_3).

^{13}C NMR (126 MHz, $CDCl_3$) δ_C: 154.7, 144.4, 137.9 (2C), 132.5, 131.6, 128.6, 126.6, 126.1, 125.7 (2C), 125.3, 124.8, 123.4, 122.7, 103.5, 59.8, 55.6, 46.8, 23.5, 23.5, 21.5 (2C).

HRMS (APCI$^+$) $[C_{23}H_{19}O]^+$ predicted 311.14304, found 311.14297 (Δ –0.22 ppm).

IR υ_{max} (s): 3291 (br), 2918, 1586, 726.

M.P. = 57 - 60 ˚C.

HRMS (CI$^+$) $[C_{20}H_{20}NO_2]^+$ predicted 306.1489, found 306.1485 (Δ 1.16 ppm).

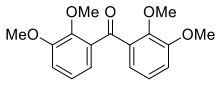

Bis(2,3-dimethoxyphenyl)methanone

This procedure has been modified from a procedure developed by Xiao and co-worker.[21] To a dried round bottom flask fitted with a condenser, Pd (231 mg,), and DPPP (165 mg) were add. Flush the flask with $Ar_{(g)}$ and add $AgNO_3$ (1.70 g,), (2,3-dimethoxyphenyl)boronic acid (1.81 g,) and dried acetone (30 ml). Purge the flask with CO 6 times then heat the mixture to 40 ˚C. The reaction was stirrer for 24 h before addition of H_2O (50 ml). The reaction mixture was extracted by DCM three times. The combined organic layer was dried with $Na_2SO_{4(s)}$ and filtered through Celite. The solvent was removed *in vacuo*. The product was purified by flash column chromatography [SiO_2, pentane/EtOAc, 5:2 then 5:3] gave yellow viscous oil. The oil was dissolved in minimum amount of Et_2O and filtered under reduced pressure to afford white solid of bis(2,3-dimethoxyphenyl)methanone (265 mg, 9%).

^{1}H NMR (400 MHz, $CDCl_3$) δ_H: 7.12 – 6.99 (m, 6H, 6C$_{Ar}$*H*), 3.87 (s, 6H, 2OC*H*$_3$), 3.64 (s, 6H, 2OC*H*$_3$).

^{13}C NMR (101 MHz, $CDCl_3$) δ_C: 196.2, 153.0 (2C), 148.0 (2C), 135.5 (2C), 123.7 (2C), 121.3 (2C), 115.3 (2C), 61.5 (2C), 56.1 (2C).

HRMS (ESI$^+$) $[C_{17}H_{19}O_5]^+$ predicted 303.1227, found 303.1228 (Δ 0.44 ppm).

IR υ_{max} (film): 2933, 2836, 2360, 1594, 1156.

Data was consistent with previously reported values.[175]

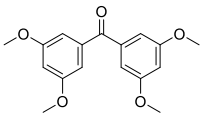

Bis(3,5-dimethoxyphenyl)methanone

In a dried round bottom flask, a mixture of bis(3,5-dimethoxyphenyl)methanol (3.28 g, 10.9 mmol, 1.0 eq.), $MnO_{2(s)}$ (28.3 g, 326 mmol, 30.0 eq.) and DCM (18 ml) was stirred vigorously at rt for 72 h. The mixture was filtered through Celite/DCM and the solvent was removed *in vacuo* to afford bis(3,5-dimethoxyphenyl)methanone as an off-white solid (3.06 g, 93%).

^{1}H NMR (400 MHz, $CDCl_3$) δ_H: 6.93 (d, *J* = 2.4 Hz, 4H, 4C$_{Ar}$*H*), 6.66 (t, *J* = 2.3 Hz, 2H, 2C$_{Ar}$*H*), 3.82 (s, 12H, 4C*H*$_3$).

^{13}C NMR (101 MHz, $CDCl_3$) δ_C: 196.1, 160.6 (4C), 139.5 (2C), 108.0 (4C), 105.0 (2C), 55.7 (4C).

Data was consistent with previously reported values.[170]

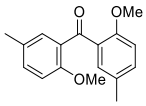

Bis(2-methoxy-5-methylphenyl)methanone

This procedure has been modified from a procedure developed by Xiao and co-worker.[21] To a dried round bottom flask fitted with a condenser, Pd (578 mg, 0.50 mmol, 0.05 eq.), and DPPP (412 mg, 1.0 mmol, 0.10 eq.) were added. The flask was flushed with $Ar_{(g)}$ before $AgNO_{3(s)}$ (1.70 g, 10 mmol, 1.0 eq.), (2-methoxy-5-

methylphenyl)boronic acid (1.66 g, 10 mmol, 1.0 eq.) and dried acetone (30 ml) were added. The flask was purged with $CO_{(g)}$ 6 times then the reaction mixture ws heated to 40 °C. The reaction was stirred for 24 h before the addition of H_2O (50 ml). Then, the reaction mixture was extracted by DCM three times. The combined organic layer was dried with $Na_2SO_{4(s)}$ and filtered through Celite. The solvent was removed *in vacuo*. The product was purified by flash column chromatography [SiO_2, pentane/EtOAc, 85:15] giving a yellow viscous oil. The oil was frozen and dried under high vacuum to afford white solid of bis(2-methoxy-5-methylphenyl)methanone (286 mg, 11%).

^{1}H NMR (400 MHz, $CDCl_3$) δ_H: 7.24 – 7.18 (m, 2H, 2C$_{Ar}$*H*), 7.14 – 7.06 (m, 2H, 2C$_{Ar}$*H*), 6.69 (d, *J* = 8.3 Hz, 2H, 2C$_{Ar}$*H*), 3.50 (s, 3H, OC*H*$_3$), 2.18 (s, 3H, C*H*$_3$).

^{13}C NMR (101 MHz, $CDCl_3$) δ_C: 195.5, 156.3 (2C), 133.0 (2C), 130.5 (2C), 130.0 (2C), 129.5(2C), 111.5 (2C), 55.8 (2C), 20.3 (2C).

HRMS (ESI$^+$) $[C_{17}H_{19}O_3]^+$ predicted 271.1329, found 271.1331 (Δ 0.68 ppm).

IR υ_{max} (film): 3650, 3318, 2980, 1979, 1597.

M.P. = 57.4 - 61.0 °C.

Melting point was consistent with previously reported values.[176]

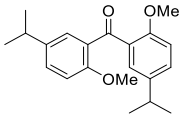

Bis(5-isopropyl-2-methoxyphenyl)methanone

This procedure has been modified from a procedure developed by Xiao and co-worker.[21] To a dried round bottom flask fitted with a condenser, Pd (578 mg, 0.50 mmol, 0.05 eq.), and DPPP (412 mg, 1.0 mmol, 0.10 eq.) were added. The flask was flushed with $Ar_{(g)}$ and $AgNO_{3(s)}$ (1.70 g, 10 mmol, 1.0 eq.), (2-methoxy-5-isopropylphenyl)boronic acid (1.94 g, 10 mmol, 1.0 eq.) and dried acetone (30 ml) were added. The flask was purged with $CO_{(g)}$ 6 times then the reaction mixture was heated to 40 °C. The reaction was stirred for 24 h before the addition of H_2O (50 ml). Then, tge reaction mixture was extracted by DCM three times. The combined organic layer was dried with $Na_2SO_{4(s)}$ and filtered through Celite. The solvent was removed *in vacuo*. The product was purified by flash column chromatography [SiO_2, pentane/EtOAc, 9:1 then 85:15] giving a yellow viscous oil of bis(5-isopropyl-2-methoxyphenyl)methanone (372 mg, 11%).

^{1}H NMR (400 MHz, $CDCl_3$) δ_H: 7.39 (d, *J* = 2.4 Hz, 2H, 2C$_{Ar}$*H*), 7.30 (dd, *J* = 2.4, 8.4 Hz, 2H, 2C$_{Ar}$*H*), 6.86 (d, *J* = 8.4 Hz, 2H, 2C$_{Ar}$*H*), 3.64 (s, 3H, OC*H*$_3$), 2.89 (hept, *J* = 6.9 Hz, 1H, C*H*), 1.24 (d, *J* = 6.9 Hz, 12H, 4CHC*H*$_3$).

^{13}C NMR (101 MHz, $CDCl_3$) δ_C: 195.8, 156.6 (2C), 140.6 (2C), 130.3(2C), 130.0(2C), 128.3(2C), 111.6 (2C), 55.9 (2C), 33.2 (2C), 24.1 (4C).

HRMS (ESI^+) $[C_{21}H_{27}O_3]^+$ predicted 327.1966, found 327.1953 (Δ −3.84 ppm).

IR υ_{max} (film): 2959, 2870, 1650, 1487, 1255.

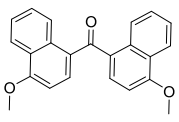

Bis(4-methoxynaphthalen-1-yl)methanone

To a dried round bottom flask with a condenser attached, $Mg_{(s)}$ (1.37 g, 56.0 mmol, 10 eq.), $I_{2(s)}$ (1 crystal) and THF (3 ml) was stirred at reflux for 10 mins until the suspension decolourised. Heating was halted before 1-bromo-4-methoxynaphthalene (2.00 g, 8.44 mmol, 1.50 eq.) was added dropwise and the stirring mixture was heated to reflux for 6 h. The mixture was cooled to rt. To a stirring solution of 4-methoxynaphthaldehyde (1.05 g, 5.62 mmol, 1.0 eq.) in THF (4 ml), the organomagnesium solution was added dropwise by syringe at 0 °C. The suspension was stirred at rt for 18h. Then $HCl_{(aq.)}$ (2 M, ca. 5 ml) and Et_2O were added to the suspension. The mixture was partitioned between the aqueous and organic layer. The aqueous layer was extracted by DCM three times. The combined organic layer was dried with anhydrous $MgSO_{4(s)}$ and the solvent was removed *in vacuo*. The crude reaction mixture was used in the next step without further purification.

In a dried round bottom flask, bis(4-methoxynaphthalen-1-yl)methanol as a crude reaction mixture (1.94 g, 5.62 mmol, 1.0 eq.), MnO_2 (14.7 g, 169 mmol, 30.0 eq.) and DCM (11 ml) were added and stirred vigorously at rt for 72 h. The mixture was filtered through Celite/DCM and the solvent was removed *in vacuo*. The crude reaction mixture was purified by flash column chromatography [SiO_2, pentane/EtOAc, 95:5 to 8:2] to give orange solid. Subsequent recrystallisation of the product in EtOAc and hexane afforded a white crystalline solid of bis(4-methoxynaphthalen-1-yl)methanone product (1.41 g, 74% over two steps).

^{1}H NMR (400 MHz, $CDCl_3$) δ_H: 8.69 – 8.61 (m, 2H, $C_{Ar}H$), 8.43 – 8.32 (m, 2H, $C_{Ar}H$), 7.65 – 7.49 (m, 6H, $C_{Ar}H$), 6.69 (d, J = 8.2 Hz, 2H, $C_{Ar}H$), 4.02 (s, 6H, CH_3).

^{13}C NMR (101 MHz, $CDCl_3$) δ_C: 198.3, 158.5, 132.9, 132.6, 130.2, 128.3, 126.0, 125.9, 125.8, 122.3, 102.2, 55.8.

HRMS (ESI^+) $[C_{20}H_{28}O_4]^+$ predicted 343.13287, found 343.13293 (Δ -0.19 ppm).

IR υ_{max} (film): 2970, 1669, 1265, 1092.

MP. = 152-154 ˚C.

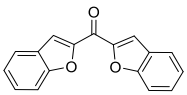
Di(benzofuran-2-yl)methanone

To a dried round bottom flask with a condenser attached, $Mg_{(s)}$ (822 mg, 33.8 mmol, 10 eq.), $I_{2(s)}$ (1 crystal) and THF (2.5 ml) was stirred at reflux for 10 mins until the suspension decolourised. Heating was halted before 2-bromobenzofuran (0.94 g, 5.08 mmol, 1.50 eq.) was added dropwise and the stirring mixture was heated to reflux for 2.5 h. The mixture was cooled to rt. To a stirring solution of benzofuran-2-carbaldehyde (495 mg, 3.38 mmol, 1.0 eq.) in THF (2 ml), the organomagnesium solution was added dropwise by syringe at 0 °C. The suspension was stirred at rt for 20h. Then $HCl_{(aq.)}$ (2 M, ca. 5 ml) and Et_2O were added to the suspension. The mixture was partitioned between the aqueous and organic layer. The aqueous layer was extracted by DCM three times. The combined organic layer was dried with anhydrous $MgSO_{4(s)}$ and the solvent was removed *in vacuo*. The crude reaction mixture was used in the next step without further purification.

In a dried round bottom flask, di(benzofuran-2-yl)methanol as a crude reaction mixture (1.00 g, 3.38 mmol, 1.0 eq.), $MnO_{2(s)}$ (8.82 g, 101 mmol, 30.0 eq.) and DCM

(6 ml) were added and stirred vigorously at rt for 72 h. The mixture was filtered through Celite/DCM and the solvent was removed *in vacuo*. The crude reaction mixture was purified by flash column chromatography [SiO_2, pentane/EtOAc, 95:5 to 8:2] to give an orange solid product (275 mg, 31% over two steps).

^{1}H NMR (400 MHz, $CDCl_3$) δ_H: 8.04 (d, *J* = 1.0 Hz, 2H, 2C_{Ar}*H*CC=O), 7.82 –7.78 (m, 2H, 2C_{Ar}*H*), 7.70 – 7.66 (m, 2H, 2C_{Ar}*H*), 7.56 – 7.51 (m, 2H, 2C_{Ar}*H*), 7.39 – 7.34 (m, 2H, 2C_{Ar}*H*).

^{13}C NMR (101 MHz, $CDCl_3$) δ_C: 171.7, 156.0 (2C), 151.8 (2C), 128.8 (2C), 127.2 (2C), 124.3 (2C), 123.7 (2C), 116.3 (2C), 112.6 (2C).

Data was consistent with previously reported values.[177]

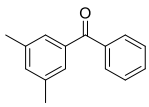

(3,5-Dimethylphenyl)(phenyl)methanone

In a dried round bottom flask, (3,5-dimethylphenyl)(phenyl)methanol (440 mg, 2.07 mmol, 1.0 eq.), $MnO_{2(s)}$ (5.40 g, 62.1 mmol, 30.0 eq.) and DCM (9 ml) was stirred vigorously at rt for 4 days. The mixture was filtered through Celite/DCM and the solvent was removed *in vacuo* to afford (3,5-dimethylphenyl)(phenyl)methanone as a colourless residue (412 mg, 94%).

^{1}H NMR (500 MHz, $CDCl_3$) δ_H: 7.83 – 7.77 (m, 2H, 2C_{Ar}*H*), 7.62 – 7.55 (m, 1H, C_{Ar}*H*), 7.48 (dd, *J* = 8.3, 7.0 Hz, 2H, 2C_{Ar}*H*), 7.42 – 7.38 (m, 2H, 2C_{Ar}*H*), 7.26 – 7.20 (m, 1H, C_{Ar}*H*), 2.38 (d, *J* = 0.8 Hz, 6H, 3C*H*$_3$).

^{13}C NMR (126 MHz, $CDCl_3$) δ_C: 197.3, 138.1, 138.1 (2C), 137.9, 134.2, 132.4 (2C), 130.2 (2C), 128.3 (2C), 127.9, 21.4 (2C).

Data was consistent with previously reported values.[178]

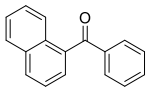 Naphthalen-1-yl(phenyl)methanone

In a dried round bottom flask, naphthalen-1-yl(phenyl)methanol (6.53 g, 27.9 mmol, 1.0 eq.), $MnO_{2(s)}$ (48.5 g, 558 mmol, 20.0 eq.) and DCM (100 ml) was stirred vigorously at rt for 3 days. The mixture was filtered through Celite/DCM and the solvent was removed *in vacuo* to afford naphthalen-1-yl(phenyl)methanone as a viscous yellow oil (6.06 g, 94%).

^{1}H NMR (500 MHz, $CDCl_3$) δ_H: 8.11 (d, *J* = 8.3 Hz, 1H, $C_{Ar}H$), 8.01 (dt, *J* = 8.2, 1.1 Hz, 1H, $C_{Ar}H$), 7.93 (dd, *J* = 7.8, 1.7 Hz, 1H, $C_{Ar}H$), 7.90 – 7.85 (m, 2H, $2C_{Ar}H$), 7.64 – 7.57 (m, 2H, $2C_{Ar}H$), 7.57 – 7.43 (m, 5H, $5C_{Ar}H$).

^{13}C NMR (126 MHz, $CDCl_3$) δ_C: 198.1, 138.5, 136.5, 133.8, 133.3, 131.4, 131.1, 130.5 (2C), 128.6 (2C), 128.5, 127.9, 127.4, 126.6, 125.8, 124.4.

HRMS (ESI$^+$) $[C_{17}H_{13}O]^+$ predicted 233.09609, found 233.09608 (Δ −0.03 ppm).

IR υ_{max} (film): 3057, 2360, 1655, 1248, 774, 711.

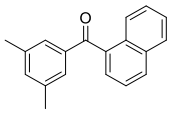 (3,5-Dimethylphenyl)(naphthalen-1-yl)methanone

In a dried round bottom flask, (3,5-dimethylphenyl)(naphthalen-1-yl)methanol (610 mg, 2.33 mmol, 1.0 eq.), $MnO_{2(s)}$ (6.06 g, 69.8 mmol, 30.0 eq.) and DCM (5 ml) was stirred vigorously at rt for 4 days. The mixture was filtered through Celite/DCM and the solvent was removed *in vacuo* to afford (3,5-dimethylphenyl)(naphthalen-1-yl)methanone as a colourless residue (531 mg, 88%).

^{1}H NMR (500 MHz, $CDCl_3$) δ_H: 8.08 (d, *J* = 8.2 Hz, 1H, $C_{Ar}H$), 8.00 (d, *J* = 8.0 Hz, 1H, $C_{Ar}H$), 7.94 – 7.91 (m, 1H, $C_{Ar}H$), 7.59 – 7.44 (m, 4H, $4C_{Ar}H$), 7.47 (s, 2H, 2*o*-$C_{Ar}H$), 7.24 (s, 1H, *p*-$C_{Ar}H$), 2.34 (s, 6H, $2CH_3$).

^{13}C NMR (126 MHz, $CDCl_3$) δ_C: 198.6, 138.6, 138.3 (2C), 136.9, 135.1, 133.9, 131.2, 131.1, 128.5, 128.3 (2C), 128.0, 127.7, 127.3, 126.5, 125.9, 124.5, 21.3 (2C).

HRMS (ESI^+) $[C_{19}H_{17}O]^+$ predicted 261.12739, found 261.12741 (Δ 0.07 ppm).

IR υ_{max} (film): 2917, 2360, 1655, 1303, 781.

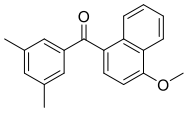

(3,5-dimethylphenyl)(4-methoxynaphthalen-1-yl)methanone

In a dried round bottom flask, (3,5-dimethylphenyl)(4-methoxynaphthalen-1-yl)methanol (985 mg, 3.40 mmol, 1.0 eq.), $MnO_{2(s)}$ (8.79 g, 10.2 mmol, 30.0 eq.) and DCM (15 ml) was stirred vigorously at rt for 4 days. The mixture was filtered through Celite/DCM and the solvent was removed *in vacuo* to afford (3,5-dimethylphenyl)(4-methoxynaphthalen-1-yl)methanone as a colourless solid (861 mg, 88%).

^{1}H NMR (500 MHz, $CDCl_3$) δ_H: 8.35 (dt, *J* = 8.0, 1.6 Hz, 2H, 2$C_{Ar}H$), 7.62 – 7.49 (m, 3H, 3$C_{Ar}H$), 7.45 (s, 2H, 2*o*-$C_{Ar}H$), 7.22 (s, 1H, *p*-$C_{Ar}H$), 6.80 (d, *J* = 8.0 Hz, 1H, C*H*), 4.08 (d, *J* = 1.3 Hz, 3H, OCH_3), 2.36 (s, 6H, 2CH_3)

^{13}C NMR (126 MHz, $CDCl_3$) δ_C: 197.9, 158.3 (2C), 139.7, 138.0, 134.4, 132.8, 131.2, 128.7, 128.2 (2C), 128.1, 125.9, 125.9 (2C), 122.3, 102.1, 55.9, 21.4 (2C).

HRMS (ESI^+) $[C_{20}H_{18}O_2{}^{23}Na]^+$ predicted 313.11990, found 313.1975 (Δ –0.48 ppm).

IR υ_{max} (s): 2981, 2360, 1647, 1227, 770.

MP. = 126 - 132 ˚C

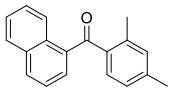
(2,4-Dimethylphenyl)(naphthalen-1-yl)methanone

In a dried round bottom flask, 2,4-dimethylphenyl)(naphthalen-1-yl)methanol (4.79 g, 18.3 mmol, 1.0 eq.), $MnO_{2(s)}$ (31.8 g, 36.6 mmol, 20.0 eq.) and DCM (92 ml) was stirred vigorously at rt for 3 days. The mixture was filtered through Celite/DCM and the solvent was removed *in vacuo* to afford (2,4-dimethylphenyl)(naphthalen-1-yl)methanone as a viscous yellow oil (4.80 g, quantitative yield).

^{1}H NMR (500 MHz, $CDCl_3$) δ_H: 8.49 – 8.43 (m, 1H, $C_{Ar}H$), 8.09 – 7.97 (m, 1H, $C_{Ar}H$), 8.01 – 7.89 (m, 1H, $C_{Ar}H$), 7.68 – 7.54 (m, 3H, 3$C_{Ar}H$), 7.52 – 7.45 (m, 1H, $C_{Ar}H$), 7.35 – 7.27 (m, 1H, $C_{Ar}H$), 7.18 (s, 1H, $C_{Ar}H$), 7.06 – 6.98 (m, 1H, $C_{Ar}H$), 2.54 (s, 3H, CH_3), 2.42 (s, 3H, CH_3).

^{13}C NMR (126 MHz, $CDCl_3$) δ_C: 200.1, 141.9, 139.0, 137.4, 136.6, 134.0, 132.5, 132.1, 131.5, 131.1, 129.5, 128.5, 127.7, 126.5, 126.2, 125.9, 124.5, 21.6, 21.0.

HRMS (ESI$^+$) $[C_{19}H_{17}O]^+$ predicted 261.12739, found 261.12744 (Δ 0.19 ppm).

IR υ_{max} (film): 2922, 2361, 1653, 777.

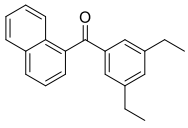

(3,5-Diethylphenyl)(naphthalen-1-yl)methanone

In a dried round bottom flask, (3,5-diethylphenyl)(naphthalen-1-yl)methanol (1.79 g, 6.2 mmol, 1.0 eq.), $MnO_{2(s)}$ (10.7 g, 123 mmol, 20.0 eq.) and DCM (30 ml) was stirred vigorously at rt for 3 days. The mixture was filtered through Celite/DCM and the solvent was removed *in vacuo* to afford (3,5-diethylphenyl)(naphthalen-1-yl)methanone as a viscous colourless oil (1.72 g, 97%).

^{1}H NMR (500 MHz, $CDCl_3$) δ_H: 8.17 – 8.11 (m, 1H, $C_{Ar}H$), 8.03 (dt, *J* = 7.9, 1.1 Hz, 1H, $C_{Ar}H$), 7.99 – 7.92 (m, 1H, $C_{Ar}H$), 7.63 – 7.49 (m, 5H, $5C_{Ar}H$), 7.31 – 7.29 (m, 1H, $C_{Ar}H$), 7.28 (s, 1H, *p*-$C_{Ar}H$), 2.73 – 2.63 (m, 4H, $2CH_2$), 1.25 (t, *J* = 7.6 Hz, 6H, $2CH_3$).

^{13}C NMR (126 MHz, $CDCl_3$) δ_C: 198.4, 144.6 (2C), 138.5, 136.8, 133.7, 132.7, 131.0, 128.3, 127.6, 127.4 (2C), 127.1, 126.4, 125.8, 124.3, 28.7 (2C), 15.5 (2C).

HRMS (ESI$^+$) $[C_{21}H_{20}O^{23}Na]^+$ predicted 311.14064, found 311.14053 (Δ –0.33 ppm).

IR υ_{max} (film): 2964, 2931, 2360, 1655, 780.

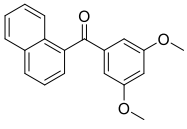

(3,5-Dimethoxyphenyl)(naphthalen-1-yl)methanone

In a dried round bottom flask, (3,5-dimethoxyphenyl)(naphthalen-1-yl)methanol (7.07 g, 26.0 mmol, 1.0 eq.), $MnO_{2(s)}$ (45.5 g, 523 mmol, 20.0 eq.) and DCM (130 ml) was stirred vigorously at rt for 3 days. The mixture was filtered through Celite/DCM and the solvent was removed *in vacuo* to afford (3,5-dimethoxyphenyl)(naphthalen-1-yl)methanone as a viscous colourless oil (7.08 g, 93%).

^{1}H NMR (500 MHz, $CDCl_3$) δ_H: 8.12 – 8.08 (m, 1H, $C_{Ar}H$), 8.00 (d, J = 8.4 Hz, 1H, $C_{Ar}H$), 7.94 – 7.90 (m, 1H, $C_{Ar}H$), 7.61 – 7.58 (m, 1H, $C_{Ar}H$), 7.56 – 7.47 (m, 3H, $3C_{Ar}H$), 7.01 (d, J = 2.2 Hz, 2H, $2C_{Ar}H$), 6.70 (q, J = 2.3, 1.7 Hz, 1H, $C_{Ar}H$), 3.80 (s, 6H, $2CH_3$).

^{13}C NMR (126 MHz, $CDCl_3$) δ_C: 197.7, 160.9 (2C), 140.4, 136.4, 133.9, 131.4, 131.1, 128.5, 127.9, 127.4, 126.6, 125.8, 124.4, 108.4 (2C), 105.8, 55.7 (2C).

HRMS (ESI^+) $[C_{19}H_{17}O_3]^+$ predicted 293.11722, found 293.11697 (Δ –0.84 ppm).

IR υ_{max} (film): 2938, 2837, 2360, 1656, 1589, 1154, 780.

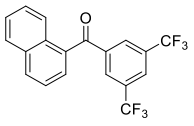

(3,5-Bis(trifluoromethyl)phenyl)(naphthalen-1-yl)methanone

In a dried round bottom flask, (3,5-bis(trifluoromethyl)phenyl)(naphthalen-1-yl)methanol (2.69 g, 7.27 mmol, 1.0 eq.), $MnO_{2(s)}$ (12.6 g, 145 mmol, 20.0 eq.) and DCM (35 ml) was stirred vigorously at rt for 3 days. The mixture was filtered through Celite/DCM and the solvent was removed *in vacuo* to afford (3,5-bis(trifluoromethyl)phenyl)(naphthalen-1-yl)methanone as a white solid (2.57 g, 96%).

^{1}H NMR (500 MHz, $CDCl_3$) δ_H: 8.33 – 8.28 (m, 2H, $2C_{Ar}H$), 8.23 – 8.17 (m, 1H, $C_{Ar}H$), 8.15 – 8.06 (m, 2H, $2C_{Ar}H$), 8.01 – 7.95 (m, 1H, $C_{Ar}H$), 7.65 – 7.52 (m, 4H, $4C_{Ar}H$).

^{13}C NMR (126 MHz, $CDCl_3$) δ_C: 194.8, 140.4, 134.1, 134.1, 133.1, 132.4 (q, *J* = 34.0 Hz, 2C), 132.4, 130.3 (q, *J* = 4.0 Hz, 2C), 129.0, 128.9, 128.2, 127.2, 126.4 – 126.3 (m), 125.4, 124.4, 123.0 (q, *J* = 273.1 Hz, 2C).

^{19}F NMR (471 MHz, $CDCl_3$) δ_F: –62.9 (s).

HRMS ($APCI^+$) $[C_{19}H_{11}OF_6]^+$ predicted 349.07086, found 349.07086 (Δ –0.01 ppm).

IR υ_{max} (s): 2981, 2360, 1662, 1122.

M.P. = 87.0 - 89.5 °C.

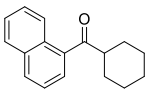
Cyclohexyl(naphthalen-1-yl)methanone

In a dried round bottom flask, cyclohexyl(naphthalen-1-yl)methanol (940 mg, 3.91 mmol, 1.0 eq.), $MnO_{2(s)}$ (11.7 g, 135 mmol, 34.5 eq.) and DCM (20 ml) was stirred vigorously at rt for 13 d. The mixture was filtered through Celite/DCM and the solvent was removed *in vacuo*. The crude reaction mixture was purified by flash column chromatography [SiO_2, petrol/EtOAc, 1:0 to 9:1] to give cyclohexyl(naphthalen-1-yl)methanone as a white solid (782 g, 84%).

^{1}H NMR (500 MHz, $CDCl_3$) δ_H: 8.29 – 8.23 (m, 1H, $C_{Ar}H$), 7.95 (dt, *J* = 8.1, 1.1 Hz, 1H, $C_{Ar}H$), 7.90 – 7.82 (m, 1H, $C_{Ar}H$), 7.71 (dd, *J* = 7.1, 1.2 Hz, 1H, $C_{Ar}H$), 7.60 – 7.45 (m, 3H, $3C_{Ar}H$), 3.20 (tt, *J* = 11.4, 3.4 Hz, 1H, C*H*), 1.99 – 1.89 (m, 2H, $2CH_aH_b$), 1.88 – 1.79 (m, 2H, $2CH_aH_b$), 1.75 – 1.67 (m, 1H, CH_aH_b), 1.60 – 1.49 (m, 2H, $2CH_aH_b$), 1.42 – 1.22 (m, 3H, $3CH_aH_b$).

^{13}C NMR (126 MHz, $CDCl_3$) δ_C: 208.7, 137.4, 134.0, 131.6, 130.6, 128.5, 127.6, 126.5, 125.8, 125.8, 124.5, 49.9, 29.1 (2C), 26.1, 25.9 (2C).

HRMS (ESI^+) $[C_{17}H_{19}O]^+$ predicted 239.14304, found 239.14311 (Δ 0.29 ppm).

IR υ_{max} (s): 2981, 2360, 774.

M.P. = 61.1 – 62.9 °C.

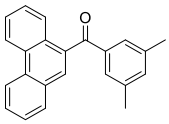

(3,5-Dimethylphenyl)(phenanthren-9-yl)methanone

In a dried round bottom flask, (3,5-dimethylphenyl)(phenanthren-9-yl)methanol (1.71 g, 5.37 mmol, 1.0 eq.), $MnO_{2(s)}$ (14.3 g, 164 mmol, 30 eq.) and DCM (27 ml) was stirred vigorously at rt for 3 d. The mixture was filtered through Celite/DCM and the solvent was removed *in vacuo*. The crude reaction mixture was purified by flash column chromatography [SiO_2, petrol/EtOAc, 1:0 to 8:2] to give (3,5-dimethylphenyl)(phenanthren-9-yl)methanone as a white solid (1.34 g, 79%).

^{1}H NMR (500 MHz, $CDCl_3$) δ_H: 8.69 – 8.60 (m, 2H, 2$C_{Ar}H$), 8.01 (dd, J = 8.3, 1.2 Hz, 1H, $C_{Ar}H$), 7.79 (dd, J = 7.9, 1.3 Hz, 1H, $C_{Ar}H$), 7.73 (s, 1H, $C_{Ar}H$), 7.68 – 7.44 (m, 6H, 6$C_{Ar}H$), 7.17 – 7.13 (m, 1H, $C_{Ar}H$), 2.24 (s, 6H, 2CH_3).

^{13}C NMR (126 MHz, $CDCl_3$) δ_C: 198.5, 138.5, 138.4 (2C), 135.9, 135.3, 131.4, 130.7, 130.3, 129.6, 129.6, 128.9, 128.3 (3C), 127.3, 127.3, 127.2, 126.8, 123.0, 122.8, 21.3 (2C).

HRMS (ESI^+) $[C_{23}H_{19}O]^+$ predicted 311.14304, found 311.14304 (Δ –0.02 ppm).

IR υ_{max} (s): 2918, 2165, 1655, 747, 724.

M.P. = 100 - 103 °C.

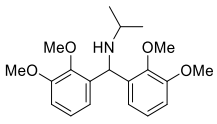

N-(bis(2,3-dimethoxyphenyl)methyl)propan-2-amine

General procedure B: bis(2,3-dimethoxyphenyl)methanone (211 mg, 0.70 mmol, 1.0 eq.), DCM (2.0 ml) $TiCl_4$ solution in DCM (0.77 ml, 1.0 M, 0.77 mmol, 1.1 eq.), isopropylamine (0.18 ml, 2.10 mmol, 3.0 eq.) $NaB(CN)H_{3(s)}$ (220 mg, 3.50 mmol, 5.0 eq.) in THF (3.5 ml), anhydrous MeOH (0.4 ml), reaction duration 18 h. *N*-(bis(2,3-dimethoxyphenyl)methyl)propan-2-amine was used without further purification.

^{1}H NMR (400 MHz, $CDCl_3$) δ_H: 7.05 – 6.92 (m, 4H, 4CH_{Ar}), 6.80 (dd, *J* = 7.7, 1.9 Hz, 2H, 2CH_{Ar}), 5.68 (s, 1H, C*H*Ar), 3.84 (s, 6H, 2OCH_3), 3.70 (s, 6H, 2OCH_3), 2.75 (hept, *J* = 6.2 Hz, 1H, C*H*Me), 1.09 (d, *J* = 6.2 Hz, 6H, 2CHCH_3).

^{13}C NMR (101 MHz, $CDCl_3$) δ_C: 152.8 (2C), 146.9 (2C), 137.9 (2C), 123.8 (2C), 120.6 (2C), 110.9 (2C), 60.3 (2C), 55.8 (2C), 51.9, 46.5, 23.2 (2C).

HRMS (ESI$^+$) $[C_{20}H_{28}O_4]^+$ predicted 346.2013, found 346.2011 (Δ −0.68 ppm).

IR υ_{max} (film): 2961, 2361, 1478, 1266.

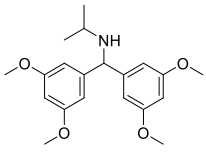

N-(bis(3,5-dimethoxyphenyl)methyl)propan-2-amine

General procedure B: bis(3,5-dimethoxyphenyl)methanone (1.06 g, 3.5 mmol, 1.0 eq.), DCM (10 ml) $TiCl_4$ solution in DCM (3.85 ml, 1.0 M, 3.85 mmol, 1.1 eq.), isopropylamine (0.90 ml, 10.5 mmol, 3.0 eq.), $NaB(CN)H_{3(s)}$ (1.10 g, 17.5 mmol, 5.0 eq.) in THF (17.5 ml), anhydrous MeOH (2.0 ml), reaction duration 17 h. *N*-(bis(3,5-dimethoxyphenyl)methyl)propan-2-amine was used without further purification (1.33 g, quantitative yield).

^{1}H NMR (400 MHz, $CDCl_3$) δ_H: 6.57 (d, *J* = 2.3 Hz, 4H, $4C_{Ar}H$), 6.30 (t, *J* = 2.3 Hz, 2H, $2C_{Ar}H$), 4.79 (s, 1H, C*H*Ar), 3.76 (s, 12H, $4OCH_3$), 2.75 (hept, *J* = 6.3 Hz, 1H, C*H*Me), 1.07 (d, *J* = 6.3 Hz, 6H, $2CH_3$).

^{13}C NMR (101 MHz, $CDCl_3$) δ_C: 160.9 (4C), 147.0 (2C), 105.5 (4C), 98.7 (2C), 64.6, 55.4 (4C), 46.4, 23.4 (2C).

HRMS (CI^+) $[C_{20}H_{27}NO_4]^+$ predicted 345.1940, found 346.2017 (Δ −0.74 ppm).

IR υ_{max} (film): 3019, 2957, 1596, 1460, 830.

MP. = 61.9 - 63.5 °C

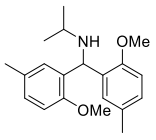

N-(bis(2-methoxy-5-methylphenyl)methyl)propan-2-amine

General procedure B: bis(2-methoxy-5-methylphenyl)methanone (286 mg, 1.06 mmol, 1.0 eq.), DCM (3.0 ml) $TiCl_4$ solution in DCM (1.16 ml, 1.0 M, 1.16 mmol, 1.1 eq.), isopropylamine (0.27 ml, 3.18 mmol, 3.0 eq.), $NaB(CN)H_{3(s)}$ (333 mg, 5.30 mmol, 5.0 eq.) in THF (5.3 ml), anhydrous MeOH (0.61 ml), reaction duration 16 h.

N-(bis(2-methoxy-5-methylphenyl)methyl)propan-2-amine was used without further purification (273 mg, 82%).

^{1}H NMR (400 MHz, $CDCl_3$) δ_H: 7.15-7.12 (m, *J* = 2.3 Hz, 2H, 2C_{Ar}*H*), 6.97 (dd, *J* = 8.3, 2.3 Hz, 2H, 2C_{Ar}*H*), 6.73 (d, *J* = 8.2 Hz, 2H, 2C_{Ar}*H*), 5.55 (s, 1H, C*H*Ar), 3.75 (s, 6H, 2OC*H*$_3$), 2.72 (hept, *J* = 6.3 Hz, 1H, C*H*Me), 2.26 (s, 6H, 2C*H*$_3$), 1.85(s, br, 1H, N*H*), 1.09 (d, *J* = 6.3 Hz, 6H, 2CHC*H*$_3$).

^{13}C NMR (101 MHz, $CDCl_3$) δ_C: 155.3 (2C), 131.9 (2C), 129.6 (2C), 129.3 (2C), 127.8 (2C), 111.0 (2C), 55.9 (2C), 52.5, 46.4, 23.3 (2C), 20.9 (2C).

HRMS (ESI$^+$) $[C_{20}H_{28}O_2N]^+$ predicted 314.2115, found 314.2114 (Δ −0.10 ppm).

IR υ_{max} (film): 2956, 2833, 1610, 1242, 1034, 804.

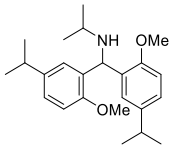

N-(bis(5-isopropyl-2-methoxyphenyl)methyl)propan-2-amine

General procedure B: bis(5-isopropyl-2-methoxyphenyl)methanone (372 mg, 1.14 mmol, 1.0 eq.), DCM (3.3 ml) $TiCl_4$ solution in DCM (1.25 ml, 1.0 M, 1.25 mmol, 1.1 eq.), isopropylamine (0.29 ml, 1.14 mmol, 1.0 eq.), $NaB(CN)H_{3(s)}$ (392 mg, 5.70 mmol, 5.0 eq.) in THF (5.7 ml), anhydrous MeOH (0.65 ml), reaction duration 16 h. N-(bis(5-isopropyl-2-methoxyphenyl)methyl)propan-2-amine was used without further purification (260 mg, 62%).

^{1}H NMR (400 MHz, $CDCl_3$) δ_H: 7.33 - 7.31 (m, 2H, 2C_{Ar}*H*), 7.12 – 7.04 (m, 2H, 2C_{Ar}*H*), 6.83-6.78 (m, 2H, 2C_{Ar}*H*), 5.59 (s, 1H, C*H*Ar), 3.81 (s, 6H, 2OC*H*$_3$), 2.91 (hept, *J* = 7.0

Hz, 2H, 2C*H*Me), 2.80 (hept, *J* = 6.4 Hz, NC*H*Me), 2.36 (s, br, 1H, N*H*), 1.28 (d, *J* = 6.9 Hz, 12H, 4CHC*H*$_3$), 1.17 (d, *J* = 6.2 Hz, 6H, 2NCHC*H*$_3$).

^{13}C NMR (101 MHz, $CDCl_3$) δ_C: 155.5 (2C), 140.4 (2C), 131.2 (2C), 127.0 (2C), 125.0 (2C), 110.64 (2C), 55.5 (2C), 53.9 (2C), 46.2, 33.5 (2C), 24.3 (2C), 24.3 (2C), 23.2 (2C).

HRMS (ESI^+) $[C_{24}36O_2N]^+$ predicted 370.2741, found 370.2733 (Δ −2.16 ppm).

IR υ_{max} (film): 2956, 2834, 1497, 1244, 1031, 810.

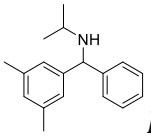

N-((3,5-dimethylphenyl)(phenyl)methyl)propan-2-amine

General procedure B: (3,5-dimethylphenyl)(phenyl)methanone (400 mg, 1.90 mmol, 1.0 eq.), DCM (5.4 ml) $TiCl_4$ solution in DCM (2.09 ml, 1.0 M, 2.09 mmol, 1.1 eq.), isopropylamine (0.49 ml, 5.71 mmol, 3.0 eq.), $NaB(CN)H_{3(s)}$ (143 mg, 2.28 mmol, 1.2 eq.) in THF (2.2 ml), anhydrous MeOH (1.08 ml), reaction duration 18 h. Following the work up procedure, *N*-((3,5-dimethylphenyl)(phenyl)methyl)propan-2-amine was obtained as a colourless viscous oil (269 mg, 56%).

The two enantiomers of *N*-((3,5-dimethylphenyl)(phenyl)methyl)propan-2-amine was separated by chiral UPC^2 [Chiralcel® OJ-H; flow: 2 mL/min; 8% heptane:IPA, 20 mM NH_3; λ = 230 nm; enantiomer (–)-(3-methyl-3-(4-phenylhexyl)cyclopentanone, t_R = 4.02 min; enantiomer (+)-3-methyl-3-(4-phenylhexyl)cyclopentanone, t_R = 4.58 min].

^{1}H NMR (500 MHz, $CDCl_3$) δ_H: 7.42 – 7.39 (m, 2H, $2C_{Ar}H$), 7.31 (dd, *J* = 8.4, 6.9 Hz, 3H, $3C_{Ar}H$), 7.23 – 7.19 (m, 1H, $C_{Ar}H$), 7.00 (s, 2H, $2C_{Ar}H$), 6.85 (s, 1H, $C_{Ar}H$), 4.91 (s, 1H, ArC*H*), 2.76 (hept, *J* = 6.3 Hz, 1H, NC*H*CH_3), 2.29 (s, 6H, Ar(CH_3)$_2$), 1.10 (d, *J* = 6.3 Hz, 6H, 2CHCH_3), 1.10 (d, *J* = 6.3 Hz, 6H, 2CHCH_3).

^{13}C NMR (126 MHz, $CDCl_3$) δ_C: 144.9, 144.7, 138.0 (2C), 128.7, 128.5 (2C), 127.5 (2C), 126.8, 125.2 (2C), 64.4, 46.3, 23.5, 23.3, 21.5 (2C).

HRMS (APCI$^+$) $[C_{18}H_{22}N]^+$ predicted 252.17468, found 252.17473 (Δ 0.21 ppm).

IR υ_{max} (film): 2960, 2920, 1599, 1167, 707.

(–)-*N*-((3,5-dimethylphenyl)(phenyl)methyl)propan-2-amine (79.6 mg, 95.5% ee): $[\boldsymbol{\alpha}]_{589}^{25}$ = –0.7 (*c* 0.88, $CHCl_3$).

(+)-*N*-((3,5-dimethylphenyl)(phenyl)methyl)propan-2-amine (82.1 mg, –89% ee): $[\boldsymbol{\alpha}]_{589}^{25}$ = +1.5 (*c* 1.04, $CHCl_3$).

B5R9_OJ-H_8(Heptane-IPA_80-20)_NH31:

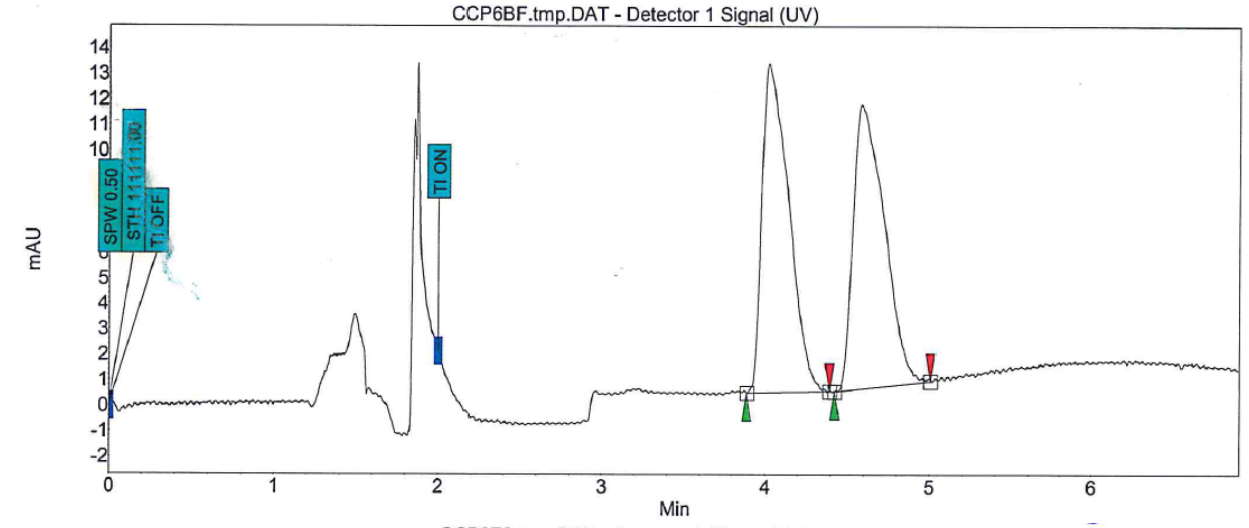

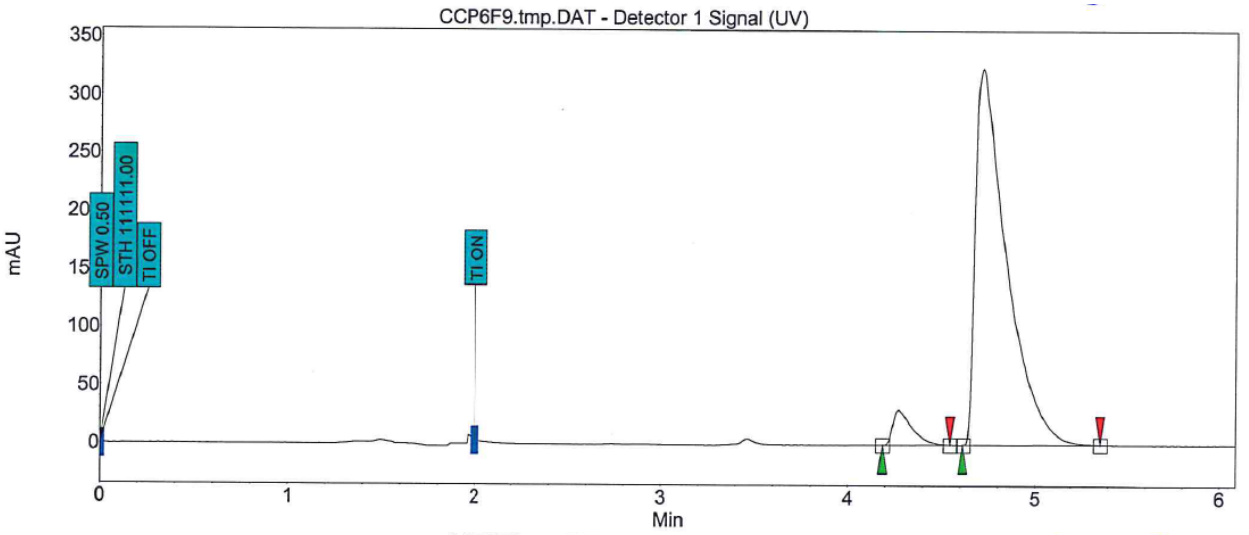

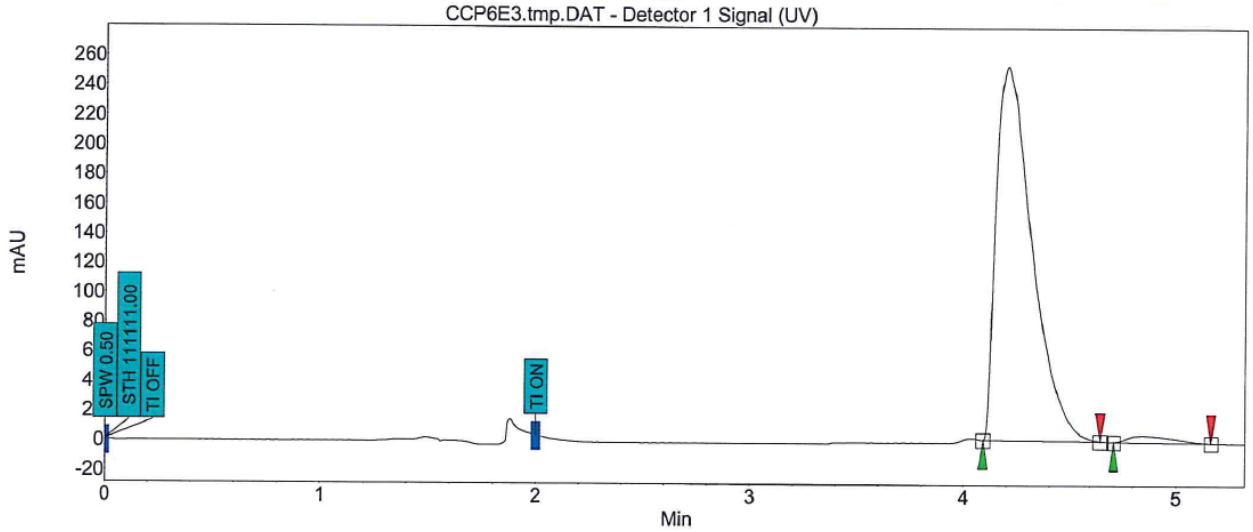

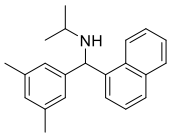

N-((3,5-dimethylphenyl)(naphthalen-1-yl)methyl)propan-2-amine

General procedure B: (3,5-dimethylphenyl)(naphthalen-1-yl)methanone (520 mg, 2.00 mmol, 1.0 eq.), DCM (5.7 ml) $TiCl_4$ solution in DCM (2.20 ml, 1.0 M, 2.20 mmol, 1.1 eq.), isopropylamine (0.52 ml, 5.99 mmol, 3.0 eq.), $NaB(CN)H_{3(s)}$ (151 mg, 2.28 mmol, 1.2 eq.) in THF (2.5 ml), anhydrous MeOH (1.14 ml), reaction duration 18 h. Following the work up procedure, *N*-((3,5-dimethylphenyl)(naphthalen-1-yl)methyl)propan-2-amine was obtained as a light pink viscous oil (355 mg, 59%).

The two enantiomers of *N*-((3,5-dimethylphenyl)(naphthalen-1-yl)methyl)propan-2-amine was separated by chiral UPLC [Chiralcel® OJ; flow: 2 mL/min; MeOH, 20 mM NH_3; λ = 300 nm; enantiomer (–)-*N*-((3,5-dimethylphenyl)(naphthalen-1-yl)methyl)propan-2-amine, t_R = 0.43 min; enantiomer (+)-*N*-((3,5-dimethylphenyl)(naphthalen-1-yl)methyl)propan-2-amine, t_R = 0.59 min].

^{1}H NMR (500 MHz, $CDCl_3$) δ_H: 8.21 – 8.15 (m, 1H, $C_{Ar}H$), 7.84 (dd, *J* = 7.9, 1.6 Hz, 1H, $C_{Ar}H$), 7.78 – 7.72 (m, 1H, $C_{Ar}H$), 7.70 (dt, *J* = 7.3, 0.9 Hz, 1H, $C_{Ar}H$), 7.51 – 7.40 (m, 3H, $3C_{Ar}H$), 7.00 (d, *J* = 1.6 Hz, 2H, $2C_{Ar}H$), 6.86 – 6.81 (m, 1H, $C_{Ar}H$), 5.68 (s, 1H ArC*H*), 2.86 (hept, *J* = 6.3 Hz, 1H, NC*H*CH_3), 2.26 (s, 6H, Ar(CH_3)$_2$), 1.14 (d, *J* = 6.3 Hz, 3H, CHCH_3), 1.12 (d, *J* = 6.3 Hz, 3H, CHCH_3).

^{13}C NMR (126 MHz, $CDCl_3$) δ_C: 144.1, 139.6, 138.0 (2C), 134.2, 131.6, 129.0, 128.8, 127.5, 126.0, 125.7 (2C), 125.7, 125.4, 125.1, 123.7, 60.0, 46.9, 23.5, 23.4, 21.5 (2C).

HRMS ($APCI^+$) $[C_{22}H_{24}N]^+$ predicted 302.19033, found 302.19019 (Δ –0.47 ppm).

IR υ_{max} (film): 2959, 1599, 1467, 778.

(–)-*N*-((3,5-dimethylphenyl)(naphthalen-1-yl)methyl)propan-2-amine (112 mg, >99.9% ee): $[\alpha]_{589}^{25}$ = –104.5 (*c* 1.82, $CHCl_3$).

(+)-*N*-((3,5-dimethylphenyl)(naphthalen-1-yl)methyl)propan-2-amine (121 mg, 97.0% ee): $[\alpha]_{589}^{25}$ = +74.3 (*c* 1.70, $CHCl_3$).

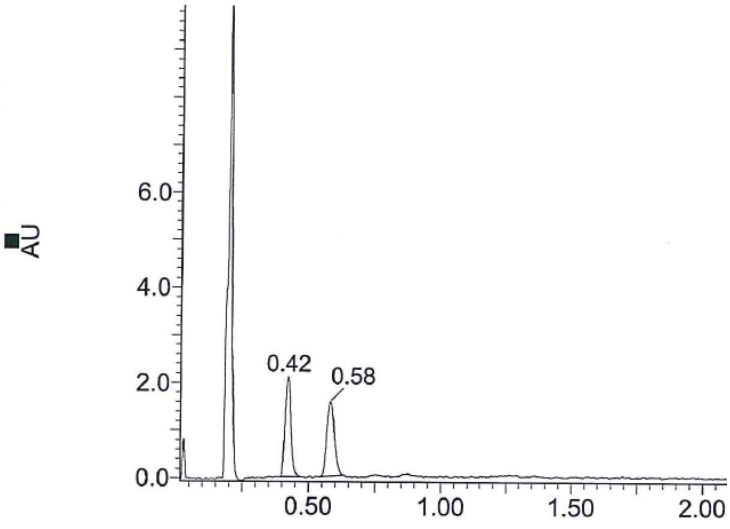

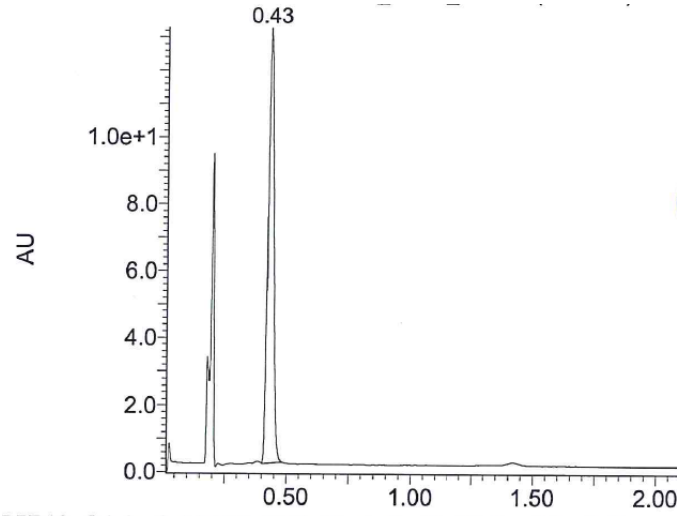

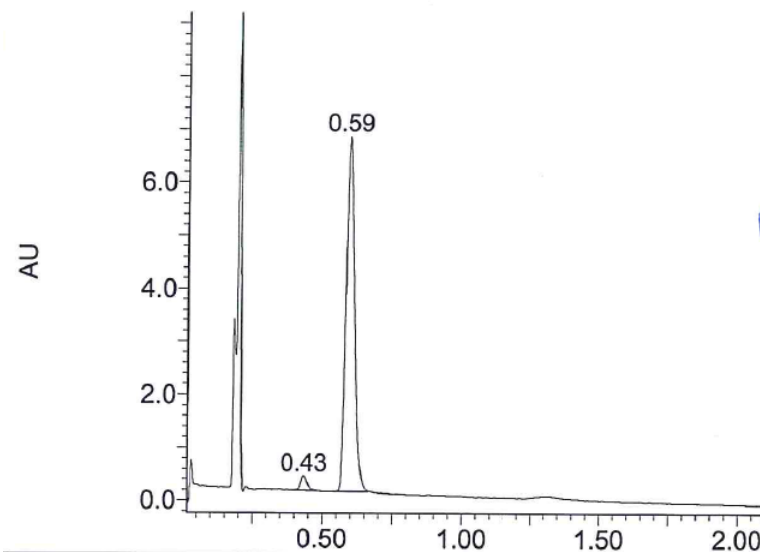

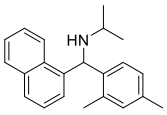

N-((2,4-dimethylphenyl)(naphthalen-1-yl)methyl)propan-2-amine

General procedure B: (2,4-dimethylphenyl)(naphthalen-1-yl)methanone (1.00 g, 3.84 mmol, 1.0 eq.), DCM (11 ml) $TiCl_4$ solution in DCM (4.23 ml, 1.0 M, 4.23 mmol, 1.1 eq.), isopropylamine (0.99 ml, 11.5 mmol, 3.0 eq.), $NaB(CN)H_3$ solution in THF (17.3 ml, 1.0 M, 17.3 mmol, 4.5 eq.), anhydrous MeOH (2.1 ml), reaction duration 2 d. Following the work up procedure, *N*-((2,4-dimethylphenyl)(naphthalen-1-yl)methyl)propan-2-amine was obtained as colourless viscous oil (684 mg, 59%).

The two enantiomers of *N*-((2,4-dimethylphenyl)(naphthalen-1-yl)methyl)propan-2-amine was separated by chiral UPC^2 [Chiralcel® OD-H; flow: 2 mL/min; 8% MeOH:MeCN 1:1, 0.2% *N,N*-dimethylisopropylamine; λ = 280 nm; enantiomer (+)-*N*-((2,4-dimethylphenyl)(naphthalen-1-yl)methyl)propan-2-amine, t_R = 5.85 min; enantiomer (–)-*N*-((2,4-dimethylphenyl)(naphthalen-1-yl)methyl)propan-2-amine, t_R = 6.41 min].

^{1}H NMR (500 MHz, $CDCl_3$) δ_H: 8.01 (d, *J* = 8.2 Hz, 1H, $C_{Ar}H$), 7.76 (dd, *J* = 7.8, 1.6 Hz, 1H, $C_{Ar}H$), 7.65 (dd, *J* = 6.7, 2.7 Hz, 1H, $C_{Ar}H$), 7.42 – 7.27 (m, 4H, $4C_{Ar}H$), 7.17 – 7.10 (m, 1H, $C_{Ar}H$), 6.92 (d, *J* = 1.8 Hz, 1H, $C_{Ar}H$), 6.88 (dd, *J* = 7.9, 1.8 Hz, 1H, $C_{Ar}H$), 5.80 (s, 1H, ArC*H*), 2.88 (hept, *J* = 6.3 Hz, 1H, $NCHCH_3$), 2.23 (s, 3H, $ArCH_3$), 2.21 (s, 3H, $ArCH_3$), 1.28 (s, br, 1H, N*H*), 1.09 (d, *J* = 6.2 Hz, 3H, $CHCH_3$), 1.03 (d, *J* = 6.3 Hz, 3H, $CHCH_3$).

^{13}C NMR (126 MHz, $CDCl_3$) δ_C: 139.2, 138.7, 136.4, 135.8, 134.2, 131.8, 131.6, 129.0, 127.6, 127.6, 126.7, 126.2, 125.6, 125.5, 125.4, 123.2, 55.9, 47.1, 23.5, 23.3, 21.1, 19.4.

HRMS (ESI^+) $[C_{22}H_{26}N]^+$ predicted 304.20598, found 304.20593 (Δ –0.14 ppm).

IR υ_{max} (film): 2960, 1465, 1166, 777.

(–)-*N*-((2,4-dimethylphenyl)(naphthalen-1-yl)methyl)propan-2-amine (97% ee): $[\alpha]_{589}^{25}$ = –39.8 (*c* 1.18, $CHCl_3$).

(+)-*N*-((2,4-dimethylphenyl)(naphthalen-1-yl)methyl)propan-2-amine (91% ee): $[\alpha]_{589}^{25}$ = +28.3 (*c* 0.93, $CHCl_3$).

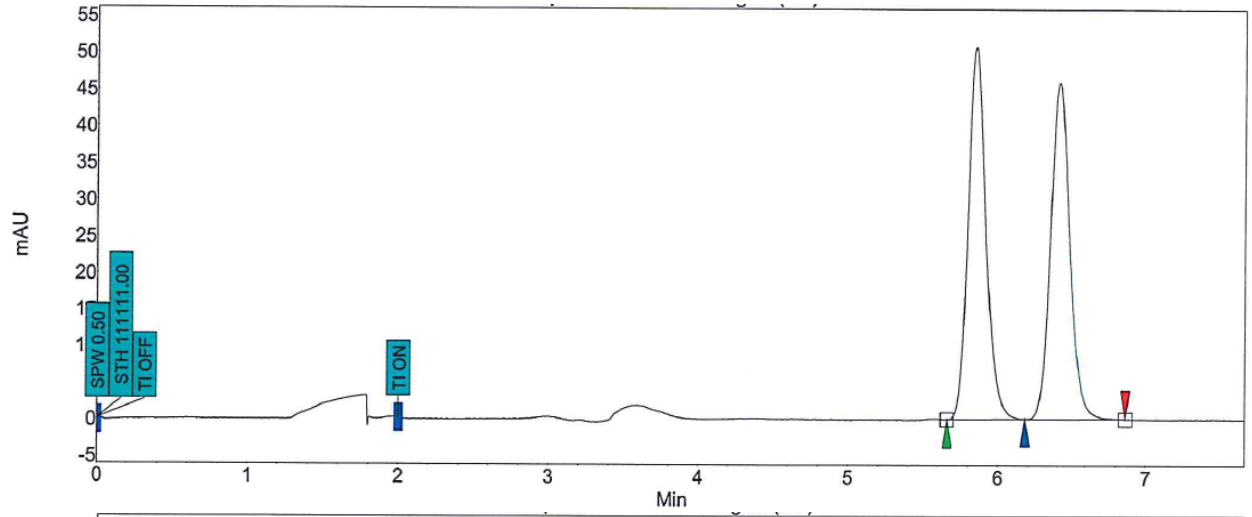

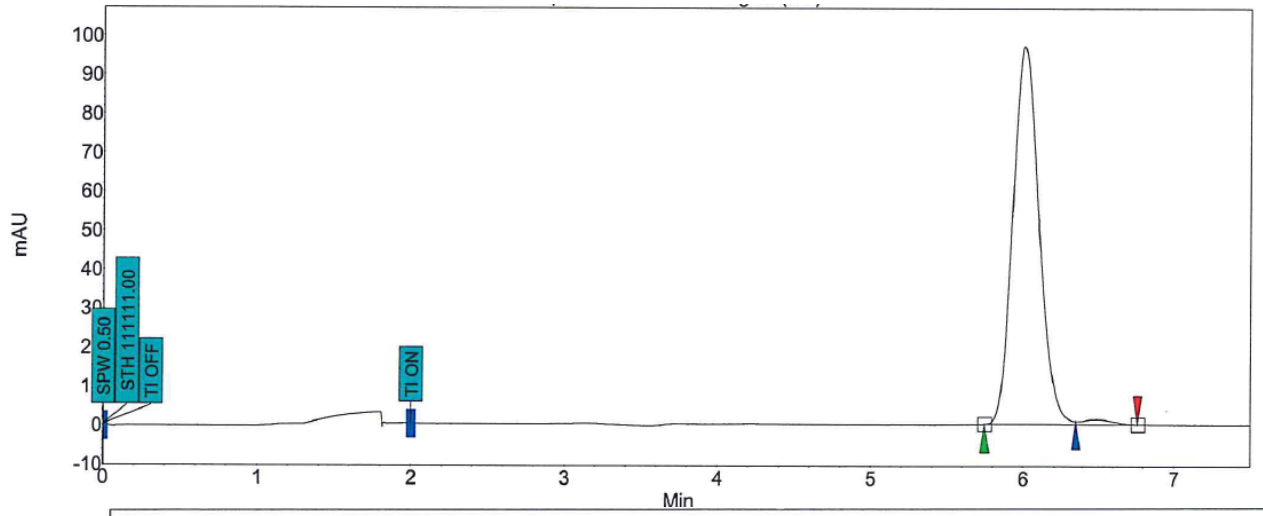

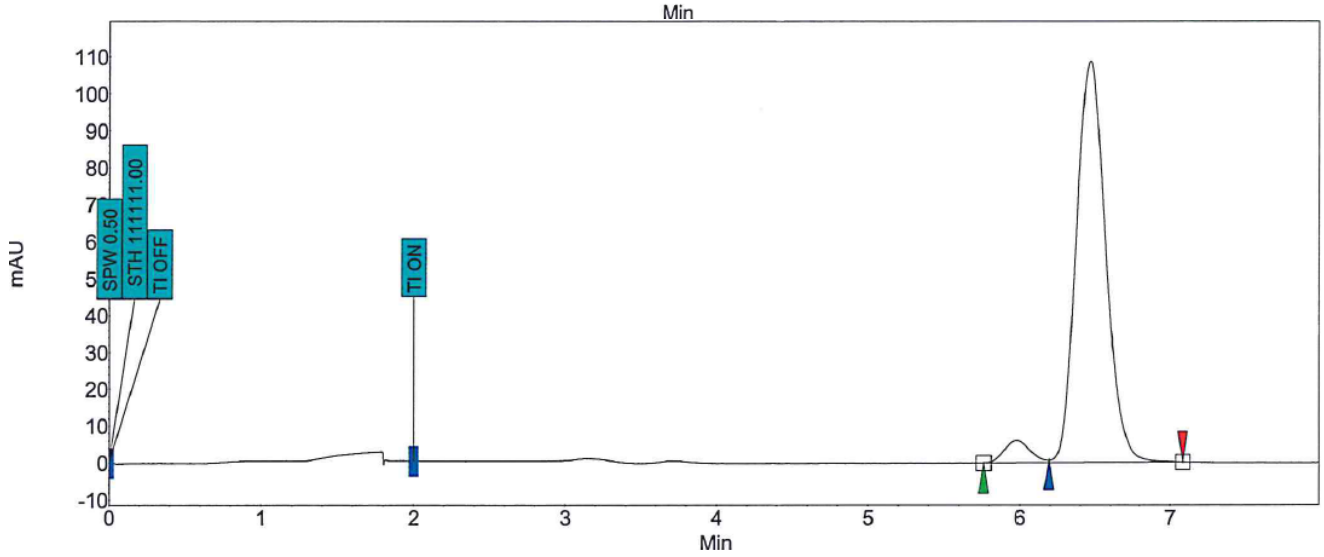

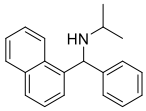

N-(naphthalen-1-yl(phenyl)methyl)propan-2-amine

General procedure B: naphthalen-1-yl(phenyl)methanone (2.32 g, 10.0 mmol, 1.0 eq.), DCM (29 ml) $TiCl_4$ solution in DCM (3.67 ml, 1.0 M, 3.67 mmol, 0.37 eq.), isopropylamine (4.3 ml, 50 mmol, 5.0 eq.), $NaB(CN)H_3$ solution in THF (50 ml, 1.0 M, 50.0 mmol, 5.0 eq.) anhydrous MeOH (5.71 ml), reaction duration 2 d. Following the work up procedure, *N*-(naphthalen-1-yl(phenyl)methyl)propan-2-amine was obtained as a light pink viscous oil (536 mg, 19%).

The two enantiomers of *N*-(naphthalen-1-yl(phenyl)methyl)propan-2-amine was separated by chiral UPLC [Chiralcel® OD-H; flow: 2 mL/min; 30% MeOH, 20 mM NH_3; $\lambda = 280$ nm; enantiomer (–)-*N*-(naphthalen-1-yl(phenyl)methyl)propan-2-amine t_R = 2.84 min; enantiomer (+)-*N*-(naphthalen-1-yl(phenyl)methyl)propan-2-amine, t_R = 3.68 min].

^{1}H NMR (500 MHz, $CDCl_3$) δ_H: 8.25 – 8.21 (m, 1H, $C_{Ar}H$), 7.92 – 7.88 (m, 1H, $C_{Ar}H$), 7.82 – 7.79 (m, 1H, $C_{Ar}H$), 7.74 (d, *J* = 7.1 Hz, 1H, $C_{Ar}H$), 7.54 – 7.45 (m, 5H, $5C_{Ar}H$), 7.36 – 7.31 (m, 2H, $2C_{Ar}H$), 7.27 – 7.22 (m, 1H, $C_{Ar}H$), 5.81 (s, 1H, ArC*H*), 2.94 (hept, *J* = 6.3 Hz, 1H, NC*H*CH_3), 1.57 (s, br, 1H, N*H*), 1.21 (d, *J* = 6.3 Hz, 3H, CHC*H*$_3$), 1.18 (d, *J* = 6.3 Hz, 3H, CHC*H*$_3$).

^{13}C NMR (126 MHz, $CDCl_3$) δ_C: 144.2, 139.6, 134.2, 131.5, 129.0, 128.6 (2C), 128.0 (2C), 127.7, 127.0, 126.1, 125.6, 125.4, 125.2, 123.6, 60.1, 46.9, 23.4 (2C).

HRMS (ESI^+) $[C_{20}H_{22}N]^+$ predicted 276.17468, found 276.17459 (Δ –0.31 ppm).

IR υ_{max} (film): 2959, 2924, 2855, 1465, 708.

(–)-*N*-(naphthalen-1-yl(phenyl)methyl)propan-2-amine (99.7% ee): $[\boldsymbol{\alpha}]_{589}^{25}$ = –51.9 (*c* 0.94, $CHCl_3$).

(+)-*N*-(naphthalen-1-yl(phenyl)methyl)propan-2-amine (99.7% ee): $[\boldsymbol{\alpha}]_{589}^{25}$= +62.2 (*c* 1.03 $CHCl_3$).

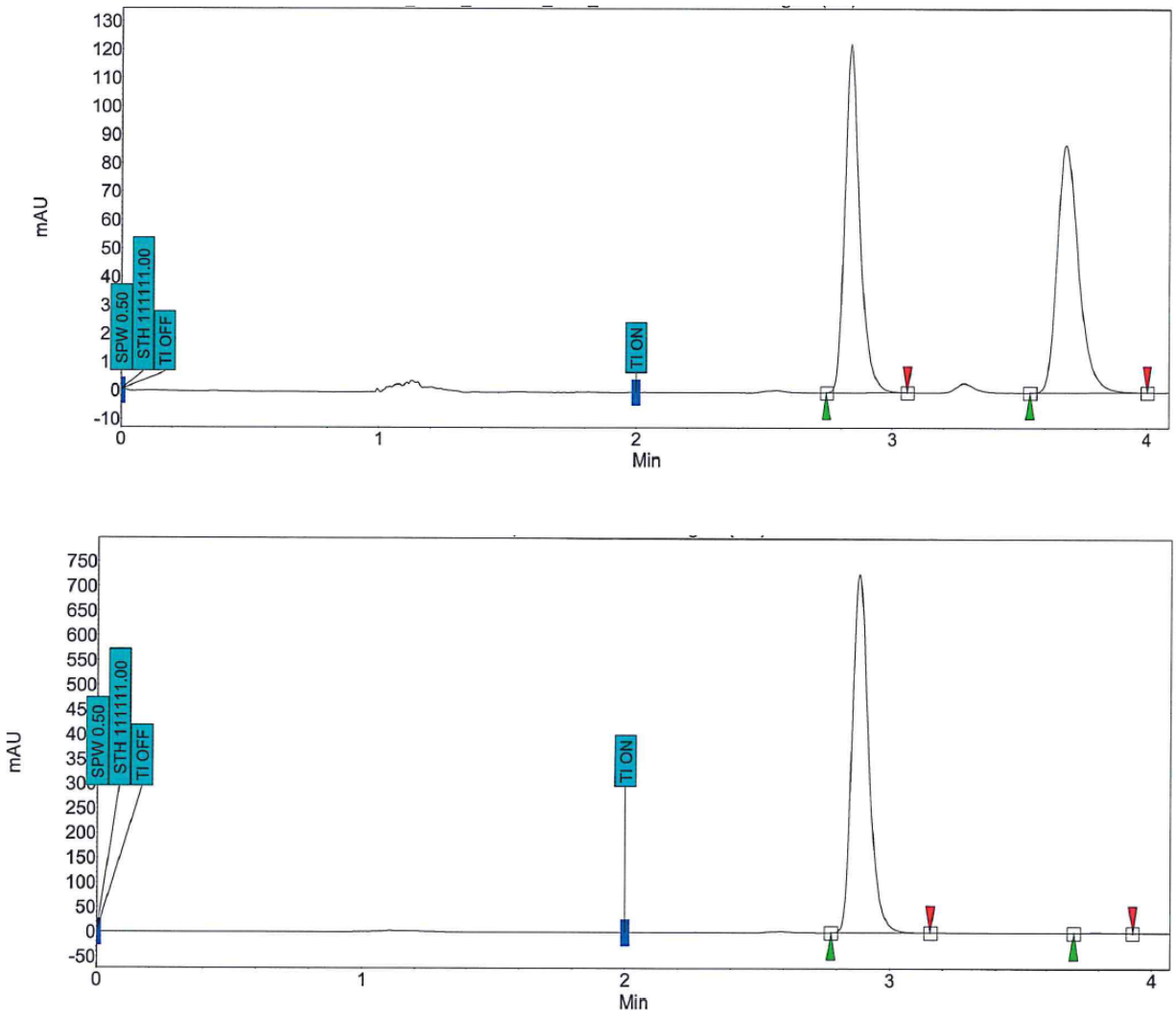

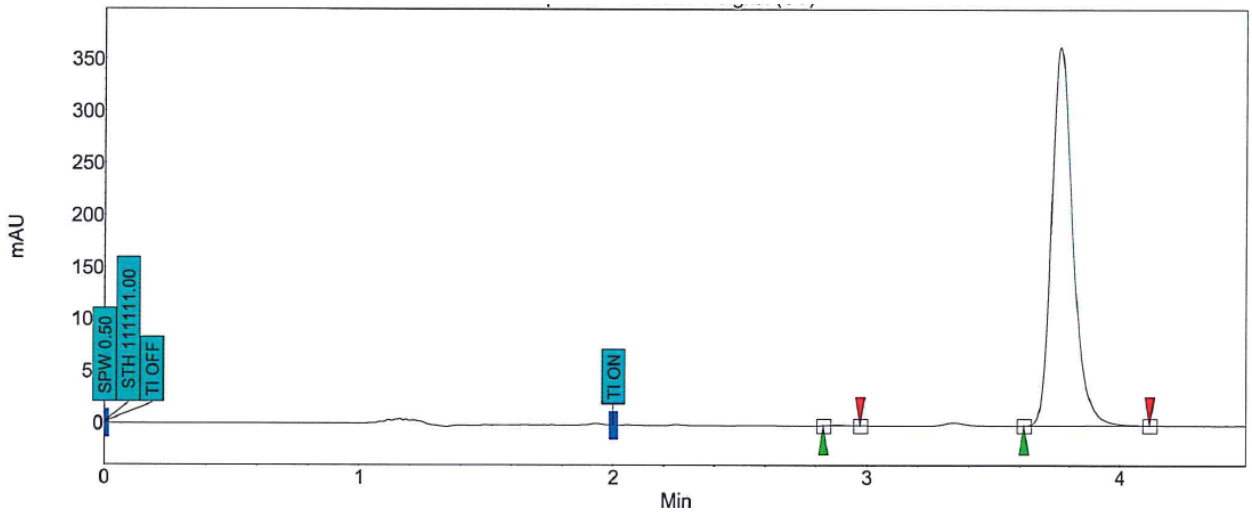

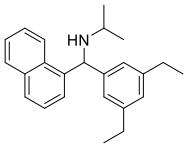

N-((3,5-diethylphenyl)(naphthalen-1-yl)methyl)propan-2-amine

General procedure B: (3,5-diethylphenyl)(naphthalen-1-yl)methanone (1.70 g, 5.90 mmol, 1.0 eq.), DCM (17 ml) $TiCl_4$ solution in DCM (7.8 ml, 1.0 M, 7.80 mmol, 1.1 eq.), isopropylamine (1.52 ml, 17.7 mmol, 3.0 eq.), $NaB(CN)H_3$ solution in THF (20.7 ml, 1.0 M, 20.7 mmol, 3.5 eq.), anhydrous MeOH (3.37 ml), reaction duration 2 d. Following the work up procedure, *N*-((3,5-diethylphenyl)(naphthalen-1-yl)methyl)propan-2-amine was obtained as a light pink viscous oil (1.34 g, 68%).

The two enantiomers of *N*-((3,5-diethylphenyl)(naphthalen-1-yl)methyl)propan-2-amine was separated by chiral UPLC [Chiralcel® OD-H; flow: 2 mL/min; 20% MeOH, 20 mM NH_3; $\lambda = 280$ nm; enantiomer (–)-*N*-((3,5-diethylphenyl)(naphthalen-1-yl)methyl)propan-2-amine, t_R = 3.22 min; enantiomer (+)-*N*-((3,5-diethylphenyl)(naphthalen-1-yl)methyl)propan-2-amine, t_R = 3.97 min].

^{1}H NMR (500 MHz, $CDCl_3$) δ_H: 8.25 (d, *J* = 8.2 Hz, 1H, $C_{Ar}H$), 7.85 (dd, *J* = 7.9, 1.6 Hz, 1H, $C_{Ar}H$), 7.76 – 7.73 (m, 1H, $C_{Ar}H$), 7.70 – 7.65 (m, 1H, $C_{Ar}H$), 7.52 – 7.41 (m, 3H, $3C_{Ar}H$), 7.08 (d, *J* = 1.6 Hz, 2H, $2C_{Ar}H$), 6.90 (d, *J* = 1.7 Hz, 1H, $C_{Ar}H$), 5.73 (s, 1H, ArC*H*), 2.88 (hept, *J* = 6.3 Hz, 1H, NC*H*CH_3), 2.59 (q, *J* = 7.6 Hz, 4H, $2CH_2CH_3$), 1.45 (s, br, 1H, N*H*), 1.20 (t, *J* = 7.6 Hz, 6H, $2CH_2CH_3$), 1.16 (d, *J* = 6.3 Hz, 3H, $CHCH_3$), 1.13 (d, *J* = 6.2 Hz, 3H, $CHCH_3$).

^{13}C NMR (126 MHz, $CDCl_3$) δ_C: 144.4, 144.0, 139.9, 134.2, 131.7, 129.0, 127.5, 126.1, 126.0, 125.7, 125.4, 125.2, 124.9 (2C), 123.7, 60.2, 46.9, 29.0 (2C), 23.5, 23.5, 15.7 (2C).

HRMS (ESI^+) $[C_{24}H_{30}N]^+$ predicted 332.23728, found 332.23718 (Δ –0.28 ppm).

IR υ_{max} (film): 2962, 2930, 1598, 1459, 778.

(–)-*(S)*-*N*-((3,5-diethylphenyl)(naphthalen-1-yl)methyl)propan-2-amine (**L44S-amine**) (99.4% ee): $[\boldsymbol{\alpha}]_{589}^{25}$= –201.3 (*c* 2.80, $CHCl_3$).

(+)-*(R)*-*N*-((3,5-diethylphenyl)(naphthalen-1-yl)methyl)propan-2-amine (98.5% ee): $[\boldsymbol{\alpha}]_{589}^{25}$= +166.7 (*c* 2.36, $CHCl_3$).

The absolute stereochemistry of **L44S-amine** was proven by X-ray crystallography of its HCl salt (see the published supporting information for crystallographyic data)[120].

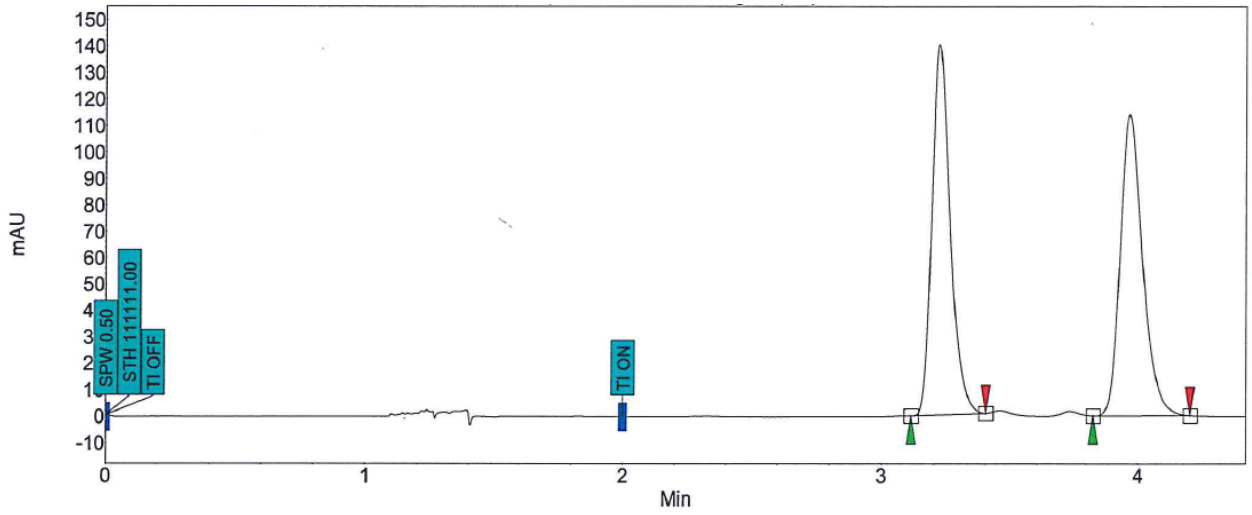
mAU
Min
SPW 0.50
STH 111111.00
TI OFF
TI ON

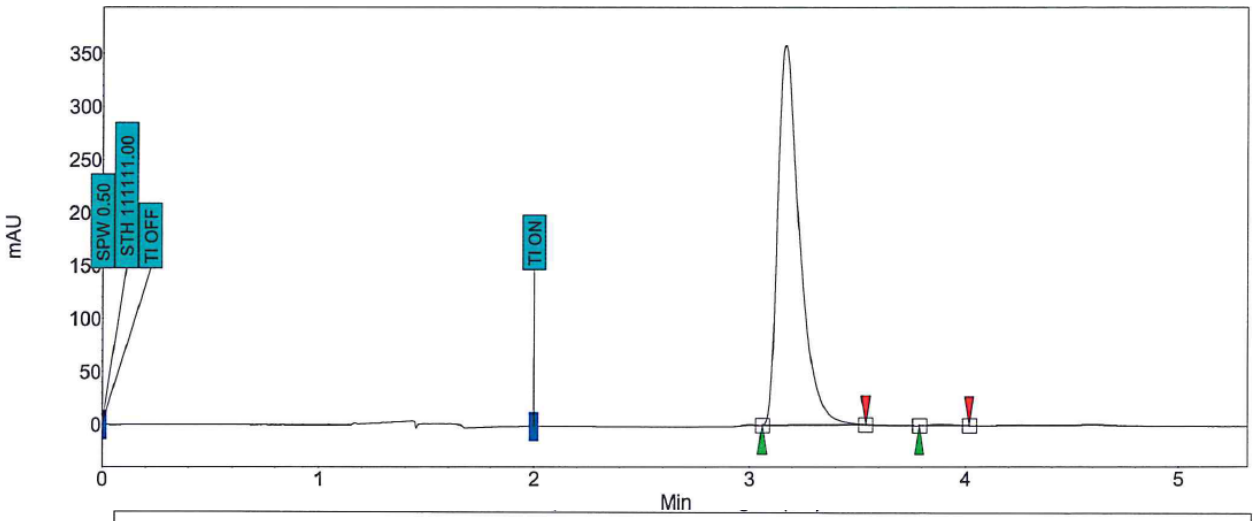
mAU
Min
SPW 0.50
STH 111111.00
TI OFF
TI ON

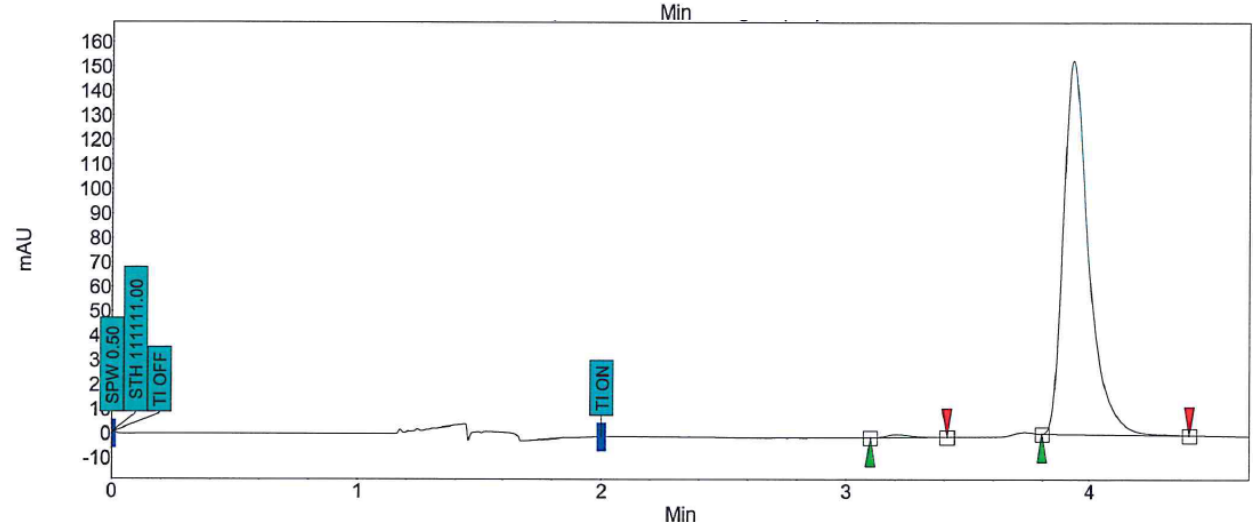
mAU
Min
SPW 0.50
STH 111111.00
TI OFF
TI ON

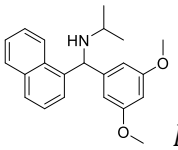

N-((3,5-dimethoxyphenyl)(naphthalen-1-yl)methyl)propan-2-amine

General procedure B: (3,5-dimethoxyphenyl)(naphthalen-1-yl)methanone (3.61 g, 12.4 mmol, 1.0 eq.), DCM (35 ml) $TiCl_4$ solution in DCM (13.6 ml, 1.0 M, 13.6 mmol, 1.1 eq.), isopropylamine (3.2 ml, 37.1 mmol, 3.0 eq.), $NaB(CN)H_3$ solution in THF (37.1 ml, 1.0 M, 37.1 mmol, 3.0 eq.), anhydrous MeOH (7.1 ml), reaction duration 2 d. Following the work up procedure, *N*-((3,5-dimethoxyphenyl)(naphthalen-1-yl)methyl)propan-2-amine was obtained as a colourless viscous oil (3.18 g, 77%).

The two enantiomers of *N*-((3,5-dimethoxyphenyl)(naphthalen-1-yl)methyl)propan-2-amine was separated by chiral UPLC [Chiralcel® OJ; flow: 2 mL/min; 5% MeOH, 20 mM NH_3; λ = 300 nm; enantiomer (–)-*N*-((3,5-dimethoxyphenyl)(naphthalen-1-yl)methyl)propan-2-amine, t_R = 0.52 min; enantiomer (+)-*N*-((3,5-dimethoxyphenyl)(naphthalen-1-yl)methyl)propan-2-amine, t_R = 0.96 min].

^{1}H NMR (500 MHz, $CDCl_3$) δ_H: 8.21 (d, *J* = 8.2 Hz, 1H, $C_{Ar}H$), 7.85 (dd, *J* = 7.8, 1.8 Hz, 1H, $C_{Ar}H$), 7.74 (d, *J* = 8.1 Hz, 1H, $C_{Ar}H$), 7.63 (d, *J* = 7.1 Hz, 1H, $C_{Ar}H$), 7.52 – 7.41 (m, 3H, $3C_{Ar}H$), 6.61 (d, *J* = 2.4 Hz, 2H, 2*o*-$C_{Ar}H$), 6.32 (t, *J* = 2.3 Hz, 1H, *p*-$C_{Ar}H$), 5.67 (s, 1H, Ar*H*), 3.74 (s, 6H, $2OCH_3$), 2.90 (hept, *J* = 6.3 Hz, 1H, $NCHCH_3$), 1.44 (s, br, 1H, N*H*), 1.16 (d, *J* = 6.3 Hz, 3H, $CHCH_3$), 1.12 (d, *J* = 6.3 Hz, 3H, $CHCH_3$).

^{13}C NMR (126 MHz, $CDCl_3$) δ_C: 161.0 (2C), 146.8, 139.5, 134.2, 131.5, 129.0, 127.7, 126.1, 125.7, 125.5, 125.3, 123.6, 106.3 (2C), 98.7, 60.3, 55.4 (2C), 47.0, 23.6, 23.3.

HRMS (ESI$^+$) $[C_{22}H_{26}O_2N]^+$ predicted 336.19581, found 336.19586 (Δ 0.17 ppm).

IR υ_{max} (film): 2959, 2836, 1593, 1152, 779.

(–)-*N*-((3,5-dimethoxyphenyl)(naphthalen-1-yl)methyl)propan-2-amine (>99.9% ee): $[\alpha]_{589}^{25}$ = –200.0 (*c* 2.55, $CHCl_3$).

(+)-*N*-((3,5-dimethoxyphenyl)(naphthalen-1-yl)methyl)propan-2-amine (99.1% ee): $[\alpha]_{589}^{25}$ = +252.8 (*c* 3.43, $CHCl_3$).

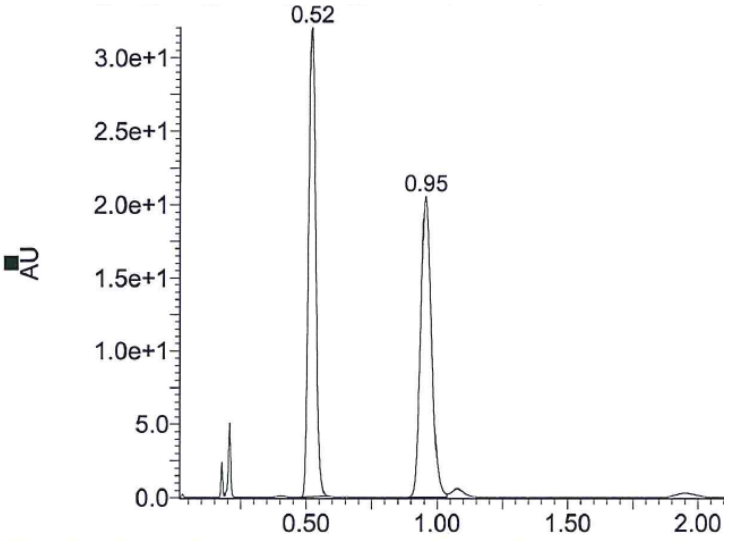

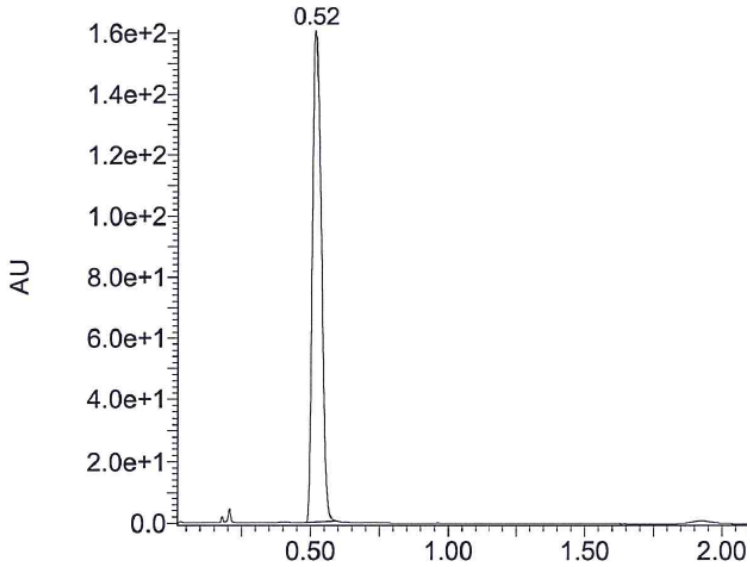

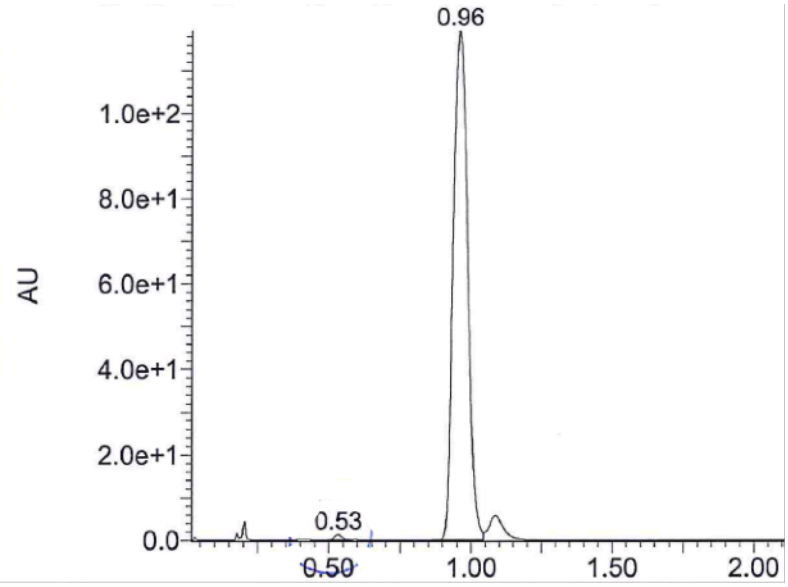

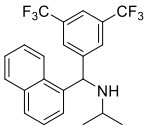

N-((3,5-bis(trifluoromethyl)phenyl)(naphthalen-1-yl)methyl)propan-2-amine

General procedure B: (3,5-bis(trifluoromethyl)phenyl)(naphthalen-1-yl)methanone (2.55 g, 6.92 mmol, 1.0 eq.), DCM (24 ml) $TiCl_4$ solution in DCM (7.6 ml, 1.0 M, 7.60 mmol, 1.1 eq.), isopropylamine (1.8 ml, 20.8 mmol, 3.0 eq.), $NaB(CN)H_3$ solution in THF (20.8 ml, 1.0 M, 20.8 mmol, 3.0 eq.), anhydrous MeOH (4.0 ml), reaction duration 2 d. Following the work up procedure, *N*-((3,5-bis(trifluoromethyl)phenyl)(naphthalen-1-yl)methyl)propan-2-amine was obtained as light pink viscous oil (2.53 g, 89%).

The two enantiomers of *N*-((3,5-bis(trifluoromethyl)phenyl)(naphthalen-1-yl)methyl)propan-2-amine was separated by chiral UPLC [Chiralcel® OD-H; flow: 2 mL/min; 5% MeOH, 20 mM NH_3; λ = 280 nm; enantiomer (–)-*N*-((3,5-bis(trifluoromethyl)phenyl)(naphthalen-1-yl)methyl)propan-2-amine, t_R = 3.03 min;

enantiomer (+)-*N*-((3,5-bis(trifluoromethyl)phenyl)(naphthalen-1-yl)methyl)propan-2-amine, t_R = 3.74 min].

^{1}H NMR (500 MHz, $CDCl_3$) δ_H: 8.16 (d, *J* = 8.3 Hz, 1H, $C_{Ar}H$), 7.98 (s, 2H, $2C_{Ar}H$), 7.90 (dd, *J* = 8.0, 1.5 Hz, 1H, $C_{Ar}H$), 7.81 (d, *J* = 7.9 Hz, 1H, $C_{Ar}H$), 7.75 (s, 1H, $C_{Ar}H$), 7.59 – 7.40 (m, 4H, $4C_{Ar}H$), 5.84 (d, *J* = 2.5 Hz, 1H, ArC*H*), 2.79 (hept, *J* = 6.3 Hz, 1H, NC*H*CH_3), 1.09 (d, *J* = 6.3 Hz, 3H, CHC*H*$_3$), 1.02 (d, *J* = 6.3 Hz, 3H, CHC*H*$_3$).

^{13}C NMR (126 MHz, $CDCl_3$) δ_C: 147.4, 138.4, 134.4, 131.7 (q, *J* = 33.2 Hz, 2C), 131.1, 129.4, 128.6, 128.1 (q, *J* = 4.0 Hz, 2C), 126.7, 125.9, 125.8, 125.7, 124.6 (q, *J* = 273.9 Hz, 2C), 122.9, 121.2-121.0 (m), 59.9, 47.6, 23.5, 23.4.

^{19}F NMR (471 MHz, $CDCl_3$) δ_F: –62.7 (s).

HRMS (ESI^+) $[C_{22}H_{20}NF_6]^+$ predicted 412.14945, found 412.15002 (Δ 1.4 ppm).

IR υ_{max} (film): 2965, 1371, 1275, 1126, 778.

(–)-*(S)*-*N*-((3,5-bis(trifluoromethyl)phenyl)(naphthalen-1-yl)methyl)propan-2-amine (**L46S-amine**) (91.4% ee): $[\boldsymbol{\alpha}]_{589}^{25}$= –408.9 (*c* 4.23, $CHCl_3$).

(+)-*N*-((3,5-bis(trifluoromethyl)phenyl)(naphthalen-1-yl)methyl)propan-2-amine (99.2% ee): $[\boldsymbol{\alpha}]_{589}^{25}$= +361.0 (*c* 3.49, $CHCl_3$).

The absolute stereochemistry of **L46S-amine** was proven by X-ray crystallography of its HCl salt (see the published supporting information for crystallographic data)[120].

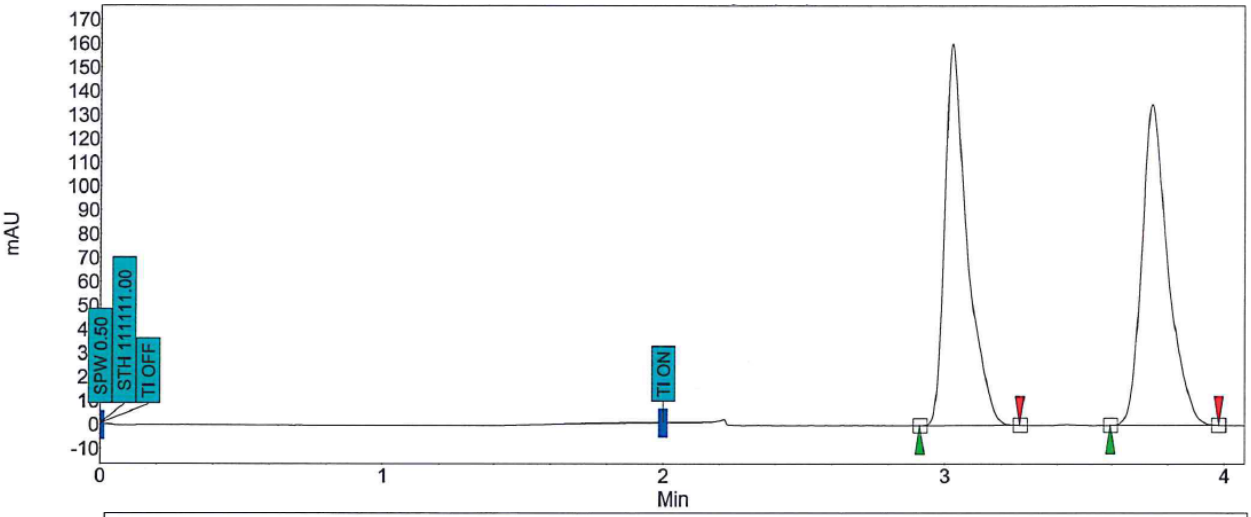

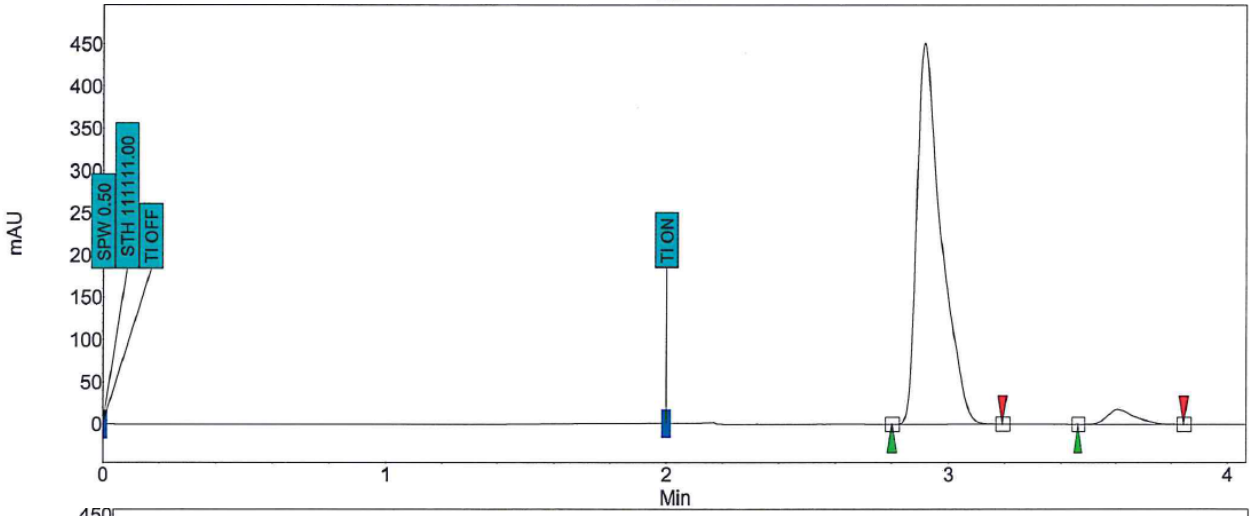

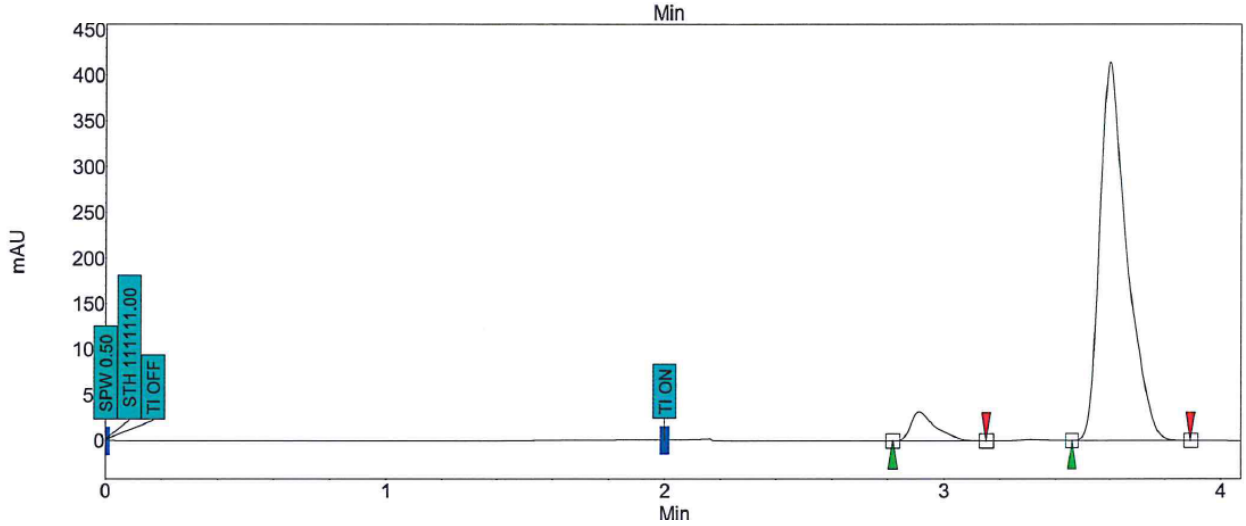

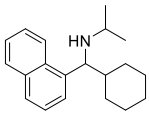

N-(cyclohexyl(naphthalen-1-yl)methyl)propan-2-amine

General procedure B: cyclohexyl(naphthalen-1-yl)methanone (2.41 g, 8.98 mmol, 1.0 eq.), DCM (26 ml) $TiCl_4$ solution in DCM (9.9 ml, 1.0 M, 9.90 mmol, 1.1 eq.), isopropylamine (2.3 ml, 26.9 mmol, 3.0 eq.), $NaB(CN)H_3$ solution in THF (26.9 ml, 1.0 M, 26.9 mmol, 3.0 eq.), anhydrous MeOH (5.1 ml), reaction duration 4 d. Following the work up procedure and purification by flash column chromatography [Basic Al_2O_3, petrol/EtOAc, 1:0 to 7:3], *N*-(cyclohexyl(naphthalen-1-yl)methyl)propan-2-amine was obtained as a colourless oil (1.47 g, 58%).

The two enantiomers of *N*-(cyclohexyl(naphthalen-1-yl)methyl)propan-2-amine was separated by chiral UPLC [Chiralpak® AS-H; flow: 2 mL/min; 15% MeOH, 20 mM NH_3; λ = 280 nm; enantiomer (–)-*N*-(cyclohexyl(naphthalen-1-yl)methyl)propan-2-amine, t_R = 2.77 min; enantiomer (+)-*N*-(cyclohexyl(naphthalen-1-yl)methyl)propan-2-amine, t_R = 3.29 min].

^{1}H NMR (400 MHz, $CDCl_3$) δ_H: 8.23 (s, br, 1H, $C_{Ar}H$), 7.93 – 7.86 (m, 1H, $C_{Ar}H$), 7.80 – 7.73 (m, 1H, $C_{Ar}H$), 7.67 – 7.43 (m, 4H, $4C_{Ar}H$), 4.42 (s, br, 1H, ArC*H*), 2.54 (hept, *J* = 6.2 Hz, 1H, NC*H*CH_3), 1.99 (s, br, 1H, N*H*), 1.76 (d, *J* = 12.8 Hz, 2H, CH_2), 1.69 – 1.56 (m, 2H, CH_2), 1.41 (s, br, 2H, 1C$H_a$$CH_b$, C*H*), 1.23 – 1.04 (m, 5H, CH_aCH_b, $2CH_2$), 1.03 (d, *J* = 6.1 Hz, 3H, CHCH_3), 0.97 (d, *J* = 6.3 Hz, 3H, CHCH_3).

^{13}C NMR (126 MHz, $CDCl_3$) δ_C: 140.3 (br), 134.0, 132.6, 129.1, 126.9, 125.6, 125.5, 125.2 (2C), 123.8 (br), 59.1 (br), 46.3, 44.9 (br), 30.9, 29.8 (br), 26.7, 26.7, 26.5, 24.6, 22.5.

HRMS (APCI$^+$) $[C_{20}H_{28}N]^+$ predicted 282.22163, found 282.22165 (Δ 0.08 ppm).

IR υ_{max} (film): 3059, 2959, 2922, 776.

(–)-*N*-(cyclohexyl(naphthalen-1-yl)methyl)propan-2-amine (99.3% ee): $[\alpha]_{589}^{25}$ = –139 (*c* 2.22, $CHCl_3$).

(+)-*N*-(cyclohexyl(naphthalen-1-yl)methyl)propan-2-amine (99.1% ee): $[\alpha]_{589}^{25}$ = +113 (*c* 1.62, $CHCl_3$).

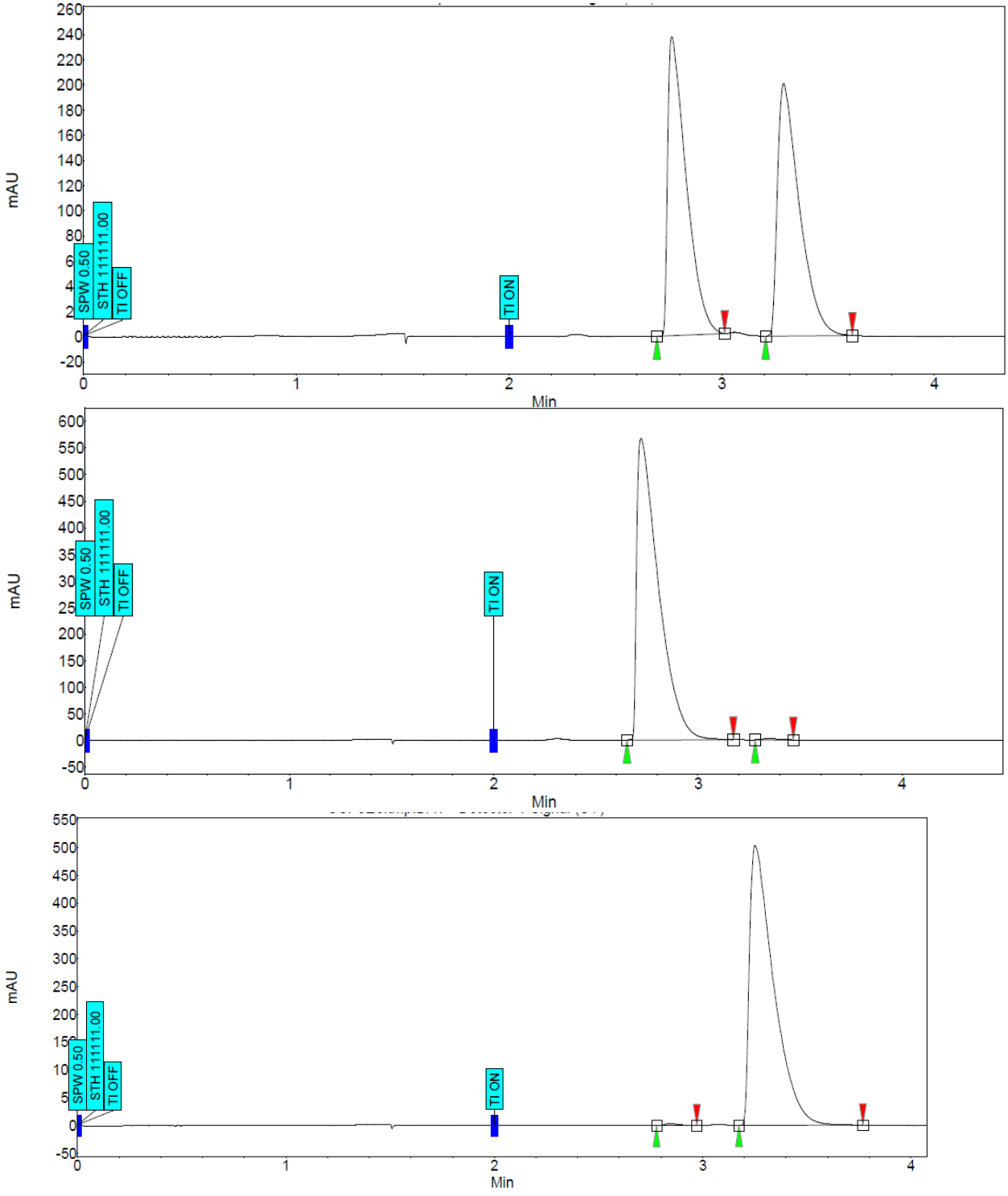

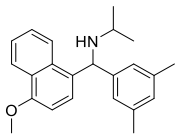

N-((3,5-dimethylphenyl)(2-methoxynaphthalen-1-yl)methyl)propan-2-amine

General procedure B: (3,5-dimethylphenyl)(2-methoxynaphthalen-1-yl)methanone (860 mg, 2.96 mmol, 1.0 eq.), DCM (8.5 ml) $TiCl_4$ solution in DCM (3.26 ml, 1.0 M, 3.26 mmol, 1.1 eq.), isopropylamine (0.76 ml, 8.89 mmol, 3.0 eq.), $NaB(CN)H_3$ solution in THF (8.9 ml, 1.0 M, 8.89 mmol, 3.0 eq.), anhydrous MeOH (1.69 ml), reaction duration 2 d. Following the work up procedure, *N*-((3,5-dimethylphenyl)(2-methoxynaphthalen-1-yl)methyl)propan-2-amine was obtained as a brown residue (827 mg, 84%).

The two enantiomers of *N*-((3,5-dimethylphenyl)(2-methoxynaphthalen-1-yl)methyl)propan-2-amine was separated by chiral UPLC [Chiralcel® OD-H; flow: 2 mL/min; 40% MeOH, 20 mM NH_3; λ = 300 nm; enantiomer (–)-*N*-((3,5-dimethylphenyl)(2-methoxynaphthalen-1-yl)methyl)propan-2-amine, t_R = 2.39 min; enantiomer (+)-*N*-((3,5-dimethylphenyl)(2-methoxynaphthalen-1-yl)methyl)propan-2-amine, t_R = 3.20 min].

^{1}H NMR (500 MHz, $CDCl_3$) δ_H: 8.34 – 8.28 (m, 1H, $C_{Ar}H$), 8.17 – 8.11 (m, 1H, $C_{Ar}H$), 7.56 (dd, *J* = 8.0, 0.6 Hz, 1H, $C_{Ar}H$), 7.53 – 7.41 (m, 2H, $2C_{Ar}H$), 7.04 – 7.00 (m, 2H, $2C_{Ar}H$), 6.87 – 6.80 (m, 2H, $2C_{Ar}H$), 5.61 (s, 1H, ArC*H*), 4.00 (s, 3H, OCH_3), 2.88 (hept, *J* = 6.3 Hz, 1H, $NCHCH_3$), 2.28 (s, 6H, $2ArCH_3$), 1.44 (s, 1H, N*H*), 1.16 (d, *J* = 6.3 Hz, 3H, $CHCH_3$), 1.13 (d, *J* = 6.3 Hz, 3H, $CHCH_3$).

^{13}C NMR (126 MHz, $CDCl_3$) δ_C: 154.7, 144.4, 137.9 (2C), 132.5, 131.6, 128.6, 126.6, 126.1, 125.7 (2C), 125.3, 124.8, 123.4, 122.7, 103.5, 59.8, 55.6, 46.8, 23.5, 23.5, 21.5 (2C).

HRMS (ESI^+) $[C_{23}H_{27}ON^{23}Na]^+$ predicted 356.19849, found 356.19836 (Δ –0.34 ppm).

IR υ_{max} (film): 2959, 1586, 1091, 760.

(–)-*N*-((3,5-dimethylphenyl)(2-methoxynaphthalen-1-yl)methyl)propan-2-amine (99.1% ee): $[\boldsymbol{\alpha}]_{589}^{25}$ = –27.6 (*c* 1.53, $CHCl_3$).

(+)-*N*-((3,5-dimethylphenyl)(2-methoxynaphthalen-1-yl)methyl)propan-2-amine (98.8% ee): $[\boldsymbol{\alpha}]_{589}^{25}$ = +30.7 (*c* 1.67, $CHCl_3$).

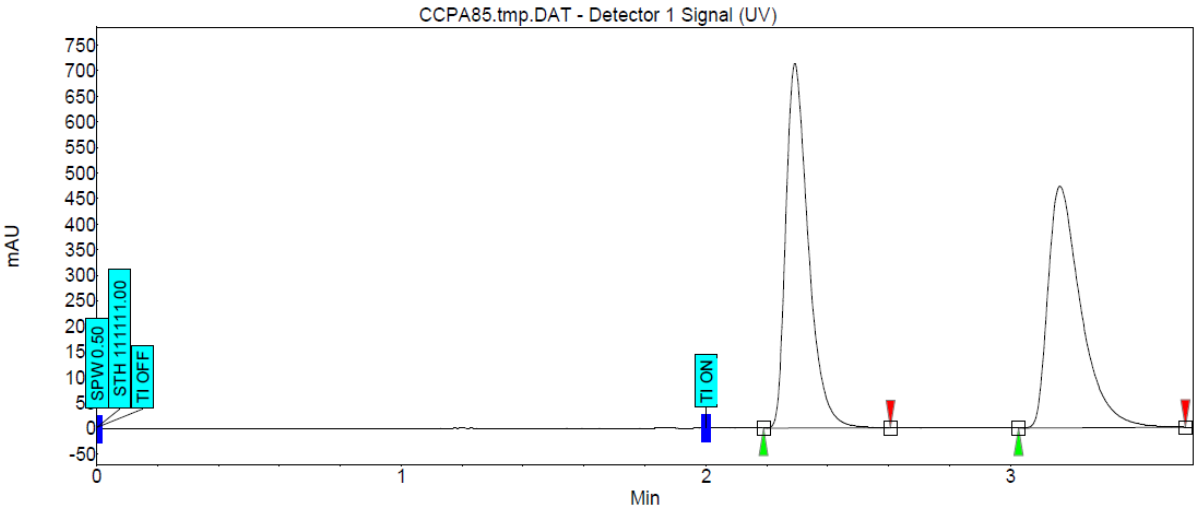

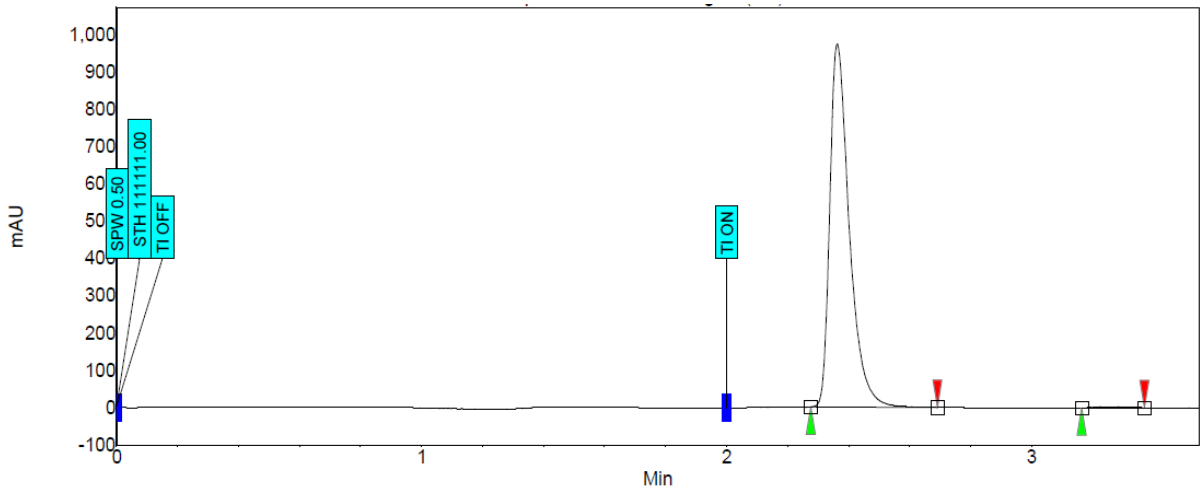

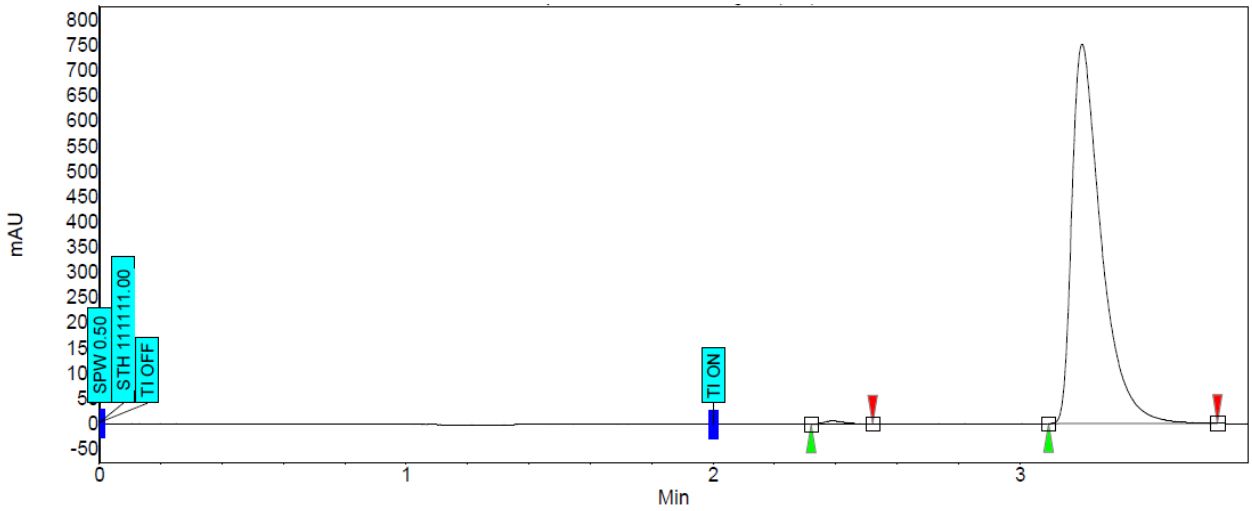

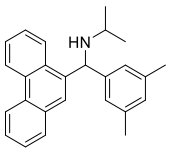

N-((3,5-dimethylphenyl)(phenanthren-9-yl)methyl)propan-2-amine

General procedure B: (3,5-dimethylphenyl)(phenanthren-9-yl)methanone (1.36 g, 4.30 mmol, 1.0 eq.), DCM (12 ml) $TiCl_4$ solution in DCM (12.0 ml, 1.0 M, 12.0 mmol, 1.1 eq.), isopropylamine (1.11 ml, 12.9 mmol, 3.0 eq.), $NaB(CN)H_3$ solution in THF (12.9 ml, 1.0 M, 12.9 mmol, 3.0 eq.), anhydrous MeOH (2.5 ml), reaction duration 2 d. Following the work up, *N*-((3,5-dimethylphenyl)(phenanthren-9-yl)methyl)propan-2-amine was obtained as an orange residue (1.34 g, 88%).

The two enantiomers of *N*-((3,5-dimethylphenyl)(phenanthren-9-yl)methyl)propan-2-amine was separated by chiral UPLC [Chiralpak® IB; flow: 2 mL/min; 20% MeOH, 20 mM NH_3; λ = 300 nm; enantiomer (+)-*N*-((3,5-dimethylphenyl)(phenanthren-9-yl)methyl)propan-2-amine, t_R = 0.53 min; enantiomer (–)-*N*-((3,5-dimethylphenyl)(phenanthren-9-yl)methyl)propan-2-amine, t_R = 0.94 min].

^{1}H NMR (400 MHz, $CDCl_3$) δ_H: 8.76 – 8.64 (m, 2H, $C_{Ar}H$), 8.18 (dd, *J* = 8.2, 1.4 Hz, 1H, $C_{Ar}H$), 8.07 (s, 1H, $C_{Ar}H$), 7.98 – 7.94 (m, 1H, $C_{Ar}H$), 7.68 – 7.50 (m, 4H, $4C_{Ar}H$), 7.07 – 7.01 (m, 2H, $2C_{Ar}H$), 6.88 – 6.82 (m, 1H, $C_{Ar}H$), 5.66 (s, 1H, ArC*H*), 2.94 (hept, *J* = 6.3 Hz, 1H, C*H*CH_3), 2.26 (s, 6H, 2ArCH_3), 1.18 (dd, *J* = 7.2, 6.3 Hz, 6H, 2CHCH_3).

^{13}C NMR (126 MHz, $CDCl_3$) δ_C: 143.9, 138.1 (2C), 137.3, 131.9, 131.1, 131.0, 130.1, 129.0, 128.9, 126.7, 126.7, 126.4, 126.1, 125.8 (3C), 124.6, 123.3, 122.5, 60.6, 47.1, 23.7, 23.4, 21.5 (2C).

HRMS (ESI^+) $[C_{26}H_{28}N]^+$ predicted 354.22163, found 354.22178 (Δ 0.43 ppm).

IR υ_{max} (film): 2961, 1600, 1091, 726.

(+)-*N*-((3,5-dimethylphenyl)(phenanthren-9-yl)methyl)propan-2-amine (99.6% ee): $[\boldsymbol{\alpha}]_{589}^{25}$ = +21.2 (*c* 1.00, $CHCl_3$).

(–)-*N*-((3,5-dimethylphenyl)(phenanthren-9-yl)methyl)propan-2-amine (97.6% ee): $[\boldsymbol{\alpha}]_{589}^{25}$ = –130 (*c* 3.00, $CHCl_3$).

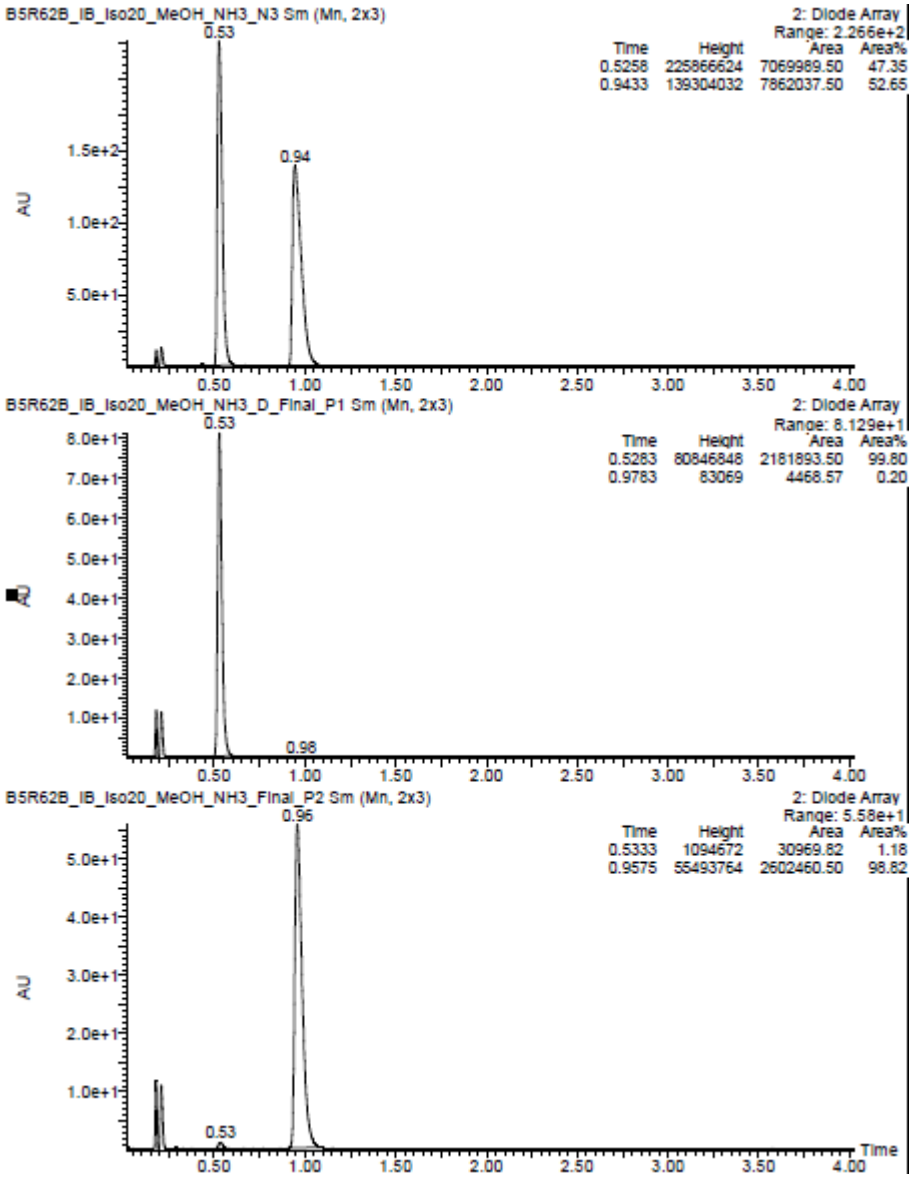

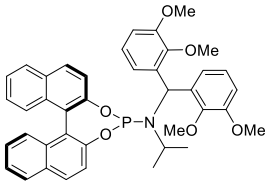

(R_a)-N-(bis(2,3-dimethoxyphenyl)methyl)-*N*-isopropyldinaphtho[2,1-*d*:1',2'-*f*][1,3,2]dioxaphosphepin-4-amine **L33**

General procedure C: $PCl_{3(l)}$ (62 µl, 0.71 mmol, 1.1 eq.) in DCM (2.5 ml), $Et_3N_{(l)}$ (0.45 ml, 3.20 mmol, 5.0 eq.), *N*-(bis(2,3-dimethoxyphenyl)methyl)propan-2-amine (223 mg, 0.64 mmol, 1.0 eq.) in DCM (2.0 ml), *(R)*-$BINOL_{(s)}$ (238 mg, 0.83 mmol, 1.3 eq.) The crude mixture was purified by flash column chromatography [SiO_2,

petrol/DCM/Et_3N, 90:9:1 then 78:21:1] to afford a mixture *N*-(bis(2,3-dimethoxyphenyl)methyl)propan-2-amine and Et_3N. To remove the residue Et_3N, small amount of MeCN and DCM was added to the mixture and the solvents were removed *in vacuo* to afford a white solid of *(R_a)-N*-(bis(2,3-dimethoxyphenyl)methyl)-*N*-isopropyldinaphtho[2,1-*d*:1',2'-*f*][1,3,2]dioxaphosphepin-4-amine (324 mg, 77%).

^{1}H NMR (400 MHz, $CDCl_3$) δ_H: 7.94 – 7.84 (m, 4H, 4CH_{Ar}), 7.57 (d, *J* = 8.8 Hz, 1H, CH_{Ar}), 7.47 (dd, *J* = 8.7, 0.9 Hz, 1H, CH_{Ar}), 7.39 (m, 3H, 3CH_{Ar})7.32 – 7.16 (m, 4H, 4CH_{Ar}), 7.14 – 7.02 (m, 3H, 3CH_{Ar}), 6.92 – 6.87 (m, 2H, 2CH_{Ar}), 6.42 (d, *J* = 16.8 Hz, 1H, C*H*Ar), 3.92 (s, 3H, OCH_3), 3.90 (s, 3H, OCH_3), 3.82 (s, 3H, OCH_3), 3.75 (s, 3H, OCH_3), 3.55 (qq, *J* = 6.6, 6.7 Hz, 1H, C*H*Me_2), 1.02 (d, *J* = 6.7 Hz, 3H, CHCH_3), 0.89 (d, *J* = 6.6 Hz, 3H, CHCH_3).

^{13}C NMR (101 MHz, $CDCl_3$) δ_C: 153.0, 152.8, 150.8 (d, *J* = 6.9 Hz), 150.3, 146.5, 146.3, 137.7 (d, *J* = 7.2 Hz), 137.2 (d, *J* = 5.4 Hz), 132.9, 132.8, 131.4, 130.6, 130.1, 129.4, 128.3, 128.3, 127.2, 125.9, 125.8, 124.7, 124.3, 124.2, 123.4, 123.4, 123.1, 123.0, 123.0, 122.9, 122.7, 121.9 (d, *J* = 2.0 Hz), 111.8, 111.5, 60.1, 60.0, 56.0, 55.9, 49.3 (d, *J* = 25.2 Hz), 47.1 (d, *J* = 5.0 Hz), 23.2, 22.1.

^{31}P NMR (162 MHz, $CDCl_3$) δ_P: 148.8.

IR υ_{max} (film): 2934, 2833, 2360, 1588, 1477.

HRMS (CI^+) $[C_{40}H_{38}NO_6P]^+$ predicted 659.2437, found 660.2532 (Δ −1.79 ppm).

MP. = 140 - 144 °C.

$[\boldsymbol{\alpha}]_{589}^{25}$= +29.3 (*c* 1.00, $CHCl_3$).

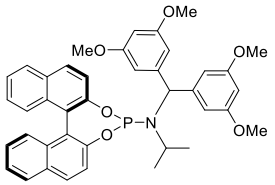

(R_a)-N-(bis(3,5-dimethoxyphenyl)methyl)-N-isopropyldinaphtho[2,1-d:1',2'-f][1,3,2]dioxaphosphepin-4-amine **L34**

General procedure C: $PCl_{3(l)}$ (34 µl, 3.85 mmol, 1.1 eq.) in DCM (10 ml), $Et_3N_{(l)}$ (2.44 ml, 17.5 mmol, 5.0 eq.), *N*-(bis(3,5-dimethoxyphenyl)methyl)propan-2-amine (1.21 g, 3.5 mmol, 1.0 eq.) in DCM (13 ml), *(S)*-$BINOL_{(s)}$ (1.30 g, 4.55 mmol, 1.3 eq.) The crude mixture was purified by flash column chromatography [SiO_2, petrol/DCM/Et_3N, 78:21:1 then 70:29:1] to afford a mixture of *N*-(bis(3,5-dimethoxyphenyl)methyl)propan-2-amine and Et_3N. To remove the residue Et_3N, small amount of MeCN and DCM was added to the mixture and the solvents were removed *in vacuo* to afford a white solid of N-(bis(3,5-dimethoxyphenyl)methyl)-N-isopropyldinaphtho[2,1-d:1',2'-f][1,3,2]dioxaphosphepin-4-amine (2.09 g, 91%).

^{1}H NMR (400 MHz, $CDCl_3$) δ_H: 7.95 – 7.78 (m, 4H, 4C$_{Ar}$*H*), 7.47 – 7.27 (m, 4H, 4C$_{Ar}$*H*), 7.29 – 7.10 (m, 4H, 4C$_{Ar}$*H*), 6.78 – 6.71 (m, 2H, 2C$_{Ar}$*H*), 6.60 – 6.53 (m, 2H, 2C$_{Ar}$*H*), 6.49 – 6.39 (m, 2H, 2C$_{Ar}$*H*), 5.56 (dd, *J* = 17.9, 3.5 Hz, 1H, C*H*Ar), 3.80 (s, 6H, 2OC*H$_3$*), 3.79 (s, 6H, 2OC*H$_3$*), 3.68 – 3.54 (m, 1H, C*H*CH_3), 1.13 – 1.00 (m, 6H, 2CHC*H$_3$*).

^{13}C NMR (101 MHz, $CDCl_3$) δ_C: 160.9, 160.7, 150.5, 150.5, 149.8, 146.06 (d, *J* = 6.0 Hz), 145.76 (d, *J* = 3.4 Hz), 137.9, 132.8, 132.7, 131.4, 130.6, 130.3, 129.5, 129.1, 128.4, 128.3, 128.3, 127.1, 127.1, 126.1, 126.0, 124.8, 124.5, 124.05 (d, *J* = 5.3 Hz),

122.3, 122.1, 121.8, 107.34 (d, *J* = 4.5 Hz), 106.91 (d, *J* = 4.0 Hz), 99.3, 98.9, 60.96 (d, *J* = 24.7 Hz), 55.4 (2C), 55.3 (2C), 47.0, 23.0, 22.9.

^{31}P NMR (162 MHz, $CDCl_3$) δ_P: 149.5 (s).

IR υ_{max} (film): 2933, 2836, 2360, 1594, 1156.

HRMS (CI^+) $[C_{40}H_{38}NO_6P]^+$ predicted 659.2437, found 660.2513 (Δ −0.56 ppm).

MP. = 114 - 118 °C.

$[\boldsymbol{\alpha}]_{589}^{25}$ = +111.3 (*c* 1.00, $CHCl_3$).

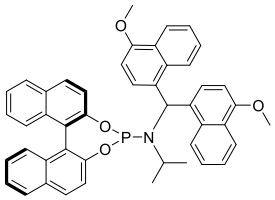

(R_a)-N-(bis(4-methoxynaphthalen-1-yl)methyl)-*N*-isopropyldinaphtho[2,1-*d*:1',2'-*f*][1,3,2]dioxaphosphepin-4-amine **L35**

General procedure B: bis(4-methoxynaphthalen-1-yl)methanone (1.41 g, 4.12 mmol, 1.0 eq.), DCM (12 ml), $TiCl_4$ solution in DCM (1.0 M, 4.53 ml, 4.53 mmol, 1.1 eq.), isopropylamine (2.12 ml, 24.8 mmol, 6.0 eq.), $NaB(CN)H_{3(s)}$ (2.59 g, 41.2 mmol, 10.0 eq.) in THF (20.6 ml), anhydrous MeOH (2.3 ml), reaction duration 40 h. The amine was used without further purification.

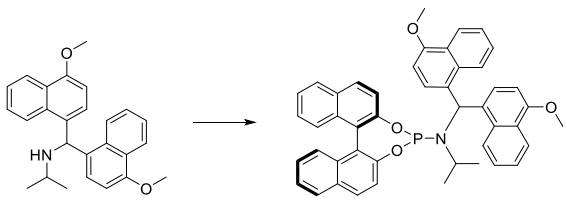

Freshly distilled $PCl_{3(l)}$ (160 µl, 1.88 mmol, 1.1 eq.) was diluted in DCM (5.0 ml) and cooled in an ice bath. $Et_3N_{(l)}$ (1.19 ml, 8.55 mmol, 5 eq.) was added dropwise to the

cooled, stirring solution of PCl_3. The ice bath was removed and the solution was left to slowly warm up to rt over 10 mins. The crude mixture of N-(bis(4-methoxynaphthalen-1-yl)methyl)propan-2-amine (660 mg, 1.71 mmol, 1.0 eq.) in DCM (3 ml) was added dropwise to the stirred solution of Et_3N. The reaction mixture was stirred at rt for 5 h before *(R)*-$BINOL_{(s)}$ (639 mg, 2.23 mmol, 1.3 eq.) was added and the mixture was continued to stir for 14 h at rt. The mixture was filtered through Celite/DCM and solvent was evaporated under reduced pressure. The crude mixture was purified by flash column chromatography [SiO_2, petrol/DCM/Et_3N, 90:9:1 then 80:19:1] to afford *N*-(bis(4-methoxynaphthalen-1-yl)methyl)-*N*-isopropyldinaphtho[2,1-*d*:1',2'-*f*][1,3,2]dioxaphosphepin-4-amine as a white solid (1.14 g, 39% over two steps).

^{1}H NMR (400 MHz, $CDCl_3$) δ_H: 8.39 – 8.31 (m, 2H, 2$C_{Ar}H$), 8.28 (s, br, 1H, $C_{Ar}H$), 8.04 (s, br, 1H, $C_{Ar}H$), 7.86 – 7.79 (m, 4H, 4$C_{Ar}H$), 7.72 – 7.65 (m, 1H, $C_{Ar}H$), 7.57 – 7.43 (m, 4H, 4$C_{Ar}H$), 7.39 – 7.29 (m, 4H, 4$C_{Ar}H$), 7.30 – 7.10 (m, 4H, 4$C_{Ar}H$), 7.00 (d, *J* = 11.6 Hz, 1H, ArCH), 6.84 (d, *J* = 8.1 Hz, 1H, $C_{Ar}H$), 6.71 (d, *J* = 8.1 Hz, 1H, $C_{Ar}H$), 3.92 (s, 3H, OCH_3), 3.68 (s, 3H, OCH_3), 3.75 (q, *J* = 6.6, 6.0 Hz, 1H, $CHCH_3$), 1.14 (s, br 3H, CHCH_3), 0.96 (s, br, 3H, CHCH_3).

^{13}C NMR (101 MHz, $CDCl_3$) δ_C: 155.2, 155.2, 149.8, 132.7(2C), 132.6, 132.0 (br), 131.8, 131.2, 130.5 (br), 130.3, 130.0(2C), 129.6 (br), 129.2 (2C), 128.8 (br), 128.2, 128.1, 127.0, 127.0, 126.7, 126.6, 126.1, 126.0, 125.8, 125.7, 124.9, 124.9, 124.5, 124.1, 124.0 (d, *J* = 5.5 Hz), 123.4, 123.2, 122.8, 122.6, 122.4, 121.4 (br), 102.9, 102.8, 55.4, 55.4, 54.2 (d, *J* = 27.4 Hz), 47.8, 24.0, 23.1.

^{31}P NMR (162 MHz, $CDCl_3$) δ_P: 148.0.

IR υ_{max} (film): 3069, 2935, 1622, 1462, 945.

HRMS (EI$^+$) $[C_{46}H_{38}NO_4P]^+$ predicted 699.2538, found 699.2547 (Δ −0.72 ppm).

M.P. = 196 - 202 °C.

$[\boldsymbol{\alpha}]_{589}^{25}$= –36.6 (*c* 1.00, $CHCl_3$).

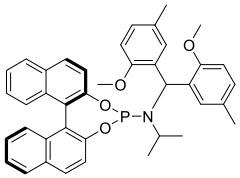

(R_a)-N-(bis(2-methoxy-5-methylphenyl)methyl)-N-isopropyldinaphtho[2,1-d:1',2'-f][1,3,2]dioxaphosphepin-4-amine **L36**

General procedure C: $PCl_{3(l)}$ (74 µl, 0.85 mmol, 1.1 eq.) in DCM (2.5 ml), $Et_3N_{(l)}$ (0.54 ml, 3.88 mmol, 5.0 eq.), *N*-(bis(2-methoxy-5-methylphenyl)methyl)propan-2-amine (243 mg, 0.78 mmol, 1.0 eq.) in DCM (2.5 ml), *(R)*-$BINOL_{(s)}$ (289 mg, 1.01 mmol, 1.3 eq.) The crude mixture was purified by flash column chromatography [SiO_2, petrol/DCM/Et_3N, 90:9:1 then 80:19:1] and filtered through a small amount of silica gel/$CHCl_3$. The purification process yielded a white solid of N-(bis(2-methoxy-5-methylphenyl)methyl)-N-isopropyldinaphtho[2,1-d:1',2'-f][1,3,2]dioxaphosphepin-4-amine (258 mg, 53%).

^{1}H NMR (400 MHz, $CDCl_3$) δ_H: 7.95 – 7.86 (m, 4H, 4$C_{Ar}H$), 7.50 – 7.18 (m, 8H, 8$C_{Ar}H$), 7.16 – 7.05 (m, 4H, 4$C_{Ar}H$), 6.83 (m, 2H, 2$C_{Ar}H$), 6.34 (d, *J* = 16.9 Hz, 1H, C*H*Ar), 3.91 (s, 3H, OCH_3), 3.84 (s, 3H, OCH_3), 3.58 – 3.47 (m, 1H, C*H*CH_3), 2.34 (s, 3H, CCH_3), 2.33 (s, 3H, CCH_3), 0.96 (d, *J* = 6.6 Hz, 3H, CHCH_3), 0.88 (d, *J* = 6.5 Hz, 3H, CHCH_3).

^{13}C NMR (101 MHz, $CDCl_3$) δ_C: 154.7, 154.5, 151.0, 150.9, 150.3, 132.9, 132.8, 131.5, 131.4 (2C), 131.3, 131.0, 130.9, 130.5, 130.1, 129.4, 128.9, 128.6, 128.6, 128.3 (2C), 127.2, 127.1, 125.9, 125.8, 124.6, 124.3, 124.2, 122.6, 122.5, 121.8, 110.7, 55.6 (2C), 49.1 (d, *J* = 30.0 Hz), 47.23 (d, *J* = 5.4 Hz), 23.0, 22.0, 21.1, 21.1.

^{31}P NMR (162 MHz, $CDCl_3$) δ_P: 149.3 (s).

IR υ_{max} (film): 2971, 2834, 2360, 1590, 1499.

HRMS (CI^+) $[C_{40}H_{38}NO_4P]^+$ predicted 627.2538, found 628.2613 (Δ 4.55 ppm).

MP. = 138 – 144 °C.

$[\alpha]_{589}^{25}$= –86.1 (*c* 1.00, $CHCl_3$).

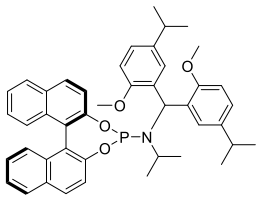

(R_a)-N-(bis(5-isopropyl-2-methoxyphenyl)methyl)-N-isopropyldinaphtho[2,1-d:1',2'-f][1,3,2]dioxaphosphepin-4-amine **L37**

General procedure C: $PCl_{3(l)}$ (68 µl, 0.77 mmol, 1.1 eq.) in DCM (2.0 ml), $Et_3N_{(l)}$ (0.49 ml, 3.52 mmol, 5.0 eq.), *N*-(bis(5-isopropyl-2-methoxyphenyl)methyl)propan-2-amine (260 mg, 0.70 mmol, 1.0 eq.) in DCM (2.7 ml), *(R)*-$BINOL_{(s)}$ (262 mg, 0.92 mmol, 1.3 eq.) The crude mixture was purified by flash column chromatography [SiO_2, petrol/DCM/Et_3N, 90:9:1 then 80:19:1] to afford a white solid of N-(bis(5-isopropyl-2-methoxyphenyl)methyl)-N-isopropyldinaphtho[2,1-d:1',2'-f][1,3,2]dioxaphosphepin-4-amine (498 mg, quantitative yield).

^{1}H NMR (400 MHz, $CDCl_3$) δ_H: 8.05 – 7.93 (m, 4H, 4$C_{Ar}H$), 7.65 – 7.55 (m, 1H, $C_{Ar}H$), 7.57 – 7.18 (m, 11H, 11$C_{Ar}H$), 6.99 – 6.90 (m, 2H, 2$C_{Ar}H$), 6.53 (dd, *J* = 16.7, 2.0 Hz,

1H, C*H*Ar), 4.00 (s, 3H, OC*H*$_3$), 3.91 (s, 3H, OC*H*$_3$), 3.72 – 3.59 (m, 1H, NC*H*Me), 3.07 – 2.93 (m, 2H, 2CC*H*CH$_3$), 1.36 (m, 12H, 4CCHC*H*$_3$), 1.14 (d, *J* = 6.8 Hz, 3H, NCHC*H*$_3$), 1.00 (d, *J* = 6.6 Hz, 3H, NCHC*H*$_3$).

^{13}C NMR (101 MHz, $CDCl_3$) δ_C: 154.9, 154.7, 151.1, 151.1, 150.4, 140.1, 140.0, 133.0, 132.8, 131.3, 131.3, 131.1, 131.0, 130.5, 130.1, 129.3, 129.1, 129.0, 128.9, 128.8, 128.3, 128.3, 127.2, 127.2, 125.9, 125.9, 125.8, 124.6, 124.3, 124.3, 122.7, 121.8, 110.5, 110.5, 49.1 (d, *J* = 29.6 Hz), 47.2 (d, *J* = 5.5 Hz), 33.5, 33.5, 24.6, 24.4, 24.4, 24.2, 23.1, 22.0.

^{31}P NMR (162 MHz, $CDCl_3$) δ_P: 149.7 (s).

IR υ_{max} (film): 3055, 2957, 2834, 1497.

HRMS (CI^+) $[C_{44}H_{46}NO_4P]^+$ predicted 683.3164, found 684.3235 (Δ −1.63 ppm).

MP. = 218 - 219 °C.

$[\boldsymbol{\alpha}]_{589}^{25}$ = −78.6 (*c* 1.00, $CHCl_3$).

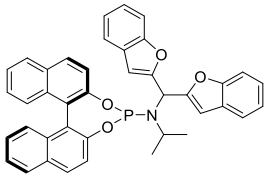

(R$_a$)-N-(di(benzofuran-2-yl)methyl)-*N*-isopropyldinaphtho[2,1-d:1',2'-f][1,3,2]dioxaphosphepin-4-amine **L38**

General procedure B: di(benzofuran-2-yl)methanone (278 mg, 1.06 mmol, 1.0 eq.), DCM (4 ml), $TiCl_4$ solution in DCM (1.0 M, 1.17 ml, 1.17 mmol, 1.1 eq.), isopropylamine (273 µl, 3.18 mmol, 3.0 eq.), $NaB(CN)H_{3(s)}$ (333 mg, 5.30 mmol,

5.0 eq.) in THF (5.3 ml), anhydrous MeOH (0.61 ml), reaction duration 40 h. The amine was used without further purification.

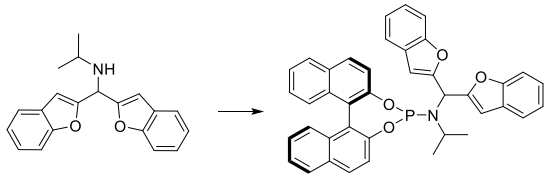

Freshly distilled $PCl_{3(l)}$ (90 µl, 1.03 mmol, 1.1 eq.) was diluted in DCM (3.0 ml) and cooled in an ice bath. $Et_3N_{(l)}$ (0.66 ml, 4.70 mmol, 5 eq.) was added dropwise to the cooled, stirring solution of PCl_3. The ice bath was removed and the solution was left to slowly warm up to rt over 10 mins. The crude mixture of N-(di(benzofuran-2-yl)methyl)propan-2-amine (286 mg, 0.94 mmol, 1.0 eq.) in DCM (3.0 ml) was added dropwise to the stirred solution of Et_3N. The reaction mixture was stirred at rt for 5 h before *(R)*-$BINOL_{(s)}$ (349 mg, 1.22 mmol, 1.3 eq.) was added and the mixture was continued to stir at rt for 17 h. The mixture was filtered through Celite/DCM and the solvent was removed under a reduced pressure. The crude mixture was purified by flash column chromatography [SiO_2, petrol/DCM/Et_3N, 80:19:1] to afford *N*-(di(benzofuran-2-yl)methyl)-*N*-isopropyldinaphtho[2,1-d:1',2'-f][1,3,2]dioxaphosphepin-4-amine as a white solid (181 mg, 31% over two steps).

^{1}H NMR (400 MHz, $CDCl_3$) δ_H: 8.01 – 7.83 (m, 3H, 3$C_{Ar}H$), 7.69 – 7.50 (m, 6H, 6$C_{Ar}H$), 7.48 – 7.16 (m, 11H, 11$C_{Ar}H$), 6.69 (s, 1H, $C_{Ar}H$), 6.61 (s, 1H, $C_{Ar}H$), 5.93 (d, *J* = 13.0 Hz, 1H, ArC*H*), 3.84 – 3.70 (m, 1H, C*H*CH_3), 1.34 (d, *J* = 6.8 Hz, 3H, CHCH_3), 1.18 (d, *J* = 6.6 Hz, 3H, CHCH_3).

^{13}C NMR (101 MHz, $CDCl_3$) δ_C: 156.3 (br), 156.1 (br), 155.1, 154.9, 149.7, 149.7 , 132.9, 132.7, 131.5, 130.8, 130.4, 129.6, 128.4, 128.3 (2C), 128.3, 127.2, 127.2, 126.1, 126.1, 124.9, 124.6, 124.5, 124.4, 124.1 (d, *J* = 6 Hz), 123.0, 122.9, 122.4 (2C), 122.1

(d, *J* = 2 Hz), 121.3, 121.2, 111.4, 111.4, 106.4 (d, *J* = 4 Hz), 105.9 (d, *J* = 2 Hz), 50.0 (d, *J* = 18 Hz), 47.7 (d, *J* = 8 Hz), 23.7, 23.7.

^{31}P NMR (162 MHz, $CDCl_3$) δ_P: 148.4 (s).

IR υ_{max} (film): 2972, 1619, 1503, 946, 731.

HRMS (CI^+) $[C_{40}H_{31}NO_4P]^+$ predicted 620.1985, found 620.1929 (Δ −9.0 ppm).

M.P. = 98.0 - 108 °C.

$[\boldsymbol{\alpha}]_{589}^{25}$ = −132.5 (*c* 1.00, $CHCl_3$).

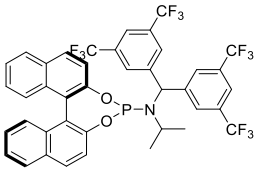

(R_a)-N-(bis(3,5-bis(trifluoromethyl)phenyl)methyl)-*N*-isopropyldinaphtho[2,1-*d*:1',2'-*f*][1,3,2]dioxaphosphepin-4-amine **L39**

General procedure C: $PCl_{3(l)}$ (1.17 µl, 13.4 mmol, 1.1 eq.) in DCM (11.0 ml), $Et_3N_{(l)}$ (8.5 ml, 61.0 mmol, 5.0 eq.), *N*-(bis(3,5-bis(trifluoromethyl)phenyl)methyl)propan-2-amine (6.07 g, 12.2 mmol, 1.0 eq.) in DCM (50.0 ml), *(R)*-$BINOL_{(s)}$ (4.55 mg, 15.9 mmol, 1.3 eq.) The crude mixture was purified by flash column chromatography [Basic Al_2O_3, petrol/DCM, 4:1] to afford a white solid of *(R_a)-N*-(bis(3,5-bis(trifluoromethyl)phenyl)methyl)-*N*-isopropyldinaphtho[2,1-*d*:1',2'-*f*][1,3,2]dioxaphosphepin-4-amine (3.41 g, 78%).

^{1}H NMR (400 MHz, $CDCl_3$) δ_H: 8.09 – 7.92 (m, 7H, 7$C_{Ar}H$), 7.91 (s, 2H, 2$C_{Ar}H$), 7.86 (d, *J* = 8.8 Hz, 1H, $C_{Ar}H$), 7.56 – 7.43 (m, 4H, 4$C_{Ar}H$), 7.40 – 7.24 (m, 4H, 4$C_{Ar}H$), 6.02 (d, *J* = 15.4 Hz, 1H, ArC*H*), 3.70 (h, *J* = 6.5 Hz, 1H, C*H*CH_3), 1.30 (d, *J* = 6.7 Hz, 3H, CHCH_3), 1.04 (d, *J* = 6.5 Hz, 3H, CHCH_3).

^{13}C NMR (101 MHz, $CDCl_3$) δ_C: 149.4 (d, *J* = 7.6 Hz), 149.2, 144.9 – 144.6 (m, 2C), 132.9 (d, *J* = 3.0 Hz), 132.5 (d, *J* = 14.8 Hz), 132.2 (d, *J* = 14.3 Hz), 131.8, 131.8, 131.0 (2C), 130.9, 129.9, 129.2 (2C), 129.1 – 128.7 (m, 2C), 128.6, 128.5, 123.2 (d, *J* = 15.1 Hz, 2C), 126.5, 126.4 (2C), 125.2, 125.0, 123.3 (q, *J* = 270.9 Hz, 4C), 123.9 (d, *J* = 4.9 Hz, 2C), 122.2 – 122.0 (m, 2C), 121.8, 121.4, 59.8 (d, *J* = 21.2 Hz), 47.6 (d, *J* = 4.1 Hz), 23.3, 23.3.

^{19}F NMR {^{1}H} (162 MHz, $CDCl_3$) δ_F: 62.8 (s), 62,9 (s).

^{31}P NMR {^{1}H} (162 MHz, $CDCl_3$) δ_P: 146.3 (s).

$[\alpha]_{589}^{25}$ = –159 (*c* 1.00, $CHCl_3$).

Data was consistent with previously reported values.[91]

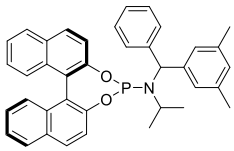

(R_a,R or *S)-N*-((3,5-dimethylphenyl)(phenyl)methyl)-*N*-isopropyldinaphtho[2,1-*d*:1',2'-*f*][1,3,2]dioxaphosphepin-4-amine **L40a**

General procedure C: $PCl_{3(l)}$ (30 µl, 0.35 mmol, 1.1 eq.) in DCM (1.0 ml), $Et_3N_{(l)}$ (0.22 ml, 1.58 mmol, 5.0 eq.), (–)-*N*-((3,5-dimethylphenyl)(phenyl)methyl)propan-2-amine (80 mg, 0.32 mmol, 1.0 eq.) in DCM (1.0 ml), *(R)*-$BINOL_{(s)}$ (118 mg, 0.41 mmol, 1.3 eq.) The crude mixture was purified by flash column chromatography [basic Al_2O_3, petrol/DCM, 85:15] to afford a white solid of *N*-((3,5-dimethylphenyl)(phenyl)methyl)-*N*-isopropyldinaphtho[2,1-*d*:1',2'-*f*][1,3,2]dioxaphosphepin-4-amine (37 mg, 20%).

^{1}H NMR (500 MHz, $CDCl_3$) δ_H: 7.93 – 7.84 (m, 3H, 3$C_{Ar}H$), 7.79 (d, *J* = 8.8 Hz, 1H, $C_{Ar}H$), 7.43 – 7.23 (m, 12H, 12$C_{Ar}H$), 7.22 – 7.17 (m, 1H, $C_{Ar}H$), 7.09 (s, 2H, 2$C_{Ar}H$), 6.95 (s, 1H, $C_{Ar}H$), 5.62 (d, *J* = 17.1 Hz, 1H, ArC*H*), 3.62 – 3.52 (m, 1H, C*H*CH_3), 2.35 (s, 6H, 2ArCH_3), 1.06 (d, *J* = 6.8 Hz, 3H, CHCH_3), 0.97 (d, *J* = 6.5 Hz, 3H, CHCH_3).

^{13}C NMR (126 MHz, $CDCl_3$) δ_C: 150.6 (d, *J* = 7.1 Hz), 150.1, 143.9 (d, *J* = 5.9 Hz), 143.4 (d, *J* = 3.9 Hz), 137.8 (2C), 132.9 (d, *J* = 1.8 Hz), 132.8, 131.5, 130.6, 130.3, 129.4, 129.2, 129.2, 128.7, 128.4, 128.3, 128.2 (2C), 127.3, 127.2, 127.0, 126.8, 126.8, 126.0, 125.9, 124.8, 124.4, 124.1 (d, *J* = 5.4 Hz), 122.6 (d, *J* = 2.1 Hz), 122.3, 121.9 (d, *J* = 2.3 Hz), 60.8 (d, *J* = 24.3 Hz), 47.0, 23.3, 23.1, 21.7 (2C).

^{31}P NMR (202 MHz, $CDCl_3$) δ_P: 149.6 (d, 17.1 Hz).

IR υ_{max} (film): 3058, 2973, 2926, 1591, 1232, 948.

HRMS (CI^+) $[C_{38}H_{35}NO_2P]^+$ predicted 568.2400, found 568.2403 (Δ –0.54 ppm).

M.P. = 89 – 93 °C.

$[\boldsymbol{\alpha}]_{589}^{25}$ = –163 (*c* 1.00, $CHCl_3$).

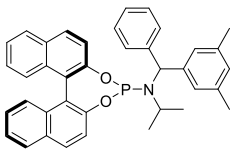

(R_a,R or *S)-N*-((3,5-dimethylphenyl)(phenyl)methyl)-*N*-isopropyldinaphtho[2,1-*d*:1',2'-*f*][1,3,2]dioxaphosphepin-4-amine **L40b**

General procedure C: $PCl_{3(l)}$ (30 µl, 0.35 mmol, 1.1 eq.) in DCM (1.0 ml), $Et_3N_{(l)}$ (0.22 ml, 1.58 mmol, 5.0 eq.), (+)-*N*-((3,5-dimethylphenyl)(phenyl)methyl)propan-2-amine (82 mg, 0.32 mmol, 1.0 eq.) in DCM (1.0 ml), *(R)*-$BINOL_{(s)}$ (118 mg,

0.41 mmol, 1.3 eq.) The crude mixture was purified by flash column chromatography [basic Al_2O_3, petrol/DCM, 85:15] to afford a white solid of *N*-((3,5-dimethylphenyl)(phenyl)methyl)-*N*-isopropyldinaphtho[2,1-*d*:1',2'-*f*][1,3,2]dioxaphosphepin-4-amine (65 mg, 35%).

^{1}H NMR (500 MHz, $CDCl_3$) δ_H: 7.97 – 7.87 (m, 3H, 3$C_{Ar}H$), 7.84 (d, *J* = 8.7 Hz, 1H, $C_{Ar}H$), 7.51 – 7.21 (m, 14H, 14$C_{Ar}H$), 6.98 (s, 2H, 2$C_{Ar}H$), 6.94 (s, 1H, $C_{Ar}H$), 5.65 (d, *J* = 17.9 Hz, 1H, ArC*H*), 3.61 (qq, *J* = 6.7, 6.6 Hz, 1H, C*H*CH_3), 2.36 (s, 6H, 2ArCH_3), 1.09 (d, *J* = 6.7 Hz, 3H, CHC*H*$_3$), 0.99 (d, *J* = 6.6 Hz, 3H, CHC*H*$_3$).

^{13}C NMR (126 MHz, $CDCl_3$) δ_C: 150.7 (d, *J* = 7.3 Hz), 150.0, 143.9 (d, *J* = 4.6 Hz), 143.6 (d, *J* = 5.4 Hz), 137.7 (2C), 132.9 (d, *J* = 1.8 Hz), 132.9, 131.4, 130.6, 130.3, 129.5, 129.1, 129.0, 128.7, 128.4 (3C), 128.3, 127.3, 127.2, 127.1, 126.9, 126.9, 126.0, 125.9, 124.8 (d, *J* = 2.8 Hz), 124.4, 124.2 (d, *J* = 5.5 Hz), 122.5 (d, *J* = 2.0 Hz), 122.4, 121.8 (d, *J* = 2.3 Hz), 60.8 (d, *J* = 25.4 Hz), 46.9, 23.2, 23.0 (d, *J* = 2.7 Hz), 21.7 (2C).

^{31}P NMR (202 MHz, $CDCl_3$) δ_P: 149.4 (d, *J* = 17.9 Hz).

IR υ_{max} (film): 3057, 2972, 2927, 1591, 1231, 948.

HRMS (CI^+) $[C_{38}H_{35}NO_2P]^+$ predicted 568.2400, found 568.2378 (Δ 3.86 ppm).

M.P. = 82 – 88 °C.

$[\boldsymbol{\alpha}]_{589}^{25}$ = –39.1 (*c* 0.50, $CHCl_3$).

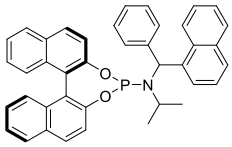

(R_a,R or *S)*-*N*-isopropyl-*N*-(naphthalen-1-yl(phenyl)methyl)dinaphtho[2,1-*d*:1',2'-*f*][1,3,2]dioxaphosphepin-4-amine **L41a**

General procedure C: $PCl_{3(l)}$ (64 µl, 0.74 mmol, 1.1 eq.) in DCM (0.5 ml), $Et_3N_{(l)}$ (0.47 ml, 3.35 mmol, 5.0 eq.), (–)-*N*-(naphthalen-1-yl(phenyl)methyl)propan-2-amine (185 mg, 0.67 mmol, 1.0 eq.) in DCM (2.4 ml), *(R)*-$BINOL_{(s)}$ (249 mg, 0.87 mmol, 1.3 eq.) The crude mixture was purified by flash column chromatography [basic Al_2O_3, petrol/DCM, 4:1] to afford a white solid of (R_a, *R* or *S*)-*N*-isopropyl-*N*-(naphthalen-1-yl(phenyl)methyl)dinaphtho[2,1-*d*:1',2'-*f*][1,3,2]dioxaphosphepin-4-amine with traces of impurity (268 mg, 70%).

^{1}H NMR (500 MHz, $CDCl_3$) δ_H: 8.05 (d, *J* = 7.2 Hz, 1H, $C_{Ar}H$), 7.97 – 7.81 (m, 7H, $7C_{Ar}H$), 7.65 (t, *J* = 7.7 Hz, 1H, $C_{Ar}H$), 7.53 (dd, *J* = 8.8, 3.8 Hz, 2H, $2C_{Ar}H$), 7.50 – 7.16 (m, 13H, $13C_{Ar}H$), 6.46 (d, *J* = 16.3 Hz, 1H, ArC*H*), 3.80 – 3.71 (m, 1H, C*H*CH_3), 1.32 (d, *J* = 6.6 Hz, 3H, CHCH_3), 0.70 (d, *J* = 6.6 Hz, 3H, CHCH_3).

^{13}C NMR (126 MHz, $CDCl_3$) δ_C: 150.5 (d, *J* = 8.2 Hz), 150.1, 143.0 (d, *J* = 9.9 Hz), 138.6 (d, *J* = 1.6 Hz), 134.0, 132.9 (2C), 132.9, 131.5, 131.0, 130.6, 130.4, 129.7 (d, *J* = 3.5 Hz, 2C), 129.0, 128.4 (2C), 128.4, 128.3, 128.2, 127.4, 127.3, 127.2, 126.6 (d, *J* = 7.6 Hz), 126.3, 126.1, 126.0, 125.6, 125.5, 124.8, 124.5, 124.2 (d, *J* = 5.4 Hz), 123.7, 122.5 (d, *J* = 2.0 Hz), 122.4, 121.8 (d, *J* = 2.3 Hz), 57.2 (d, *J* = 28.0 Hz), 46.7 (d, *J* = 4.1 Hz), 23.4, 22.9.

^{31}P NMR (202 MHz, $CDCl_3$) δ_P: 149.2 (d, *J* = 16.1 Hz).

IR υ_{max} (film): 3059, 2971, 2972, 1591,1231, 948.

HRMS (CI$^+$) $[C_{40}H_{33}NO_2P]^+$ predicted 590.2243, found 590.2248 (Δ –0.78 ppm).

M.P. = 108 - 118 °C.

$[\alpha]_{589}^{25}$= +21.3 (*c* 1.00, $CHCl_3$).

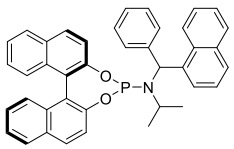

(R_a, R or *S)*- *N*-isopropyl-*N*-(naphthalen-1-yl(phenyl)methyl)dinaphtho[2,1-*d*:1',2'-*f*][1,3,2]dioxaphosphepin-4-amine **L41b**

General procedure C: $PCl_{3(l)}$ (64 µl, 0.74 mmol, 1.1 eq.) in DCM (0.5 ml), $Et_3N_{(l)}$ (0.47 ml, 3.35 mmol, 5.0 eq.), (+)-*N*-(naphthalen-1-yl(phenyl)methyl)propan-2-amine (177 mg, 0.64 mmol, 1.0 eq.) in DCM (2.4 ml), *(R)*-$BINOL_{(s)}$ (249 mg, 0.87 mmol, 1.3 eq.) The crude mixture was purified by flash column chromatography [basic Al_2O_3, petrol/DCM, 4:1] to afford a white solid of (R_a, *R* or *S*)-*N*-isopropyl-*N*-(naphthalen-1-yl(phenyl)methyl)dinaphtho[2,1-*d*:1',2'-*f*][1,3,2]dioxaphosphepin-4-amine (125 mg, 32%).

^{1}H NMR (500 MHz, $CDCl_3$) δ_H: 8.30 (d, *J* = 7.1 Hz, 1H, $C_{Ar}H$), 7.94 – 7.85 (m, 4H, $4C_{Ar}H$), 7.76 – 7.66 (m, 2H, $2C_{Ar}H$), 7.51 – 7.30 (m, 8H, $8C_{Ar}H$), 7.30 – 7.03 (m, 9H, $9C_{Ar}H$), 6.41 (d, *J* = 13.3 Hz, 1H, Ar*CH*), 3.64 (h, *J* = 6.4 Hz, 1H, *CH*CH_3), 1.12 (d, *J* = 6.4 Hz, 3H, CHCH_3), 1.04 (s, br, 3H, CHCH_3).

^{13}C NMR (126 MHz, $CDCl_3$) δ_C: 150.4, 149.9, 142.6 (d, *J* = 8.2 Hz), 139.1, 134.0, 132.9, 132.7, 131.5, 131.0, 130.5, 130.3, 129.8 (d, *J* = 3.0 Hz, 2C), 129.3, 128.8, 128.4, 128.3, 128.3 (2C), 128.1, 127.3, 127.2, 127.1, 126.1 (2C), 126.0, 125.9, 125.6, 125.4, 124.8,

124.3, 124.2 (d, *J* = 5.3 Hz), 123.7, 122.5 (d, *J* = 1.9 Hz), 122.0, 121.7 (d, *J* = 2.3 Hz), 57.8 (d, *J* = 20.4 Hz), 47.8, 23.9, 23.2.

^{31}P NMR (202 MHz, $CDCl_3$) δ_P: 149.8 (s, br)

IR υ_{max} (film): 3056, 2972, 1591, 1231, 947.

HRMS (CI^+) $[C_{40}H_{33}NO_2P]^+$ predicted 590.2243, found 590.2226 (Δ 2.96 ppm).

(**M.P.** was unobtainable due to thermal decomposition.)

$[\boldsymbol{\alpha}]_{589}^{25}$ = –156.9 (*c* 1.00, $CHCl_3$).

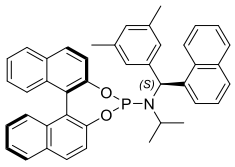

(R_a,S)-N-((3,5-dimethylphenyl)(naphthalen-1-yl)methyl)-*N*-isopropyldinaphtho[2,1-*d*:1',2'-*f*][1,3,2]dioxaphosphepin-4-amine **L42S**

General procedure C: $PCl_{3(l)}$ (31 µl, 0.35 mmol, 1.1 eq.) in DCM (1.0 ml), $Et_3N_{(l)}$ (0.22 ml, 1.58 mmol, 5.0 eq.), (–)-*N*-((3,5-dimethylphenyl)(naphthalen-1-yl)methyl)propan-2-amine (90.2 mg, 0.30 mmol, 1.0 eq.) in DCM (1.0 ml), *(R)*-$BINOL_{(s)}$ (120 mg, 0.41 mmol, 1.3 eq.) The crude mixture was purified by flash column chromatography [basic Al_2O_3, petrol/DCM, 4:1] to afford a white solid of *N*-((3,5-dimethylphenyl)(naphthalen-1-yl)methyl)-*N*-isopropyldinaphtho[2,1-*d*:1',2'-*f*][1,3,2]dioxaphosphepin-4-amine (62.2 mg, 34%).

^{1}H NMR (500 MHz, $CDCl_3$) δ_H: 8.01 – 7.83 (m, 8H, 8$C_{Ar}H$), 7.67 – 7.60 (m, 1H, $C_{Ar}H$), 7.55 – 7.34 (m, 7H, 7$C_{Ar}H$), 7.28 – 7.16 (m, 3H, 3$C_{Ar}H$), 6.94 (s, 2H, 2$C_{Ar}H$), 6.86 (s, 1H,

$C_{Ar}H$), 6.39 (d, *J* = 15.8 Hz, 1H, ArC*H*), 3.79 – 3.69 (m, 1H, C*H*CH_3), 2.26 (s, 6H, 2ArCH_3), 1.28 (d, *J* = 6.3 Hz, 3H, CHCH_3), 0.68 (d, *J* = 6.5 Hz, 3H, CHCH_3).

^{13}C NMR (126 MHz, $CDCl_3$) δ_C: 150.5 (d, *J* = 7.8 Hz), 150.2, 142.8 (d, *J* = 9.8 Hz), 138.8 (d, *J* = 1.9 Hz), 137.7 (2C), 133.9, 132.9 (d, *J* = 2.1 Hz, 2C), 131.4, 131.2 (d, *J* = 1.7 Hz), 130.6, 130.3, 129.5, 129.1, 128.9, 128.3, 128.3, 128.1, 127.6, 127.6, 127.3, 127.1, 126.8 (d, *J* = 7.7 Hz), 126.2, 126.0, 126.0, 125.5, 125.4, 124.8, 124.5, 124.2 (d, *J* = 5.4 Hz), 123.8, 122.6 (d, *J* = 1.9 Hz), 122.3, 121.9 (d, *J* = 2.2 Hz), 57.1 (d, *J* = 27.4 Hz), 46.6 (d, *J* = 3.9 Hz), 23.4, 22.9, 21.6 (2C).

^{31}P NMR (202 MHz, $CDCl_3$) δ_P: 149.5 (d, *J* = 15.9 Hz).

IR υ_{max} (film): 3053, 2971, 2927, 1591, 1231, 948.

HRMS (CI^+) $[C_{42}H_{36}NO_2P]^+$ predicted 618.2556, found 618.2582 (Δ –4.14 ppm).

M.P. = 118 - 122 °C.

$[\boldsymbol{\alpha}]_{589}^{25}$= +51.4 (*c* 1.00, $CHCl_3$).

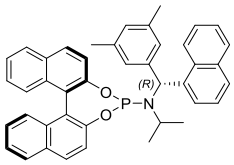

(R_a,R)-*N*-((3,5-dimethylphenyl)(naphthalen-1-yl)methyl)-*N*-isopropyldinaphtho[2,1-*d*:1',2'-*f*][1,3,2]dioxaphosphepin-4-amine **L42R**

General procedure C: $PCl_{3(l)}$ (31 µl, 0.35 mmol, 1.1 eq.) in DCM (1.0 ml), $Et_3N_{(l)}$ (0.22 ml, 1.58 mmol, 5.0 eq.), (+)-*N*-((3,5-dimethylphenyl)(naphthalen-1-yl)methyl)propan-2-amine (97.8 mg, 0.30 mmol, 1.0 eq.) in DCM (1.0 ml), *(R)*-$BINOL_{(s)}$ (120 mg, 0.41 mmol, 1.3 eq.) The crude mixture was purified by flash

column chromatography [basic Al_2O_3, petrol/DCM, 4:1] to afford a white solid of (R_a, *R* or *S*)-*N*-((3,5-dimethylphenyl)(naphthalen-1-yl)methyl)-*N*-isopropyldinaphtho[2,1-*d*:1',2'-*f*][1,3,2]dioxaphosphepin-4-amine (136 mg, 68%). See the published supporting information for crystallographic data.[120]

^{1}H NMR (500 MHz, $CDCl_3$) δ_H: 8.25 (d, *J* = 7.2 Hz, 1H, $C_{Ar}H$), 7.96 – 7.86 (m, 4H, $4C_{Ar}H$), 7.78 – 7.68 (m, 2H, $2C_{Ar}H$), 7.65 – 7.31 (m, 8H, $8C_{Ar}H$), 7.30 – 7.17 (m, 4H, $4C_{Ar}H$), 6.86 (s, 1H, $C_{Ar}H$), 6.83 (s, 2H, $2C_{Ar}H$), 6.34 (d, *J* = 13.9 Hz, 1H, ArC*H*), 3.62 (h, *J* = 6.5 Hz, 1H, C*H*CH_3), 2.24 (s, 6H, $2ArCH_3$), 1.13 (d, *J* = 6.2 Hz, 3H, $CHCH_3$), 0.94 (s, br, 3H, $CHCH_3$).

^{13}C NMR (126 MHz, $CDCl_3$) δ_C: 150.6, 150.0, 142.5 (d, *J* = 7.7 Hz), 139.4, 137.6 (2C), 134.0, 132.9 (d, *J* = 1.6 Hz), 132.7, 131.4, 131.1, 130.5, 130.2, 129.3, 129.0, 128.8, 128.4, 128.3, 128.0, 127.6 (d, *J* = 3.1 Hz, 2C), 127.2, 127.2, 126.4, 126.1, 126.0, 125.8, 125.5, 125.5, 124.7, 124.3, 124.2 (d, *J* = 5.3 Hz), 123.7, 122.6 (d, *J* = 1.9 Hz), 122.1, 121.7 (d, *J* = 2.3 Hz), 57.6 (d, *J* = 22.3 Hz), 47.7, 23.7 (br), 23.1 (br), 21.6 (2C).

^{31}P NMR (202 MHz, $CDCl_3$) δ_P: 150.0 (s, br).

IR υ_{max} (film): 3053, 2969, 1591, 1230, 947.

HRMS (CI^+) $[C_{42}H_{36}NO_2P]^+$ predicted 618.2556, found 618.2538 (Δ 2.98 ppm).

(**M.P.** was unobtainable due to thermal decomposition.)

$[\boldsymbol{\alpha}]_{589}^{25}$ = –228 (*c* 1.00, $CHCl_3$).

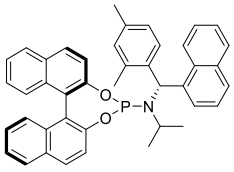

(R_a,*R*)-*N*-(-(2,4-dimethylphenyl)(naphthalen-1-yl)methyl)-*N*-isopropyldinaphtho[2,1-*d*:1',2'-*f*][1,3,2]dioxaphosphepin-4-amine **L43R**

General procedure C: $PCl_{3(l)}$ (82 µl, 0.94 mmol, 1.1 eq.) in DCM (1.3 ml), $Et_3N_{(l)}$ (0.59 ml, 4.26 mmol, 5.0 eq.), (+)-(*R*)-*N*-((2,4-dimethylphenyl)(naphthalen-1-yl)methyl)propan-2-amine (258 mg, 0.85 mmol, 1.0 eq.) in DCM (3.0 ml), *(R)*-$BINOL_{(s)}$ (317 mg, 1.11 mmol, 1.3 eq.) The crude mixture was purified by flash column chromatography [basic Al_2O_3, petrol/DCM, 4:1] to afford a white solid of (R_a,)-*N*-((*R*)-(2,4-dimethylphenyl)(naphthalen-1-yl)methyl)-*N*-isopropyldinaphtho[2,1-*d*:1',2'-*f*][1,3,2]dioxaphosphepin-4-amine (357 mg, 68%). See the published supporting information for crystallographic data.[120]

^{1}H NMR (500 MHz, $CDCl_3$) δ_H: 8.03 (s, br, 1H, $C_{Ar}H$), 7.92 – 7.74 (m, 6H, $6C_{Ar}H$), 7.71 (s, br, 1H, $C_{Ar}H$), 7.56 – 7.40 (m, 4H, $4C_{Ar}H$), 7.39 – 7.31 (m, 3H, $3C_{Ar}H$), 7.27 – 7.09 (m, 5H, $5C_{Ar}H$), 7.03 (s, 1H, $C_{Ar}H$), 6.93 (d, *J* = 7.9 Hz, 1H, $C_{Ar}H$), 6.52 (d, *J* = 12.5 Hz, 1H, Ar*CH*), 3.75 – 3.65 (m, 1H, *CH*CH_3), 2.41 (s, 3H, ArCH_3), 2.31 (s, 3H, ArCH_3), 1.09 (d, *J* = 6.8 Hz, 3H, CHCH_3), 0.90 (d, *J* = 6.6 Hz, 3H, CHCH_3).

^{13}C NMR (126 MHz, $CDCl_3$) δ_C: 150.6 (d, *J* = 7.3 Hz), 150.0, 138.8, 138.7 (d, *J* = 6.4 Hz), 137.0, 135.6, 134.2, 132.9, 132.8, 131.7, 131.4, 131.1, 130.6 (d, *J* = 5.2 Hz), 130.4, 130.2, 129.3, 129.1, 128.3 (4C), 127.2, 127.1, 126.5, 126.2, 126.0, 125.9, 125.6, 125.1, 124.7, 124.3, 124.2 (d, *J* = 5.5 Hz), 123.5, 122.6, 122.4, 121.6, 55.1 (d, *J* = 27.1 Hz), 47.9, 24.2, 23.0, 21.2, 20.0.

^{31}P NMR (202 MHz, $CDCl_3$) δ_P: 147.8 (d, *J* = 12.2 Hz).

IR υ_{max} (film): 3058, 2973, 1591, 1231, 947.

HRMS (CI$^+$) $[C_{42}H_{37}NO_2P]^+$ predicted 618.2556, found 618.2565 (Δ –1.39 ppm).

M.P. = 80 - 85 °C.

$[\boldsymbol{\alpha}]_{589}^{25}$= +38.2 (*c* 2.00, $CHCl_3$).

For the other diasteromer: (*R*$_a$,*S*)-*N*-(-(2,4-dimethylphenyl)(naphthalen-1-yl)methyl)-*N*-isopropyldinaphtho[2,1-*d*:1',2'-*f*][1,3,2]dioxaphosphepin-4-amine: $[\boldsymbol{\alpha}]_{589}^{25}$= –174.7 (*c* 1.00, $CHCl_3$).

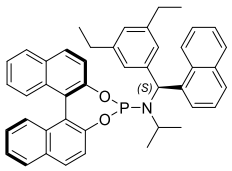

(*R*$_a$,*S*)- *N*-((3,5-diethylphenyl)(naphthalen-1-yl)methyl)-*N*-isopropyldinaphtho[2,1-*d*:1',2'-*f*][1,3,2]dioxaphosphepin-4-amine **L44S**

General procedure C: $PCl_{3(l)}$ (167 µl, 1.91 mmol, 1.1 eq.) in DCM (2.7 ml), $Et_3N_{(l)}$ (1.21 ml, 8.68 mmol, 5.0 eq.), (–)-*(S)*-*N*-((3,5-diethylphenyl)(naphthalen-1-yl)methyl)propan-2-amine (556 mg, 1.68 mmol, 1.0 eq.) in DCM (6.0 ml), *(R)*-$BINOL_{(s)}$ (646 mg, 2.26 mmol, 1.3 eq.) The crude mixture was purified by flash column chromatography [basic Al_2O_3, petrol/DCM, 4:1] to afford a white solid of (*R*$_a$,*S*)-*N*-((3,5-diethylphenyl)(naphthalen-1-yl)methyl)-*N*-isopropyldinaphtho[2,1-*d*:1',2'-*f*][1,3,2]dioxaphosphepin-4-amine (992 mg, 92%).

^{1}H NMR (500 MHz, $CDCl_3$) δ_H: 7.87 – 7.70 (m, 8H, 8$C_{Ar}H$), 7.51 (t, *J* = 7.7 Hz, 1H, $C_{Ar}H$), 7.42 – 7.21 (m, 7H, 7$C_{Ar}H$), 7.20 – 7.03 (m, 3H, 3$C_{Ar}H$), 6.88 (s, 2H, 2$C_{Ar}H$), 6.79 (s, 1H, $C_{Ar}H$), 6.31 (d, *J* = 15.7 Hz, 1H, ArCH), 3.63 (qq, *J* = 6.6 Hz, 1H, $CHCH_3$), 2.47 (q,

J = 7.6 Hz, 4H, 2C*H*$_2$CH$_3$), 1.17 (d, *J* = 6.6 Hz, 3H, CHC*H*$_3$), 1.07 (t, *J* = 7.6 Hz, 6H, 2CH$_2$C*H*$_3$), 0.60 (d, *J* = 6.6 Hz, 3H, CHC*H*$_3$).

^{13}C NMR (126 MHz, $CDCl_3$) δ_C: 150.6 (d, *J* = 8.0 Hz), 150.2, 144.1, 143.0 (d, *J* = 9.1 Hz, 2C), 138.9 (d, *J* = 2.2 Hz), 133.9, 133.3 – 132.7 (m, 2C), 131.4, 131.2 (d, *J* = 1.8 Hz), 130.6, 130.3, 129.5, 128.9, 128.3, 128.3, 128.1, 127.3, 127.2, 126.9 (d, *J* = 7.7 Hz), 126.7, 126.6, 126.4, 126.2, 126.0, 126.0, 125.5, 125.4, 124.8, 124.4, 124.2 (d, *J* = 5.4 Hz), 123.9, 122.6 (d, *J* = 2.0 Hz), 122.4, 121.8 (d, *J* = 2.3 Hz), 57.3 (d, *J* = 27.4 Hz), 46.7 (d, *J* = 3.5 Hz), 29.0 (2C), 23.4, 22.9, 15.7 (2C).

^{31}P NMR (202 MHz, $CDCl_3$) δ_P: 149.7 (d, *J* = 15.7 Hz).

IR υ_{max} (film): 3054, 2965, 2931, 1592, 1231, 948.

HRMS (CI$^+$) $[C_{44}H_{41}NO_2P]^+$ predicted 646.2869, found 646.2845 (Δ 3.79 ppm).

M.P. = 74 – 78 °C.

$[\boldsymbol{\alpha}]_{589}^{25}$ = +34.4 (*c* 1.00, $CHCl_3$).

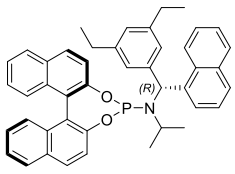

(*R*$_a$,*R*)- *N*-((3,5-diethylphenyl)(naphthalen-1-yl)methyl)-*N*-isopropyldinaphtho[2,1-*d*:1',2'-*f*][1,3,2]dioxaphosphepin-4-amine **L44R**

General procedure C: $PCl_{3(l)}$ (167 µl, 1.91 mmol, 1.1 eq.) in DCM (2.7 ml), $Et_3N_{(l)}$ (1.21 ml, 8.68 mmol, 5.0 eq.), (+)-*(R)*-*N*-((3,5-diethylphenyl)(naphthalen-1-yl)methyl)propan-2-amine (575 mg, 1.74 mmol, 1.0 eq.) in DCM (6.0 ml), *(R)*-BINOL$_{(s)}$ (646 mg, 2.26 mmol, 1.3 eq.) The crude mixture was purified by flash

column chromatography [basic Al_2O_3, petrol/DCM, 4:1] to afford a white solid of (*R*$_a$,*R*)- *N*-((3,5-diethylphenyl)(naphthalen-1-yl)methyl)-*N*-isopropyldinaphtho[2,1-*d*:1',2'-*f*][1,3,2]dioxaphosphepin-4-amine (522 mg, 47%).

^{1}H NMR (500 MHz, $CDCl_3$) δ_H: 8.14 (d, *J* = 7.1 Hz, 1H, $C_{Ar}H$), 7.83 – 7.74 (m, 4H, $4C_{Ar}H$), 7.65 – 7.56 (m, 2H, $2C_{Ar}H$), 7.54 (s, br, 1H, $C_{Ar}H$), 7.42 (s, br, 1H, $C_{Ar}H$), 7.34 – 7.05 (m, 11H, $11C_{Ar}H$), 6.81 – 6.76 (m, 3H, $3C_{Ar}H$), 6.27 (d, *J* = 14.2 Hz, 1H, ArC*H*), 3.57 – 3.46 (m, 1H, C*H*CH_3), 2.45 (q, *J* = 7.5 Hz, 4H, $2CH_2CH_3$), 1.06 (t, *J* = 7.6 Hz, 6H, $2CH_2CH_3$), 1.01 (d, *J* = 6.4 Hz, 3H, $CHCH_3$), 0.85 (s, br, 3H, $CHCH_3$).

^{13}C NMR (126 MHz, $CDCl_3$) δ_C: 150.6 (d, *J* = 6.4 Hz), 150.0, 144.1 (2C), 142.6 (d, *J* = 7.7 Hz), 139.4, 133.9, 132.9 (d, *J* = 1.7 Hz), 132.7, 131.4, 131.2, 130.5, 130.2, 129.3, 128.8, 128.4, 128.3, 128.0, 127.2, 127.1, 126.6 (d, *J* = 3.2 Hz, 2C), 126.5, 126.4, 126.1, 126.0, 125.8, 125.5, 125.4, 124.7, 124.3, 124.2 (d, *J* = 5.2 Hz), 123.8, 122.5 (d, *J* = 2.0 Hz), 122.1, 121.8 (d, *J* = 2.2 Hz), 57.7 (d, *J* = 22.8 Hz), 47.7, 28.9 (2C), 23.6, 23.0, 15.8 (2C).

^{31}P NMR (202 MHz, $CDCl_3$) δ_P: 150.5 (s, br).

IR υ_{max} (film): 3055, 2965, 2930, 1592, 1231, 948.

HRMS (CI^+) $[C_{44}H_{41}NO_2P]^+$ predicted 646.2869, found 646.2859 (Δ 1.62 ppm).

(**M.P.** was unobtainable due to thermal decomposition.)

$[\alpha]_{589}^{25}$ = –104.1 (*c* 0.50, $CHCl_3$).

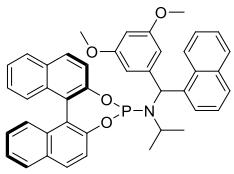

(R_a,R or *S)-N*-((3,5-dimethoxyphenyl)(naphthalen-1-yl)methyl)-*N*-isopropyldinaphtho[2,1-*d*:1',2'-*f*][1,3,2]dioxaphosphepin-4-amine **L45a**

General procedure C: $PCl_{3(l)}$ (366 µl, 4.19 mmol, 1.1 eq.) in DCM (3.0 ml), $Et_3N_{(l)}$ (2.66 ml, 19.1 mmol, 5.0 eq.), (–)-*N*-((3,5-dimethoxyphenyl)(naphthalen-1-yl)methyl)propan-2-amine (1.28 g, 3.81 mmol, 1.0 eq.) in DCM (8.0 ml), *(R)*-$BINOL_{(s)}$ (1.42 mg, 4.95 mmol, 1.3 eq.) The crude mixture was purified by flash column chromatography [basic Al_2O_3, petrol/DCM, 4:1] to afford a white solid of (R_a,*S*)-*N*-((3,5-dimethoxyphenyl)(naphthalen-1-yl)methyl)-*N*-isopropyldinaphtho[2,1-*d*:1',2'-*f*][1,3,2]dioxaphosphepin-4-amine (2.28 g, 92%).

^{1}H NMR (500 MHz, $CDCl_3$) δ_H: 7.86 – 7.71 (m, 8H, 8$C_{Ar}H$), 7.48 (t, *J* = 7.7 Hz, 1H, $C_{Ar}H$), 7.41 – 7.21 (m, 7H, 7$C_{Ar}H$), 7.18 – 7.04 (m, 3H, 3$C_{Ar}H$), 6.42 (d, *J* = 2.2 Hz, 2H, 2$C_{Ar}H$), 6.27 (d, *J* = 15.3 Hz, 1H, ArCH), 6.23 (t, *J* = 2.2 Hz, 1H, $C_{Ar}H$), 3.71 – 3.59 (m, 1H, $CHCH_3$), 3.60 (s, 6H, 2OCH_3), 1.20 (d, *J* = 6.6 Hz, 3H, CHCH_3), 0.59 (d, *J* = 6.6 Hz, 3H, CHCH_3).

^{13}C NMR (126 MHz, $CDCl_3$) δ_C: 160.8 (2C), 150.6 (d, *J* = 7.9 Hz), 150.0, 145.6 (d, *J* = 9.0 Hz), 138.3 (d, *J* = 2.3 Hz), 133.9, 132.9 (2C), 131.5, 131.2 (d, *J* = 1.6 Hz), 130.6, 130.4, 129.5, 129.0, 128.4, 128.3 (2C), 127.3, 127.1, 126.9 (d, *J* = 7.5 Hz), 126.3, 126.1, 126.0, 125.6, 125.4, 124.8, 124.5, 124.2 (d, *J* = 5.4 Hz), 123.6, 122.5, 122.5, 122.3, 121.7 (d, *J* = 2.3 Hz), 108.3 (2C), 98.8, 57.2 (d, *J* = 26.6 Hz), 55.4 (2C), 46.8 (d, *J* = 2.7 Hz), 23.4, 22.9.

^{31}P NMR (202 MHz, $CDCl_3$) δ_P: 148.7 (d, *J* = 15.3 Hz).

IR υ_{max} (film): 3058, 2970, 2836, 1593, 1231, 947.

HRMS (CI$^+$) $[C_{42}H_{37}NO_4P]^+$ predicted 650.2455, found 650.2400 (Δ 2.27 ppm).

M.P. = 116 – 121 °C.

$[\boldsymbol{\alpha}]_{589}^{25}$ = +24.4 (*c* 1.00, $CHCl_3$).

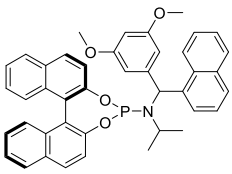

(R_a,R or *S)-N*-((3,5-dimethoxyphenyl)(naphthalen-1-yl)methyl)-*N*-isopropyldinaphtho[2,1-*d*:1',2'-*f*][1,3,2]dioxaphosphepin-4-amine **L45b**

General procedure C: $PCl_{3(l)}$ (366 µl, 4.19 mmol, 1.2 eq.) in DCM (3.0 ml), $Et_3N_{(l)}$ (2.66 ml, 19.1 mmol, 5.3 eq.), (+)-*N*-((3,5-dimethoxyphenyl)(naphthalen-1-yl)methyl)propan-2-amine (1.20 g, 3.59 mmol, 1.0 eq.) in DCM (8.0 ml), *(R)*-$BINOL_{(s)}$ (1.42 mg, 4.95 mmol, 1.4 eq.) The crude mixture was purified by flash column chromatography [basic Al_2O_3, petrol/DCM, 4:1] to afford a white solid of (R_a,*R*)-*N*-((3,5-dimethoxyphenyl)(naphthalen-1-yl)methyl)-*N*-isopropyldinaphtho[2,1-*d*:1',2'-*f*][1,3,2]dioxaphosphepin-4-amine (2.02 g, 87%).

^{1}H NMR (500 MHz, $CDCl_3$) δ_H: 8.15 – 8.09 (m, 1H, $C_{Ar}H$), 7.84 – 7.75 (m, 4H, $C_{Ar}H$), 7.57 (t, *J* = 7.7 Hz, 2H, $C_{Ar}H$), 7.50 – 6.85 (m, 12H, $C_{Ar}H$), 6.33 (s, 2H, $C_{Ar}H$), 6.22 (d, *J* = 14.5 Hz, 2H, $C_{Ar}H$, ArCH), 3.60 (s, 6H, 2OCH_3), 3.57 – 3.50 (m, 1H, $CHCH_3$), 1.04 (d, *J* = 6.4 Hz, 3H, CHCH_3), 0.90 (s, 3H, CHCH_3).

^{13}C NMR (126 MHz, $CDCl_3$) δ_C: 160.7 (2C), 150.4, 149.9, 145.2 (d, *J* = 7.4 Hz), 138.8, 133.9, 132.9, 132.6, 131.5, 131.1, 130.5, 130.3, 129.3, 128.8, 128.4, 128.3, 128.2, 127.2, 127.1, 126.2, 126.2, 126.1, 125.9, 125.6, 125.4, 124.8, 124.3, 124.1, 123.5,

122.4 (d, *J* = 1.9 Hz), 122.0, 121.7 (d, *J* = 2.2 Hz), 108.3 (2C), 98.9, 57.7 (d, *J* = 20.6 Hz), 55.3 (2C), 47.8, 23.8, 23.1.

^{31}P NMR (202 MHz, $CDCl_3$) δ_P: 149.4 (s, br).

IR υ_{max} (film): 3055, 2969, 2836, 1594, 1231, 947.

(**HRMS** cannot be obtained by ESI, EI, CI and APCI ionisation methods.)

(**M.P.** was unobtainable due to thermal decomposition.)

$[\boldsymbol{\alpha}]_{589}^{25}$ = −125 (*c* 0.50, $CHCl_3$).

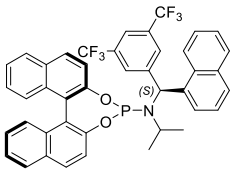

(*R*$_a$,*S*)-*N*-((3,5-bis(trifluoromethyl)phenyl)(naphthalen-1-yl)methyl)-*N*-isopropyldinaphtho[2,1-*d*:1',2'-*f*][1,3,2]dioxaphosphepin-4-amine

L46S

General procedure C: $PCl_{3(l)}$ (210 µl, 2.41 mmol, 1.1 eq.) in DCM (3.0 ml), $Et_3N_{(l)}$ (1.53 ml, 10.9 mmol, 5.0 eq.), (–)-*(S)*-*N*-((3,5-bis(trifluoromethyl)phenyl)(naphthalen-1-yl)methyl)propan-2-amine (902 mg, 2.19 mmol, 1.0 eq.) in DCM (8.0 ml), *(R)*-$BINOL_{(s)}$ (816 mg, 2.85 mmol, 1.3 eq.) The crude mixture was purified by flash column chromatography [basic Al_2O_3, petrol/DCM, 4:1] to afford a white solid of (*R*$_a$,*S*)-*N*-((3,5-bis(trifluoromethyl)phenyl)(naphthalen-1-yl)methyl)-*N*-isopropyldinaphtho[2,1-*d*:1',2'-*f*][1,3,2]dioxaphosphepin-4-amine (1.29 mg, 81%).

^{1}H NMR (500 MHz, $CDCl_3$) δ_H: 7.98 – 7.83 (m, 11H, 11$C_{Ar}H$), 7.65 (t, *J* = 7.7 Hz, 1H, $C_{Ar}H$), 7.55 – 7.34 (m, 7H, 7$C_{Ar}H$), 7.31 – 7.17 (m, 3H, 3$C_{Ar}H$), 6.60 (d, *J* = 15.6 Hz, 1H, ArC*H*), 3.85 – 3.76 (m, 1H, C*H*CH_3), 1.32 (d, *J* = 6.6 Hz, 3H, CH_3), 0.76 (d, *J* = 6.6 Hz, 3H, CH_3).

^{13}C NMR (126 MHz, $CDCl_3$) δ_C: 150.0 (d, *J* = 7.6 Hz), 149.6, 146.6 (d, *J* = 2.9 Hz), 136.3, 134.1, 132.9 (2C), 131.8 (q, *J* = 33.3 Hz, 2C), 131.6, 130.8, 130.7, 130.6, 129.8, 129.5 (2C), 129.4, 129.2, 128.4 (2C), 127.4, 127.3, 127.2, 126.8, 126.3, 126.2, 126.0, 125.5, 125.0, 124.7, 124.0 (d, *J* = 4.9 Hz), 123.4 (q, *J* = 273.9 Hz, 2C), 123.0, 122.2, 121.8 (2C), 121.6 – 121.2 (m), 56.7 (d, *J* = 26.2 Hz), 47.1, 23.3, 23.1.

^{31}P NMR (202 MHz, $CDCl_3$) δ_P: 148.5 (s).

^{19}F NMR (471 MHz, $CDCl_3$) δ_F: –62.6 (s).

IR υ_{max} (film): 3062, 1591, 1231, 948.

HRMS (CI^+) $[C_{42}H_{31}F_6NO_2P]^+$ predicted 726.1991, found 726.1967 (Δ 3.33 ppm).

M.P. = 126 – 128 °C.

$[\boldsymbol{\alpha}]_{589}^{25}$ = –2.3 (*c* 0.25, $CHCl_3$).

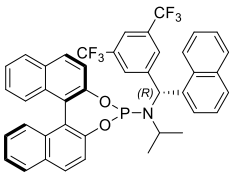

(*R*$_a$,*R*)-*N*-((3,5-bis(trifluoromethyl)phenyl)(naphthalen-1-yl)methyl)-*N*-isopropyldinaphtho[2,1-*d*:1',2'-*f*][1,3,2]dioxaphosphepin-4-amine

L46R

General procedure C: $PCl_{3(l)}$ (118 µl, 1.35 mmol, 1.1 eq.) in DCM (2.0 ml), $Et_3N_{(l)}$ (0.86 ml, 6.15 mmol, 5.0 eq.), (+)-*(R)*-*N*-((3,5-bis(trifluoromethyl)phenyl)(naphthalen-1-yl)methyl)propan-2-amine (506 mg, 1.23 mmol, 1.0 eq.) in DCM (4.0 ml), *(R)*-$BINOL_{(s)}$ (458 mg, 1.60 mmol, 1.3 eq.) The crude mixture was purified by flash column chromatography [basic Al_2O_3, petrol/DCM, 4:1] to afford a white solid of (R_a,*R*)-*N*-((3,5-bis(trifluoromethyl)phenyl)(naphthalen-1-yl)methyl)-*N*-isopropyldinaphtho[2,1-*d*:1',2'-*f*][1,3,2]dioxaphosphepin-4-amine (536 mg, 60%).

^{1}H NMR (500 MHz, $CDCl_3$) δ_H: 8.11 (d, *J* = 7.2 Hz, 1H, $C_{Ar}H$), 7.91 – 7.78 (m, 4H, $4C_{Ar}H$), 7.69 (s, 1H, $C_{Ar}H$), 7.64 (t, *J* = 7.7 Hz, 2H, $2C_{Ar}H$), 7.59 (s, 2H, $2C_{Ar}H$), 7.44 (s, br, 1H, $C_{Ar}H$), 7.41 – 7.34 (m, 1H, $C_{Ar}H$), 7.33 – 7.22 (m, 4H, $4C_{Ar}H$), 7.22 – 7.09 (m, 5H, $5C_{Ar}H$), 7.08 (s, br, 1H, $C_{Ar}H$), 6.41 (d, *J* = 14.5 Hz, 1H, ArC*H*), 3.58 – 3.48 (m, 1H, C*H*CH_3), 1.04 (d, *J* = 6.5 Hz, 3H, C*H*$_3$), 0.91 (s, 3H, C*H*$_3$).

^{13}C NMR (126 MHz, $CDCl_3$) δ_C: 150.0 (d, *J* = 7.5 Hz), 149.5, 146.1 (d, *J* = 7.5 Hz), 136.8, 134.1, 132.9 (d, *J* = 1.7 Hz), 132.7, 131.7 (q, *J* = 31.8 Hz, 2C), 131.6, 130.7, 130.6 (2C), 129.5 (3C), 129.3, 129.1, 128.5, 128.3, 127.2, 127.2, 126.7 (2C), 126.2, 126.1, 126.0, 125.6, 125.0, 124.6, 124.0 (d, *J* = 5.2 Hz), 123.4 (q, *J* = 272.9 Hz, 2C), 122.7, 122.1 (d, *J* = 2.0 Hz), 121.8 (d, *J* = 2.3 Hz), 121.7, 121.48 – 121.24 (m), 56.9 (d, *J* = 22.5 Hz), 47.9, 23.6, 23.0.

^{31}P NMR (202 MHz, $CDCl_3$) δ_P: 148.0 (s).

^{19}F NMR (471 MHz, $CDCl_3$) δ_F: −62.8 (s).

IR υ_{max} (film): 3061, 1591, 1231, 949.

HRMS (CI$^+$) $[C_{42}H_{31}F_6NO_2P]^+$ predicted 726.1991, found 726.2019 (Δ –3.85 ppm).

M.P. = 125 – 130 °C.

$[\alpha]_{589}^{25}$ = –103 (*c* 0.50, $CHCl_3$).

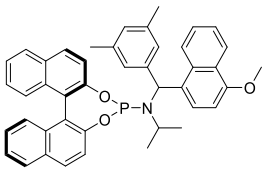

(*R*$_a$,*R or S*)-*N*-((3,5-dimethylphenyl)(4-methoxynaphthalen-1-yl)methyl)-*N*-isopropyldinaphtho[2,1-*d*:1',2'-*f*][1,3,2]dioxaphosphepin-4-amine

L47a

General procedure C: $PCl_{3(l)}$ (97 µl, 1.11 mmol, 1.1 eq.) in DCM (1.0 ml), $Et_3N_{(l)}$ (1.48 ml, 5.05 mmol, 5.0 eq.), (–)-*N*-((3,5-dimethylphenyl)(4-methoxynaphthalen-1-yl)methyl)propan-2-amine (337 mg, 1.01 mmol, 1.0 eq.) in DCM (4.0 ml), *(R)*-$BINOL_{(s)}$ (376 mg, 1.31 mmol, 1.3 eq.) The crude mixture was purified by flash column chromatography [basic Al_2O_3, petrol/DCM, 4:1] to afford a white solid of ((*R*$_a$,*R or S*)-*N*-((3,5-dimethylphenyl)(4-methoxynaphthalen-1-yl)methyl)-*N*-isopropyldinaphtho[2,1-*d*:1',2'-*f*][1,3,2]dioxaphosphepin-4-amine (489 mg, 75%).

^{1}H NMR (400 MHz, $CDCl_3$) δ_H: 8.41 – 8.32 (m, 1H, $C_{Ar}H$), 7.97 – 7.83 (m, 5H, $5C_{Ar}H$), 7.76 (d, *J* = 8.1 Hz, 1H, $C_{Ar}H$), 7.54 – 7.33 (m, 7H, $C7_{Ar}H$), 7.32 – 7.13 (m, 3H, $3C_{Ar}H$), 7.01 – 6.91 (m, 3H, $3C_{Ar}H$), 6.87 (s, 1H, $C_{Ar}H$), 6.29 (d, *J* = 15.7 Hz, 1H, ArC*H*), 4.07 (s, 3H, OCH_3), 3.79 – 3.66 (m, 1H, $CHCH_3$), 2.28 (s, 6H, $Ar(CH_3)_2$), 1.24 (d, *J* = 6.6 Hz, 3H, $CHCH_3$), 0.76 (d, *J* = 6.6 Hz, 3H, $CHCH_3$).

^{13}C NMR (101 MHz, $CDCl_3$) δ_C: 155.0, 150.6 (d, *J* = 7.9 Hz), 150.1, 143.4 (d, *J* = 8.9 Hz), 137.6 (2C), 132.9 (2C), 132.0, 131.4, 130.5, 130.4 (d, *J* = 2.7 Hz), 130.2, 129.5, 128.9, 128.3 (2C), 127.5, 127.4, 127.3, 127.2, 127.1, 126.7, 126.0, 125.9, 125.9, 124.9, 124.7,

124.4, 124.2 (d, *J* = 5.2 Hz), 123.6, 122.7, 122.6, 122.4, 121.8, 103.2, 56.9 (d, *J* = 27.9 Hz), 55.6, 46.7, 23.3, 23.0, 21.7 (2C).

^{31}P NMR (162 MHz, $CDCl_3$) δ_P: 149.5 (s).

IR υ_{max} (film): 2970, 1588, 1231, 947.

(**HRMS** cannot be obtained by ESI, EI, CI and APCI ionisation methods.)

M.P. = 140 - 142 °C.

$[\alpha]_{589}^{25}$ = +15.8 (*c* 0.50, $CHCl_3$).

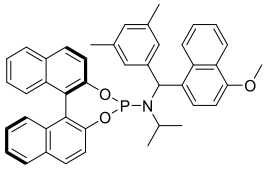

(*R*$_a$,*R or S*)-*N*-((3,5-dimethylphenyl)(4-methoxynaphthalen-1-yl)methyl)-*N*-isopropyldinaphtho[2,1-*d*:1',2'-*f*][1,3,2]dioxaphosphepin-4-amine

L47b

General procedure C: $PCl_{3(l)}$ (97 µl, 1.11 mmol, 1.1 eq.) in DCM (1.0 ml), $Et_3N_{(l)}$ (1.48 ml, 5.05 mmol, 5.0 eq.), (+)-*N*-((3,5-dimethylphenyl)(4-methoxynaphthalen-1-yl)methyl)propan-2-amine (332 mg, 0.99 mmol, 1.0 eq.) in DCM (4.0 ml), *(R)*-$BINOL_{(s)}$ (376 mg, 1.31 mmol, 1.3 eq.) The crude mixture was purified by flash column chromatography [basic Al_2O_3, petrol/DCM, 4:1] to afford a white solid of ((*R*$_a$,*R or S*)-*N*-((3,5-dimethylphenyl)(4-methoxynaphthalen-1-yl)methyl)-*N*-isopropyldinaphtho[2,1-*d*:1',2'-*f*][1,3,2]dioxaphosphepin-4-amine (603 mg, 94%).

^{1}H NMR (400 MHz, $CDCl_3$) δ_H: 8.36 (dd, *J* = 8.4, 1.3 Hz, 1H, $C_{Ar}H$), 8.07 (d, *J* = 8.1 Hz, 1H, $C_{Ar}H$), 7.94 – 7.84 (m, 2H, $2C_{Ar}H$), 7.75 (d, *J* = 8.1 Hz, 1H, $C_{Ar}H$), 7.57 (s, br, 2H,

2$C_{Ar}H$), 7.48 – 7.13 (m, 10H, 10$C_{Ar}H$), 7.03 (d, *J* = 8.1 Hz, 1H, $C_{Ar}H$), 6.85 (s, 3H, 3$C_{Ar}H$), 6.23 (d, *J* = 14.3 Hz, 1H, ArC*H*), 4.11 (s, 3H, OCH_3), 3.66 – 3.53 (m, 1H, C*H*CH_3), 2.25 (s, 6H, Ar(CH_3)$_2$), 1.10 (d, *J* = 6.4 Hz, 3H, CHCH_3), 0.94 (s, br, 3H, CHCH_3).

^{13}C NMR (126 MHz, $CDCl_3$) δ_C: 155.1, 150.7 (d, *J* = 6.8 Hz), 150.0, 143.0, 137.5 (2C), 132.9 (d, *J* = 1.7 Hz), 132.7, 131.9, 131.4, 131.1 (d, *J* = 1.9 Hz), 130.5, 130.2, 129.3, 128.8, 128.4, 128.3, 127.5, 127.4, 127.2, 127.2, 126.7, 126.0, 125.8, 124.9, 124.7, 124.3, 124.2 (d, *J* = 5.4 Hz), 123.5, 122.6, 122.6, 122.6, 122.2, 121.7 (d, *J* = 2.2 Hz), 103.2, 57.3 (d, *J* = 23.2 Hz), 55.7, 47.6, 23.7, 22.9, 21.6 (2C).

^{31}P NMR (162 MHz, $CDCl_3$) δ_P: 150.7 (s).

IR υ_{max} (film): 2970, 1588, 1231, 947.

(**HRMS** cannot be obtained by ESI, EI, CI and APCI ionisation methods.)

M.P. = 154 - 158 °C and 164 - 166 °C.

$[\boldsymbol{\alpha}]_{589}^{25}$ = –65.4 (*c* 0.43, $CHCl_3$).

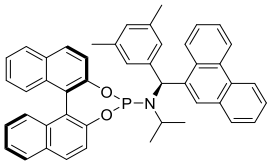

(*R*$_a$,*S*)-*N*-(3,5-dimethylphenyl)(phenanthren-9-yl)methyl)-*N*-isopropyldinaphtho[2,1-*d*:1',2'-*f*][1,3,2]dioxaphosphepin-4-amine **L48S**

General procedure C: $PCl_{3(l)}$ (131 µl, 1.50 mmol, 1.1 eq.) in DCM (2.8 ml), $Et_3N_{(l)}$ (0.95 ml, 6.79 mmol, 5.0 eq.), (+)-(*S*)-*N*-((3,5-dimethylphenyl)(phenanthren-9-yl)methyl)propan-2-amine (480 mg, 1.36 mmol, 1.0 eq.) in DCM (4.0 ml), *(R)*-$BINOL_{(s)}$ (507 mg, 1.77 mmol, 1.3 eq.) The crude mixture was purified by flash

column chromatography [SiO_2, petrol/DCM/Et_3N, 80:20:1] to afford a white solid of (R_a,*S*)-*N*-(3,5-dimethylphenyl)(phenanthren-9-yl)methyl)-*N*-isopropyldinaphtho[2,1-*d*:1',2'-*f*][1,3,2]dioxaphosphepin-4-amine (779 mg, 86%). See the published supporting information for crystallographic data.[120]

^{1}H NMR (400 MHz, $CDCl_3$) δ_H: 8.89 – 8.77 (m, 2H, 2$C_{Ar}H$), 8.46 (s, 1H, $C_{Ar}H$), 8.24 – 8.15 (m, 1H, $C_{Ar}H$), 8.11 – 7.93 (m, 5H, 5$C_{Ar}H$), 7.84 – 7.66 (m, 4H, 4$C_{Ar}H$), 7.66 – 7.41 (m, 5H, 5$C_{Ar}H$), 7.41 – 7.23 (m, 3H, 3$C_{Ar}H$), 7.10 (s, 2H, 2$C_{Ar}H$), 6.95 (s, 1H, $C_{Ar}H$), 6.45 (d, *J* = 16.5 Hz, 1H, ArC*H*), 3.95 – 3.83 (m, 1H, C*H*CH_3), 2.34 (s, 6H, Ar(CH_3)$_2$), 1.43 (d, *J* = 6.6 Hz, 3H, CHCH_3), 0.80 (d, *J* = 6.6 Hz, 3H, CHCH_3).

^{13}C NMR (101 MHz, $CDCl_3$) δ_C: 150.6, 150.5, 150.2, 142.4, 142.3, 137.7 (2C), 137.2, 132.9 (2C), 131.6, 131.4, 130.8, 130.6, 130.4, 130.4, 129.5, 129.2, 129.2, 128.4, 128.3, 127.8 (d, *J* = 2.7 Hz), 127.7, 127.3, 127.1, 126.9, 126.9, 126.8, 126.3, 126.1, 126.0, 124.8, 124.6, 124.5, 124.2 (d, *J* = 5.5 Hz), 123.3, 122.6, 122.5, 122.3, 121.8 (d, *J* = 2.3 Hz), 57.3 (d, *J* = 28.0 Hz), 46.6 (d, *J* = 4.5 Hz), 23.3, 22.8, 21.6 (2C).

^{31}P NMR {^{1}H} (162 MHz, $CDCl_3$) δ_P: 149.7 (s).

IR υ_{max} (film): 3054, 2971, 1951, 1591, 1231, 948.

(**HRMS** cannot be obtained by ESI, EI, CI and APCI ionisation methods. The structure was confirmed by X-ray crystallography.)

M.P. = 176 - 177 °C.

$[\boldsymbol{\alpha}]_{589}^{25}$ = +86.4 (*c* 1.00, $CHCl_3$).

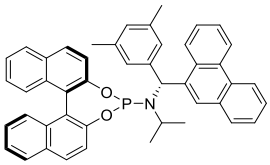

(*R*$_a$,*R*)-*N*-(3,5-dimethylphenyl)(phenanthren-9-yl)methyl)-*N*-isopropyldinaphtho[2,1-*d*:1',2'-*f*][1,3,2]dioxaphosphepin-4-amine **L48R**

General procedure C: $PCl_{3(l)}$ (131 µl, 1.50 mmol, 1.1 eq.) in DCM (2.8 ml), $Et_3N_{(l)}$ (0.95 ml, 6.79 mmol, 5.0 eq.), (–)-(*R*)-*N*-((3,5-dimethylphenyl)(phenanthren-9-yl)methyl)propan-2-amine (480 mg, 1.36 mmol, 1.0 eq.) in DCM (4.0 ml), *(R)*-$BINOL_{(s)}$ (507 mg, 1.77 mmol, 1.3 eq.) The crude mixture was purified by flash column chromatography [SiO_2, petrol/DCM/Et_3N, 80:20:1] to afford a white solid of (*R*$_a$,*R*)-*N*-(3,5-dimethylphenyl)(phenanthren-9-yl)methyl)-*N*-isopropyldinaphtho[2,1-*d*:1',2'-*f*][1,3,2]dioxaphosphepin-4-amine (832 mg, 92%).

^{1}H NMR (400 MHz, $CDCl_3$) δ_H: 8.71 – 8.63 (m, 2H, 2$C_{Ar}H$), 8.56 (s, 1H, $C_{Ar}H$), 8.11 – 8.02 (m, 1H, $C_{Ar}H$), 7.85 – 7.74 (m, 2H, 2$C_{Ar}H$), 7.67 – 7.54 (m, 3H, 3$C_{Ar}H$), 7.47 (t, *J* = 7.7 Hz, 2H, 2$C_{Ar}H$), 7.34 – 7.05 (m, 10H, 10$C_{Ar}H$), 6.80 (s, 2H, 2$C_{Ar}H$), 6.76 (s, 1H, $C_{Ar}H$), 6.21 (d, *J* = 14.1 Hz, 1H, ArC*H*), 3.56 (h, *J* = 6.5 Hz, 1H, C*H*CH_3), 2.12 (s, 6H, Ar(CH_3)$_2$), 1.07 (d, *J* = 6.3 Hz, 3H, CHCH_3), 0.87 (s, br, 3H, CHCH_3).

^{13}C NMR (101 MHz, $CDCl_3$) δ_C: 150.5, 150.0, 141.9, 137.9, 137.7 (2C), 132.9, 132.7, 131.8, 131.4, 130.8, 130.5, 130.4 (2C), 130.3, 129.4, 129.1, 129.1, 128.4, 128.3, 127.7, 127.7, 127.2 (2C), 127.1, 127.0, 126.8, 126.8, 126.3, 126.0, 125.9, 124.8, 124.5, 124.3, 124.2 (d, *J* = 5.0 Hz), 123.2, 122.7, 122.6, 122.0, 121.8, 57.9 (d, *J* = 22.2 Hz), 47.7, 23,7, 23,1, 21.6 (2C).

^{31}P NMR (162 MHz, $CDCl_3$) δ_P: 150.1 (d, *J* = 148.6 Hz).

IR υ_{max} (film): 3058, 2970, 2930, 1591, 1231, 947.

(**HRMS** could not be obtained by ESI, EI, CI and APCI ionisation methods.)

M.P. = 177 - 179 °C.

$[\boldsymbol{\alpha}]_{589}^{25}$ = –132 (*c* 1.00, $CHCl_3$).

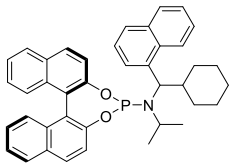

(*R_a*,*R or S*)-*N*-(cyclohexyl(naphthalen-1-yl)methyl)-*N*-isopropyldinaphtho[2,1-*d*:1',2'-*f*][1,3,2]dioxaphosphepin-4-amine **L49a**

General procedure C: $PCl_{3(l)}$ (204 µl, 2.34 mmol, 1.1 eq.) in DCM (3.0 ml), $Et_3N_{(l)}$ (1.48 ml, 10.65 mmol, 5.0 eq.), (–)-*N*-(cyclohexyl(naphthalen-1-yl)methyl)propan-2-amine (599 mg, 2.13 mmol, 1.0 eq.) in DCM (7.0 ml), *(R)*-$BINOL_{(s)}$ (793 mg, 2.77 mmol, 1.3 eq.) The crude mixture was purified by flash column chromatography [Basic Al_2O_3, petrol/DCM, 4:1] to afford a white solid of ((*R_a*,*R or S*)-*N*-(cyclohexyl(naphthalen-1-yl)methyl)-*N*-isopropyldinaphtho[2,1-*d*:1',2'-*f*][1,3,2]dioxaphosphepin-4-amine (1.09 g, 86%).

^{1}H NMR (400 MHz, $CDCl_3$) δ_H: 8.24 – 8.16 (m, 2H, 2$C_{Ar}H$), 8.07 (d, *J* = 8.7 Hz, 1H, $C_{Ar}H$), 8.01 – 7.88 (m, 4H, 4$C_{Ar}H$), 7.84 (d, *J* = 8.0 Hz, 1H, $C_{Ar}H$), 7.76 – 7.62 (m, 2H, 2$C_{Ar}H$), 7.62 – 7.35 (m, 7H, 7$C_{Ar}H$), 7.33 – 7.23 (m, 2H, 2$C_{Ar}H$), 4.99 – 4.87 (m, 1H, ArCH), 3.63 – 3.48 (m, 1H, $CHCH_3$), 3.05 – 2.98 (m, 1H, CH_aH_b), 2.49 – 2.41 (m, 1H, ArCHCH), 2.01 – 1.94 (m, 1H, CH_aH_b), 1.70 (d, *J* = 11.9 Hz, 1H, CH_aH_b), 1.55 – 1.48 (m, 1H, CH_aH_b), 1.40 – 1.14 (m, 6H, CH_2, CH_aH_b, CH_3), 1.12 – 0.86 (m, 3H, CH_2, CH_aH_b), 0.32 (d, *J* = 6.7 Hz, 3H, CH_3).

^{13}C NMR (101 MHz, $CDCl_3$) δ_C: 150.9 (d, *J* = 8.4 Hz), 150.3, 142.9, 133.7, 133.0, 132.9, 131.9, 131.5, 130.6, 130.5, 129.6, 129.3, 128.4, 128.3, 127.4, 127.3 (2C), 127.2, 126.1, 126.0 (3C), 125.3, 124.3 (d, *J* = 5.5 Hz), 124.3, 124.2, 123.1, 122.6, 122.5, 121.6, 57.6 (d, *J* = 19.5 Hz), 46.4 (d, *J* = 4.7 Hz), 45.0 (d, *J* = 25.4 Hz), 32.0, 31.5, 26.7 (2C), 26.6, 22.9, 21.5.

^{31}P NMR (162 MHz, $CDCl_3$) δ_P: 147.3 (s).

IR υ_{max} (film): 3056, 2923, 2850, 1592, 1232, 947.

HRMS (CI^+) $[C_{40}H_{39}NO_2P]^+$ predicted 596.2713, found 596.2723 (Δ –1.69 ppm).

M.P. = 165 - 167 °C.

$[\boldsymbol{\alpha}]_{589}^{25}$ = –95.2 (*c* 1.00, $CHCl_3$).

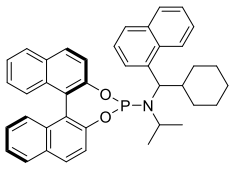

(*R_a*,*R or S*)-*N*-(cyclohexyl(naphthalen-1-yl)methyl)-*N*-isopropyldinaphtho[2,1-*d*:1',2'-*f*][1,3,2]dioxaphosphepin-4-amine **L49b**

General procedure C: $PCl_{3(l)}$ (204 µl, 2.34 mmol, 1.1 eq.) in DCM (3.0 ml), $Et_3N_{(l)}$ (1.48 ml, 10.65 mmol, 5.0 eq.), (+)-*N*-(cyclohexyl(naphthalen-1-yl)methyl)propan-2-amine (594 mg, 2.11 mmol, 1.0 eq.) in DCM (7.0 ml), *(R)*-$BINOL_{(s)}$ (793 mg, 2.77 mmol, 1.3 eq.) The crude mixture was purified by flash column chromatography [basic Al_2O_3, petrol/DCM, 4:1] to afford a white solid of ((*R_a*,*R or S*)-*N*-(cyclohexyl(naphthalen-1-yl)methyl)-*N*-isopropyldinaphtho[2,1-*d*:1',2'-*f*][1,3,2]dioxaphosphepin-4-amine (1.21 g, 96%).

^{1}H NMR (400 MHz, $CDCl_3$) δ_H: 8.27 (dd, *J* = 7.4, 3.7 Hz, 1H, $C_{Ar}H$), 8.20 (d, *J* = 8.5 Hz, 1H, $C_{Ar}H$), 8.05 (d, *J* = 8.7 Hz, 1H, $C_{Ar}H$), 8.01 – 7.90 (m, 2H, $2C_{Ar}H$), 7.91 – 7.81 (m, 2H, $2C_{Ar}H$), 7.76 – 7.67 (m, 2H, $2C_{Ar}H$), 7.65 – 7.52 (m, 3H, $3C_{Ar}H$), 7.55 – 7.43 (m, 2H, $2C_{Ar}H$), 7.47 – 7.35 (m, 2H, $2C_{Ar}H$), 7.33 – 7.23 (m, 2H, $2C_{Ar}H$), 7.11 (d, *J* = 8.8 Hz, 1H, $C_{Ar}H$), 4.82 (dd, *J* = 16.3, 10.9 Hz, 1H, ArC*H*), 3.52 – 3.39 (m, 1H, C*H*CH_3), 2.74 (d, *J* = 13.0 Hz, 1H, CH_aH_b), 2.50 – 2.35 (m, 1H, ArCHC*H*), 2.06 – 1.96 (m, 1H, CH_aH_b), 1.78 – 1.68 (m, 1H, CH_aH_b), 1.56 – 1.33 (m, 2H, CH_2), 1.34 – 1.15 (m, 2H, CH_aH_b, CH_aH_b), 1.13 – 0.85 (m, 6H, CH_aH_b, CH_2, CH_3), 0.41 (d, *J* = 6.8 Hz, 3H, CH_3).

^{13}C NMR (101 MHz, $CDCl_3$) δ_C: 150.7 (d, *J* = 6.4 Hz), 150.2, 142.6, 133.6, 133.0, 132.7, 131.8, 131.5, 130.6, 130.4, 129.5, 129.3, 128.4, 128.3, 127.3, 127.2, 127.2, 126.1, 126.0, 125.9, 125.9, 125.5 (d, *J* = 12.7 Hz), 125.2, 124.8, 124.4, 124.3 (d, *J* = 5.0 Hz),123.4, 122.6, 122.4, 121.9, 58.2 (d, *J* = 18.6 Hz), 46.2, 44.4 (d, *J* = 27.1 Hz), 31.9 (d, *J* = 4.8 Hz), 31.5, 26.7, 26.6, 26.5, 22.2, 21.7.

^{31}P NMR (162 MHz, $CDCl_3$) δ_P: 149.3 (s).

IR υ_{max} (film): 3057, 2930, 1591, 1232, 948.

HRMS (CI^+) $[C_{40}H_{39}NO_2P]^+$ predicted 596.2713, found 596.2728 (Δ –2.53 ppm).

M.P. = 168 - 170 °C.

$[\alpha]_{589}^{25}$ = –178 (*c* 1.00, $CHCl_3$).

3.6 Computational experimental section

3.6.1 Quantitative structure – selectivity relationship (QSSR)

Quantitative relationship between the experimentally observed enantioselectivities of ACA and the chemical descriptors of the corresponding ligands were analysed in

R-statistics package in the form of multiple linear least squares regression.[62] Initially for **Model I** (first generation ligands, n = 11, **Figure 3-7**), 28 chemical descriptors were computed based on optimised ligand structures or only aryl rings capped with methyl group. For **Model II** (first and second generation ligands, n = 30, **Figure 3-12**), 12 relevant chemical descriptors based on aryl rings were computed. Each descriptor (x_i) was scaled to dimensionless values (x) using **Equation 1-2**.

Chemical descriptors considered in a selection process were:

HOMO energies of aryl substituents (**HOMO**) were calculated at the B3LYP/6-31G(d) level of theory. The aryl groups were considered in isolation from the rest of the ligand structures and were capped with a methyl group as shown in **Figure 3-15**. For substituents that possess multiple stable conformations, their HOMO energies are reported as an averaged value weighed by their corresponding Boltzmann factors for the two most stable conformations at 298 K.

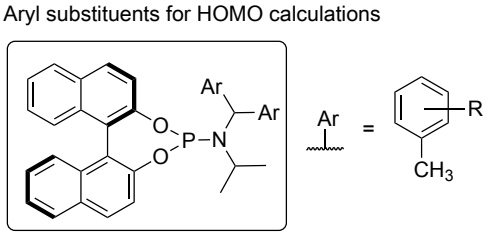

Figure 3-15 Aryl substituents connected to a methyl group instead of the rest of the ligand

The first and second generation Sterimol parameters: L, B_1, B_2, B_3, B_4 and B_5, were derived from *Molecular Modelling Pro Plus 7.0* on the optimised structures of methyl capped aryl rings (B3LYP/6-31g(d)) unless stated otherwise. Exponential term of B_1 is also calculated ($\mathbf{e^{B1}}$). For the diethyl aryl substituent, we used the second most stable conformation (energy higher that the most stable conformation by 0.009 kJ/mol) because this conformation has a much smaller B_1 value.[57]

Dihedral angles for P-N-C-C_{Ar} (**dih**), SCF GIAO magnetic sheilding of P atoms (**NMR**) and Natural charges on P, N, α-C to N, *ipso*-C, *ortho*-C and *para*-C atoms (**P**, **N**, **aC**, **bC1**, **bC2**, **gC1**, and **gC2** respectively), were obtained by Gaussian 09 at B3LYP/6-31G(d,p) from optimised ligand structures (B97D/6-31G(d) with DCM-SMD solvation). Averaged charges of the two *ortho*-Cs and *para*-Cs are represented as **bCav** and **gCav** respectively.

QSAR descriptors were obtained from Spartan'14 on optimised ligand structures (ωB97X-D[179]/6-31G(d)), namely, molecular orbital energy (**MO**), Natural charges (**Nat**), and Mulliken charges (**Mul**) on Phosphorus, accessible area (**AccArea**), polar area (**Pol**), accessible polar area (**AccPol**), maximum and minimum ionisation potential (**MaxIE** and **MinIE**), local ionisation potential (**loc**) and polarisability (**pol**).

Table 3-7 Experimental enantiomeric excess (ΔΔG‡ in kJ/mol) and ligand descriptors (scaled to dimensionless values over 11 ligands) for the first generation ligands.

Lig	dih	NMR	P	N	aC	bC1	bC2	bCav	gC1	gC2	gCav	MO	Nat	Mul	AccArea
L24	-1.458	-0.675	0.359	-2.183	-1.166	1.370	1.161	1.273	1.584	-0.468	0.118	-0.129	-0.277	-1.930	-1.236
L1	0.906	0.467	-0.205	-0.113	0.117	0.040	-0.038	0.002	-0.751	-0.483	-0.662	-2.451	-0.447	0.345	-1.225
L25	0.868	0.193	-0.205	0.301	0.544	-0.403	-0.403	-0.404	-0.650	-0.444	-0.596	-0.132	-0.362	0.453	-0.462
L26	0.851	0.173	0.077	0.301	0.758	0.582	0.744	0.663	-0.776	-0.512	-0.695	0.135	-0.277	0.561	0.165
L27	1.030	0.022	0.359	-0.113	0.972	0.927	0.796	0.866	-0.801	-0.516	-0.707	0.122	-0.277	1.211	2.263
L28	-1.196	-0.609	0.359	-0.113	-1.380	1.124	1.318	1.222	1.496	-0.502	0.060	1.190	-0.277	0.778	0.618
L29	0.837	0.706	-0.205	0.301	0.758	0.040	0.066	0.053	-0.387	-0.497	-0.554	-0.126	-0.447	0.453	1.141
L30	0.911	2.130	-0.205	-0.527	-0.097	0.434	0.275	0.358	-0.475	-0.416	-0.513	Nd	2.942	-0.630	-0.791
L31	-0.844	-0.259	-0.487	-0.113	0.972	-1.487	-1.498	-1.497	-0.512	-0.396	-0.509	1.208	-0.447	0.345	-0.110
L32	-0.840	0.038	-2.180	2.371	-2.021	-1.881	-2.019	-1.955	-0.500	2.237	1.759	0.183	-0.870	0.345	-0.515
L33	-1.065	-2.187	2.334	-0.113	0.544	-0.748	-0.403	-0.582	1.771	1.997	2.299	Nd	0.739	-1.930	0.153

Table 3-8 Experimental enantiomeric excess (ΔΔG‡ in kJ/mol) and ligand descriptors (scaled to dimensionless values over 11 ligands) for the first generation ligands. (Continues)

Lig	Pol Area	Acc Pol Area	MaxIE	MinlE	Loc	Polz	L	B1	e^{B1}	B5	B3	B4	E_{HOMO}	ΔΔG‡
L24	-0.160	-0.068	-0.346	0.189	0.170	-1.162	-0.93	-0.46	-0.38	-1.22	-0.45	-1.22	-0.88	3.15
L1	-0.561	-0.492	-0.579	0.221	0.386	-1.014	-0.93	-0.46	-0.38	-1.22	-0.45	-1.22	-0.88	3.45
L25	-0.390	-0.401	-0.731	0.102	0.329	-0.044	0.35	-0.01	-0.17	-1.21	-0.50	-1.23	-0.20	3.01
L26	-0.334	-0.362	-0.734	0.153	0.322	-0.044	-0.72	-0.46	-0.38	0.11	1.28	0.13	-0.30	5.71

L27	-0.488	-0.860	-0.771	0.469	0.339	2.786	0.47	3.12	3.15	1.23	2.75	1.13	-0.20	1.02
L28	0.132	0.292	-0.683	-0.046	0.381	-0.531	-0.91	-0.46	-0.38	1.14	-0.40	1.22	1.00	5.56
L29	0.107	0.522	-0.175	0.079	0.396	0.351	1.74	-0.46	-0.38	-0.10	-0.35	-0.06	0.94	4.13
L30	-2.076	-1.858	1.553	2.157	-1.609	-0.131	-0.11	-0.27	-0.30	0.54	-0.45	0.59	-2.21	0.18
L31	1.754	1.973	2.068	-0.708	1.449	-0.360	1.90	-0.15	-0.24	-1.21	-0.48	-1.23	1.04	3.15
L32	1.606	1.412	1.096	-0.288	0.177	-0.308	-0.96	-0.36	-0.34	1.13	-0.44	1.21	0.85	4.67
L33	0.409	-0.158	-0.700	-2.327	-2.340	0.458	0.10	-0.03	-0.19	0.83	-0.50	0.65	0.83	4.02

Table 3-9 Experimental enantiomeric excess (ΔΔG‡ in kJ/mol) and ligand descriptors (scaled to dimensionless values over 30 ligands) for the first and second generations ligands.

Lig	ΔΔG‡	R1	R2	R1L	R1B1	R1B5	R1B3	R1B4	R2L	R2B1	R2B5	R2B3	R2B4
L24	3.15	-0.62396	-0.60743	-0.67	-0.42	-1.7	-0.69	-1.68	-0.71	-0.43	-1.68	-0.69	-1.67
L1	3.45	-0.62396	-0.60743	-0.67	-0.42	-1.7	-0.69	-1.68	-0.71	-0.43	-1.68	-0.69	-1.67
L25	3.01	-0.14635	-0.12569	0.72	0.23	-1.69	-0.73	-1.69	0.67	0.22	-1.67	-0.73	-1.68
L26	5.71	-0.21826	-0.19822	-0.44	-0.42	-0.24	0.92	-0.24	-0.48	-0.43	-0.21	0.92	-0.21
L27	1.02	-0.14188	-0.12118	0.84	4.73	0.98	2.28	0.82	0.80	4.74	1.03	2.28	0.87
L28	5.56	0.70819	0.73625	-0.64	-0.42	0.88	-0.64	0.93	-0.69	-0.43	0.93	-0.64	0.98
L29	4.13	0.66356	0.69123	2.22	-0.42	-0.47	-0.59	-0.44	2.17	-0.43	-0.44	-0.59	-0.41
L30	0.18	-1.57372	-1.56541	0.22	-0.15	0.22	-0.69	0.25	0.18	-0.16	0.27	-0.69	0.29
L31	3.15	0.73646	0.76476	2.39	0.02	-1.69	-0.71	-1.69	2.35	0.01	-1.67	-0.71	-1.68
L32	4.67	0.60354	0.6307	-0.70	-0.28	0.87	-0.68	0.91	-0.74	-0.29	0.92	-0.68	0.97
L33	4.02	0.58811	0.61513	0.45	0.19	0.55	-0.73	0.32	0.41	0.18	0.59	-0.73	0.36
L40a	3.29	-0.62396	-0.19822	-0.67	-0.42	-1.70	-0.69	-1.68	-0.48	-0.43	-0.21	0.92	-0.21
L40b	4.75	-0.21826	-0.60743	-0.44	-0.42	-0.24	0.92	-0.24	-0.71	-0.43	-1.68	-0.69	-1.67
L41a	3.94	-0.62396	0.73625	-0.67	-0.42	-1.70	-0.69	-1.68	-0.69	-0.43	0.93	-0.64	0.98
L41b	4.22	0.70819	-0.60743	-0.64	-0.42	0.88	-0.64	0.93	-0.71	-0.43	-1.68	-0.69	-1.67
L42S	4.99	-0.21826	0.73625	-0.44	-0.42	-0.24	0.92	-0.24	-0.69	-0.43	0.93	-0.64	0.98
L42R	5.39	0.70819	-0.19822	-0.64	-0.42	0.88	-0.64	0.93	-0.48	-0.43	-0.21	0.92	-0.21
L43R	5.54	0.70819	0.07842	-0.64	-0.42	0.88	-0.64	0.93	0.67	-0.09	-0.22	-0.65	-0.20
L44S*	5.54	-0.24579	0.73625	-0.70	-0.15	0.61	1.76	0.43	-0.69	-0.43	0.93	-0.64	0.98
L44R*	6.05	0.70819	-0.22599	-0.64	-0.42	0.88	-0.64	0.93	-0.74	-0.16	0.65	1.76	0.48
L45a	4.86	0.9036	0.73625	0.42	0.57	0.78	1.26	0.82	-0.69	-0.43	0.93	-0.64	0.98
L45b	4.03	0.70819	0.93335	-0.64	-0.42	0.88	-0.64	0.93	0.38	0.56	0.82	1.26	0.87
L46S	2.3	-2.43421	0.73625	0.21	1.79	0.25	1.47	0.14	-0.69	-0.43	0.93	-0.64	0.98
L46R	4.63	0.70819	-2.43335	-0.64	-0.42	0.88	-0.64	0.93	0.16	1.78	0.29	1.47	0.18
L47a	5.25	-0.21826	1.48062	-0.44	-0.42	-0.24	0.92	-0.24	2.32	0.25	0.93	-0.63	0.97
L47b	6.45	1.44618	-0.19822	2.37	0.26	0.88	-0.63	0.91	-0.48	-0.43	-0.21	0.92	-0.21
L48S	6.83	-0.21826	0.79178	-0.44	-0.42	-0.24	0.92	-0.24	2.12	-0.43	0.93	2.14	0.98
L48R	6.68	0.76324	-0.19822	2.16	-0.42	0.88	2.14	0.93	-0.48	-0.43	-0.21	0.92	-0.21
L49a	1.56	0.70819	-3.24726	-0.64	-0.42	0.88	-0.64	0.93	-0.66	0.69	-1.16	-0.88	-1.14
L49b	0.87	-3.24114	0.73625	-0.61	0.70	-1.18	-0.88	-1.16	-0.69	-0.43	0.93	-0.64	0.98

3.6.2 Construction of regression models

Next is to select parameters to be included in a model using data from **Table 3-7** and **Table 3-8**. This was done using an automated stepwise forward regression incorporated in *R* to obtain a starting model (**Model I-0**). The parameters were excluded from this model until the resultant correlation has a good fit ($R^2 \approx 1$) with least parameter used (**Model I-1 = Model I** showed in **Figure 1**, manuscript). Further exclusion of parameters (**Model I-2** and **Model I-3**) resulted in reduction in R^2 to 0.86 and 0.76 respectively. Leave-one-out cross validation (LOOCV) was carried out for **Model I** giving the cross-validated correlation coefficient (q^2) of 0.87, higher than recommended value of 0.5.[63] Models with cross-terms were also explored but the resultant models contain parameters which are not statistically significant, therefore those models were discarded.

3.6.2.1 Stepwise forward regression:

```
null=lm(ddG~1)
full=lm(ddG ~ dih + NMR + P + N + aC + bC1 + bC2 + bCav + gC1 + gC2 + gCav + MO + Nat +
Mul    + AccArea + MinlE + Loc + PolArea + AccPolArea + MaxIE + Polz + L + B1 + eB1 +
B5 + B3 + B4 + R1)

step(null, scope=list(lower=null, upper=full), direction="forward")

Step:  AIC=-Inf
Model I-0: ddG ~ R1 + L + B1 + B3 + gC2 + MaxEI + eB1 + bC2 + P + dih
```

3.6.2.2 Multiple Linear least squared regression (Model I-1):

```
Model I-1 <- lm(ddG ~ R1 + L + B1 + B3)
```

Coefficients:	Estimate	Std. Error	t value	Pr(>|t|)	
(Intercept)	3.3908	0.1599	21.205	7.17E-07	***
R1	1.2206	0.1724	7.078	0.0004	***
L	-0.5441	0.1822	-2.986	0.0244	*
B1	-1.72	0.3043	-5.652	0.0013	**
B3	1.3033	0.2969	4.39	0.0046	**

```
---
```

```
Signif. codes:  0 ‘***’ 0.001 ‘**’ 0.01 ‘*’ 0.05 ‘.’ 0.1 ‘ ’ 1

Residual standard error: 0.5303 on 6 degrees of freedom
Multiple R-squared:  0.942,  Adjusted R-squared:  0.9033
F-statistic: 24.34 on 4 and 6 DF,  p-value: 0.0007484
```

3.6.2.3 Multiple Linear least squared regression (Model I-2):

```
Model I-2 <- lm(ddG ~ R1 + B1 + B3)

Coefficients:  Estimate     Std. Error   t value      Pr(>|t|)
(Intercept)    3.3908       0.2334       14.526       1.75E-06     ***
R1             1.036        0.235        4.408        0.0031       **
B1             -2.0283      0.4179       -4.854       0.0019       **
B3             1.5267       0.4194       3.64         0.0083       **
---
Signif. codes:  0 ‘***’ 0.001 ‘**’ 0.01 ‘*’ 0.05 ‘.’ 0.1 ‘ ’ 1

Residual standard error: 0.7742 on 7 degrees of freedom
Multiple R-squared:  0.8557, Adjusted R-squared:  0.7938
F-statistic: 13.83 on 3 and 7 DF, p-value: 0.002505
```

3.6.2.4 Multiple Linear least squared regression (Model I-3):

```
Model I-3 <- lm(ddG ~ R1 + L + B1)

                            Std.
Coefficients:     Estimate     Error        t value      Pr(>|t|)
(Intercept)    3.3908       0.3038       11.16        1.03E-05     ***
R1             1.2153       0.3276       3.709        0.00756      **
L              -0.7456      0.335        -2.226       0.06136      .
B1             -0.5974      0.3135       -1.906       0.09838      .
---
Signif. codes:  0 ‘***’ 0.001 ‘**’ 0.01 ‘*’ 0.05 ‘.’ 0.1 ‘ ’ 1

Residual standard error: 1.008 on 7 degrees of freedom
Multiple R-squared:  0.7555, Adjusted R-squared:  0.6507
F-statistic:  7.21 on 3 and 7 DF,  p-value: 0.01514
```

Selection of parameters for the combined training ligands (n = 30) was carried out in the same way using data from **Table 3-9**. The starting model (**Model II-0**) was derived by forward selection. Based on this, three models with good fit are listed: **Model II-1** with R^2 = 0.85, **Model II-2** with R^2 = 0.83 and **Model II-3** with R^2 = 0.75. The fit of **Model II-2** only slightly increased compared to **Model II-1** (**Model II-2** has one parameter more). To help selecting the best model, Leave-one-out cross

validation (LOOCV) was carried out giving the cross-validated correlation coefficient (q^2) of 0.71, 0.66 and 0.65 for **Model II-1, II-2** and **II-3** respectively. Balancing the fit with the number of parameters used, q^2 and its significance (see later under 'Analysis of variance'), we selected model **Model II-2** as the best model (shown as **Model II** in **Figure 3**, manuscript). Once again non-linear models containing cross-terms were discarded on the ground of statistical significance.

3.6.2.5 Stepwise forward regression:

```
null=lm(ddG~1)
full=lm(ddG ~ R1 + R2 + R1L + R1B1+ R1B5 + R1B3 + R1B4 + R2L + R2B1 + R2B5 + R2B3 +
R2B4)
step(null, scope=list(lower=null, upper=full), direction="forward")

Step:  AIC=-13.14
ddG ~ R1 + R2B1 + R2B3 + R1B3 + R1L + R2 + R1B1
```

3.6.2.6 Multiple Linear least squared regression (Model II-1):

Model II-1 <- lm(ddG ~ R1 + R2B3 + R1B3 + R2 + R1B1 +R2L)

Coefficients:	**Estimate**	**Std. Error**	**t value**	**Pr(>|t|)**	
(Intercept)	4.1723	0.1365	30.576	< 2e-16	***
R1	0.7929	0.1509	5.253	2.50E-05	***
R2B3	0.5499	0.1525	3.607	0.001485	**
R1B3	0.6147	0.1605	3.829	0.000859	***
R2	0.6952	0.1509	4.607	0.000124	***
R1B1	-1.0622	0.1641	-6.473	1.32E-06	***
R2L	-0.297	0.1475	-2.013	0.055949	.

```
---
Signif. codes:  0 ‘***’ 0.001 ‘**’ 0.01 ‘*’ 0.05 ‘.’ 0.1 ‘ ’ 1

Residual standard error: 0.7474 on 23 degrees of freedom
Multiple R-squared:  0.8517, Adjusted R-squared:  0.813
F-statistic: 22.01 on 6 and 23 DF,  p-value: 1.852e-08
```

3.6.2.7 Multiple Linear least squared regression (Model II-2):

Model II-2 <- lm(ddG ~ R1 + R2B3 + R1B3 + R2 + R1B1)

Coefficients:	**Estimate**	**Std. Error**	**t value**	**Pr(>|t|)**	
(Intercept)	4.172	0.1449	28.797	< 2e-16	***

R1	0.7404	0.1578	4.691	9.12E-05	***	
R2B3	0.5136	0.1607	3.196	0.003881	**	
R1B3	0.6497	0.1694	3.835	0.000798	***	
R2	0.5946	0.1512	3.933	0.000624	***	
R1B1	-1.095	0.1734	-6.317	1.57E-06	***	

Signif. codes: 0 ‘***’ 0.001 ‘**’ 0.01 ‘*’ 0.05 ‘.’ 0.1 ‘ ’ 1

Residual standard error: 0.7935 on 24 degrees of freedom
Multiple R-squared: 0.8255, Adjusted R-squared: 0.7892
F-statistic: 22.71 on 5 and 24 DF, p-value: 2.214e-08

3.6.2.8 Multiple Linear least squared regression (Model II-3):

Model II-3 <- lm(ddG ~ R1 + R1B3 + R2 + R1B1)
Call:
lm(formula = ddG ~ R1 + R1B3 + R2 + R1B1, data = all)

Coefficients:	**Estimate**	**Std. Error**	**t value**	**Pr(>|t|)**	
(Intercept)	4.172	0.1695	24.617	< 2e-16	***
R1	0.8911	0.1762	5.057	3.22E-05	***
R1B3	0.7411	0.1953	3.794	0.000839	***
R2	0.5307	0.1753	3.027	0.005655	**
R1B1	-0.9566	0.1964	-4.872	5.20E-05	***

Signif. codes: 0 ‘***’ 0.001 ‘**’ 0.01 ‘*’ 0.05 ‘.’ 0.1 ‘ ’ 1

Residual standard error: 0.9283 on 25 degrees of freedom
Multiple R-squared: 0.7513, Adjusted R-squared: 0.7115
F-statistic: 18.88 on 4 and 25 DF, p-value: 2.899e-07

3.6.3 Analysis of variance

Once the models with best fits are identified, the significance of each parameter was tested by analysis of variance (ANOVA) which is an algorithm implemented in *R* statistical package. A parameter is significant at 5% level of confident if its F value is higher than the critical value for the given degree of freedom. For **Model I**, all parameters are significant within 5% level of confidence.

3.6.3.1 Analysis of Variance Table for Model I:

Degree of freedom: 6, Critical value (P = 0.05)= **5.9874**.

	F value	Pr(>F)
R1	72.257	0.0001451 ***
L	48.808	0.0004280 ***

```
B1          25.652    0.0022997 **
B3          25.382    0.0023614 **
---
Signif. codes:  0 ‘***’ 0.001 ‘**’ 0.01 ‘*’ 0.05 ‘.’ 0.1 ‘ ’ 1
```

For **Model II-1**, 4 out of 6 parameters are significant within 5% level of confidence. $\mathbf{L^{R2}}$ and $\mathbf{B_3^{R2}}$ lie in the borderline. For **Model II-2**, 5 out of 6 parameters are significant within 5% level of confidence. Only $\mathbf{B_3^{R2}}$ lies in the borderline. For **Model II-3**, all parameters are significant within 5% level of confidence.

3.6.3.2 Analysis of Variance Table for Model II-1:

```
Degree of freedom: 23, Critical value (P = 0.05)= 4.2793.
       F value    Pr(>F)
R1         53.5720    1.905e-07 ***
R2B3       4.1899      0.0522588 .
R1B3       7.7430     0.0105838 *
R2         17.5405    0.0003523 ***
R1B1       44.9750    7.681e-07 ***
R2L        4.0527     0.0559493 .
---
Signif. codes:  0 ‘***’ 0.001 ‘**’ 0.01 ‘*’ 0.05 ‘.’ 0.1 ‘ ’ 1
```

3.6.3.3 Analysis of Variance Table for Model II-2:

```
Degree of freedom: 24, Critical value (P = 0.05) = 4.2597.
       F value    Pr(>F)
R1         47.5268    3.953e-07 ***
R2B3       3.7171      0.0657724 .
R1B3       6.8693     0.0149777 *
R2         15.5612    0.0006058 ***
R1B1       39.9000    1.572e-06 ***
---
Signif. codes:  0 ‘***’ 0.001 ‘**’ 0.01 ‘*’ 0.05 ‘.’ 0.1 ‘ ’ 1
```

3.6.3.4 Analysis of Variance Table for Model II-3:

```
Degree of freedom: 25, Critical value (P = 0.05) = 4.2417.
       F value    Pr(>F)
R1         34.7293    3.779e-06 ***
R1B3       6.7852     0.015256 *
R2         10.2816    0.003657 **
R1B1       23.7336    5.195e-05 ***
---
Signif. codes:  0 ‘***’ 0.001 ‘**’ 0.01 ‘*’ 0.05 ‘.’ 0.1 ‘ ’ 1
```

3.7 Density functional theory (DFT) calculations

All transition state (TS) calculations were computed by *Gaussian09* programme.[118] The TS geometry optimisations were carried out with B97D functional using 6-31G(d) basis set for C, H, N, O, P, Si atoms and LANL2DZ with effective core potential treatment (ecp) for Cu^{+} ion.[116] Energy corrections were evaluated on the optimised TS structures at B97D/def2-TZVPP level of theory and solvation was taken into account using implicit Solvation Model based on Density (SMD) in DCM. All the transition structures possess a single imaginary harmonic vibrational frequency. The enantiomeric excess was calculated at 273 K. Graphics were generated by Pymol.[180] The non-covalent interaction index (NCI) reflects changes in the curvature of the electron density and was obtained from the promolecular density (molecular density calculated from the sum of atomic density) using NCIPLOT, treating the ligand separately from the rest of the transition state complex.[181] All energetic terms were reported in kJ/mol.

Transition States	ΔΔG‡ (kJ/mol)	Product	Normalised Boltzmann factor (273 K)
(S,S)-**TS1**	0.00	*(-)*-3	0.49
(S,R)-**TS2**	2.2(1)	*(+)*-3	0.19
(S,S)-**TS3**	2.8(8)	*(-)*-3	0.14
(S,S)-**TS4**	2.9(4)	*(-)*-3	0.13
(S,R)-**TS5**	7.0(4)	*(+)*-3	0.02
(S,S)-**TS6**	7.6(4)	*(-)*-3	0.01
(S,R)-**TS7**	10.2(5)	*(+)*-3	0.00
(S,R)-**TS8**	11.8(2)	*(+)*-3	0.00

Table 3-10 Transition states and their relative Gibbs free energies with **L1** (S_a-BINOL).

The total of 8 transition structures at the stereodetermining carbocupration step were calculated. The TSs energies and their corresponding Boltzmann factors are tabulated in **Table 3-10**. The key bond distances (Å) in the two lowest energy TSs; **TS1** (lead to major enantiomer of product) and **TS2** (lead to the minor enantiomer

of product) are shown in red in **Figure 3-16**. The distances (Å) between copper and the *ipso*- and *ortho*-carbon are shown in grey. These diatances show the closer proximity of the copper and one other aryl ring in (*S*,*S*)-**TS**s compared to those in (*S*,*R*)-**TS**s. The averaged Cu-C distance in (*S*,*S*)-**TS1** is 3.00 Å, which is 0.39 Å shorter than (*S*,*R*)-**TS2** (3.39 Å). In all four of the (*S*,*S*)-**TS** structures, the Cu-C distances are closer than the sum of the two van der Waals radii of each element (vdW radii: C 1.70 Å and Cu 1.40 Å).

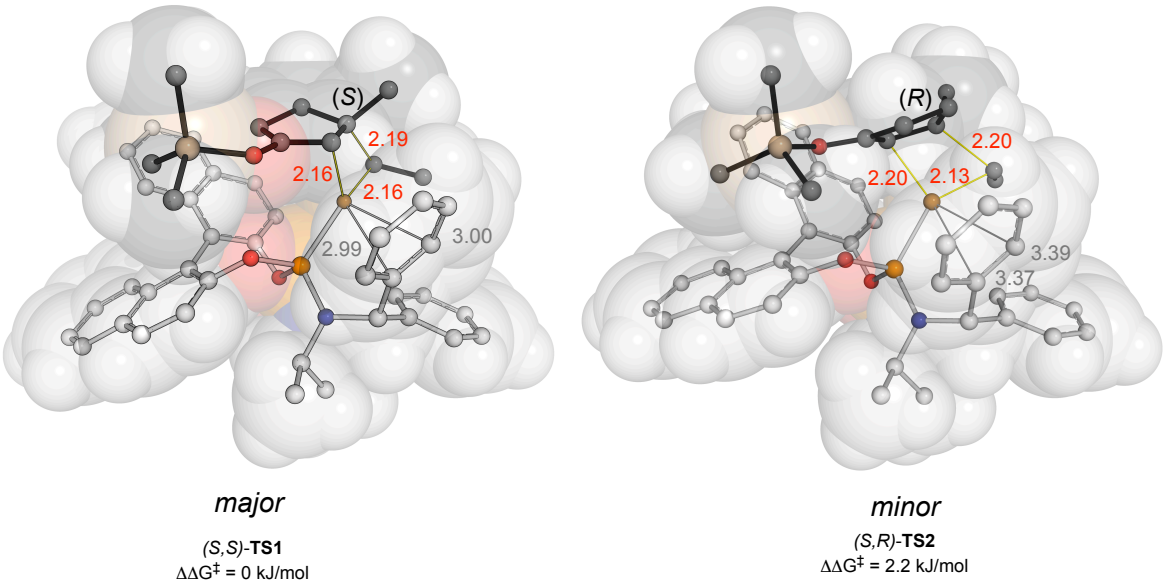

Figure 3-16 Transition structures (*S*,*S*)-**TS1** and (*S*,*R*)-**TS2** and the key distances (Å).

To quantitatively probe the Cu-C interaction, a non-covalent interaction isosurface (NCI plot) of the lowest energy TS (**TS1**) was carried out (**Figure 3-17**). The plot highlights the strongest favourable interaction between Cu and P atom as purple area and the weaker interaction between Cu-C as blue area. We previously reported quantitative analysis of this type of interaction in a related system.[91]

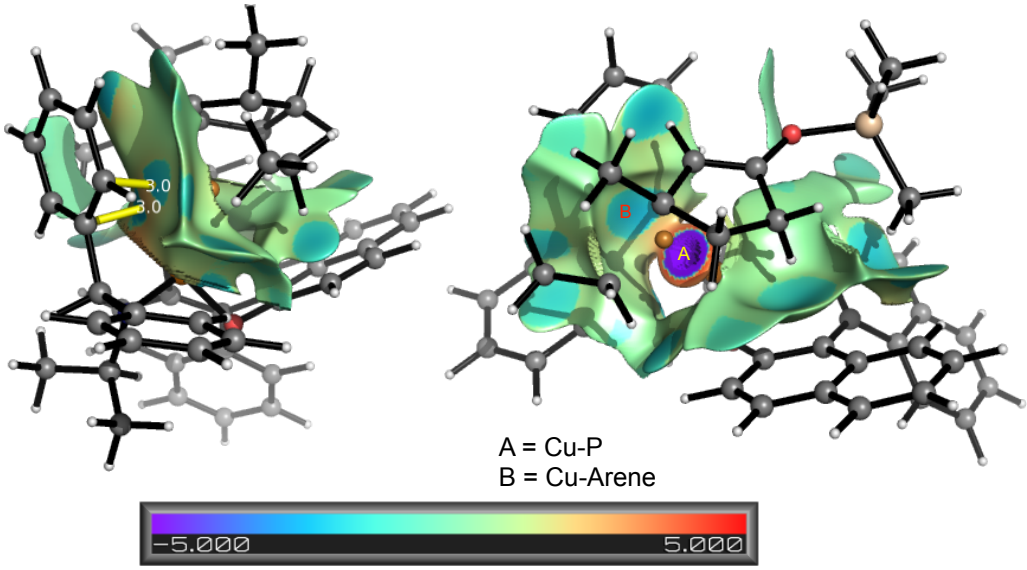

Figure 3-17 NCI index of the lowest energy transition state (*S*,*S*)-**TS1**.

3.7.1 Cartesian Coordinates

All TS coordinates can be found in published material.[120]

4 Hydrogenation of dihydroisoquinoline core towards the synthesis of Almorexant®

4.1 Introduction

Orexin peptides play a crucial role in regulating the sleep-wake cycle in mammals. Abnormal production of orexins was found to be a cause of chronic neurodegenerative diseases such as narcolepsy (involuntary daytime sleepiness) and cataplexy (loss of muscle response to stimuli).[182] Orexins refer to two peptides: Orexin A and Orexin B. They are endogenous agonists of OX1 and OX2 receptors respectively. Almorexant® was identified as an antagonist to both protein receptors and therefore recognised as a potential treatment for sleeping disorders (**Scheme 4-1**). This feature has drawn much attention from multiple pharmaceutical companies in attempts to synthesise Almorexant® at scale.[183] The key step in the synthesis of Almorexant® is an enantioselective reduction of dihydroisoquinoline **1** to afford the chiral amine intermediate **2** (**Scheme 4-1**).

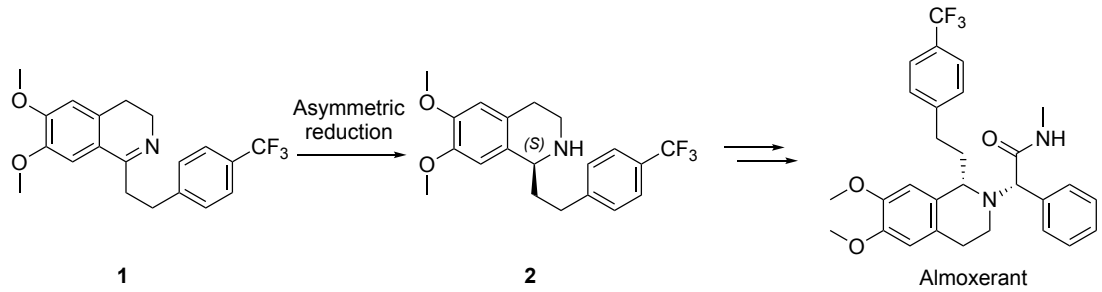

Scheme 4-1. Synthetic route to Almorexant from dihydroisoquinoline **1**.

Chiral amines are important motifs in pharmaceuticals, however the enantiomeric synthesis of chiral amines remains a challenging task.[184] Recent advances in the field of enantioselective reduction strategies allow access to chiral amines. Of particular importance is an enantioselective transition metal catalysed

hydrogenation as demonstrated by the Nobel prize awarded to Noyori in 2001. Noyori's contribution on asymmetric amine reduction is shown in **Scheme 4-2** giving up to 99% yield and 97% ee.[185] Noyori's ligands are available in both *R* and *S* forms which means we can access either enantiomer of the products.

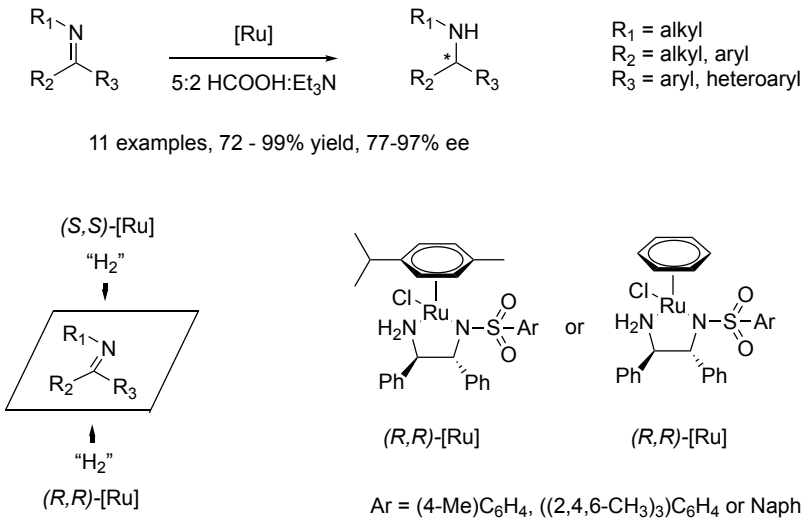

Scheme 4-2 Noyori's asymmetric transfer hydrogenation on imines.[185]

In addition to Noyori's work, asymmetric reduction of dihydroisoquinolines has been achieved with Noyori's based Ru-diamine catalyst (**3**) developed by Xiao,[186] titanocene catalyst **4** developed by Buchwald,[187] Ir-pyrrolidine diphosphene **5**[188] and Ir-BINAP catalyst **6**[189] developed by Morimoto (**Scheme 4-3**). In general, these reduction conditions give high to excellent ee (79-99% ee). Except for catalyst **3**, these catalysts require harsh conditions with H_2 pressure from 33 to 133 atm, with substrate to catalyst ratios (S:C) in a range of 20 – 100.

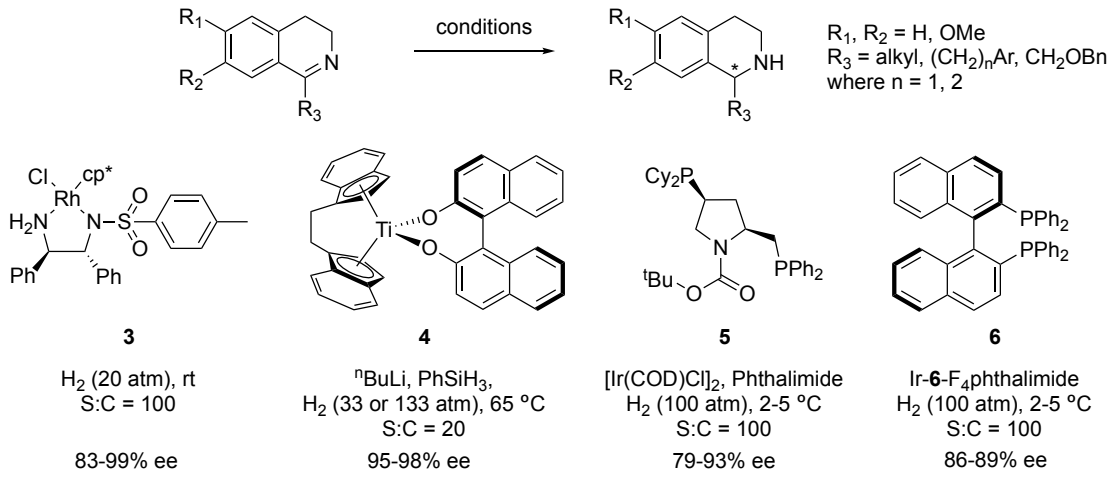

Scheme 4-3 Examples of transition metal catalysed asymmetric hydrogenation of dihydroisoquinoline.[190]

Lefort and coworkers, in a collaboration between Actelion Pharmaceuticals, GlaxoSmithKline and DSM, have explored two methods of homogenous hydrogenation in an attempt to synthesise Almorexant®: asymmetric transfer hydrogenation using Noyori's Ru catalyst **7** (**Scheme 4-4a**) and asymmetric hydrogenation with $[Ir(COD)Cl]_2$ and TaniaPhos (**8**) (**Scheme 4-4b**).[183] Each method has its own merits and drawbacks. Asymmetric hydrogen transfer using Ru catalyst **7** and formic acid as hydrogen source was found to give good yield and ee (95%, 81-95% ee), but failed to reproduce desirable results in a larger scale synthesis. In asymmetric hydrogenation with molecular hydrogen, their optimised reaction conditions with $[Ir(COD)Cl]_2$ and TaniaPhos (**8**) gave high yield and enantioselectivity (>99%, 94% ee). However, the cost of TaniaPhos (**8**) makes its use on a larger scale prohibitive.

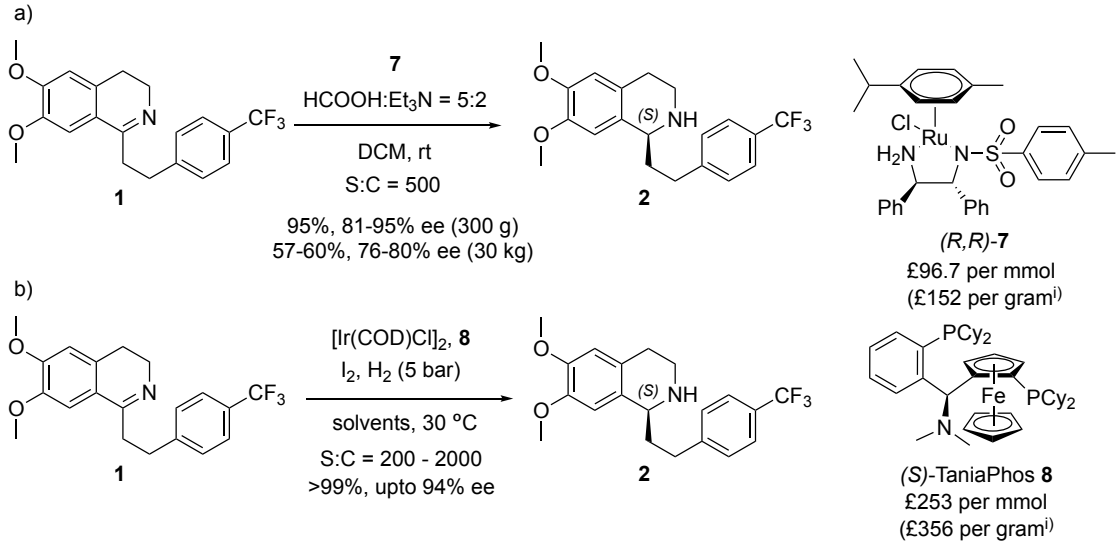

Scheme 4-4 a) Synthesis of **2** by asymmetric transfer hydrogenation using catalyst **7** b) Synthesis of **2** by asymmetric hydrogenation using $[Ir(COD)Cl]_2$ and **8** [i]Price quoted from Merck (Sigma-Aldrich) as of August 2018.

Lefort and coworkers has also illustrated that chirality in asymmetric hydrogenation can be induced with phosphoramidite ligands.[183] The team explored 19 ligands some of which are shown in **Scheme 4-5**. They discovered that Feringa's ligand (**L1**) gave mediocre selectivity (57% ee). Ligands with small substituents on the amido group with 3,3'-disubstituted BINOL gave the highest ee (**L2**-**L6**, upto 79% ee,). None of these were superior to TaniaPhos (**8**).

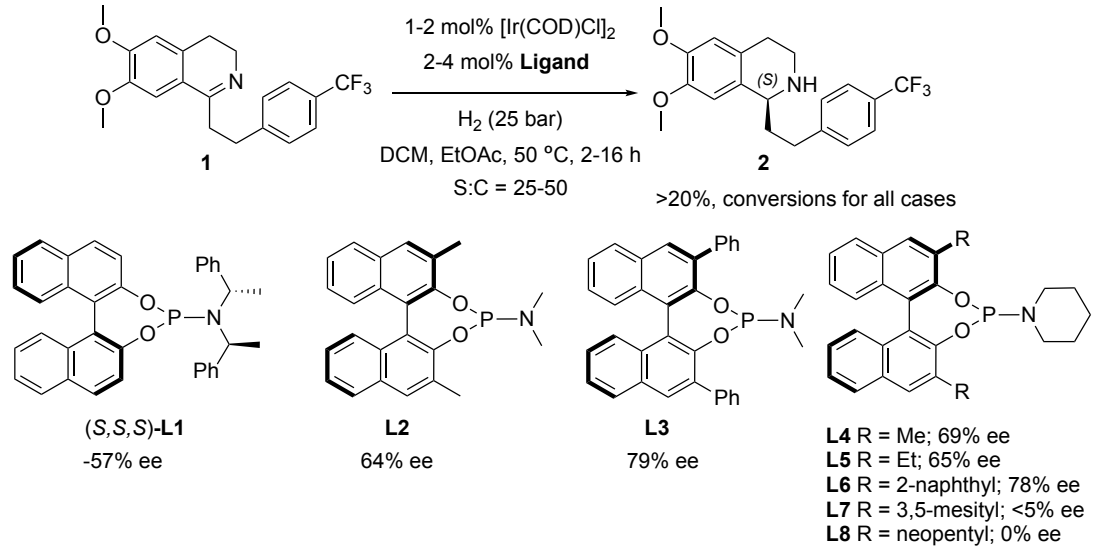

Scheme 4-5 Asymmetric hydrogenation ligand screening results by Lefort and co-workers.[183]

Inspired by these results, we aimed to develop new chiral phosphoramidite ligands that give high yield and ee and are scalable. Compared to other sources of chirality,

the BINOL) backbone is the most attractive as it is relatively cheap (ca. £1 per gram or £0.29 per mmol on 1 kg scale from RCA chiral specialist) and commercially available in both *R* and *S* enantiomers. Our approach is to modify the amido moeity because this strategy is more synthetically tractable than modifying the BINOL backbone. Once again, we have taken a systematic, combinatorial approach to aid the design of the chiral ligands using QSSR models.

4.2 Results and Discussion

4.2.1 Screening Reaction conditions

Reported reaction conditions were modified such that hydrogenations were done at lower pressures (1-6 atm). Reactions were carried out in two steps; preformation of the catalysts followed by hydrogenation. Reactions were repeated to ensure reproducibility (**Table 4-1**). DCM was found to give lower ee than EtOAc when used as reaction solvent (entries 1-n vs entries 2-n, **Table 4-1**). Reactions performed at atmospheric pressure of H_2 with elevated temperature resulted in complex mixtures (entry 2, **Table 4-1**). We found that the quality of the Ir source was crucial for good and consistent enantioselectivity. Using a slightly older batch of $[Ir(COD)Cl]_2$ (orange) resulted in lower conversion and ee than the $[Ir(COD)Cl]_2$ (red) purchased from Strem (entries 4-n, **Table 4-1**). With this new batch of Ir precatalyst, the solvent used in catalyst preformation did not significantly affect the results (entries 5-n, **Table 4-1**). Using conditions as described in entries 4-n, we increased the reaction pressure to 6 bar. This markedly increases the conversion and slightly increases the ee (95%, −84% ee, entry 6-1, **Table 4-1**). From these results, we decided to use conditions described in entries 4 for screening.

Table 4-1 Reaction screening conditions with **L1**

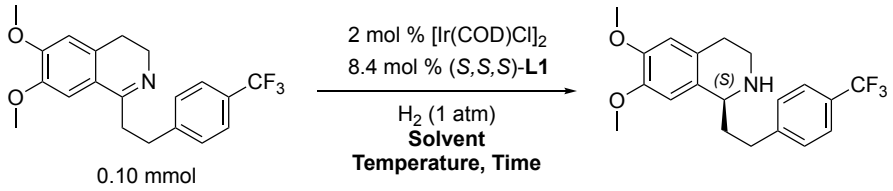

0.10 mmol

1 **2**

Entry	Solvent	Conditions for catalyst preformation	Temperature	Time	Conversion[a]	ee
1-1	DCM	DCM/rt/4h	rt	3.5 days	36%, 64%[b]	−52%
1-2	DCM	DCM/rt/5h	rt	2 days	37%, 61%[b]	−52%
2-1	EtOAc	DCM/rt/4h	50	1 h	9%	Not conclusive
	,,	,,	,,	16 h	33%	Not conclusive
3-1	EtOAc	DCM/rt/4h	rt	16 h	35%	−74%
3-2	EtOAc	DCM/rt/4h	rt	16 h	39%	−72%
3-3	EtOAc	DCM/rt/4h	rt	16 h	20%	−69%
4-1[c]	EtOAc	DCM/rt/1h	rt	16 h	29%	−79%
4-2[c]	EtOAc	DCM/rt/1h	rt	16 h	46%	−81%
5-1[c]	EtOAc	EtOAc/rt/1h	rt	16 h	46 %	−81%
5-2[b]	EtOAc	EtOAc/rt/1h	rt	16 h	40 %	−82%
6-1[c,d]	EtOAc	DCM/rt/1h	rt	16 h	95%	−84%

[a]Conversion based on ^{1}H and ^{19}F NMR of crude reaction mixture, [b]unreacted starting material **1** using $MeNO_2$ as internal standard, [c]$[Ir(COD)Cl]_2$ purchased from Strem [d] H_2 pressure 6 bar.

To examine the metal-ligand complex, we monitored the complexation of $[Ir(COD)Cl]_2$ and **L1** (Ir:**L1** = 1:2) in DCM-d_4 by ^{31}P NMR spectroscopy. We clearly observed that the newly purchased $[Ir(COD)Cl]_2$ from Strem bound to ligand within 1 hr, whereas the homemade, older batch of $[Ir(COD)Cl]_2$ did not fully form the Ir(**L1**)$_2$ complex even after 16 h (**Figure 4-1**). As a result, we decided to use $[Ir(COD)Cl]_2$ purchased from Strem and run the catalyst formation step for 1 hr (stir a solution of $[Ir(COD)Cl]_2$ and the ligands for 1 hr under inert atmosphere) in the subsequent ligand screening.

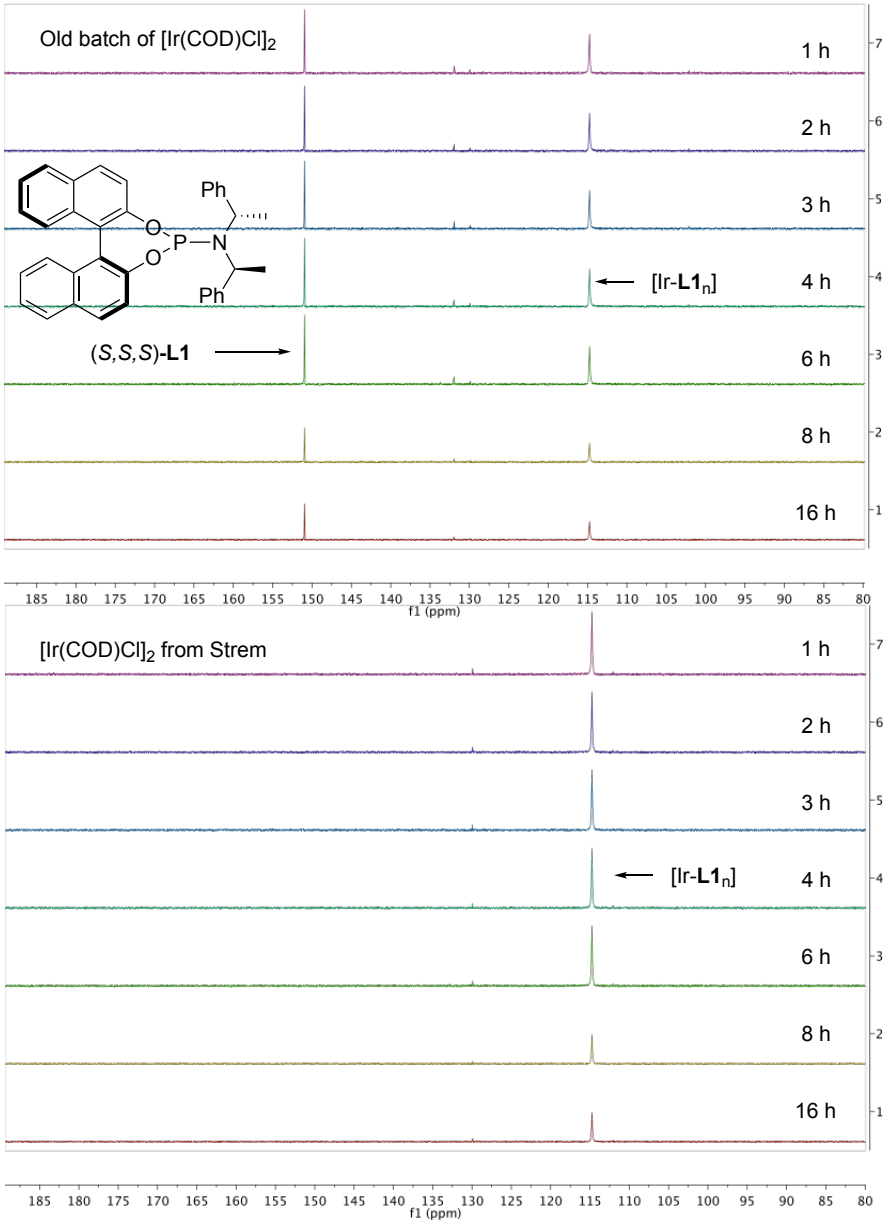

Figure 4-1 ^{31}P NMR of $[Ir(COD)Cl]_2$ and **L1** (1:2) in DCM-d_4 over 16 hr. (n = 1-2)

4.3 Ligand screening

Using the identified reaction conditions, we first screened phosphoramidite ligands bearing Feringa's amine with various backbones (**L9**-**L13**, **Scheme 4-6**). These ligands all gave poor ee's (2 -20% ee, **L9**-**L13**). Comparing the same backbone, if the substituents on amido group are larger, the enantioselectivity dropped almost completely (**L3** vs **L9**).

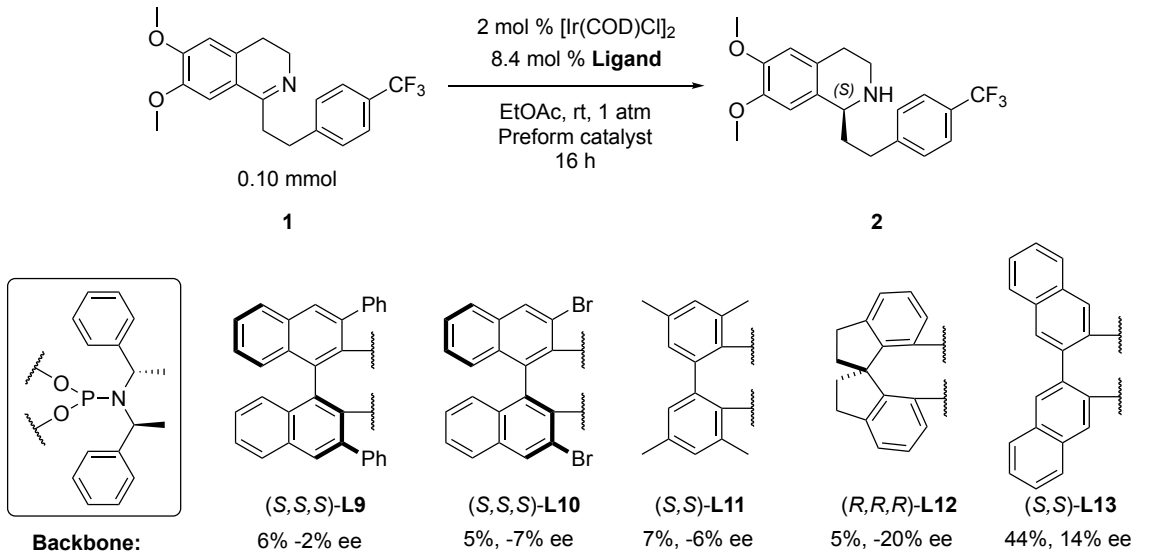

Scheme 4-6 Screening conditions and results with different backbone of the ligands. Conversions based on ^{1}H NMR spectroscopy of the crude reaction mixture. Ee's were determined by HPLC using a non-racemic stationary phase.

We then modified the amido part of the ligands and maintained the unsubstituted BINOL as a backbone (**L1**, **L14**-**L19**, **Figure 4-2**). Every result is reported as an average of two repeats (n = 2) unless specified otherwise. The average standard deviation of measured ee is 2% (0.14 kJ/mol). The yields are based on ^{1}H and ^{19}F NMR spectrum of the crude reaction mixture. The ee's were obtained by chiral supercritical fluid chromatography (SFC) analysis of the crude reaction mixture.

In our screening conditions, Feringa's ligand (**L1**) gave the best selectivity (80% ee) whereas the diastereomer of the ligand (mismatched stereochemistry) performed much worse (–52% ee). In every case, the absolute sense of the stereochemistry of the product **2** is determined by the axial chirality of the BINOL backbone where (*R*)-BINOL gives (*S*)-**2** (reported as positive % ee) and *vice versa,* regardless of the chirality of the amido substituents (if any). A slightly modified version of **L1** (Phenyl to 2-Naphthyl) led to a decrease in ee to –52% ee (**L14**). Having only one fluoride substituent on one of the phenyl rings also decreased the ee compared to **L1** (–70%, **L15**).

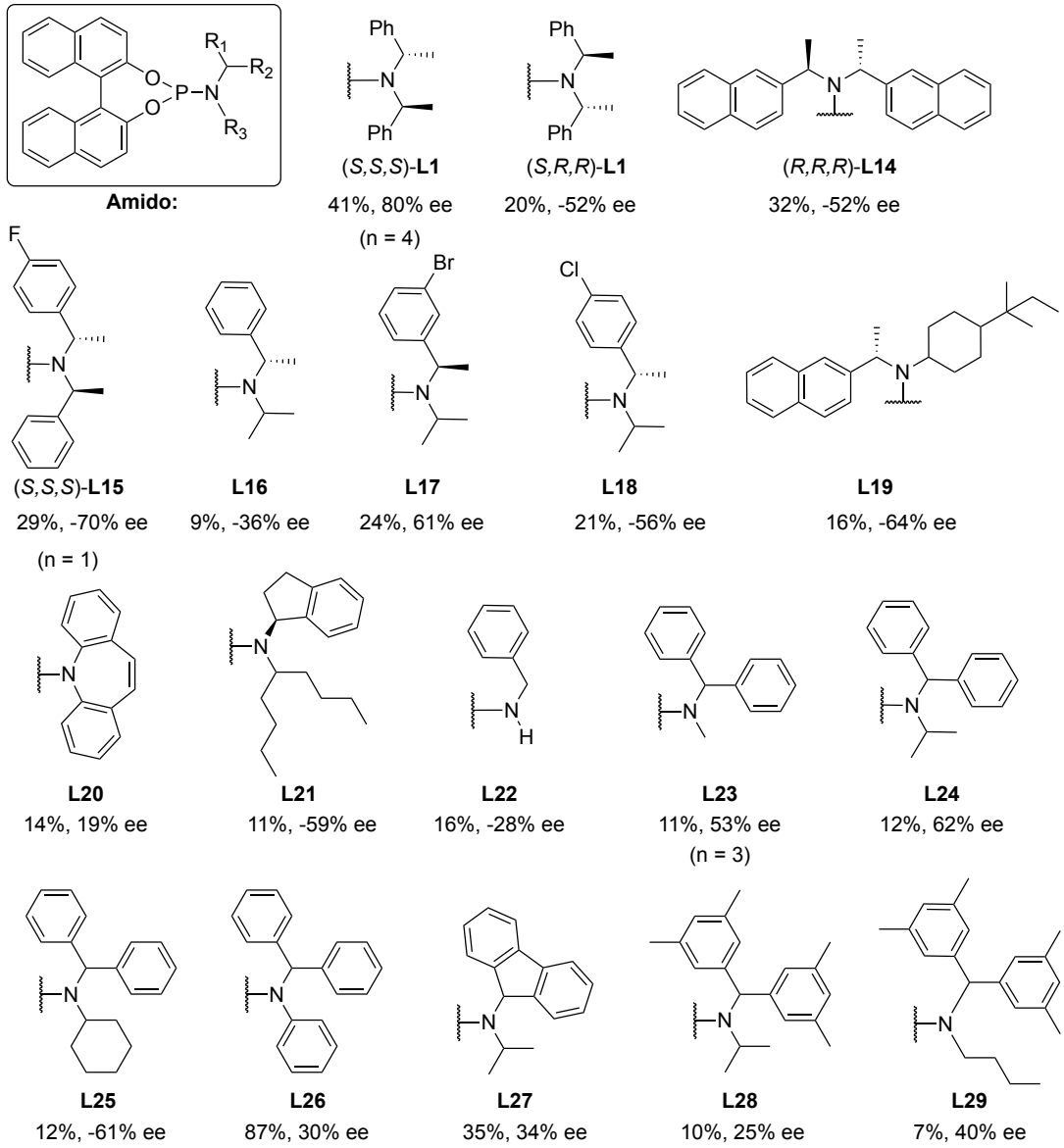

Figure 4-2 Screening results of phosphoramidite ligands with BINOL backbone. Conversions based on ^{1}H NMR spectroscopy of the crude reaction mixture. Ee's were determined by HPLC using a non-racemic stationary phase. Reaction condition used is shown in **Scheme 4-6**.

When we decreased the size of the amido part by switching one substituent to isopropyl, ee also decreases, (–36% ee, **L16**). Halide substitutions on ligands of type **L16** slightly improved the ee (up to 61% ee, **L17** and **L18**). Replacing one of the substituent of **L14** to a conformationally locked substituted cyclohexyl gave slightly better ee (–64% ee, **L19**).

Carreira's ligand (**L20**) gave poor ee of 19%. Another commercially available ligand developed in our group, **L21** gave moderate ee (–59% ee). Benzyl amine

substitution also gave poor ee (–28% ee, **L22**). Having two phenyls on one amido substituent (R_1, R_2 = Ph) and varying only R_3 give mediocre ee when R_3 is a methyl, isopropyl or cyclohexyl (53-62% ee, **L23-L25**). Interestingly, for R_1 = R_2 = R_3 = phenyl (**L26**), the yield increases to 87% but the enantioselectivity was reduced to 30% ee. When the two phenyls are connected i.e. fluorenyl, the yield increases slightly but the ee is reduced compared to **L24** (35%, 34% ee, **L27**). Again, compared to **L24**, dimethyl substituents at meta position (**L28**) gave lower ee but comparable yield (10%, 25% ee). Change from the isopropyl group (**L28**) to a ^{n}butyl increases the ee to 40% (**L29**).

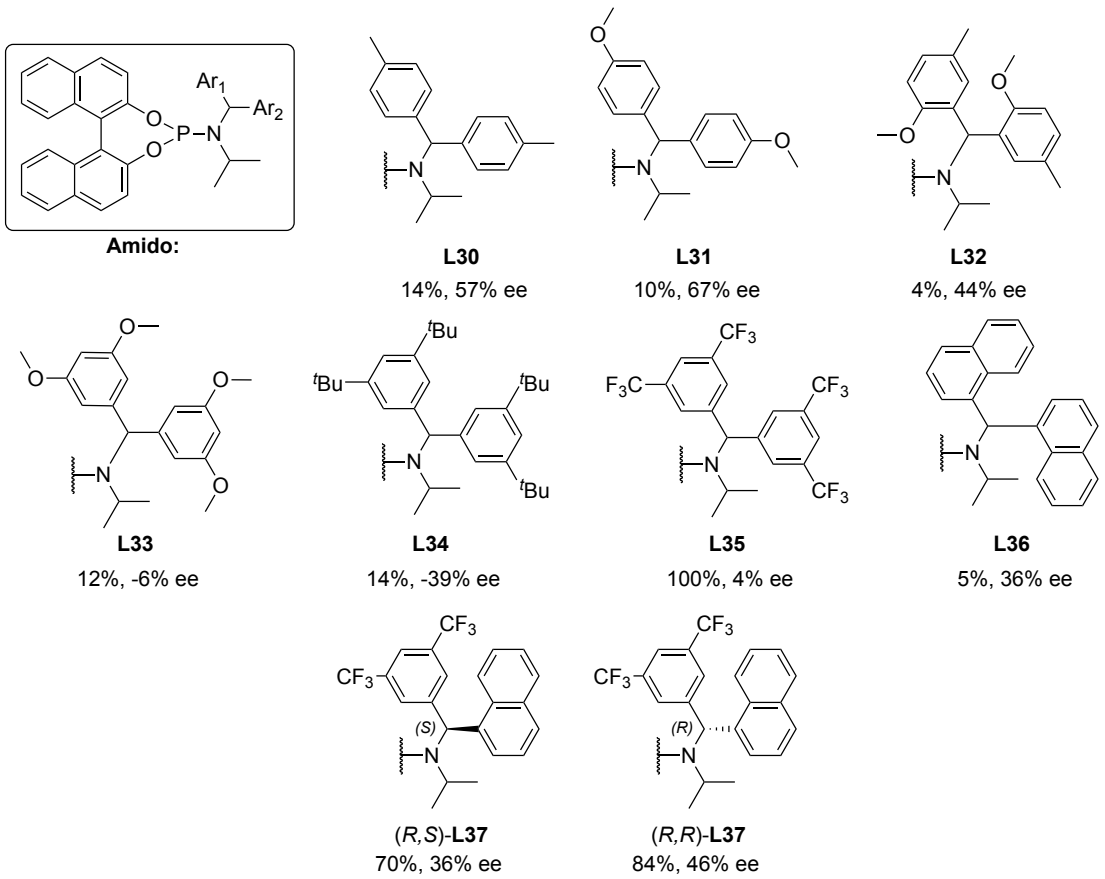

Figure 4-3 Ligand screening varying the aryl moiety. Conversions based on ^{1}H NMR spectroscopy of the crude reaction mixture. Ee's were determined by HPLC using a non-racemic stationary phase. Reaction condition used is shown in **Scheme 4-6**.

When we fixed the BINOL backbone and R_3 as an isopropyl and only varied the identity of the aromatic rings (Ar_1 and Ar_2), we saw a large range of reaction yield

(4% - 100%, **Figure 4-3**). Compared to **L24** (with unsubstituted Ph), the *p*-methyl variation gave a comparable yield and ee (14%, 57% ee **L30** vs 12%, 62% ee **L24**) while *p*-methoxy substitution (**L31**) gave marginal increase in ee compared to **L24** (10%, 67% ee). However, combining the two substituents with different substitution pattern (Me,- OMe-, **L32**) led to worse yield and ee (4%, 44% ee). Ligand with two methoxy substituents at *meta* position (**L33**) gave very poor yield and ee (12%, –6% ee). Switching the *meta*-substituents to ^{t}butyl (**L34**) gave poor yield and ee (14%, –39% ee). Surprisingly, bistrifluoromethyl substituents (**L35**) gave *full* conversion to product near racemic (100%, 4% ee). Naphthyl rings (**L36**) performed poorly (5%, 36% ee). When one aryl is naphthyl, the other bis(CF_3) substituted aryl (**L37**), both diastereomers of the ligand gave good yield but poor to moderate ee where the ligand with mismatched stereochemistry performed worse than the matching diastereomer (70%, 36% ee, (*R,S*)-**L37** vs 84%, 46% ee, (*R,R*)-**L37**). Notably, the fact that (*R,R*)-**L37** gave higher ee than either **L35** and **L36** suggested a synergistic effect between the two rings.

To summarise, Feringa's ligand ((*S,S,S*)-**L1**) gave highest ee whereas the bis-CF_3-substituted ligand gave the best yield. In all cases except **L1** and its variant **L15**, most ligands gave ee's lower than 70%. The presence of chirality in the amido group does not guarantee good ee. When R_1, R_2 = aryl and R_3 = ^{n}Bu or phenyl, these motifs improved the yield or ee compared to the corresponding ligands with R_3 = isopropyl. The effect of electron-donating groups on ee and yield is not clear but electron-withdrawing groups drastically increase the yield.

4.4 QSSR models

Using the aforementioned results to design a ligand that gives good yield and ee based on chemical intuition alone is somewhat challenging. To extract more information, we used these ligand screening data to construct a QSSR model. The approach used to construct the QSSR models is analogous to that previously described.

4.4.1 Training data

The training data collected is shown in **Table 4-2**. This data only include the ligands with unsubstituted BINOL backbone. The substituents on the amido part are ranked based on sizes where R_1 and R_2 are the same size or larger than R_3 and R_4 (collectively named R_{34}), and R_1 is larger than R_2 etc. (**Figure 4-4**). We excluded ligands where R_1 and R_2 are connected, namely **L20**, **L21** and **L27** as they do not add much value to the model (their substructures are similar to those already in the training set and they all gave yield and ee in the middle range). Excluding them will also enable the systematic ranking of the amido substituents as described above.

Table 4-2 Training ligands and their substituents, yield (%) and ΔΔG‡ (kJ/mol) are reports as averaged.

Ligand	R_1	R_2	R_{34}	R_3	R_4	yield	ΔΔG‡
L1sss	Ph	Me	CH(Me)Ph	Ph	Me	0.41	5.41
L1srr	Ph	Me	CH(Me)Ph	Ph	Me	0.20	2.82
L2rrr	2-Naph	Me	CH(Me)2-Naph	2-Naph	Me	0.32	4.71
L3	Ph	Ph	^{i}pr	Me	Me	0.12	3.59
L6	4-MeC_6H_4	4-MeC_6H_4	^{i}pr	Me	Me	0.14	3.21
L7	4-OMeC_6H_4	4-OMeC_6H_4	^{i}pr	Me	Me	0.10	4.02
L8	3,5diMeC_6H_3	3,5diMeC_6H_3	^{i}pr	Me	Me	0.10	1.27
L9	3,5ditBuC_6H_3	3,5ditBuC_6H_3	^{i}pr	Me	Me	0.14	2.02
L5	1-Naph	1-Naph	^{i}pr	Me	Me	0.05	1.87
L13rs	3,5-diCF_3	Naph	^{i}pr	Me	Me	0.84	2.47
L13rr	1-Naph	3,5-diCF_3	^{i}pr	Me	Me	0.70	1.87
L11	3,5-diOMe	3,5-diOMe	^{i}pr	Me	Me	0.12	0.27
L12	2-OMe,5-Me	2-OMe,5-Me	^{i}pr	Me	Me	0.04	2.41
L10	3,5-diCF_3	3,5-diCF_3	^{i}pr	Me	Me	1.00	0.20

L14ss	Ph	Me	^{i}pr	Me	Me	0.09	1.88
L15rr	3-BrC_6H_4	Me	^{i}pr	Me	Me	0.24	3.51
L16ss	4-ClC_6H_4	Me	^{i}pr	Me	Me	0.21	3.14
L17	3,5-diMeC_6H_3	3,5-diMeC_6H_3	^{n}Bu	^{n}Pr	H	0.07	2.10
L18	Ph	Ph	Me	H	H	0.11	2.97

4.4.2 Ligand descriptors

We have collected 66 computed electronics and steric parameters describing each substituent of the ligands (R_1-R_4) in the training set (**Table 4-2**) from Gaussian 09 and Spartan'16. Some parameters are highly correlated to each other (dark blue for positively correlated or dark red for negatively correlated, **Figure 4-4**). These strongly correlated parameters are to be avoided in QSSR models due to meaningless correlations that might arise from linear combinations of confounded parameters.

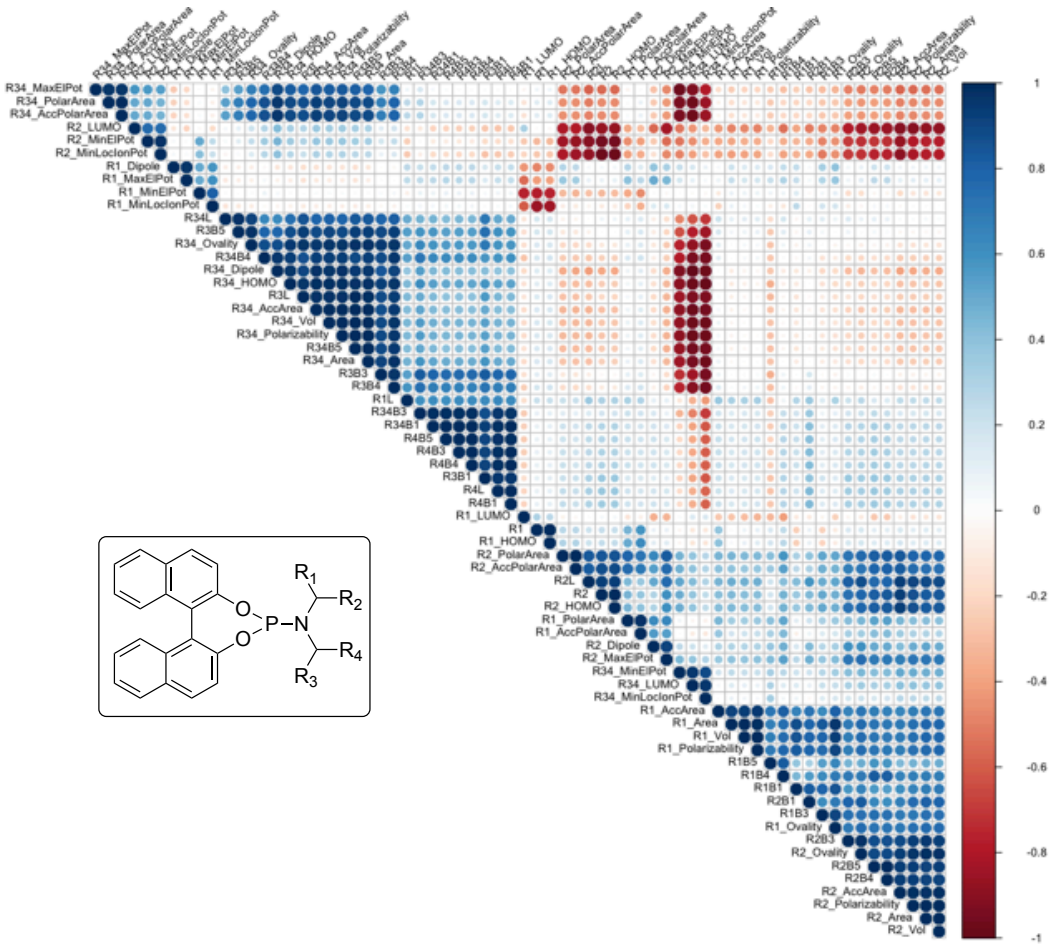

Figure 4-4 Pearson correlation matrix of computed descriptors.

As before, these parameters are standardised such that the values are scaled and unitless.

4.4.3 External testing set

We have used the training data to construct preliminary QSSR models. We noticed that these training data are heavily biased towards having R_{34} = ^{i}Pr. Based on the preliminary QSSR models, the ranking as R_3 and R_4 were not useful in describing the yield or ee, so we discarded the R_3 and R_4 notation and only used R_1, R_2 and R_{34}. The preliminary models were then tested against unseen data (testing set, **Table 4-3**). In the selection of the ligands for testing set, we intended to select ligands whose

structures are varied from the training set (R_{34} other than ^{i}Pr). These preliminary models failed to account for the external testing set given to validate it.

Table 4-3 Testing ligands and their substituents, yield (%) and ΔΔG‡ (kJ/mol) are reports as averaged.

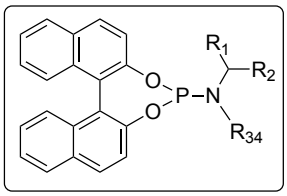

Ligand	R_1	R_2	R_{34}	yield	ΔΔG‡
L15	4-FC_6H_4	Me	CH(Me)Ph	0.29	4.30
L19	2-Naph	Me	Me(C_6H_{10})CMe_2Et	0.16	3.76
L22	Bn	H	H	0.16	1.40
L25	Ph	Ph	cyclohexane	0.12	1.51
L26	Ph	Ph	Ph	0.87	3.48

4.5 Future work

We have a database of yields and ee values from a variety of BINOL-based phoshoramidite ligands. The current preliminary models failed the external validation test, most likely because they were overtrained on R_{34} = ^{i}Pr. New models will be developed where we will shuffle the testing data into the training data to give a more balanced training set and new descriptors will be generated. If that still fails to produce rigorous models that pass external validation, the fundamental assumption of linear regression will be revised. However, the use of non-linear regression can lead to very complicated models that are then hard to interpret. Furthermore, there are additional degrees of freedom associated with fitting a non-linear model that typically necessitate a much larger quantity of training data. Further statistical work regarding model construction is on-going.

4.6 Experimental section

4.6.1 General experimental information

$Ir(cod)Cl_2$ was used as purchased from Strem. Anhydrous DCM and toluene was obtained from mBraun SPS-800 solvent purification system equipped with anhydrous alumina columns. Anhydrous EtOAc was dried over 4 Å molecular sieves. Anhydrous MeOH and other solvents were used as purchased. Thin layer chromatography (TLC) plates were examined under UV light (λ_{max} = 254 nm) and stained using Dragendorff's reagent ($Bi(NO_3)_3$, CH_3COOH and KI).

^1H, ^{13}C and ^{19}F NMR spectra were measured by Bruker AVIII400, AVII400, and Ascend™ 400 MHz machines in $CDCl_3$ solvent. Chemical shifts were reported in part per million, referenced to solvent residue peaks. Scalar coupling patterns were described as singlet (s), doublet (d), triplet (t), quartet (q) or multiplet (m). Broad peaks are indicated as (br). Coupling constants (*J*) were quoted to one decimal place. Chemical shifts were quoted to two decimal places in ^1H NMR and one decimal place in ^{13}C NMR and ^{31}P NMR. HSQC, COSY, DEPTQ and HMBC based experiments were performed to aid the assignment of spectra.

Chiral SFC (supercritical fluid chromatography) separations were conducted on a Waters Acquity UPC2 system using Waters Empower software. Chiralpak® columns (150 × 3 mm, particle size 3 μm) were used. Solvents used were of HPLC grade (Fisher Scientific, Sigma Aldrich or Rathburn). Solvents used were of HPLC grade (Fisher Scientific, Sigma Aldrich or Rathburn); all eluent systems were isocratic.

Infra-red spectra were recorded on a Bruker Tensor 27 FTIR spectrometer equipped with a PIKE Miracle Attenuated Total Reflectance sampling accessory using a solid

sample or thin film for liquid compounds. IR data was reported in wavenumbers (cm^{-1}).

High Resolution Mass spectra were carried out by internal service at the university of Oxford. Electron spray ionisation (ESI+) were recorded on a Fisons Platform II.

Chemical names were generated from CambridgeSoft ChemBioDraw Ultra 17.1 programme. Optical rotations ($[\alpha]_D^T$) were recorded from a Perkin Elmer 241 Polarimeter and are reported in degree·ml(·g·dm)$^{-1}$. Samples were prepared at concentration (c) measured in mg·ml^{-1}.

4.6.2 General procedures

4.6.2.1 General procedure 4-A. Hydrogenation conditions for ligand screening

This procedure was based on a literature reported procedure.[183] 6,7-Dimethoxy-1-(4-(trifluoromethyl)phenethyl)-3,4-dihydroisoquinoline in a form of the mesylate salt (45.95 mg, 0.1 mmol, 1.0 eq.) was added to $NaHCO_{3(sat)}$ and EtOAc mixture. The aqueous layer was extracted with EtOAc three times. The solvent was removed from the combined organic layer and the crude mixture was dried under high vacuum for 2 hr. In the mean time, in a dried capped glass Radley's Carousel 12 Plus Reaction Station™ tubes filled with $Ar_{(g)}$, a chiral ligand (0.84 mol%, 0.084 eq.) was added. Then a solution of $(Ir(COD)Cl)_2$ (1.34 mg, 0.2 mol%, 0.02 eq.) in DCM (0.5 ml) was added by syringe. The reaction mixture was stirred under $Ar_{(g)}$ for 1 hr before the solvent was removed and the carousel tubes were purged with $H_{2(g)}$. A solution of 6,7-dimethoxy-1-(4-(trifluoromethyl)phenethyl)-3,4-dihydroisoquinoline (36.3 mg, 0.1 mmol, 1.0 eq.) in EtOAc (5 ml, dried under 4 Å MS and degassed) was added by syringe. The reaction mixture was stirred at rt overnight. The crude mixture was

concentrated. The conversion was estimated by ^{1}H and ^{19}F NMR of the crude mixture in $CDCl_3$. The enantiomeric excess of the product was analysed by chiral SFC.

4.6.3 Experimental details

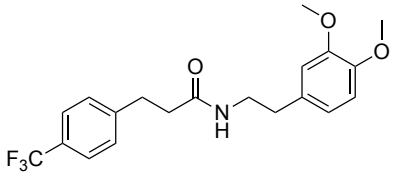

N-(3,4-dimethoxyphenethyl)-3-(4-(trifluoromethyl)phenyl)propanamide

N-(3,4-dimethoxyphenethyl)-3-(4-(trifluoromethyl)phenyl)propanamide was synthesized according to the literature reported procedure.[191] In a Dean-Stark distillation apparatus, 3-(4-(trifluoromethyl)phenyl)propanoic acid (24 g, 110 mmol, 1.0 eq.) and 2-(3,4-dimethoxyphenyl)ethan-1-amine (Homoveratrylamine) (19.9 g, 110 mmol, 1.0 eq.) was stirred at reflux in toluene (350ml) for 4 days. The toluene was occasionally topped up to maintain the total volume of approx. 350 ml and water was occasionally removed. The reaction mixture was then left to cool to room temperature. White solid was formed upon cooling. The solid was filtered and washed with ice cold toluene. Solvent was removed in high vacuum to afford *N*-(3,4-dimethoxyphenethyl)-3-(4-(trifluoromethyl)phenyl)propanamide as white needles (41.5 g, 109 mmol, 99%).

^{1}H NMR (400 MHz, $CDCl_3$) δ_H: 7.52 (d, *J* = 8.2 Hz, 2H, 2$C_{Ar}H$), 7.29 (d, *J* = 8.2 Hz, 2H, 2$C_{Ar}H$), 6.76 (d, *J* = 8.1 Hz, 1H, $C_{Ar}H$), 6.66 (d, *J* = 1.9 Hz, 1H, $C_{Ar}H$), 6.60 (dd, *J* = 8.1, 1.9 Hz, 1H, $C_{Ar}H$), 5.41 (t, *J* = 6.0 Hz, 1H, N*H*), 3.85 (s, 3H, OCH_3), 3.84 (s, 3H, OCH_3), 3.47 (dt, *J* = 7.0, 6.0 Hz, 2H, NCH_2), 3.00 (t, *J* = 7.6 Hz, 2H, ArCH_2), 2.69 (t, *J* = 7.0 Hz, 2H, ArCH_2), 2.42 (t, *J* = 7.6 Hz, 2H, COCH_2).

^{13}C NMR (101 MHz, $CDCl_3$) δ_C: 171.5, 149.2, 147.8, 145.2 (2C), 131.3, 128.9 (2C), 125.5 (q, *J* = 3.7 Hz, 2C), 124.4 (q, *J* = 276.9 Hz), 120.7, 111.9, 111.4, 56.0, 56.0, 40.8, 38.0, 35.3, 31.4.

^{19}F NMR (471 MHz, $CDCl_3$) δ_F: −62.3 (s).

IR υ_{max} (film): 3305, 2945, 2534, 2160, 2026, 1329, 1111.

HRMS (ESI^+) $[C_{20}H_{23}O_3NF_3]^+$ predicted 382.16245, found 382.16318 (Δ 1.89 ppm).

M.P. = 130 - 132 °C.

^{1}H NMR spectral data was consistent with previously reported values.[192]

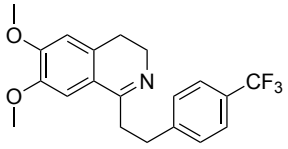

6,7-Dimethoxy-1-(4-(trifluoromethyl)phenethyl)-3,4-dihydroisoquinoline

6,7-Dimethoxy-1-(4-(trifluoromethyl)phenethyl)-3,4-dihydroisoquinoline was synthesised using modified procedure based on the literature reported procedure.[193] To a flame dried round bottom flask fitted with a reflux condenser, *N*-(3,4-dimethoxyphenethyl)-3-(4-(trifluoromethyl)phenyl)propanamide (2.11 g, 5.53 mmol, 1.0 eq) was stirred in toluene (300 ml). $POCl_{3(l)}$ (1.2 ml, 1.23 mmol, 2.22 eq.) was added by syringe and the solution was heated to 100 °C and stirred for 2 hr. The reaction mixture was left to cool down to room temperature. The reaction mixture was added portionwise to a stirring iced cold $NaHCO_3$ solution. The basicity of the solution was modulated to be within pH = 7-8 by aan ddition of a concentrated $NaOH_{(aq)}$ solution. The resultant suspension was stirred vigourously until all the solid suspension was dissolved before the mixture was partitioned between organic

and aqueous phases. The solvent was removed from the organic solution *in vacuo*. Methanesulfonic acid (0.43 ml, 1.2 mmol, 1.01 eq.) was added to the concentrated crude mixture. Filter the solid with toluene. Solvent was removed in high vacuum to afford methanesulfonic acid salt of 6,7-dimethoxy-1-(4-(trifluoromethyl)phenethyl)-3,4-dihydroisoquinoline as white solid (2.5 g, 5.53 mmol, quant.).

Characterisation data for the free amine:

^{1}H NMR (400 MHz, $CDCl_3$) δ_H: 7.51 (d, *J* = 8.0 Hz, 2H, $2C_{Ar}H$), 7.32 (d, *J* = 8.0 Hz, 2H, $2C_{Ar}H$), 6.92 (s, 1H, $C_{Ar}H$), 6.69 (s, 1H, $C_{Ar}H$), 3.89 (s, 3H, OCH_3), 3.84 (s, 3H, OCH_3), 3.68 – 3.59 (m, 2H, $ArCH_2CH_2N$), 3.10 – 3.02 (m, 2H, $ArCH_2$), 3.01 – 2.92 (m, 2H, $ArCH_2$), 2.63 – 2.54 (m, 2H, NCH_2).

^{13}C NMR (101 MHz, $CDCl_3$) δ_C: 165.2, 150.9, 147.5, 146.2, 131.6, 128.8 (2C), 128.3 (q, *J* = 32.5 Hz), 125.3 (q, *J* = 3.7 Hz, 2C), 124.4 (q, *J* = 272.6 Hz), 21.8, 110.4, 108.4, 56.2, 56.0, 47.0, 37.1, 32.8, 25.8.

^{19}F NMR (471 MHz, $CDCl_3$) δ_F: −62.3 (s).

IR υ_{max} (s): 3019, 2937, 2848, 1281, 1102.

HRMS (ESI^+) $[C_{20}H_{21}O_2NF_3]^+$ predicted 364.15189, found 364.15207 (Δ 0.49 ppm).

M.P. = 92 - 95 °C.

Characterisation data for the methanesulfonate salt:

^{1}H NMR (400 MHz, $CDCl_3$) δ_H: 13.68 (s, br, 1H, N*H*), 7.47 (d, *J* = 8.0 Hz, 2H, $2C_{Ar}H$), 7.31 (d, *J* = 8.0 Hz, 2H, $2C_{Ar}H$), 6.96 (s, 1H, $C_{Ar}H$), 6.75 (s, 1H, $C_{Ar}H$), 3.95 (s, 3H, OCH_3), 3.81 (s, 1H, OCH_3), 3.84-3.79 (m, 2H, NCH_2), 3.46 – 3.37 (m, 2H, $ArCH_2$), 3.18 – 3.09 (m, 2H, $ArCH_2$), 2.87 (t, *J* = 8.0 Hz, 2H, $ArCH_2CH_2N$), 2.79 (s, 3H, $CH_3SO_3^-$).

^{13}C NMR (151 MHz, $CDCl_3$) δ_C: 176.4, 156.8, 149.1, 142.6, 134.0, 129.4 (q, *J* = 32.5 Hz), 129.1 (2C), 125.9 (q, *J* = 3.8 Hz, 2C), 124.1 (q, *J* = 272.2 Hz), 117.3, 111.4, 111.2, 56.7, 56.6, 41.1, 39.6, 34.4, 34.1, 25.6.

^{19}F NMR (471 MHz, $CDCl_3$) δ_F: −62.5 (s).

IR υ_{max} (s): 2980, 1331, 1219, 1159, 1108, 1034.

M.P. = 167-170˚C.

M.P. was consistent with previously reported values.[191]

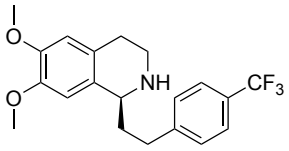

(*S*)-6,7-dimethoxy-1-(4-(trifluoromethyl)phenethyl)-1,2,3,4-tetrahydroisoquinoline

(*S*)-6,7-dimethoxy-1-(4-(trifluoromethyl)phenethyl)-1,2,3,4-tetrahydroisoquinoline

General procedure 4-A A glass tube reinforced with steel mesh charged with (*S*,*S*,*S*)-Feringa's Ligand (4.53 mg) was purge and filled with $H_{2(g)}$ atmosphere (5 bar). The condensed crude reaction mixture was purified by flash column chromatography [SiO_2, petrol/EtOAc/MeOH = 3:6:1] to afford (*S*)-6,7-dimethoxy-1-(4-(trifluoromethyl)phenethyl)-1,2,3,4-tetrahydroisoquinoline as a pale yellow residue (31.8 mg, 0.09 mmol, 87%).

Racemic synthesis

6,7-Dimethoxy-1-(4-(trifluoromethyl)phenethyl)-1,2,3,4-tetrahydroisoquinoline was synthesised according to the literature reported procedure.[191]

To a flame dried round bottom flask, 6,7-dimethoxy-1-(4-(trifluoromethyl)phenethyl)-3,4-dihydroisoquinoline (181.7 mg, 0.50 mmol, 1.0 eq.), $NaBH_{4(s)}$ (56.0 mg, 1.5 mmol, 3.0 eq.) and anhydrous MeOH (2.27 ml, 0.22 m) was added. The reaction mixture was stirred at 0 °C for 2 hr. The crude reaction mixture was condensed and H_2O (ca. 5 ml) was added. The suspension was extracted by EtOAc three times. The combined organic layer was dried with $MgSO_{4(s)}$ and solvent was removed *in vacuo*. The residue was dried under high vacuum to afford 6,7-dimethoxy-1-(4-(trifluoromethyl)phenethyl)-1,2,3,4-tetrahydroisoquinoline as a pale yellow residue (199.8 mg, 0.55 mmol, quant.).

^{1}H NMR (400 MHz, $CDCl_3$) δ_H: 7.54 (d, *J* = 8.0 Hz, 2H, $2C_{Ar}H$), 7.34 (d, *J* = 8.0 Hz, 2H, $2C_{Ar}H$), 6.58 (s, 1H, $C_{Ar}H$), 6.56 (s, 1H, $C_{Ar}H$), 3.98 – 3.92 (m, 1H, C*H*), 3.85 (s, 3H, OCH_3), 3.83 (s, 3H, OCH_3), 3.28 – 3.18 (m, 1H, ArC$H_aH_bCH_2N$), 3.05 – 2.97 (m, 1H, $ArCH_aH_bCH_2N$), 2.93 – 2.59 (m, 4H, CH_2N, ArCH_2), 2.17 – 1.95 (m, 2H, ArCH_2), 1.56 (s, br, 1H, N*H*).

^{13}C NMR (101 MHz, $CDCl_3$) δ_C: 147.5, 147.4, 146.8, 131.1, 128.8 (2C), 128.3 (q, *J* = 32.0 Hz), 127.5, 127.2 (q, J = 271.2 Hz), 25.4 (q, *J* = 4.0 Hz, 2C), 112.0, 109.2, 56.2, 56.0, 55.1, 41.1, 38.1, 32.4, 29.6.

^{19}F NMR (471 MHz, $CDCl_3$) δ_F: −62.3 (s).

IR υ_{max} (s): 2935, 2834, 1615, 1514, 1325, 1114.

HRMS (ESI^+) $[C_{20}H_{23}O_2NF_3]^+$ predicted 366.16754, found 366.16757 (Δ 0.09 ppm).

SFC analysis indicated an enantiomeric excess of 84% [Chiralpak® IB-3; 1500 psi, 30 °C, flow: 1.5 mL/min; 1% to 30% MeOH:^{i}PrOH(99:1) in 8 min; λ = 284.6 nm; major enantiomer, t_R = 5.61 min; minor enantiomer, t_R = 6.22 min].

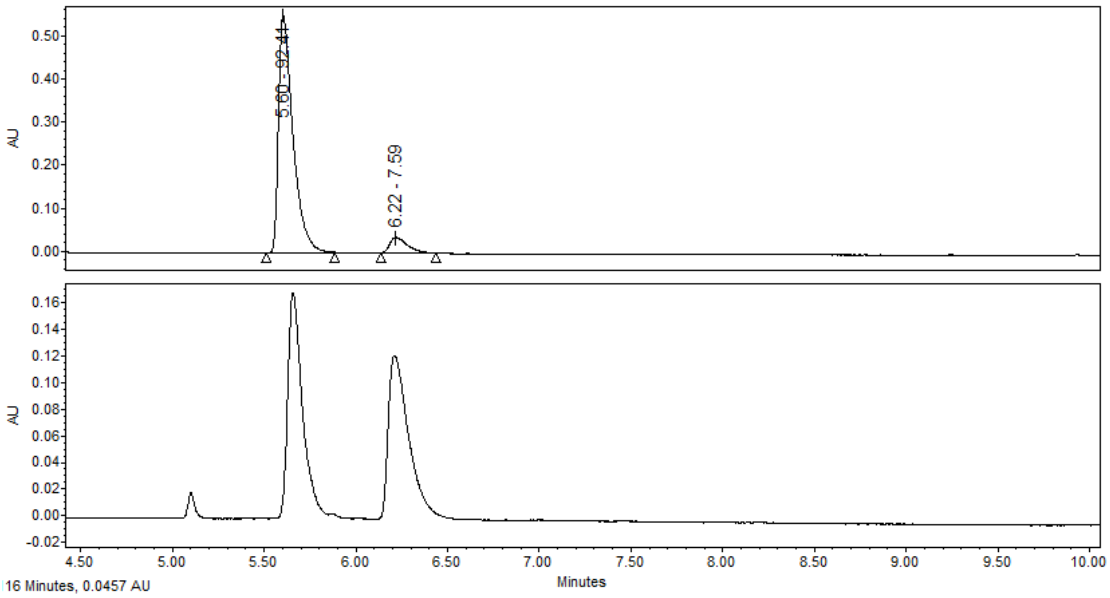

$[\alpha]_{589}^{25}$ = −17.4 (*c* 1.5, $CHCl_3$).

4.7 Computational experimental section

The chemical descriptors of the corresponding ligands were computed using g09, *Molecular Modelling Pro Plus 7.0*[119] or Spartan'16 as described below.[194] The Pearson correlation matrix using *R*-statistics package.[62] The total of 66 chemical descriptors based on substituents on amido part were computed. Each descriptor (x_i) was scaled to dimensionless values (x) using equation below.

$$x = \frac{x_i - \bar{x}}{s}$$

Where $\bar{x} = \frac{1}{N}\sum_{i=1}^{N} x_i$ (sample mean of x), N = number of data points,

$$s = \sqrt{\frac{1}{N-1}\sum_{i=1}^{N}(x_i - \bar{x})^2}$$ (sample standard deviation of x).

The descriptors of each substituent (R_n) is labeled Rn_descriptor. For example, the dipole moment of R_1 is called **R1_dipole** except for Highest occupied molecular orbital energy (HOMO energy) of R_1 and R_2 calculated by g09, these are named **R1**

and **R2** respectively. Table containing all the data for each descriptor can be found in Oxford University Research Archive.

HOMO energies of R_1 and R_2 substituents (under label **R1** and **R2**) were calculated at the B3LYP/6-31g(d) level of theory with a methyl group at the disconnection point from the rest of the ligand. For substituents that possess multiple stable conformations, their HOMO energies are reported as an averaged value weighed by their corresponding Boltzmann factors at 298 K.

The first and second generation Sterimol parameters: L, B_1, B_2, B_3, B_4 and B_5, were derived from *Molecular Modelling Pro Plus 7.0*[119] for the optimised structures of methyl capped substituents (B3LYP/6-31g(d)) unless stated otherwise. Exponential term of B_1 is also calculated ($\mathbf{e^{B1}}$).

QSAR descriptors obtained from Spartan'16[194] on optimised methyl-capped substituent structures (ωB97X-D/6-31G(d)): Highest occupied molecular orbital energy (**HOMO**), lowest unoccupied molecular orbital energy (**LUMO**), dipole moment (**Dipole**), molecular ovality (**Ovality**), surface area (**Area**), molecular volume (**Vol**), accessible area (**AccArea**), polar area (**PolarArea**), accessible polar area (**AccPolArea**), maximum and minimum electrostatic potential (**MaxEIPot** and **MinEIPot**), minimum local ionisation potential (**MinLocIonPot**) and polarisability (**Polarizability**).

5 Summary and Outlook

A crucial element in successfully developing efficient asymmetric catalytic reactions is finding a suitable chiral catalyst. Ligand discovery/development is not always easy to achieve. The most common practice often relies on trial and error. To move away from this, we have adopted a systematic approach that integrates traditional experimental screening approaches with statistical models (QSSR) and DFT calculations. Our aim is to increase useful information drawn from the experimental results, rather than just relying on chemical intuition alone.

We have applied this approach to two copper catalysed conjugate addition reactions and an iridium catalysed hydrogenation, all of which involved chiral phosphoramidite ligands. The QSSR models are shown to be both predictive and informative. This approach is not limited to only transition metal catalysed reaction or only with phosphoramidite-type ligands. In theory, it is applicable to any asymmetric transformation of interest involving any type of ligand. However, there are limitations. First is the practicality of the ligand screening. It is crucial that the results are reproducible. The synthetic tractability of ligands themselves can be a constraint. Therefore a group of chiral ligands with more modular structures is preferred.

A challenge in pursuing QSSR approaches is the creation of a quantitative model from numerous possible parameters. A 'Goldilocks' zone for a QSSR model is where the model is complex enough to allow for useful predictions yet simple enough to allow for physiochemical interpretations. A linear regression is an ideal form that allows for a straightforward interpretation. We used an automated model

generation method, a forward selection, to give a linear model. However, a linear relationship is an assumption. An alternative to an automated regression generation method such as forward regression is to use a machine-learning algorithm for regression generation. This lifts the constraints of a linear model. However, there are also drawbacks. To train the algorithm, thousands of data points are required which is generally prohibitive in the academic laboratory setup. Collaboration between academia and industry provides one way forward in this regard. Another drawback is that the model interpretation will become a challenge instead, preventing mechanistic insight to be gained.

Synthetic chemists who are invested in experimental work may find this approach helpful in terms of increasing the amount of useful information from hard-earned experimental results. There are pros and cons for using different tools to aid ligand discovery. The bottleneck of this approach is the time taken to synthesise the ligands and test them. This approach may not always result in a faster process yet but certainly offers a structured and systematic way to develop new chiral ligands.

6 References

[1] L. D. Barron, in *Strateg. Life Detect.* (Eds.: O. Botta, J.L. Bada, J. Gomez-Elvira, E. Javaux, F. Selsis, R. Summons), Springer US, Boston, MA, **2008**, pp. 187–201.
[2] E. Eliel, S. Wilen, L. Mander, *Stereochemistry Of Organic Compounds*, Wiley, Chichester, **1994**.
[3] K. Soai, T. Shibata, H. Morioka, K. Choji, *Nature* **1995**, *378*, 767–768.
[4] D. G. Blackmond, *Proc. Natl. Acad. Sci.* **2004**, *101*, 5732–5736.
[5] "Thalidomide - American Chemical Society", can be found under https://www.acs.org/content/acs/en/molecule-of-the-week/archive/t/thalidomide.html, 2018.
[6] K. V. Chuang, C. Xu, S. E. Reisman, *Science* **2016**, *353*, 912–915.
[7] K. C. Nicolaou, D. Pappo, K. Y. Tsang, R. Gibe, D. Y.-K. Chen, *Angew. Chem. Int. Ed.* **2008**, *47*, 944–946.
[8] J. M. Brunel, *Chem. Rev.* **2005**, *105*, 857–898.
[9] E. Christmann, E. Brase, *Asymmetric Synthesis: The Essentials, 2Nd, Completely Revised Edition*, John Wiley & Sons, **2007**.
[10] B. M. Trost, *Angew. Chem. Int. Ed. Engl.* **1995**, *34*, 259–281.
[11] R. Noyori, *Angew. Chem. Int. Ed.* **2002**, *41*, 2008–2022.
[12] G. A. Crispino, P. T. Ho, K. B. Sharpless, *Science* **1993**, *259*, 64–66.
[13] T. Katsuki, K. B. Sharpless, *J. Am. Chem. Soc.* **1980**, *102*, 5974–5976.
[14] T. P. Yoon, E. N. Jacobsen, *Science* **2003**, *299*, 1691–1693.
[15] M. Berthod, G. Mignani, G. Woodward, M. Lemaire, *Chem. Rev.* **2005**, *105*, 1801–1836.
[16] L. A. Paquette, *Chiral Reagents for Asymmetric Synthesis*, John Wiley & Sons, **1999**.
[17] D. Seebach, A. K. Beck, A. Heckel, *Angew. Chem. Int. Ed.* **2001**, *40*, 92–138.
[18] G. Desimoni, G. Faita, K. A. Jørgensen, *Chem. Rev.* **2006**, *106*, 3561–3651.
[19] J. F. Teichert, B. L. Feringa, *Angew. Chem. Int. Ed.* **2010**, *49*, 2486–2528.
[20] B. L. Feringa, *Acc. Chem. Res.* **2000**, *33*, 346–353.
[21] M. Diéguez, O. Pàmies, C. Claver, *Chem. Rev.* **2004**, *104*, 3189–3216.
[22] R. Roberts, *Serendipity*, Wiley, New York, **1989**.
[23] A. McNally, C. K. Prier, D. W. C. MacMillan, *Science* **2011**, *334*, 1114–1117.
[24] L. Lefort, J. A. F. Boogers, A. H. M. de Vries, J. G. de Vries, *Org. Lett.* **2004**, *6*, 1733–1735.
[25] R. B. C. Jagt, P. Y. Toullec, E. P. Schudde, J. G. de Vries, B. L. Feringa, A. J. Minnaard, *J. Comb. Chem.* **2007**, *9*, 407–414.
[26] C. L. Barhate, L. A. Joyce, A. A. Makarov, K. Zawatzky, F. Bernardoni, W. A. Schafer, D. W. Armstrong, C. J. Welch, E. L. Regalado, *Chem. Commun.* **2017**, *53*, 509–512.
[27] H. H. Jo, C.-Y. Lin, E. V. Anslyn, *Acc. Chem. Res.* **2014**, *47*, 2212–2221.
[28] B. T. Herrera, S. L. Pilicer, E. V. Anslyn, L. A. Joyce, C. Wolf, *J. Am. Chem. Soc.* **2018**, *140*, 10385–10401.
[29] E. G. Shcherbakova, V. Brega, T. Minami, S. Sheykhi, T. D. James, P. Anzenbacher, *Chem. – Eur. J.* **2016**, *22*, 10074–10080.
[30] E. G. Shcherbakova, T. Minami, V. Brega, T. D. James, P. Anzenbacher, *Angew. Chem. Int. Ed.* **2015**, *54*, 7130–7133.

[31] Y. Zhao, T. M. Swager, *J. Am. Chem. Soc.* **2015**, *137*, 3221–3224.
[32] T. A. Feagin, D. P. V. Olsen, Z. C. Headman, J. M. Heemstra, *J. Am. Chem. Soc.* **2015**, *137*, 4198–4206.
[33] K. N. Houk, P. H.-Y. Cheong, *Nature* **2008**, *455*, 309–313.
[34] Q. Peng, F. Duarte, R. S. Paton, *Chem. Soc. Rev.* **2016**, *45*, 6093–6107.
[35] G.-J. Cheng, X. Zhang, L. W. Chung, L. Xu, Y.-D. Wu, *J. Am. Chem. Soc.* **2015**, *137*, 1706–1725.
[36] M. Żyła-Karwowska, L. Moshniaha, H. Zhylitskaya, M. Stępień, *J. Org. Chem.* **2018**, *83*, 5199–5209.
[37] Q. Zhang, Y. Liu, T. Wang, X. Zhang, C. Long, Y.-D. Wu, M.-X. Wang, *J. Am. Chem. Soc.* **2018**, *140*, 5579–5587.
[38] J. M. Brown, R. J. Deeth, *Angew. Chem. Int. Ed.* **2009**, *48*, 4476–4479.
[39] R. N. Straker, Q. Peng, A. Mekareeya, R. S. Paton, E. A. Anderson, *Nat. Commun.* **2016**, *7*, 1–9.
[40] M. F. L. Parker, S. Osuna, G. Bollot, S. Vaddypally, M. J. Zdilla, K. N. Houk, C. E. Schafmeister, *J. Am. Chem. Soc.* **2014**, *136*, 3817–3827.
[41] Y. Guan, S. E. Wheeler, *Angew. Chem. Int. Ed.* **2017**, *56*, 9101–9105.
[42] V. P. Ananikov, D. G. Musaev, K. Morokuma, *J. Mol. Catal. Chem.* **2010**, *324*, 104–119.
[43] C. Bo, F. Maseras, *Dalton Trans.* **2008**, *0*, 2911–2919.
[44] E. Hansen, A. R. Rosales, B. Tutkowski, P.-O. Norrby, O. Wiest, *Acc. Chem. Res.* **2016**, *49*, 996–1005.
[45] P. J. Donoghue, P. Helquist, P.-O. Norrby, O. Wiest, *J. Am. Chem. Soc.* **2009**, *131*, 410–411.
[46] A. Tropsha, *Mol. Inform.* **2010**, *29*, 476–488.
[47] L. P. Hammett, *J. Am. Chem. Soc.* **1937**, *59*, 96–103.
[48] L. P. Hammett, *Chem. Rev.* **1935**, *17*, 125–136.
[49] J. C. Dearden, M. T. D. Cronin, K. L. E. Kaiser, *SAR QSAR Environ. Res.* **2009**, *20*, 241–266.
[50] C. B. Santiago, J.-Y. Guo, M. S. Sigman, *Chem. Sci.* **2018**, *9*, 2398–2412.
[51] S. Tan, *US Environ. Prot. Agency-Environ. Dir. Wash. DC* **2005**.
[52] S. Winstein, N. J. Holness, *J. Am. Chem. Soc.* **1955**, *77*, 5562–5578.
[53] R. Ruzziconi, S. Spizzichino, L. Lunazzi, A. Mazzanti, M. Schlosser, *Chem. – Eur. J.* **2009**, *15*, 2645–2652.
[54] M. Charton, *J. Org. Chem.* **1976**, *41*, 2217–2220.
[55] M. Charton, *J. Am. Chem. Soc.* **1975**, *97*, 1552–1556.
[56] R. W. Taft, *J. Am. Chem. Soc.* **1952**, *74*, 2729–2732.
[57] a) Verloop, A. in Drug Design Vol. III (ed. Ariens, E. J.) 133 (Academic Press, **1976**), p.165. b) Verloop, A. In IUPAC Pesticide Chemistry; Miyamoto, J., Ed.; Pergamon: Oxford, **1983**; Vol. 1, p 339.
[58] M. Urbano-Cuadrado, J. J. Carbó, A. G. Maldonado, C. Bo, *J. Chem. Inf. Model.* **2007**, *47*, 2228–2234.
[59] J. Jover, N. Fey, J. N. Harvey, G. C. Lloyd-Jones, A. G. Orpen, G. J. J. Owen-Smith, P. Murray, D. R. J. Hose, R. Osborne, M. Purdie, *Organometallics* **2012**, *31*, 5302–5306.
[60] N. Fey, A. G. Orpen, J. N. Harvey, *Coord. Chem. Rev.* **2009**, *253*, 704–722.
[61] N. Fey, J. N. Harvey, G. C. Lloyd-Jones, P. Murray, A. G. Orpen, R. Osborne, M. Purdie, *Organometallics* **2008**, *27*, 1372–1383.

[62] *R Core Team* (**2013**). R: A language and environment for statistical computing. R Foundation for Statistical Computing, Vienna, Austria. ISBN 3-900051-07-0, URL: http://www.R-project.org/.
[63] A. Tropsha, P. Gramatica, V. K. Gombar, *QSAR Comb. Sci.* **2003**, *22*, 69–77.
[64] A. Golbraikh, A. Tropsha, *J. Mol. Graph. Model.* **2002**, *20*, 269–276.
[65] D. M. Hawkins, *J. Chem. Inf. Comput. Sci.* **2004**, *44*, 1–12.
[66] S. Wold, W. J. Dunn, *J. Chem. Inf. Comput. Sci.* **1983**, *23*, 6–13.
[67] J. D. Oslob, B. Åkermark, P. Helquist, P.-O. Norrby, *Organometallics* **1997**, *16*, 3015–3021.
[68] R. Wehrens, H. Putter, L. M. . Buydens, *Chemom. Intell. Lab. Syst.* **2000**, *54*, 35–52.
[69] C. Rücker, G. Rücker, M. Meringer, *J. Chem. Inf. Model.* **2007**, *47*, 2345–2357.
[70] V. Consonni, D. Ballabio, R. Todeschini, *J. Chem. Inf. Model.* **2009**, *49*, 1669–1678.
[71] G. Schüürmann, R.-U. Ebert, J. Chen, B. Wang, R. Kühne, *J. Chem. Inf. Model.* **2008**, *48*, 2140–2145.
[72] K. S. Kannan, K. Manoj, *Appl. Math. Sci.* **2015**, *9*, 2317–2324.
[73] C. Zhang, C. B. Santiago, J. M. Crawford, M. S. Sigman, *J. Am. Chem. Soc.* **2015**, *137*, 15668–15671.
[74] R. L. Lipnick, *Sci. Total Environ.* **1991**, *109–110*, 131–153.
[75] G. M. Maggiora, *J. Chem. Inf. Model.* **2006**, *46*, 1535–1535.
[76] T. Fujita, D. A. Winkler, *J. Chem. Inf. Model.* **2016**, *56*, 269–274.
[77] Z. L. Niemeyer, A. Milo, D. P. Hickey, M. S. Sigman, *Nat. Chem.* **2016**, *8*, 610–617.
[78] S. E. Denmark, N. D. Gould, L. M. Wolf, *J. Org. Chem.* **2011**, *76*, 4337–4357.
[79] K. C. Harper, E. N. Bess, M. S. Sigman, *Nat. Chem.* **2012**, *4*, 366–374.
[80] K. C. Harper, M. S. Sigman, *Science* **2011**, *333*, 1875–1878.
[81] H. Huang, H. Zong, G. Bian, H. Yue, L. Song, *J. Org. Chem.* **2014**, *79*, 9455–9464.
[82] H. Huang, H. Zong, B. Shen, H. Yue, G. Bian, L. Song, *Tetrahedron* **2014**, *70*, 1289–1297.
[83] M. Orlandi, J. A. S. Coelho, M. J. Hilton, F. D. Toste, M. S. Sigman, *J. Am. Chem. Soc.* **2017**, *139*, 6803–6806.
[84] Y. Luo, N. G. Berry, A. J. Carnell, *Chem. Commun.* **2012**, *48*, 3279–3281.
[85] S. Aguado-Ullate, M. Urbano-Cuadrado, I. Villalba, E. Pires, J. I. García, C. Bo, J. J. Carbó, *Chem. – Eur. J.* **2012**, *18*, 14026–14036.
[86] J. M. Crawford, E. A. Stone, A. J. Metrano, S. J. Miller, M. S. Sigman, *J. Am. Chem. Soc.* **2018**, *140*, 868–871.
[87] E. N. Bess, A. J. Bischoff, M. S. Sigman, *Proc. Natl. Acad. Sci.* **2014**, *111*, 14698–14703.
[88] M. Orlandi, M. J. Hilton, E. Yamamoto, F. D. Toste, M. S. Sigman, *J. Am. Chem. Soc.* **2017**, *139*, 12688–12695.
[89] M. S. Sigman, K. C. Harper, E. N. Bess, A. Milo, *Acc. Chem. Res.* **2016**, *49*, 1292–1301.
[90] H. Gonzalez-Diaz, S. Arrasate, A. Juan, N. Sotomayor, E. Lete, A. Speck-Planche, J. Ruso, F. Luan, M. Cordeiro, *Curr. Drug Metab.* **2014**, *15*, 470–488.
[91] R. Ardkhean, P. M. C. Roth, R. M. Maksymowicz, A. Curran, Q. Peng, R. S. Paton, S. P. Fletcher, *ACS Catal.* **2017**, *7*, 6729–6737.
[92] B. E. Rossiter, N. M. Swingle, *Chem. Rev.* **1992**, *92*, 771–806.
[93] G. M. Villacorta, C. P. Rao, S. J. Lippard, *J. Am. Chem. Soc.* **1988**, *110*, 3175–3182.
[94] N. Krause, A. Hoffmann-Röder, *Synthesis* **2001**, *2001*, 171–196.

[95] A. H. M. de Vries, A. Meetsma, B. L. Feringa, *Angew. Chem. Int. Ed. Engl.* **1996**, *35*, 2374–2376.
[96] B. L. Feringa, M. Pineschi, L. A. Arnold, R. Imbos, A. H. M. de Vries, *Angew. Chem. Int. Ed. Engl.* **1997**, *36*, 2620–2623.
[97] A. Alexakis, J. Vastra, J. Burton, C. Benhaim, P. Mangeney, *Tetrahedron Lett.* **1998**, *39*, 7869–7872.
[98] A. Alexakis, J. E. Bäckvall, N. Krause, O. Pàmies, M. Diéguez, *Chem. Rev.* **2008**, *108*, 2796–2823.
[99] T. Jerphagnon, M. G. Pizzuti, A. J. Minnaard, B. L. Feringa, *Chem. Soc. Rev.* **2009**, *38*, 1039–1075.
[100] S. R. Harutyunyan, T. den Hartog, K. Geurts, A. J. Minnaard, B. L. Feringa, *Chem. Rev.* **2008**, *108*, 2824–2852.
[101] R. M. Maksymowicz, A. J. Bissette, S. P. Fletcher, *Chem. – Eur. J.* **2015**, *21*, 5668–5678.
[102] R. M. Maksymowicz, P. M. C. Roth, S. P. Fletcher, *Nat. Chem.* **2012**, *4*, 649–654.
[103] P. M. C. Roth, M. Sidera, R. M. Maksymowicz, S. P. Fletcher, *Nat. Protoc.* **2014**, *9*, 104–111.
[104] P. M. C. Roth, S. P. Fletcher, *Org. Lett.* **2015**, DOI 10.1021/acs.orglett.5b00021.
[105] Z. Gao, S. P. Fletcher, *Chem. Sci.* **2016**, *8*, 641–646.
[106] E. E. Maciver, R. M. Maksymowicz, N. Wilkinson, P. M. C. Roth, S. P. Fletcher, *Org. Lett.* **2014**, *16*, 3288–3291.
[107] P. M. C. Roth, S. P. Fletcher, *Org. Lett.* **2015**, *17*, 912–915.
[108] M. Sidera, P. M. C. Roth, R. M. Maksymowicz, S. P. Fletcher, *Angew. Chem. Int. Ed.* **2013**, *52*, 7995–7999.
[109] S. R. Harutyunyan, F. López, W. R. Browne, A. Correa, D. Peña, R. Badorrey, A. Meetsma, A. J. Minnaard, B. L. Feringa, *J. Am. Chem. Soc.* **2006**, *128*, 9103–9118.
[110] C. B. Santiago, A. Milo, M. S. Sigman, *J. Am. Chem. Soc.* **2016**, *138*, 13424–13430.
[111] H. Huang, H. Zong, G. Bian, L. Song, *J. Org. Chem.* **2012**, *77*, 10427–10434.
[112] S. Harutyunyan, Ed. , *Progress in Enantioselective Cu(I)-Catalyzed Formation of Stereogenic Centers*, Springer International Publishing, **2016**.
[113] A. Alexakis, N. Krause, S. Woodward, *Copper-Catalyzed Asymmetric Synthesis*, John Wiley & Sons, **2013**.
[114] J. Schwartz, J. A. Labinger, *Angew. Chem. Int. Ed. Engl.* **1976**, *15*, 333–340.
[115] D. W. Hart, J. Schwartz, *J. Am. Chem. Soc.* **1974**, *96*, 8115–8116.
[116] S. Grimme, *J. Comput. Chem.* **2006**, *27*, 1787–1799.
[117] C. Puchot, O. Samuel, E. Dunach, S. Zhao, C. Agami, H. B. Kagan, *J. Am. Chem. Soc.* **1986**, *108*, 2353–2357.
[118] *Gaussian 09*, Revision D.01, Frisch, M. J.; Trucks, G. W.; Schlegel, H. B.; Scuseria, G. E.; Robb, M. A.; Cheeseman, J. R.; Scalmani, G.; Barone, V.; Mennucci, B.; Petersson, G. A.; Nakatsuji, H.; Caricato, M.; Li, X.; Hratchian, H. P.; Izmaylov, A. F.; Bloino, J.; Zheng, G.; Sonnenberg, J. L.; Hada, M.; Ehara, M.; Toyota, K.; Fukuda, R.; Hasegawa, J.; Ishida, M.; Nakajima, T.; Honda, Y.; Kitao, O.; Nakai, H.; Vreven, T.; Montgomery, J. A., Jr.; Peralta, J. E.; Ogliaro, F.; Bearpark, M.; Heyd, J. J.; Brothers, E.; Kudin, K. N.; Staroverov, V. N.; Kobayashi, R.; Normand, J.; Raghavachari, K.; Rendell, A.; Burant, J. C.; Iyengar, S. S.; Tomasi, J.; Cossi, M.; Rega, N.; Millam, N. J.; Klene, M.; Knox, J. E.; Cross, J. B.; Bakken, V.; Adamo, C.; Jaramillo, J.; Gomperts, R.; Stratmann, R. E.; Yazyev, O.; Austin, A. J.; Cammi, R.; Pomelli, C.; Ochterski, J. W.; Martin, R. L.; Morokuma, K.; Zakrzewski, V. G.; Voth,

G. A.; Salvador, P.; Dannenberg, J. J.; Dapprich, S.; Daniels, A. D.; Farkas, Ö.; Foresman, J. B.; Ortiz, J. V.; Cioslowski, J.; Fox, D. J. Gaussian, Inc., Wallingford CT, **2009**.
[119] *Molecular Modelling Pro Plus v 7.0*, Norgwyn Montgomery Software Inc.,. Quinn, J. A. and co-workers
[120] R. Ardkhean, M. Mortimore, R. S. Paton, S. P. Fletcher, *Chem. Sci.* **2018**, *9*, 2628–2632.
[121] S. F. Brady, M. P. Singh, J. E. Janso, J. Clardy, *J. Am. Chem. Soc.* **2000**, *122*, 2116–2117.
[122] G. Majetich, J. M. Shimkus, *J. Nat. Prod.* **2010**, *73*, 284–298.
[123] K. D. Wellington, R. C. Cambie, P. S. Rutledge, P. R. Bergquist, *J. Nat. Prod.* **2000**, *63*, 79–85.
[124] H. Kuhl, *Climacteric* **2005**, *8*, 3–63.
[125] H. Zhou, Y.-H. Tang, Y. Zheng, *Brain Res.* **2006**, *1092*, 207–213.
[126] W.-K. P. Cho, *United States Patent: 7612058 - Methods for Inhibiting Sterol Absorption*, **2009**, 7612058.
[127] T. Ling, F. Rivas, *Tetrahedron* **2016**, *72*, 6729–6777.
[128] K. W. Quasdorf, L. E. Overman, *Nature* **2014**, *516*, 181–191.
[129] X. Gu, Y. Dai, T. Guo, A. Franchino, D. J. Dixon, J. Ye, *Org. Lett.* **2015**, *17*, 1505–1508.
[130] I. Marek, Y. Minko, M. Pasco, T. Mejuch, N. Gilboa, H. Chechik, J. P. Das, *J. Am. Chem. Soc.* **2014**, *136*, 2682–2694.
[131] M. Shimizu, *Angew. Chem. Int. Ed.* **2011**, *50*, 5998–6000.
[132] J. P. Das, I. Marek, *Chem. Commun.* **2011**, *47*, 4593–4623.
[133] M. P. Sibi, S. Manyem, *Tetrahedron* **2000**, *56*, 8033–8061.
[134] M. Vuagnoux-d'Augustin, A. Alexakis, *Chem. – Eur. J.* **2007**, *13*, 9647–9662.
[135] C. Hawner, K. Li, V. Cirriez, A. Alexakis, *Angew. Chem. Int. Ed.* **2008**, *47*, 8211–8214.
[136] L. Palais, A. Alexakis, *Chem. – Eur. J.* **2009**, *15*, 10473–10485.
[137] K. Kikushima, J. C. Holder, M. Gatti, B. M. Stoltz, *J. Am. Chem. Soc.* **2011**, *133*, 6902–6905.
[138] D. Müller, C. Hawner, M. Tissot, L. Palais, A. Alexakis, *Synlett* **2010**, *2010*, 1694–1698.
[139] C. Hawner, D. Müller, L. Gremaud, A. Felouat, S. Woodward, A. Alexakis, *Angew. Chem. Int. Ed.* **2010**, *49*, 7769–7772.
[140] S. Kehrli, D. Martin, D. Rix, M. Mauduit, A. Alexakis, *Chem. – Eur. J.* **2010**, *16*, 9890–9904.
[141] L. Palais, A. Alexakis, *Chem. – Eur. J.* **2009**, *15*, 10473–10485.
[142] M. W. Paixão, N. Holub, C. Vila, M. Nielsen, K. A. Jørgensen, *Angew. Chem. Int. Ed.* **2009**, *48*, 7338–7342.
[143] S. Liu, Q. Wang, L. Ye, Z. Shi, Z. Zhao, X. Yang, K. Ding, X. Li, *Tetrahedron* **2016**, *72*, 5115–5120.
[144] D. Martin, S. Kehrli, M. d'Augustin, H. Clavier, M. Mauduit, A. Alexakis, *J. Am. Chem. Soc.* **2006**, *128*, 8416–8417.
[145] T. L. May, M. K. Brown, A. H. Hoveyda, *Angew. Chem. Int. Ed.* **2008**, *47*, 7358–7362.
[146] J. Buter, R. Moezelaar, A. J. Minnaard, *Org. Biomol. Chem.* **2014**, *12*, 5883–5890.

[147] M. K. Brown, T. L. May, C. A. Baxter, A. H. Hoveyda, *Angew. Chem. Int. Ed.* **2007**, *46*, 1097–1100.
[148] T. L. May, J. A. Dabrowski, A. H. Hoveyda, *J. Am. Chem. Soc.* **2011**, *133*, 736–739.
[149] M. Vuagnoux-d'Augustin, S. Kehrli, A. Alexakis, *Synlett* **2007**, *2007*, 2057–2060.
[150] P. Wipf, W. Xu, J. H. Smitrovich, R. Lehmann, L. M. Venanzi, *Tetrahedron* **1994**, *50*, 1935–1954.
[151] E. Rideau, F. Mäsing, S. P. Fletcher, *Synthesis* **2015**, *47*, 2217–2222.
[152] R. M. Maksymowicz, M. Sidera, P. M. C. Roth, S. P. Fletcher, *Synthesis* **2013**, *45*, 2662–2668.
[153] Z. Gao, S. P. Fletcher, *Chem. Commun.* **2018**, *54*, 3601–3604.
[154] Z. Gao, S. P. Fletcher, *Chem. Commun.* **2017**, *53*, 10216–10219.
[155] D. Caprioglio, S. P. Fletcher, *Chem. Commun.* **2015**, *51*, 14866–14868.
[156] R. M. Maksymowicz, P. M. C. Roth, A. L. Thompson, S. P. Fletcher, *Chem. Commun.* **2013**, *49*, 4211–4213.
[157] R. L. Reyes, T. Harada, T. Taniguchi, K. Monde, T. Iwai, M. Sawamura, *Chem. Lett.* **2017**, *46*, 1747–1750.
[158] A. Bondi, *J. Phys. Chem.* **1964**, *68*, 441–451.
[159] P. Wipf, J. H. Smitrovich, *J. Org. Chem.* **1991**, *56*, 6494–6496.
[160] B. Huber, B. Roling, *Electrochimica Acta* **2011**, *56*, 6569–6572.
[161] S. E. Hampton, B. Baragaña, A. Schipani, C. Bosch-Navarrete, J. A. Musso-Buendía, E. Recio, M. Kaiser, J. L. Whittingham, S. M. Roberts, M. Shevtsov, et al., *ChemMedChem* **2011**, *6*, 1816–1831.
[162] B. M. Trost, S. M. Silverman, J. P. Stambuli, *J. Am. Chem. Soc.* **2011**, *133*, 19483–19497.
[163] M. M. Alam, R. Varala, S. R. Adapa, *Synth. Commun.* **2003**, *33*, 3035–3040.
[164] R. C. Gadwood, I. M. Mallick, A. J. DeWinter, *J. Org. Chem.* **1987**, *52*, 774–782.
[165] R. S. Bhosale, S. V. Bhosale, S. V. Bhosale, T. Wang, P. K. Zubaidha, *Tetrahedron Lett.* **2004**, *45*, 7187–7188.
[166] Y. Moritani, D. H. Appella, V. Jurkauskas, S. L. Buchwald, *J. Am. Chem. Soc.* **2000**, *122*, 6797–6798.
[167] B. M. Trost, J. Xie, N. Maulide, *J. Am. Chem. Soc.* **2008**, *130*, 17258–17259.
[168] H. Ren, W. D. Wulff, *J. Am. Chem. Soc.* **2011**, *133*, 5656–5659.
[169] S. Tartaglia, F. Pace, P. Scafato, C. Rosini, *Org. Lett.* **2008**, *10*, 3421–3424.
[170] A. Kabro, T. Roisnel, C. Fischmeister, C. Bruneau, *Chem. – Eur. J.* **2010**, *16*, 12255–12261.
[171] S. M. Manolikakes, M. Ellwart, C. I. Stathakis, P. Knochel, *Chem. – Eur. J.* **2014**, *20*, 12289–12297.
[172] H. Komagawa, Y. Maejima, T. Nagano, *Synlett* **2016**, *27*, 789–793.
[173] D. P. Papahatjis, T. Kourouli, A. Makriyannis, *J. Heterocycl. Chem.* **1996**, *33*, 559–562.
[174] G. W. Kabalka, Z. Wu, Y. Ju, *Tetrahedron* **2001**, *57*, 1663–1670.
[175] Y. Li, W. Lu, D. Xue, C. Wang, Z.-T. Liu, J. Xiao, *Synlett* **2014**, *25*, 1097–1100.
[176] R. L. Letsinger, A. W. Schnizer, *J. Org. Chem.* **1951**, *16*, 869–873.
[177] Y. Shang, C. Wang, X. He, K. Ju, M. Zhang, S. Yu, J. Wu, *Tetrahedron* **2010**, *66*, 9629–9633.
[178] Q. Zhou, S. Wei, W. Han, *J. Org. Chem.* **2014**, *79*, 1454–1460.
[179] J.-D. Chai, M. Head-Gordon, *Phys. Chem. Chem. Phys.* **2008**, *10*, 6615–6620.

[180] The PyMOL Molecular Graphics System, Version 2.0 Schrödinger, LLC.
[181] E. R. Johnson, S. Keinan, P. Mori-Sánchez, J. Contreras-García, A. J. Cohen, W. Yang, *J. Am. Chem. Soc.* **2010**, *132*, 6498–6506.
[182] C. Brisbare-Roch, J. Dingemanse, R. Koberstein, P. Hoever, H. Aissaoui, S. Flores, C. Mueller, O. Nayler, J. van Gerven, S. L. de Haas, et al., *Nat. Med.* **2007**, *13*, 150–155.
[183] G. K. M. Verzijl, A. H. M. de Vries, J. G. de Vries, P. Kapitan, T. Dax, M. Helms, Z. Nazir, W. Skranc, C. Imboden, J. Stichler, et al., *Org. Process Res. Dev.* **2013**, *17*, 1531–1539.
[184] T. C. Nugent, M. El-Shazly, *Adv. Synth. Catal.* **2010**, *352*, 753–819.
[185] N. Uematsu, A. Fujii, S. Hashiguchi, T. Ikariya, R. Noyori, *J. Am. Chem. Soc.* **1996**, *118*, 4916–4917.
[186] C. Li, J. Xiao, *J. Am. Chem. Soc.* **2008**, *130*, 13208–13209.
[187] C. A. Willoughby, S. L. Buchwald, *J. Am. Chem. Soc.* **1992**, *114*, 7562–7564.
[188] T. Morimoto, K. Achiwa, *Tetrahedron Asymmetry* **1995**, *6*, 2661–2664.
[189] T. Morimoto, N. Suzuki, K. Achiwa, *Tetrahedron Asymmetry* **1998**, *9*, 183–187.
[190] J.-H. Xie, S.-F. Zhu, Q.-L. Zhou, *Chem. Rev.* **2011**, *111*, 1713–1760.
[191] T. Weller, R. Koberstein, H. Aissaoui, M. Clozel, W. Fischli, *Substituted 1,2,3,4-Tetrahydroisoquinoline Derivatives*, **2005**, WO2005118548 (A1).
[192] S. Erbeck, R. Koberstein, A. Soi, A. Zistler, *Method for Obtaining an Optically Pure 1,2,3,4 Tetrahydro-Isoquinoline Derivative*, **2010**, WO2010064212 (A1).
[193] V. De, D. Domin, M. Helms, C. Imboden, R. Koberstein, Z. Nazir, W. Skranc, M. Stanek, W. Tschebull, G. Verzijl, *Trisubstituted 3,4-Dihydro-1h-Isoquinolin Compound, Process for Its Preparation, and Its Use*, **2009**, WO2009083903 (A1).
[194] Spartan 16, Y. Shao, L.F. Molnar, Y. Jung, J. Kussmann, C. Ochsenfeld, S.T. Brown, A.T.B. Gilbert, L.V. Slipchenko, S.V. Levchenko, D.P. O'Neill, R.A. DiStasio Jr., R.C. Lochan, T. Wang, G.J.O. Beran, N.A. Besley, J.M. Herbert, C.Y. Lin, T. Van Voorhis, S.H. Chien, A. Sodt, R.P. Steele, V.A. Rassolov, P.E. Maslen, P.P. Korambath, R.D. Adamson, B. Austin, J. Baker, E.F.C. Byrd, H. Dachsel, R.J. Doerksen, A. Dreuw, B.D. Dunietz, A.D. Dutoi, T.R. Furlani, S.R. Gwaltney, A. Heyden, S. Hirata, C-P. Hsu, G. Kedziora, R.Z. Khalliulin, P. Klunzinger, A.M. Lee, M.S. Lee, W.Z. Liang, I. Lotan, N. Nair, B. Peters, E.I. Proynov, P.A. Pieniazek, Y.M. Rhee, J. Ritchie, E. Rosta, C.D. Sherrill, A.C. Simmonett, J.E. Subotnik, H.L. Woodcock III, W. Zhang, A.T. Bell, A.K. Chakraborty, D.M. Chipman, F.J. Keil, A.Warshel, W.J. Hehre, H.F. Schaefer, J. Kong, A.I. Krylov, P.M.W. Gill and M. Head-Gordon, *Phys. Chem. Chem. Phys.,* **8**, 3172 (2006).